



5-1996

# Impact Biomechanics of the Human Body

Tyler A. Kress

*University of Tennessee - Knoxville*

---

## Recommended Citation

Kress, Tyler A., "Impact Biomechanics of the Human Body." PhD diss., University of Tennessee, 1996.  
[https://trace.tennessee.edu/utk\\_graddiss/2516](https://trace.tennessee.edu/utk_graddiss/2516)

This Dissertation is brought to you for free and open access by the Graduate School at Trace: Tennessee Research and Creative Exchange. It has been accepted for inclusion in Doctoral Dissertations by an authorized administrator of Trace: Tennessee Research and Creative Exchange. For more information, please contact [trace@utk.edu](mailto:trace@utk.edu).

To the Graduate Council:

I am submitting herewith a dissertation written by Tyler A. Kress entitled "Impact Biomechanics of the Human Body." I have examined the final electronic copy of this dissertation for form and content and recommend that it be accepted in partial fulfillment of the requirements for the degree of Doctor of Philosophy, with a major in Engineering Science.

John N. Snider, Major Professor

We have read this dissertation and recommend its acceptance:

Jack F. Wasserman, Milt Bailey, John Hungerford

Accepted for the Council:

Dixie L. Thompson


Vice Provost and Dean of the Graduate School

(Original signatures are on file with official student records.)

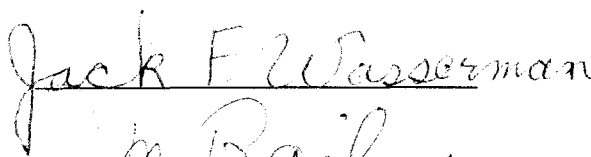
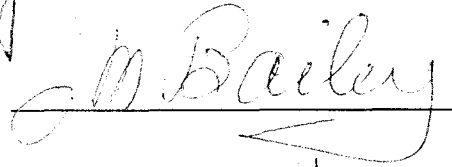
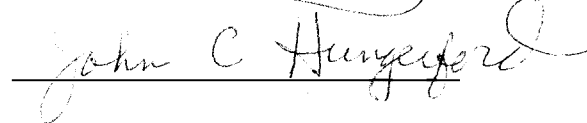
---

To the Graduate Council:

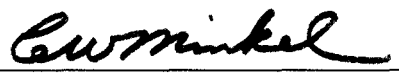
I am submitting herewith a dissertation written by Tyler A. Kress entitled "Impact Biomechanics of the Human Body." I have examined the final copy of this dissertation for form and content and recommend that it be accepted in partial fulfillment of the requirements for the degree of Doctor of Philosophy, with a major in Engineering Science.

  
John N. Snider, Major Professor

We have read this dissertation  
and recommend its acceptance:

Accepted for the Council:

  
Associate Vice Chancellor and  
Dean of The Graduate School

# **IMPACT BIOMECHANICS OF THE HUMAN BODY**

**A Dissertation  
Presented for the  
Doctor of Philosophy  
Degree  
The University of Tennessee, Knoxville**

**Tyler A. Kress  
May 1996**



## **DEDICATION**

**This dissertation is  
dedicated to my parents,**

**Tom and Dee Kress,**

**two amazing people  
who I love and respect tremendously.**

## **ACKNOWLEDGMENTS**

My first “thank you” is to the caring individuals (and their families) who have bequeathed their bodies for the purposes of scientific research. It is these deceased who truly make the world a better place for the living. Cadaveric research is crucial in the field of biomechanics.

Appreciation is in order to the various sponsors of my research - three of which include the Japan Automobile Manufacturer’s Association (JAMA), Inc., Mercury Marine Corporation, and Outboard Marine Corporation. There are other sponsors to thank, but they must remain unnamed because of proprietary and contractual reasons.

I would like to express extraordinary thanks to my father, Dr. Tom Kress, and my major professor, Dr. John Snider. My dad is beyond compare with respect to his gift to me as an ideal father and incredible teacher throughout my life. It is hard to express my gratitude to Dr. Snider for all that he has done. I am fortunate to have such a friend, mentor, and second father-figure.

Many thanks to my mother too. She is the perfect mom and perfect person. Words could never do her justice!

I would like to mention and thank my brother, Reid, and sister, Wendy, for their constant support and encouragement throughout my life. They are the best siblings a person could ever have. My family support circle is fantastic - including Ann and all of my nieces and nephews.

Appreciation is also in order for my other committee members (I have already mentioned the Chairman, Dr. John Snider). Dr. John Hungerford, Dr. Jack Wasserman, and Dr. Milt Bailey gave valued time and comments and provided me with an enjoyable experience in completing my dissertation. Dr. Hungerford and his wife, Ruth, are super people who are both a pleasure to be around. I have always found a knowledgeable teacher and great friend in Dr. Wasserman and was fortunate enough to have him as my first major professor (i.e., for my Master's). My thanks go out to Dr. Bailey too - he's definitely a great guy.

Special thanks are in high order for my great buddy and work partner, David Porta. A person could not have a better friend than David or his wonderful wife, Nancy. Their daughter, Layne, is a shining example of the success of a good gene pool. David is an incredible research partner, and one major side benefit of knowing him is that he has a stupendous knack for teaching. This has proven invaluable to me when it comes to anatomy! Anyway, David's contributions to this dissertation and to me as a friend are countless and treasurable. Thanks for everything.

Next, I would like to thank a very special person, Cherie Alexander. After recently doing one of her many unselfish acts, she asked me, "Am I your favorite student now?" She is much more than a student and I hope she knows that. Cherie helps me in many ways and I could not begin to thank her enough. I

think she is an awesome person. She has a heart of gold and will always mean a great deal to me.

So many “thank yous” are in order for so many people: Dr. Hal Aikens for his continued support and professional attitude toward me during my Ph.D. work and employment in the Industrial Engineering (IE) Department; Dr. James Bontadelli, for his professionalism and demeanor with regard to the operations of the graduate program in IE; my long-time (and still) best friend, Billy Smiddy, for always being there for everything; thanks to Cheryl and the girls, too; thank you to Ann Lacava for being her usual helpful, friendly self; to Carl Worley for being “the greatest” to me and my family in so many ways; and to Adam and Julie Baranowski, Mollie Parris, and Stephen Duma for their contributions. I should also mention my good friend, Dave Halstead, for his sacrifices during the crunch hours of document preparation; and, of extreme importance are three fantastic people who make my life so much easier and my day-to-day so much more enjoyable - Donna Bodenheimer, Linda Chatham, and Karen Homes. I think the world of these three ladies and they are all excellent at their jobs.

My final “thank you” is reserved for Paige Rose. I have not even known her for a year, yet I feel as if I have been her friend forever. She has been a true inspiration during the final phases of the Ph.D. process. Thanks for being the wonderful person that you are and for your constant thoughtfulness.

## ABSTRACT

The research reported on in this dissertation has been systematically developed through a series of interrelated studies and experiments. The purpose has been to understand and characterize the effects of severe impact loading on the human body that results from accidents involving automobiles, motorcycles, boats, other vehicles, pedestrians, swimmers, et cetera. Previous work in this arena has relied strongly on simulations of human body anatomy, has focused on the microscopic mechanical properties of bone and soft tissue, or has resorted to analytical modeling.

Literature regarding mechanical properties of human tissue is plentiful. The experimental results in comparison among researchers are often quite variable, probably due to the complexity and diversity of the hard and soft materials that compose the human body. The majority of the research involves mechanical properties of human and animal bones and rarely is a full intact bone or specimen used for testing purposes. Instead, small cube samples are usually tested under static conditions. One reason for the widespread use of small cubes is their ease of use in material testing. The mechanical properties, however, of a full intact bone and/or intact specimen are much different than those found in a small cube section of bone or a dissected soft tissue part. This is due to the anisotropic and viscoelastic nature of these materials. When bone is combined with the various soft tissue components (muscles, tendons, ligaments, vessels, nerves, fascia, fat, skin, et cetera), a “black box” complex

composite structure is created that needs to be characterized as a “material” of its own.

Hence, more realistic data is needed about impact trauma effects on the human body. This research helps “bridge-the-gap” to this previous research through the use of various intact cadaveric specimens. The approach has been to develop a unique impact biomechanics laboratory, an air bag research laboratory, and various other testing apparatuses. In addition, existing facilities such as a drop tower, standard structural mechanical test equipment, and, in one instance, a specialized marine research facility were used when appropriate.

This research focuses on macroscopic effects of impact loading and includes: impact loading of human legs and tibias, impact behavior of thighs and femurs, comparison of embalmed versus unembalmed specimens, fracture patterns of long bones, impact response of the frontal bone and face, and response of the spine. The study also includes evaluation of the air bag as a protective device and evaluation of a particular cage guard design for boat propellers as a safety device.

Reduction or prevention of impact injury through design of protective devices/safer environments requires certain biomechanical information. This includes a characterization of how the body region of interest responds to impact forces in terms of mechanical parameters such as force-time histories of impact, accelerations/decelerations, and deformations in the tissue structures. Also, mechanisms by which the tissues fail, mechanical parameters by which they

respond, and the values of the injury criteria are important results in impact biomechanics research. These “biomechanical behaviors” and “injury characterizations” are the essence of the different parts of this dissertation.

## TABLE OF CONTENTS

### PART 1: INTRODUCTION

Background and Overview.....	2
Objectives .....	4
Previous Work of Others .....	9
Introductory Statement.....	9
Impact Biomechanics .....	11
Mechanical Properties of Bone .....	12
Major Conclusions .....	18
General Recommendations .....	24
Bibliography .....	26

### PART 2: IMPACT RESPONSE OF THE LEG AND TIBIA

Abstract.....	34
Introduction .....	34
Experimental Approach .....	35
Experimental Results .....	39
Discussion .....	51
Bibliography .....	53

### PART 3: GENERAL IMPACT BEHAVIOR OF THIGHS AND FEMURS

Abstract.....	55
Introduction .....	56
Materials and Methods .....	56
Results.....	60
Discussion .....	61
Conclusions .....	63

### PART 4: IMPACT RESPONSE OF THE FEMUR

Abstract.....	65
Introduction .....	66
Methodology .....	67
Results and Discussion.....	75
Conclusions .....	84
Bibliography .....	89



## **PART 5: AN IMPACT RESPONSE COMPARISON OF UNEMBALMED VS. EMBALMED LEGS**

Abstract.....	91
Introduction .....	92
Objective.....	94
Methodology .....	95
Results .....	101
Discussion .....	106

## **PART 6: FRACTURE PATTERNS OF LONG BONES**

Abstract.....	110
Introduction .....	110
Objective.....	113
Experimental Method .....	115
Results .....	121
Observations and Conclusions .....	122
Bibliography .....	127
Appendix.....	129

## **PART 7: IMPACT RESPONSE OF THE FRONTAL BONE AND FACE**

Abstract.....	133
Introduction .....	134
Materials and Methods .....	135
Results .....	139
Data Evaluation and Discussion .....	141
Conclusions .....	148
Remarks .....	148
Bibliography .....	149

## **PART 8: IMPACT RESPONSE OF THE SPINE**

Abstract.....	151
Introduction .....	151
Methodology .....	152
Results .....	153
Discussion .....	153
Bibliography .....	154

## **PART 9: BIOMECHANICAL EFFECTIVENESS OF A SAFETY DEVICE: THE AIR BAG**

Abstract.....	157
Introduction.....	158
Air Bag System .....	159
Review of Air Bag Induced Injuries.....	163
Discussion .....	171
Bibliography .....	172

## **PART 10: BIOMECHANICAL EFFECTIVENESS OF A SAFETY DEVICE: A BOAT MOTOR CAGE TYPE PROPELLER GUARD**

Abstract.....	179
Introduction.....	180
Methodology .....	181
Instrumentation and Specimen Evaluation .....	183
Results.....	184
Discussion and Recommendations.....	185

## **APPENDICES**

Appendix A: Research Overview of “Dynamic Response of the Human Leg to Impact Loading” .....	189
Appendix B: Velocity Response of Centrifuge from the Center for Research in Special Environments at the State University of New York .....	228
Appendix C: Post-test Dissection and X-ray Data .....	233
Appendix D: Dissection Measurements: Cortical Thickness and Weights .....	294
Appendix E: Characteristics of Tested Tibias .....	298
Appendix F: Cadaver Information .....	301
Appendix G: Addendum to Biomechanical Effectiveness of a Safety Device: A Boat Motor Cage-type Propeller Guard .....	304
Appendix H: Causal Mechanisms of Air Bag Induced Eye Injuries from Actual Cases .....	339
Vita.....	343

## LIST OF TABLES

TABLE	PAGE
<b>PART 1: INTRODUCTION</b>	
1. Historical Perspective of Some of the Pioneering Research of Impact Biomechanics .....	13
2. Technical Constants for Human Bones .....	16
3. Mechanical Properties of Wet Compact Human Bone (20-39 Yrs.) .....	17
4. Static Properties of Bone .....	18
<b>PART 2: IMPACT RESPONSE OF THE LEG AND TIBIA</b>	
1. Ultimate Failure Force for Embalmed Human Tibias Impacted with Pipe and Transducer at Varying Speeds.....	44
2. Ultimate Strength of the Embalmed Human Tibia Submitted to Anterior-Posterior Impact Loading .....	48
<b>PART 3: GENERAL IMPACT BEHAVIOR OF THIGHS AND FEMURS</b>	
1. Dynamic Response Characteristics of the Human Femur to Impact Loading .....	60
2. Dynamic Response Characteristics of the Human Thigh to Impact Loading .....	61
<b>PART 4: IMPACT RESPONSE OF THE FEMUR</b>	
1. Types of Fractures Occurring in L-M Loaded Femurs .....	76
2. Types of Fractures Occurring in A-P Loaded Femurs.....	78
3. Independent Variables and Torque Data on Femurs Loaded in Torsion at Low Strain Rates.....	79
4. Independent Variables and Torque Data for Femurs Loaded in L-M Bending with Torsional Preload .....	80
5. Results from A-P Impact of Fresh Long Bones of Two Individuals .....	82
6. Summary of the Response Characteristics of the Human Femur.....	83
7. Some Calculated Dynamic Response Characteristics from Selected Data of the Human Femur .....	84

## **PART 5: AN IMPACT RESPONSE COMPARISON OF UNEMBALMED VS. EMBALMED LEGS**

1. Specimen Data .....	97
2. Test Data .....	101
3. Damage Summary (Dissection Results) .....	102

## **PART 6: FRACTURE PATTERNS OF HUMAN CADAVER LONG BONES**

1. Summary Data of the Dynamic Response Characteristics of Human Long Bones .....	130
--	-----

## **PART 7: IMPACT RESPONSE OF THE FRONTAL BONE AND FACE**

1. Cadaver Data and Test Measurements .....	139
2. Clinical Diagnoses from Axial and Coronal CT Scans .....	140
3. Calculated Energy Values .....	147

## **PART 8: IMPACT RESPONSE OF THE SPINE**

1. Experimental Matrix .....	153
2. Primary Injury Results .....	153

## **PART 9: BIOMECHANICAL EFFECTIVENESS OF A SAFETY DEVICE: THE AIR BAG**

1. AIS Rating of Most Severe Injury as a Percentage of Drivers in Each Category of Restraint.....	165
2. Most Severely Injured Body Region as a Percentage of Drivers in Each Category of Restraint.....	165
3. Distribution of Individual Injuries Sustained by Belted Drivers in Collisions Which Resulted in the Deployment of an Air Bag System .....	166
4. Type and Location of Occupant Injuries Caused by Air Bags.....	167
5. Characterization of Air Bag Induced Injuries.....	168
6. Suggested Causation of Some Eye Injuries Related to Air Bags .....	169

**PART 10: BIOMECHANICAL EFFECTIVENESS OF A SAFETY DEVICE:  
A BOAT MOTOR CAGE-TYPE PROPELLER GUARD**

1. Test Conditions and Resultant Fractures.....	182
---	-----

## LIST OF FIGURES

FIGURE	PAGE
<b>PART 1: INTRODUCTION</b>	
1. A systems engineering approach to impact biomechanics .....	6
<b>PART 2: IMPACT RESPONSE OF THE LEG AND TIBIA</b>	
1. Idealized cross-sectional view of the human tibia .....	47
2. Ultimate failure force versus maximum bending stress for nine embalmed human tibias .....	48
3. Ultimate failure force versus energy absorption capacity for nine embalmed human tibias .....	50
4. Ultimate failure force versus average cortex thickness for nine embalmed human tibias .....	51
<b>PART 3: GENERAL IMPACT BEHAVIOR OF THE THIGHS AND FEMURS</b>	
1. Test set-up for axial (or longitudinal) impact of intact human cadaver thighs .....	59
2. Lateral x-ray view of the comminuted knee .....	62
<b>PART 4: IMPACT RESPONSE OF THE FEMUR</b>	
1. Sample force-time plot produced by crash simulator during impact .....	69
2. Diagram of axially loaded femur showing cross-sections of stress calculation: S = shaft, T = trochanter, N = neck .....	81
<b>PART 5: AN IMPACT RESPONSE COMPARISON OF UNEMBALMED VS. EMBALMED LEGS</b>	
1. Test set-up .....	99
2. Embalmed leg 308L .....	104
3. Unembalmed leg 301R .....	104
4. Sample force plots (specimens 301Ru and 301Le) .....	105
5. Impact resulting in no fracture .....	108

## **PART 6: FRACTURE PATTERNS OF HUMAN CADAVER LONG BONES**

1. Fracture patterns .....	114
2. Wheeled cart set-up .....	117
3. Sketch showing “swinging pipe” approach .....	117
4. Photographs of actual test specimens showing fracture patterns .....	118
5. Fracture pattern from impacts using apparatus in figure 2 .....	119
6. Fracture patterns from impacts using apparatus in figure 3 .....	120
7. Fractured bone after special treatment showing tensile wedge stress fractures .....	127
8. Relationship between torsional loading direction and resulting spiral fracture direction .....	127

## **PART 7: IMPACT RESPONSE OF THE FRONTAL BONE AND FACE**

1. Mounting of head .....	138
2. Rotational movement of impacted head .....	143
3. Translational movement of impacted head .....	143
4. Force-time plot of test 8a: non-fracture .....	145
5. Force-time plot of test 8c: fracture .....	145

## **PART 9: BIOMECHANICAL EFFECTIVENESS OF A SAFETY DEVICE: THE AIR BAG**

1. Example of typical timeline for air bag deployment process and driver movement .....	160
--	-----

## **PART 10: BIOMECHANICAL EFFECTIVENESS OF A SAFETY DEVICE: A BOAT MOTOR CAGE-TYPE PROPELLER GUARD**

1. Photograph of cage-type guard mounted on propeller in which the forward direction of travel for the boat is to the right .....	181
--	-----

**PART 1**  
**INTRODUCTION**



## **BACKGROUND AND OVERVIEW**

A wide range of research projects have been conducted over the past decade that have had impact biomechanics and human safety as their central themes. A primary reason for these projects was to better understand biomechanics from the viewpoint of human tolerances, capabilities, and limitations. Important to this understanding is the structural characterization of the human body and its individual components.

Specifically, multiple experimental studies were designed and carried out in the attempt to address some important biomechanical and safety objectives. Significant progress includes the design and installation of state-of-the-art impact testing laboratories; the completion of significant impact tests using human legs, animal legs, and simulated leg structures; and development of a basic understanding of the response of the human leg to impact loading. Other contributions include biological and structural material testing, testing of various intact human body parts, and evaluation of an alternative leg impact response measurement system.

One long-term research program titled “Dynamic Response of the Human leg to Impact Loading” intended to describe and quantify the dynamic response of the human leg to impact loading such as encountered when a pedestrian or cyclist is struck by an automobile. A research overview written during the project is presented in Appendix A. The resulting information is valuable as a guide for designing safer vehicles and protective systems. Several experimental protocols

yielded interesting results relating to the impact response of the human leg and its various bony components.

Another research program sponsored by two major outboard motor corporations, examined human trauma resulting from contact with outboard boat motors. An objective of the study was to evaluate the effectiveness of a propeller cage as a protective device. The tests utilized a unique integration of human cadaver legs and upper-body dummy components.

In conjunction with a large automobile corporation, the biomechanical effectiveness of the air bag as a safety device was also evaluated. This project involved a thorough review of air bag design to develop a comprehensive understanding of the restraint system and its risk factors. Information was also collected on the clinical aspects of actual cases. This has afforded some information important on the specific causal mechanisms of injuries from air bags.

A variety of other biomechanical-related studies have been performed, but for the purposes of this dissertation, discussion will be limited to the above-mentioned work and a couple of other experimental efforts: one involves impact response of the frontal bone and face and the other involves the spine.

Immediately following this part (i.e. part 1) of the dissertation, there will be nine more parts and the appendices. Parts 2-6 are all “modules” that represent experimental studies concerning the human leg and its various components. Each module has certain objectives that are addressed. Part 7 is the

presentation about the impact response of the frontal bone and face, and part 8 is the study about the spine's impact behavior. The remaining two parts, 9 and 10, are the sections that discuss the biomechanical effectiveness of two different safety devices: the air bag and a boat-motor cage-type propeller guard.

## **OBJECTIVES**

The understanding of the relationships between engineering aspects of accidents and anatomical damage to the human body is one aspect of biomechanics. Applied forces and their distributions need to be assessed as they relate to human injury. The field of biomechanics and understanding injury and trauma involves applying engineering principles, primarily elastic/plastic structural mechanical equations and Newton's Law, to determine forces and their distributions as they pertain to the human body's responses. Consequently, it is extremely important to gather as much data as possible relating impact inputs to their respective anatomical outputs as evaluation of product design and development of protective schemes proceed. An underlying purpose of the research efforts presented in this dissertation has been to study the human body's response to impact loading. Responses of the human body (failure modes and injuries) depend on loading profiles that cause various relative motions and internal forces/stresses within the human body. These failure modes and injuries also depend on the resultant rates of changes in velocities

(accelerations/decelerations) to the different parts of the body (e.g. joints and visceral organs).

It is important that research proceeds in the area of impact biomechanics, and that discussions are presented in such a way to document input profiles with their respective injury results. Proceeding in this manner will help contribute to the top-level objectives of the field of impact biomechanics. Some of the top-level objectives are as follows: to have appropriate experimental capabilities for accident reconstruction purposes; to help develop and evaluate prosthetic designs; to be able to reduce impact injuries; to be able to reconstruct/understand accident conditions as indicated from the resultant injuries; to aid in design of protective gear to help prevent/mitigate injuries; and to aid in dummy design.

Figure 1 illustrates the interrelationships among various aspects of impact biomechanics research and indicates the role played by this work.

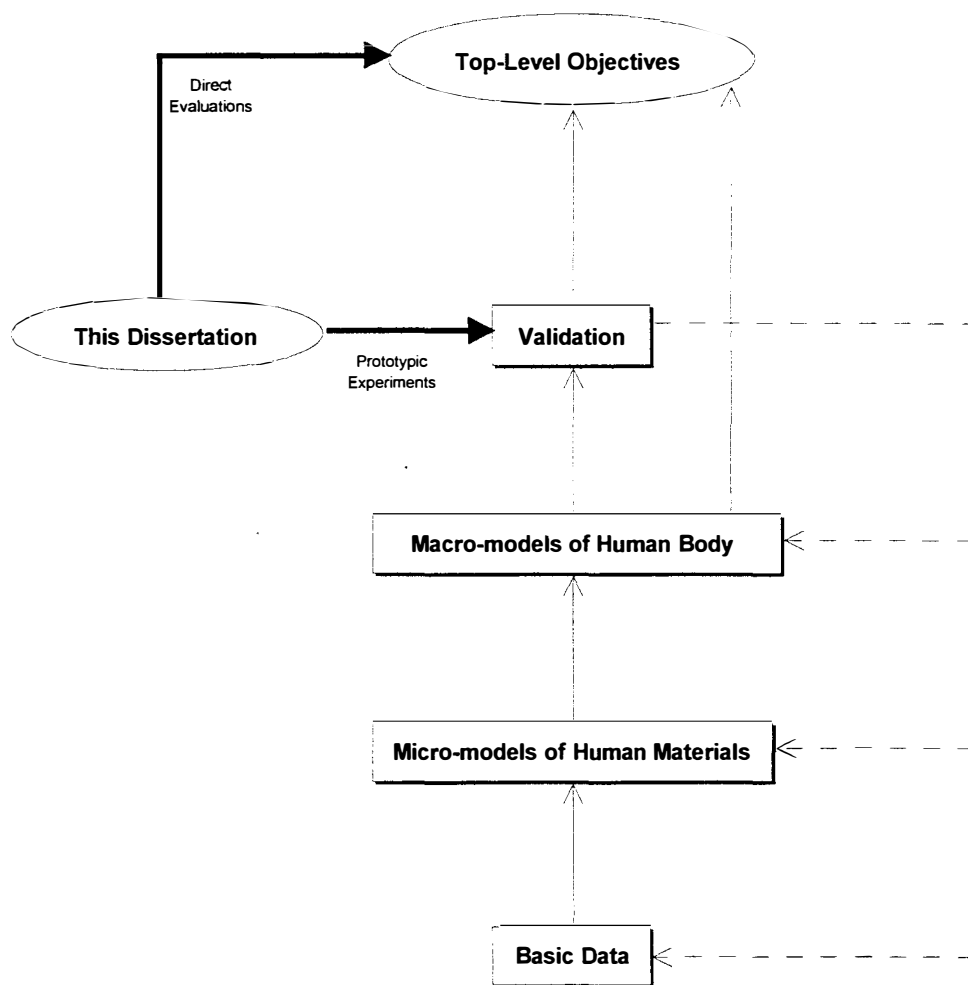


**FIGURE 1.** A systems engineering approach to impact biomechanics.

At the bottom level, there is a need for basic biomechanical structural data for the components of the human body. These consist of fundamental properties of bone, muscle, ligament, tendon, and other tissues (e.g. failure strength of bone in compression, tension, torsion, or bending; moduli of elasticity, etc.).

The fundamental data feed into micro-models for kinetic calculations of motions and accelerations at the finite element local level where the applied forces serve as initial and boundary conditions.

The resultant local kinetics are coupled to the macro-response of major body components such as legs, arms, torso, head, or the entire body as a whole. Macro-models for these are primarily based on Newton's Law relating mass, acceleration, and applied forces. The results feed back into the local kinetics for the redistribution of forces and the local responses. This coupling, along with the basic property data, ultimately determines the failure modes and the extent of injury.

Because any such combination of micro- and macro-models of the human body's response to applied forces can only be at some level of approximation to the real behavior, the results must be validated and the level of uncertainty determined. Such validation requires precisely the type of experiments reported on in this work. The results of such research serve to both validate calculational models and to provide feedback/guidance on how to develop such models in the first place. They give insight into the required degree of complexity and sophistication as well as point to the needs of basic data.

Such research can also provide direct resolution of some of the top-level objectives for impact biomechanics without need to resort to basic data and models. Examples of this would be the biomechanical effectiveness of safety devices research such as reported on in parts 9 and 10 of this dissertation.

It is believed that the impact failure of human tissue and the resulting extent of damage is describable in terms of classical elastic/plastic mechanics of non-isotropic composite materials. Consequently, a 3-D finite element computer representation of human structures could be developed in which the material properties are allowed to be dependent on strain rate, spatial position, and direction. Strain rate dependent properties (modules of elasticity, yield stress, ultimate stress, ultimate strain, Poisson's ratio) could be measured for real human samples oriented in the radial, circumferential, and axial directions. These properties could be input, initially uniformly, into the computer model which could be exercised under impact loading simulation conditions. The model results could then be compared with actual impact experiments on real complete human specimens in terms of energy absorbed to failure, extent of damage, stress/strain distributions, and displacements. The model property values and distributions could be adjusted to obtain a "best" correspondence between the model and the test results. The "validated" model could then be subjected to a sensitivity study to determine the most sensitive parameters and how their variations affect the calculated results. The results of this would be a set of desirable properties and their distributions for a physical model.

The impact loading experiments performed as part of the research for this dissertation provide response data of real complete human specimens in terms of force/time histories, extent of damage, energy absorbed to failure, displacements, et cetera.

Specifically, the first six parts concentrate on the response of the lower extremity to impact loading. Part 6 presents a comprehensive summary about the fracture patterns of human long bones including most of those tested for parts 1 through 5. For a good summary discussion with regard to the majority of the findings from the lower extremity research refer to the observations and conclusions section of Part 6 on page 122.

Parts 7 and 8 provide additional impact response data for other areas of the human body. Few studies have determined energy absorption values and tolerance levels from strikes to the supraorbital rims, frontal sinuses, and junctions of the nasal and ethmoid bones of human cadaver heads. Also, interesting dynamic effects and injury response mechanisms are presented with respect to dynamic axial loading of the human cadaver spine.

## **PREVIOUS WORK OF OTHERS**

### **Introductory Statement**

The field of biomechanics encompasses many different disciplines, some of which include engineering, physics, anatomy, and physiology. The knowledge of these disciplines as it is applied to studying trauma due to impact to the body



is referred to as impact biomechanics. Mechanical energy is transformed into failure of tissue structures by applied forces and induced stresses. Quantification of these stresses, determination of risk factors, and evaluation of safety alternatives require a knowledge of physical details of the impact conditions and the mechanical and dynamic behavior of the tissues involved. The goals of impact biomechanics are to understand how injuries occur and how they can be minimized through the application of that knowledge. Specifically, reduction or prevention of impact injury through design of protective devices/safer environments requires certain biomechanical information. The information includes a characterization of how the body region of interest responds to impact forces in terms of mechanical parameters such as force applications, accelerations/decelerations, and deformations in the tissue structures. Also, mechanisms by which the tissues fail, mechanical parameters by which they respond, and the values of the injury criteria are important elements in impact biomechanics research.

There has been significant research with regard to the material properties of human and animal tissue. Yamada (1973) was responsible for publishing much of the early work, yet these efforts involved slow-loading of the tissues and may not accurately define dynamic material properties (Kress, 1989). McElhaney (1966) is one of the few researchers to study dynamic material properties. Although he impacted animal tissues at higher velocities, he used small samples of tissues instead of whole bone or intact specimens. Also, large

changes occurred in velocity of the striking object during impact. This makes assessment of the actual forces imparted to the specimens difficult. So, there is a definite need for research/experimentation involving high-speed loading of whole bone or intact specimens in order to characterize the human's dynamic response and allow failure modes to be adequately understood and modeled. The research undertaken for this dissertation was intended to help fill this need.

### **Impact Biomechanics**

Research to understand ballistic impact has been documented by Werner Goldsmith (Goldsmith, 1960). The biomedical aspects of impact have also received intense attention (Aldman and Chapon, 1984), especially in the study of injuries obtained during automobile accidents (Melvin et al., 1975). The majority of this work has focused on injuries of the head and neck. The work has also emphasized human body dynamics resulting in both specialized computer codes and the development of anthropomorphic dummies for testing. The use of these dummies has been limited, however, because of the lack of impact failure simulation. The literature on the determination of human and animal tissue material properties is extensive and well summarized in several articles and books (e.g., see Yamada, 1970). Although most previous works obtain properties by slow loading, there has been significant work with impact loads (McElhaney, 1966; and others). Some inadequacies of previous works are that

complete bone and leg samples have not been used and the impact and failure have occurred with significant change of the velocity of the striking object.

Table 1 provides a historical perspective of some of the pioneering research of impact biomechanics.

### **Mechanical Properties Of Bone**

The mechanical properties of bone are well discussed in the literature. Researchers Yamada (1970), Evans (1973) and McElhaney (1966) pioneered the study of mechanical properties of bone. The data have been periodically updated by Currey (1960), Reilly and Burnstein (1974), Carter and Spengler (1978), Fung (1981), Van Buskirk and Ashman (1989), and Cowin et al. (1987). A thorough and detailed discussion of the mechanical properties of bone is given in Bone Mechanics by Cowin (1989).

A good characterization of leg bone properties is essential to the development of a synthetic bone for impact studies. If leg bone properties were completely characterized for both static and dynamic conditions, then a polymer or some other material could be “designed” to have those properties. “Designed” in this context means that the synthetic bone material properties can be altered by using blends and fillers so that the properties match those of real bone.

**TABLE 1. Historical Perspective of Some of the Pioneering Research of Impact Biomechanics**

Date	Scientist	Contribution
1940's	Hugh De Haven	Provided first insights into human tolerance of crash loads; established the Automotive Crash Injury Research Programme at Cornell University
1941 1946	Sir Hugh Cairns	Helmet studies (Army and motorcycle)
1942	De Haven	Published a paper establishing the groundwork for whole-body tolerance
1942	John Lane (Australia)	Noted that aircraft should be certified in two ways - airworthy and crashworthy (this gave birth to the term "crashworthiness")
1945	Gurdjian	Cadaveric studies
1951	Stapp	Volunteer studies
1954	Mathewson and Severy	Dummy testing
By mid-1950's	Various contributors	A body of knowledge existed that gave insights into general frequencies of traffic collisions and injuries, and a means whereby forces and accelerations applied to car occupants could be modified
1960	Sheldon	Paper entitled "On the Natural History of Falls in Old Age"
1962	Aldman (Sweden)	Anatomical positioning for seatbelt analysis complemented with dynamic property data
1962	Snyder	Tibia testing (4448 N)
1962-1963	Ford Motor Company Garrett Huelke Gissane and Bull	Examined the real world of collisions
1966	William Haddon, Director	Establishment of the National Highway Safety Bureau by an Act of Congress
1966	Young	Cadaver leg testing (6543 N)
1966	Goldsmith	Stress-strain behavior during impact
1967	Frank and Mather	Tibias of younger people and males were more resistant to fracture than tibias of older people and females; 75 N-m (using 4.22 m/s falling weight broke the tibia in 50% of tests)
1969	Mackey	Collision aspects of road accidents
1973	Kramer, Burow & Heger	Tested 209 cadavers (most > 60 years of age) for "bumper type" tibial impact velocity of 6.7 m/s produced fracture in 50% of tests
1960's 1970's 1980's 1990's	Various contributors	Researchers produced voluminous literature on various human kinematics under impact conditions; very important information regarding the composition and mechanical properties of bone was also provided

In biological terms, bone is described as a connective tissue, an aggregation of similarly specialized cells united in the performance of a particular function. In bioengineering terms, bone can be viewed as a nonhomogeneous anisotropic composite. In the literature, bone is often divided into two categories, especially with reference to its mechanical properties. These categories are dehydrated and hydrated, and are often referred to as old and fresh, or dry and wet. In general, dry bone is brittle and fails at a strain of approximately 0.4%; wet bone fails at a strain of about 1.2%. Wet, of course, is of most interest to this dissertation because it best represents the *in vivo* bone.

The volumetric composition of bone tissue can be divided into almost equal thirds: water, minerals, and collagenous matrix. Even among like bones from human to human, this composition can vary. When considering human leg bones, variations exist with age, sex, and whether or not the individual has experienced bone disease. About two-thirds of the weight of bone, or half its volume, is inorganic material with the composition of hydroxyapatite, present as tiny elongated crystals approximately 200 Å long with an average cross-section of 2500 Å<sup>2</sup>. The remainder of the bone is collagen fibers. Water and salt significantly affect the mechanical properties. The role of water in bone is somewhat obscure as discussed by Timmins and Wall (1977); however, variation in water content with age is fairly well documented, so a correlation might be drawn between water content and ductility.

Bone has been assumed to be transversely isotropic (Lang, 1970; Reilly et al., 1974; Reilly et al., 1975; Yoon and Katz, 1976) and also to be an orthotropic material (Van Buskirk et al., 1981; Ashman et al., 1984; Knetts and Malmeisters, 1977). In order to obtain technical constants for human bone, researchers have used two methods: 1) ultrasound, in which the measured velocities are used to determine elastic coefficients and technical constants are then found by matrix inversion, and 2) standard testing in which load machines are used to make direct measurements. Table 2 (Cowin, 1989) presents the technical constants for human bone measured by various investigators. The material symmetry generally assumed is that of transverse isotropy (TI) or orthotropy (ORTH).

An important observation is that stiffness in the circumferential direction is always greater than the stiffness in the radial direction. Yanson et al. (1974), suggest that the lower stiffness in the radial direction is associated with the greater permeability in that direction. Blood flow is less in the circumferential direction as opposed to the radial direction; thus, for cortical tissue of long bones, an orthotropic assumption might be more accurate.

**TABLE 2. Technical Constants for Human Bones**

Group	Reilly and Burnstein	Yoon and Katz	Knets et al.	Ashman et al.
Bone	Femur	Femur	Tibia	Femur
Symmetry	TI	TI	ORTH	ORTH
Method	M	U	M	U
$E_1$ (GPa)	11.5	18.8	6.91	12.0
$E_2$ (GPa)	11.5	18.8	8.51	13.4
$E_3$ (GPa)	17.0	27.4	18.4	20.0
$G_{12}$ (GPa)	3.6 <sup>a</sup>	7.17	2.41	4.53
$G_{13}$ (GPa)	3.3	8.71	3.56	5.61
$G_{23}$ (GPa)	3.3	8.71	4.91	6.23
$\nu_{12}$	0.58	0.312	0.49	0.376
$\nu_{13}$	0.31 <sup>a</sup>	0.193	0.12	0.222
$\nu_{23}$	0.31 <sup>a</sup>	0.193	0.14	0.235
$\nu_{21}$	0.58	0.312	0.62	0.422
$\nu_{31}$	0.46	0.281	0.32	0.371
$\nu_{32}$	0.46	0.281	0.31	0.350

Note: E = Modulus of Elasticity

G = Modulus of Rigidity

$\nu$  = Poisson's Ratio

Note: The "three" direction is coincident with the long axis of the bone; the "one" and "two" directions are radial and circumferential, respectively. Method U is ultrasound and method M is standard machine testing. TI, transverse isotropy; ORTH, orthotropy.

<sup>a</sup>not measured

Source: Cowin, S.C. Bone Mechanics. Boca Raton, Florida: CRC Press, Inc., 1989.

Viscoelasticity, the effect of strain rate on the stress-strain curve, is important with respect to bone response to impact loadings. McElhaney (1966) indicated that the embalmed human femur in compression is stiffer and stronger at higher strain rates. Carter and Hayes (1976) found that both strength and modulus of elasticity were approximately proportional to the 0.06 power of strain rate.

Some mechanical properties of human leg bones are presented in Table 3 (data taken from Yamada, 1970 and Fung, 1981).

Generally, it is known that the strength of bone varies with the age and sex of the human, the location of the bone, the orientation of the load, the strain rate, and the specimen condition (dry or wet). The higher strain rate effect may be especially significant, with higher ultimate strengths being obtained at higher strain rates. Another note is that the strength and modulus of elasticity of spongy bone are much smaller than those of compact bone (Yamada, 1970, presents human vertebrae data as support).

**TABLE 3. Mechanical Properties of Wet Compact Human Bone (20-39 Yrs.)**

Mechanical Property	Value
Ultimate Tensile Strength (Femur)	124 MPa
Ultimate Tensile Strength (Tibia)	174 MPa
Ultimate Percentage Elongation (Femur)	1.41
Ultimate Percentage Elongation (Tibia)	1.50
Modulus of Elasticity in Tension (Femur)	17.6 GPa
Modulus of Elasticity in Tension (Tibia)	18.4 GPa
Ultimate Compressive Strength (Femur)	170 MPa
Ultimate Percentage Contraction (Femur)	1.85
Ultimate Shear Strength (Femur)	54 MPa
Torsional Modulus of Elasticity (Femur)	3.2 GPa

Sources: Yamada, H. In F.G. Evans (ed.), Strength of Biological Materials. Baltimore: Williams and Wilkins, 1970. Fung, Y.C. Biomechanics: Mechanical Properties of Living Tissue. New York: Springer-Verlag (1981).

The literature provides a basis for comparison of real bone properties to those of simulant bone. Motoshima (1959) tested long wet leg bones of 13 fresh



cadavers ranging from 20 to 83 years old. Some of Motoshima's results are presented in Table 4 and will serve as an excellent static comparison in the search for a bone simulant.

**TABLE 4. Static Properties of Bone**

Mechanical Property	Value
$E_t$ , Modulus of Elasticity (tension)	$1.0 \times 10^{10}$ Pa
$\sigma_{yt}$ , Yield Stress (tension)	$1.3 \times 10^8$ Pa
$\sigma_{yb}$ , Yield Stress (bending)	$4.3 \times 10^7$ Pa
$\sigma_{ub}$ , Ultimate Bending Stress	$5.9 \times 10^8$ Pa

Source: Motoshima, T. "Studies on the Strength for Bending of Human Long Extremity Bones." The 64<sup>th</sup> Japan Anatomy Conference, Kyoto, Japan: The Kyoto Prefectural University of Medicine, 1959.

## MAJOR CONCLUSIONS

Parts 2 through 10 of this dissertation each contain subsections associated with "discussion" or "conclusions." Significant detail about the different findings and observations from the various research efforts are in these subsections. The following remarks are intended to serve as an executive summary of the majority of these conclusions and observations. Background details, methodology, and results that substantiate these remarks are contained throughout the body of the dissertation.

(1) It appears reasonable to combine the data from varying loading directions (A-P, P-A, L-M, AND M-L). In other words, the resultant fracture types seem to be extremely similar regardless of the direction of the impact.

(2) Intact leg impacts promote more comminution type fractures than bare bone impacts. It is believed that the impactor continues to impart forces and energy on the intact leg bones because of the containment provided by the surrounding soft tissue. Also, the inertial constraints of the foot mass and upper leg/body components cause a wrap-around effect that results in increased comminution as the specimen stretches around the impactor.

(3) Embalmed intact leg fractures exhibit greater comminution than unembalmed. The embalment process causes significant increase in stiffness of the soft tissue containment.

(4) It is reasonable to assume that transverse, oblique, segmental, and tension wedge fractures are all just different manifestations of tensile failure. Even high comminution fractures probably originate as tensile fractures but get further fragmented due to other influences.

(5) Compressive wedge type failures are extremely rare in long bones. This is expected as human bone is approximately 1.5 times stronger in compression than it is in tension.

(6) Although the femur is stronger and has a different cross-sectional geometric shape, its fracture patterns as a result of transverse loading are generally the same as those for the tibia.

(7) The most common fracture pattern is the tension wedge and is followed closely by the oblique fracture.

(8) Transverse and oblique fractures generally have jagged edges.

(9) Spiral fractures have the “smoothest” break edge, perhaps indicating that it follows some pre-existing engineering structural line. Wedge fracture lines tend to follow curved paths similar to the spiral fracture path.

(10) Tensile wedge fractures clearly originate at a location directly opposite of the point of impact and the wedge segment radiates back through the bone initially forming a  $90^\circ$  vertex angle (propagates  $45^\circ$  from the horizontal both superiorly and inferiorly) indicating possible transition along the lines of principal stress (transition from purely tensile to shear).

(11) The only bare bones with high comminution were those that were extremely osteoporotic or loaded axially at high speeds (e.g. a knee impact).

(12) Because of the high incidence of tension wedges, this fracture pattern can be used as an indicator of the direction of impact.

(13) Many oblique fractures also have tensile wedge patterns that are not detected by x-ray.

(14) The fracture patterns of low speed impacts (1.2 m/s) are very similar to those of high speed (7.5 m/s) with the exception that high comminution is not observed in the low speed fractures. This is somewhat of a unique observation because it has been commonly thought that the butterfly wedge results only from high speed impacts.

(15) Spiral fractures only appear when the bones are subjected to torsional loads. Furthermore, if long bones are loaded in pure torsion then spiral

fractures will result 100% of the time.

(16) Approximately two out of three spiral fractures of the femur were located at the proximal third.

(17) A torsional loading direction is herein defined as being “clockwise” if the top is held and the bottom is twisted in the clockwise direction (looking up). Contrary to popular belief, a clockwise torsional load will result in the spiral portion of the fracture being oriented like a right-hand screw. This interesting observed fracture behavior is indicative that the bone is failing in tension rather than shear when loaded in torsion.

(18) Segmental fractures are much more prevalent in femurs than tibias.

(19) Transverse loading to the tibia/fibula most often results in a segmental fracture of the fibula.

(20) Analysis of stored computer images of selected bones provided no evidence of the presence of surface stress risers that could have caused fracture or crack propagation.

(21) Fractures resulting from 7.5 m/s (16.8 mph) impacts can cause serious soft tissue injuries.

(22) There is no noticeable differences in injury severity associated with cylindrical impactor radii varying from 1-inch to 4-inches.

(23) Comminuted fractures can occur without entrapment (crushing injury). For 7.5 m/s impacts of intact legs, the inertial restraint of the tibia from the upper thigh and foot is sufficient enough to result in comminuted fractures

without any additional support. For low speed tests (static and 1.2 m/s), simply-supported legs have resultant bone fractures comparable to inertially supported legs at high speeds.

(24) Age changes in bone can exist, although these changes do not seem to significantly affect fracture patterns (except when compared to babies or small infants). Such changes can include mineral mass, volume, density, and mechanical properties. During dynamic loading situations when ultimate strength is exceeded, bone basically fails as a brittle material (young or old). So, the fractured patterns do not vary too much, unless severe osteoporotic changes have occurred. Such osteoporosis can increase the incidence of high comminution (shatter).

(25) For impact loading of the long bone shaft, arthritic changes did not seem to affect the resultant fracture pattern of the entire bone. In other words, a fair supposition would be that arthritis only affects failure patterns when they involve joints.

(26) Impact to the supraorbital rims, given the other methodological conditions, at speeds near 7.2 m/s will almost always cause severe to critical injury.

(27) The occurrence of skeletal injury to the cranium and face is better indicated by the energy absorption value rather than the tolerance level. Energy accounts for the total time that force is applied, whereas tolerance level is only a peak force value at a specified time (at which the first fracture just begins).

(28) Forces that are transmitted through the spine and the resultant injuries of the spine are increased as specimen drop height and impact velocity are increased.

(29) The major mechanism of vertebral column injuries (i.e. the cervical, thoracic, lumbar, or sacral regions) is the inertial effects of the various masses of the human body. For example, cervical failure from axial loading through contact with the head results from inertial effects or momentum associated with the mass of the torso and the rest of the body. Another example would be whiplash - this injury occurs because of the inertial effects of the head mass.

(30) Air bags are an effective injury prevention device in that they reduce the number of resulting deaths, and mitigate major injuries. However, they are a relatively “new” design and can still “evolve.” The most significant factors associated with induced injuries are the absence of tethers on air bags, closeness to the air bag module or proximity to the steering wheel, and high velocity of deployment (high capacity inflator).

(31) The intent of this last “finding” is to provide general discussion about design issues associated with biomechanics and injury prevention. It is important to realize that injury prevention ideas are not always as simple as they may appear “on the surface.” Any time a protective product is created or the design of an existing system that interfaces with the human is changed for the purposes of injury reduction or prevention, many issues must be considered (mainly whole body effects or injuries). For example, increased leg protection

can be provided to a motorcyclist by wearing shin guards, however prevention of leg fracture may result in increased head injury. In short, expected resultant real-life impact injuries can be decreased to localized areas of the human body, but the “trade-off” often includes other body region injuries which could increase the seriousness of the whole-body damage. An interesting discussion about the safety effectiveness of a cage-type propeller guard is provided in Part 10 and Appendix G of this dissertation. This is another example of a proposed product that may appear (“on the surface”) to be a good idea, but the results of biomechanical experimentation reveal that this is not case. It is therefore apparent that, in order to completely understand the effectiveness of new product designs associated with protection or with human interfacing, appropriate biomechanical testing and analyses are needed.

## **GENERAL RECOMMENDATIONS**

The body of this dissertation contains significant discussion about possible future work. The following is a list of recommended items for consideration with regard to continued research in the area of impact biomechanics:

- (1) development of the micro- and macro-models discussed earlier in this part of the dissertation;
- (2) additional impact research on the arm, thorax, pelvic, and shoulder;

(3) more impact response research evaluating the effects on the major internal organs;

(4) additional impact experimentation on the skull with loads being at different locations;

(5) more studies to understand closed-head injuries (e.g. tolerance levels associated with diffuse axonal injury);

(6) additional validation studies with full cadavers in simulated accidents;

(7) continued development of improved artificial frangible bone surrogates along with other human tissue surrogates;

(8) development of improved dummy designs of the human body;

(9) research to develop “smarter” air bags in which the vehicle is equipped with diagnostics/instrumentation that can detect seat position, occupant anthropometrics, and belt use, so that inflation dynamics and tether length can be “customized”;

(10) improvement of underwater-related testing procedures and additional experimentation;

(11) testing to improve the fundamental (basic) property database; and

(12) emphasis on the acceptance of biomechanical testing/evaluations for the purposes of understanding the efficacy of product designs.



## BIBLIOGRAPHY

- Abendschein, W. and G.W. Hyatt. "Ultrasonic and Selected Properties of Bone." Relat. Res. 69(1970).
- Aldman, Bertil, "Living Tissue Properties." The Biomechanics of Impact Trauma. Amsterdam: Elsevier Science Publishers B.V., 1984.
- Aldman, Bertil, ed., and Andre Chapon, ed. The Biomechanics of Impact Trauma. Amsterdam, Netherlands: Elsevier Science Publishers B.V., 1984.
- Ambarder, J.D. and C.D. Ferris "A Simple Technique for Measuring Certain Elastic Moduli in Bone." Biomed Sci. Instr. 12(1976).
- Ashman, R.B. "Ultrasonic Determination of the Elastic Properties of Cortical Bone: Techniques and Limitations." Ph.D. Dissertation. Tulane University, New Orleans: 1982.
- Ashman, R.B., S. C. Cowin, W.C. Van Buskirk, and J.C. Rice. "A Continuous Wave Technique for the Measurement of the Elastic Properties of Bone." J. Biomechan. 17 (1984).
- Ashman, R.B., M. Donofrio, S.C. Cowin and W.C. Van Buskirk. "Postmortem Changes in the Elastic Properties of Bone." Proc. 28th Annu. New Orleans: 1982.
- Beer, P. Ferdinand, and Russell E. Johnston Jr. Mechanics of Materials. New York, NY: McGraw-Hill, Inc., 1981.
- Bickley, E. Harmon, et al. "An Improved Method for the Preservation of Teaching Specimens." Arch. Pathol. Lab Med., 105(1981).
- Bensusan, J.S., D.T. Davy, K.G. Heiple and P.J. Verdin. "Tensile, Compressive and Torsional Testing of Cancellous Bone." Trans. Orthop. Res. Society. 8(1983).
- Blitz, R.M and E.D. Pellegrino. "The Chemical Anatomy of Bone." J. Bone Jt. Surg. 51A(1969).
- Bonfield, W. and A.E. Tully. "Ultrasonic Analysis of Young's Modulus of Cortical Bone." J. Biomed. Eng. 4(1982).
- Burris, C.L. "A Correlation of Quasistatic and Ultrasonic Measurements of the Elastic Properties of Cortical Bone." Ph.D. Dissertation. Tulane University, New Orleans: May, 1983.
- Carter, D.R., W.E. Caler, D.M. Spengler and V.H. Fawkel. "Uniaxial Fatigue of Human Cortical Bone - The Influence of Tissue Physical Characteristics." J. Biomech. 14 (1986).
- Carter, D.R. and W.C. Hayes. "Bone Compressive Strength: The Influence of Density and Strain Rate." Science. 194(1976).
- Carter, D.R. and W.C. Hayes. "The Compressive Behavior of Bone as a Two-Phase Porous Structure." J. Bone Jt. Surg. 59A(1977).
- Carter, D.R., W.C. Hayes and D.J. Schurman. "Fatigue Life of Compact Bone: II. Effects of Microstructure and Density." J. Biomech. 9(1976).

- Carter, D.R., G.H. Schwab and D.M. Spengler. "Tensile Fracture of Cancellous Bone." Acta Orthop. 51(1980).
- Carter, D.R. and D.M. Spengler. "Mechanical Properties and Composition of Cortical Bone." Clin. Orthop. 135(1978).
- Cezayirlioglu, H., E. Bahnink, D.T. Davy and K.G. Heiple. "Anisotropic Yield Behavior of Bone Under Combined Axial Force and Torque." J. Biomech. 18(1985).
- Chapon, Andre. "Experimental Models in Biomechanics of Impacts." The Biomechanics of Impact Trauma. Amsterdam: Elsevier Science Publishers B.V., 1984.
- Christensen, R.M. Theory of Viscoelasticity. New York: Academic Press, 1971.
- Crowninshield, R.D. and M.H. Pope. "The Response of Compact Bone in Tension at Various Strain Rates." Ann. Biomed. Eng. 2(1974).
- Cowin, S.C. Bone Mechanics. Boca Raton, Florida: CRC Press, Inc., 1989.
- Cowin, S.C. et al. "The Properties of Bone" in Handbook of Bioengineering. Skalak, R. and S. Chien, Editors-in-Chief, McGraw-Hill, New York, NY: 1987.
- Cowin, S.C. "On the Strength Anisotropy of Bone and Wood." J. Appl. Mech. 46(1979).
- Crandell, S.H., N. Dahl and T.J. Lardner. An Introduction to the Mechanics of Solids (2 ed.). New York: McGraw-Hill, 1978.
- Currey, J.D. "Anelasticity of Inelastic Flow in Bone." J. Exp. Biol. 43(1965).
- Currey, J.D. "Difference in the Blood Supply of Bone of Different Histological Types." O.J. Microsc. Sci., 1960.
- Currey, J.D. "The Mechanical Consequences of Variation in the Mineral Content of Bone." J. Biomech. 2(1969).
- Currey, J.D. "The Relationship Between the Stiffness and the Mineral Content of Bone." J. Biomech. 2(1969).
- Currey, J.D. What is bone for? -- Property-function relationships in bone." In Mechanical Properties of Bone. S.C. Cowin (ed.) New York: ASME, 1981.
- Dally, James, W., et al. Instrumentation for Engineering Measurements. New York: John Wiley & Sons, Inc., 1984.
- Evans, F.G. Mechanical Properties of Bone. Charles C. Thomas, Springfield, Illinois: 1973.
- Evans, F. Gaynor, and Milton Lebow. "Regional Differences in Some of the Physical Properties of the Human Femur." J. Applied Physiol. 2(1951).
- Fung, Y.C. Biomechanics: Mechanical Properties of Living Tissues. New York: Springer-Verlag (1981).
- Galante, J., W. Rosker and R.D. Day. "Physical Properties of Trabecular Bone." Calif. Tiss. Res. 5(1970).
- Glimcher, M.J. "Composition, Structure and Organization of Bone and Other Mineralized Tissues and the Mechanisms of Calcification." Handbook of

- Physiology: Endocrinology. 7(1976).
- Goldsmith, Werner. Impact: The Theory and Physical Behaviour of Colliding Solids. Bungay, Suffolke, Great Britain: Richard Clay and Company, Ltd., 1960.
- Gong, J.K., J.S. Arnold and S.H. Cohn. "Composition of Trabecular and Cortical Bone." Anat. Rec. 149(1964).
- Hayes, M.A. and L.W. Morland. "The Response Functions of an Anisotropic Linear Viscoelastic Material." Trans. Soc. Theol. 13(1969)
- Henderson, N.J., et al. "Rigid Fixation and Myoplastic Techniques for the Salvage of Major Tibial Injuries." International Orthopaedics. Springer-Verlag: 1982.
- Hight, T.K. and J.F. Brandeau. "Mathematical Modeling of the Stress-Strain Rate Behavior of Bone Using the Ramberg-Osgood Equation." J. Biomech. 16(1983).
- Hirsch, Arthur, E. "The Tolerance of Man to Impact." Annals of the New York Academy of Sciences. 152(1968).
- Hodgson, M.S. and G.S. Nakamra. "Mechanical Impedence and Impact Response of the Human Cadaver Zygoma." J. Biomech. Great Britain: 1(1968).
- Huelke, Donald F., et al. "Bone Fractures Produced by High Velocity Impacts." Am. J. Annt. 1967.
- Huiskes, R. "On the Modeling of Long Bones in Structural Analysis." J. Biomech. 15(1982).
- Katoh, T., K. Sakamaki and T. Nakamura. "A New Method for Measurement of Bone Mineral Deposition Pattern - Using a Dual Energy Radiographic Densitometry Method in a Single Exposure." Bull. Tokyo Med. Dent. Univ. 28(1981).
- Kenedi, R.M., ed. Biomechanics and Related Bioengineering Topics. London: Pergamon Press Ltd., 1965.
- Kerr, S.A., K. Kouris, C.E., Webber and T.J. Kennett. "Coherent Scattering and the Assessment of Mineral Concentrations in Trabecular Bone." Phys. Med. Biol. 25(1980).
- King, William F., and Harold J. Mertz. Human Impact Response: Measurement and Simulation. New York, NY: Plenum Press, 1973.
- Kirby, J.S. "Impact Testing and Analysis." Engineering Science Preprints., Society of Engineering Sciences, Inc., 1987.
- Knets, I. and A. Malmeisters. "Deformability and Strength of Human Compact Bone Tissue." In G. Brankov (ed.), Mechanics of Biological Solids: Proceedings of the Euromech Colloquium 68. September, 1975.
- Kress, T.A. "Mechanical Behavior of Lower Limbs in Response to Impact Loading: Facility Deployment and Initial Results." Master's Thesis. University of Tennessee, Knoxville: 1989.
- Kress, T.A., et al. "Determination of Lower Limb Failure Modes and Tissue

- Damage by Impact Loading." Proc. of the VI International Cong. on Exp. Mech. Bethel, CT: The Society for Experimental Mechanics, Inc., 1(1988).
- Kress, T.A. and J.F. Wasserman. "Laboratory Experiment for the Evaluation of the Shear Modulus and the Maximum Shear Stress of Fresh, Dry, and Plastinized Canine Bone." Proc. of the 13th Annual Northeast Bioengineering Conf. New York, NY: IEEE, Inc., 2(1987).
- Kress, T.A. and J.F. Wasserman. "The Effects of Plastinization Process on Torsional Properties of Canine Bone." Developments in Theoretical and Applied Mechanics. Biloxi, MS: University of Mississippi Press, 14(1988).
- Krolner, B., S. Pors Nielsen, B. Lund, O.H. Sorensen and A. Chrenholdt. "Measurement of Bone Mineral Content (BMC) of the Lumbar Spine: I. Theory and Application of a New Two-Dimensional Dual Photon Attenuation Method." Scand. J. Clin. Lab. Invest. 40(1980).
- Lafferty, J.F. and P.V.V. Raju. "The Influence of Stress Frequency on the Fatigue Strength of Cortical Bone." J. Biomed. Eng. 101(1979).
- Lakes, R.S. and J.L. Katz. "Interrelationships Among the Viscoelastic Functions for Anisotropic Solids: Application to Calcified Tissues and Related Systems." J. Biomech. 7(1974).
- Lakes, R.S. and J.L. Katz. "Viscoelastic Properties of Wet Cortical Bone: III. A Non-Linear Constitutive Equation." J. Biomech. 12(1979).
- Lakes, R.S., J.L. Katz and S.S. Sternstein. "Viscoelastic Properties of Wet Cortical Bone: I. Torsional and Biaxial Studies." J. Biomech. 12(1979).
- Lang, S.B. "Ultrasonic Method for Measuring Elastic Coefficients of Bone and Results on Fresh and Dry Bovine Bones." IEEE Trans. Biomed. Eng. 17(1970).
- Leichter, I., S.Y. Margulies, A. Weinreb., J. Mizrahi, G.C. Robin, B. Conforty, M. Makin, and B. Bloch. "The Relationship Between Bone Density, Mineral Content and Mechanical Strength in the Femoral Neck." Clin. Orthop. 163(1982).
- Marino, A.A., R. O. Becker and C.H. Bachman. "Dielectric Determination of Bound Water of Bone." Phys. Med. Biol. 12(1967).
- Martens, M., et al. "Mechanical Behaviour of Femoral Bones in Bending Loading." J. Biomechanics. Great Britain: Pergammon Journals Ltd., 19(1986).
- Mather, B. Sherwood. "Observations on the Effects of Static and Impact Loading on the Human Femur." J. Biomechanics. Great Britain: Pergammon Press, 1968.
- McElhaney, J.H. "Dynamic Response of Bone and Muscle Tissue." J. Appl. Physiol. 21(1966).
- McElhaney, James. "Effect of Embalming on the Mechanical Properties of Beef Bone." J. Appl. Physiol., 1964.
- Melvin, J.W., et al. "Impact Response of the Lower Extremities." SAE Paper No.

751159. Nineteenth Stapp Car Crash Conference Proceedings. 1975.
- Modern Plastics Encyclopedia. New York, NY: McGraw-Hill Book Company, 1988.
- Motishima, T. "Studies on the Strength for Bending of Human Long Extremity Bones." The 64th Japan Anatomy Conference, Kyoto, Japan: The Kyoto Prefectural University of Medicine, 1959.
- Padgaonkar, A.J., et al. "A Three-Dimensional Mathematical Simulation of Pedestrian - Vehicle Impact with Experimental Verification." Journal of Biomechanical Engineering. 99(1977).
- Park, Joon Bu. Biomaterials Science and Engineering. New York: Plenum Press, 1984.
- Pelker, R.R. and S. Saha. "Stress Wave Propagation in Bone." J. Biomech. 16(1983).
- "Polyamide Plastics." Encyclopedia of Polymer Science and Technology: Plastics, Resins, Rubbers, Fibers. New York, NY: John Wiley & Sons, Inc. 10 (1969).
- Reilly, D.T. and A.H. Burnstein. "The Elastic and Ultimate Properties of Compact Bone Tissue." J. Biomech. 8(1975).
- Reilly, D.T. and A.H. Burnstein. "The Mechanical Properties of Cortical Bone." J. Bone Jt. Surg. 56A(1974).
- Reilly, D.T., A.H. Burnstein and V.H. Frankel. "The Elastic Modulus for Bone." J. Biomech. 7(1974),
- Rockwood, Charles A., and David P. Green. Fractures. 2 vols. Philadelphia: J. B. Lippincott Company, 1975.
- Robertson, D.M. and D.C. Smith. "Compressive Strength of Mandibular Bone as a Function of Microstructure and Strain Rate." J. Biomech. 11(1978).
- Saha, S. and W.C. Hayes. "Tensile Impact Properties of Human Compact Bone." J. Biomechanics. Great Britain: Pergamon Press, 9(1976).
- Saha, S. and W.C. Hayes. "Instrumented Tensile-Impact Properties of Human Compact Bone." Experimental Mechanics. 14(1974).
- Saulgozis, Y. "Differences and Correlations Between the Elastic Characteristics of the Compact Bone Tissue of the Human Tibia." Polymer Mechanics. 11(1976).
- Sedlin, E.D. and C. Hirsch. "Factors Affecting the Determination of the Physical Properties of Femoral Cortical Bone." Acta Orthop. Scand. 37(1966).
- Segal, Bernard L., and David G. Kilpatrick. Engineering in the Practice of Medicine. Baltimore, Maryland: The Williams & Wilkins Company, 1967.
- Skalak, Richard, and Shu Chien, eds. Handbook of Bioengineering. New York: McGraw-Hill Book Company, 1987.
- Snider, J.N. et al. "The Response of the Human Lower Leg to Impact Loading." Biomechanics of Impacts. Bergisch-Gladbach (FRG): International Research Council of Biokinetics of Impacts, 1988.
- Stapp, John P., ed. Eleventh Stapp Car Crash Conference. New York, NY:

- Society of Automotive Engineers, Inc., 1967.
- Stapp, John P., ed. Nineteenth Stapp Car Crash Conference. Warrendale, Pennsylvania: Society of Automotive Engineers, Inc., 1975.
- Stapp, John P., ed. Seventeenth Stapp Car Crash Conference. New York, NY: Society of Automotive Engineers, Inc., 1973.
- Stapp, John P., ed. Twenty-Fifth Stapp Car Crash Conference. Warrendale, Pennsylvania: Society of Automotive Engineers, Inc., 1981.
- Stone, J.L., G.S. Beaupre and W.C. Hayes. "Multiaxial Strength Characteristics of Trabecular Bone." J. Biomech. 9(1983).
- Swanson, S.A.V., M.A.R. Freeman and W.H. Day. "The Fatigue Properties of Human Cortical Bone." Med. Biol. Eng. 9(1971).
- Tadokoro, Hidetoshi. "Load Measuring Method of Occupant's Leg on Motorcycle Collision." The 11th International Conference on Experimental Safety Vehicles. May, 1987.
- Timmins, P.A. and J.C. Wall. "Bone Water." Calif. Tiss. Res. 23(1977).
- Torzilli, P.A., K. Takabe, A.H. Burnstein and K.G. Heiple. "Structural Properties of Immature Canine Bone." J. Biomech. Eng. 103(1981).
- Torzilli, P.A., K. Takabe, A.H. Burnstein, J.M. Zika, and K.G. Heiple. "The Material Properties of Immature Bone." J. Biomech. Eng. 104(1982).
- Tsai, S.W. and E.M. Wu. "A General Theory of Strength for Anisotropic Materials." J. Compos. Mater. 5(1971).
- Van Buskirk, W.C. and R.B. Ashman. "The Elastic Moduli of Bone." In S.C. Cowin (ed.), Mechanical Properties of Bone. New York: American Society of Mechanical Engineers, 1981.
- Van Buskirk, W.C., S.C. Cowin and R.N. Ward. "Ultrasonic Measurement of Orthotropic Elastic Constants of Bovine Femoral Bone." J. Biomech. Eng. 103(1981).
- Von Hagens, Gunther. "Emulsifying Resins for Plastination." Bochum, 25(1979).
- Von Hagens, Gunther. "Impregnation of Soft Biological Specimens with Thermosetting Resins and Elastomers." Anat. Rec., 194(1979).
- Vose, G.P. and A.L. Kubala. "Bone Strength - Its Relationship to X-Ray Determined Ash Content." Hum. Biol. 31(1959).
- Walker, James. Nightline. ABC News, New York: Journal Graphics, Inc., December 5, 1988.
- Welkowitz, Walter, and Sid Deutsch. Biomedical Instruments: Theory and Design. New York, NY: Academic Press, Inc., 1976.
- Yamada, H. Strength of Biological Materials. New York : Robert E. Krieger Publishing Co., 1973.
- Yamada, H. In F.G. Evans (ed.), Strength of Biological Materials. Baltimore: Williams & Wilkins, 1970.
- Yanson, K.A. I.V. Knets and Y.Z. Saulgozis. "Physiological Significance of Changes in Bone Volume Associated with Deformation." Polymer Mechanics [trans. of Mekhanika Polimerov]. 10(1974).

Yoon, H.S. and J.L. Katz. "Ultrasonic Wave Propagation in Human Cortical Bone: II. Measurements of Elastic Properties and Micro-Hardness." J. Biomech. 9(1976).

Zettas, James P., et al. "Injury Patterns in Motorcycle Accidents." The Journal of Trauma. The Williams & Wilkins Co., 19(1979).

## **PART 2**

### **IMPACT RESPONSE OF THE LEG AND TIBIA**



## **ABSTRACT**

It has been widely reported that injury to the leg is the most common form of non-fatal trauma associated with motorcycle accidents. Furthermore, it has also been reported that the majority of motorcycle leg injuries resemble those experienced by pedestrians in that they do not involve crush. Rather, these injuries appear to involve only a direct impact between the leg and an opposing rigid object. Often the soft tissue of the limb is injured from the inside out in that sharp bone fragments and jagged ends lacerate the soft tissue as relative motion occurs. The complexity of understanding these results is due to a combination of impact effects, biological material properties, and human geometric considerations. This research provides some fundamental data for cadaver leg and bone impact response. It is sponsored by the Japan Automobile Manufacturers Association (JAMA), Inc. for the investigation of design modifications to automobiles and motorcycles to reduce the seriousness of collision injuries. To conduct this research, a unique test facility has been developed that simulates collisions between automobiles and pedestrians, motorcycles, or bicycles. Results are presented and discussed for the purposes of understanding fracture behavior of the human leg and tibia.

## **INTRODUCTION**

This work is part of a research project entitled “Dynamic Response of the Human Leg to Impact Loading.” The intent of the research project is to describe

and quantify the dynamic response of the human lower leg to impact loading as encountered when pedestrians or cyclists are struck by automobiles. The approach has been to develop a test facility that simulates collisions between automobiles and pedestrians, motorcycles, or bicycles. The facility was designed so that it would produce leg injuries comparable to those normally seen by surgeons.

Some long-term objectives of the project are (1) to develop a physical model of the leg which responds to impact as the human leg does, (2) to produce design modifications of automobiles and motorcycles for improved safety, (3) to develop impact/injury computer models that can be used to guide in the design of a wide variety of personal protective equipment, and (4) to aid in developing improved surgical techniques. This section presents some results for the purposes of understanding fracture behavior of the human leg and tibia during impact loading.

## **EXPERIMENTAL APPROACH**

In order to better understand lower leg impact injuries and identify specific countermeasures, a facility was developed to simulate impact conditions on cadaver, animal, and model specimens with impact velocities up to 13.41 meters per second (30 miles per hour) and with impact masses up to several hundred kilograms.

The apparatus used in this facility consists of three main components: the cart accelerator system, the specimen holding device and the impactor support cart with its associated guideway. In operation, the cart accelerator system propels the impactor support cart to the desired velocity, after which the impactor strikes the test specimen. The impactor support cart is then stopped by means of direct impact onto energy-absorbing bales of wood fiber. Specimen recoil energy is dissipated by means of frictional losses associated with the movement of a pivoting horizontal arm which supports the specimen and through specimen contact with an energy-absorbing padding. The pivoting horizontal arm can also serve as a rigid support.

The facility was designed for a variety of impact conditions including the ability to produce free-hanging and crushing injuries. Impact speeds can range from 0.6 meters per second (m/s) up to a maximum of about 13.4 m/s. Different impacting surfaces and bumpers can be mounted on the support cart. Five impacting surfaces have been used to date: (1) a section of a Chevrolet automobile bumper, (2) a 4.1275-cm diameter steel pipe (1.5875 cm thick), (3) a 7.62 cm diameter steel pipe (1.5875 cm thick), (4) a flat plate (7.62 cm x 20.32 cm x 0.3175 cm), and (5) a flat plate (7.62 cm x 20.32 cm x 0.3175 cm) covered with a polymer. The 4.1275-centimeter diameter pipe was used for most tests because the resultant injuries from the test using that pipe corresponded closely to those seen clinically.

A PCB quartz piezoelectric force transducer (Model 208A04) was mounted on the impact bumper to transmit the force exerted on the bone directly to the transducer. When connected to a PCB power unit and a Hewlett Packard (Model 3562) signal analyzer, the PCB transducer generates a high-level, low-impedance analog output signal with a force constant of 1.124 mv/N that is linear up to a force value of 31,360 N.

Two different mounting set-ups were used for the specimens: (1) simple-support (pin-pin), and (2) inertial constraint (pin-foot mass). Impacts were directed at the midshaft and the distal one-third of the tibia. Most impacts were delivered from the front (anterior-posterior), but some were directed from the side (lateral-medial). The impactor was rigidly attached to a track-guided cart traveling at selected speeds. Two measurement systems have been used to time the cart travel over a given distance. One uses a spotlight and a photosensitive receiving cell to turn a "clock" on and off as the cart passes. The other system uses microswitches that are separated by a given distance and are triggered by the moving cart. Piezoelectric transducers and accelerometers were used to obtain the force and acceleration data.

This facility and other complementary laboratories with state-of-the-art data acquisition provide the capability of testing a variety of specimens ranging from bone to a full cadaver or dummy. Mechanical properties of various materials including bone can be determined, and bone simulant specimens can be developed.

A variety of dynamic response experiments have been conducted to date. These include intact cadaver legs, human tibias, human femurs, intact goat legs, dog bones (humeri, femora, tibiae - mechanical properties only), horse bones, bakelite as a bone simulant, and fiber-reinforced polyamide as a bone simulant (Kress, 1988).

In the tests, the following bone and motion parameters were measured and recorded: impactor velocity, force during impact, cart acceleration, bone dimensions, and end damage state. For some tibia specimens, cortical bone volume was determined, after removal of the marrow, by carefully measuring the displaced volumes when the bones were immersed in a beaker of water. High-speed camera (up to 11,000 frames/second) and other video camera documentation were used during some of the tests. In addition to the direct test documentation, most specimens were x-rayed and then carefully dissected and photographed. The experimental data are qualitatively compared with real injuries seen in clinical settings such as hospital emergency rooms. Typical motorcycle and pedestrian impact accidents often result in severe damage to the vascular and neurological components of the lower leg. Comminuted fractures with compression and tension butterfly wedges are very common among accident victims admitted to the emergency room. Comparison of x-rays of clinical patients and experimental specimens confirmed that the damage produced by the experimental apparatus is comparable to the clinical damage.

## EXPERIMENTAL RESULTS

The first objective of the research program was to design and develop a facility for conducting simulated automobile/leg impact testing. Automobile accidents that produce leg injuries to pedestrians or cyclists typically involve velocities ranging from 3.048 m/s (10 fps) to 13.411 m/s (44 fps). During the injury phase of impact the change of velocity of the automobile is negligible. Therefore, design criterion of the impact facility was to produce an impact velocity of at least 13.4 m/s with very little change in velocity during impact.

Use of high-speed camera films showed that the cart velocity decreased less than 3% after impact when compared to the calibration curve. This was also verified by an accelerometer mounted on the cart. This decrease was independently confirmed using a "switch" system in which two microswitches turned a clock on and off to time the cart travel over a fixed distance after impact.

A number of separate experiments were conducted to provide program guidance and direction. These experiments provided information in such areas as evaluation of specimen support conditions, determination of preservation effects on specimen response, and exploratory tests for impactor geometry.

Other tests were conducted to provide information pertaining to the behavior of the lower leg during impact loading. Some of those tests are reported on here. They can be sub-categorized as follows: (1) Specimen Support Condition, (2) Horse Bone Tests, (3) Impactor Geometry Exploratory Tests, (4) Femur Lateral Impact, (5) Initial Human Tibia Tests, (6) Simply

Supported Leg, (7) Tibia Tests for Ultimate Failure Strength, (8) Bending Stress and, (9) Energy Absorption Capacity.

**SPECIMEN SUPPORT CONDITION** - The initial testing was designed to answer the question of whether the leg had to be trapped between the motorcycle and automotive bumper (crushing injury) or if the limb was restrained by its own inertia. The mechanics of the fracture and the resultant injury have remained a subject of speculation. This information is clearly needed for computer modeling. High-speed photography showed that, for the human, the lower leg acted as if it was simply supported during the initial impact up to fracture. Animal testing confirmed this because the legs of a goat could not be fractured until a mass was added to the limb to simulate a foot.

Twenty-six human cadaver legs and ten goat legs were impacted at speeds varying from 4.5 m/s to 10.4 m/s (15 to 34 feet per second). These velocities are characteristic of the typical automobile/motorcycle accident in which lower leg injury results in loss of limb due to neurological and vascular complications. Thirty-five of the specimens were fractured by this process illustrating the significance of inertial restraint of the foot.

**HORSE BONE TESTS** - Impact testing was performed on eight equine leg bones in order to compare the strength of hydrated bone with that of dehydrated bone. Dehydrated bones have material properties that are usually different from their "fresh" or hydrated state.

The energy absorption capacity was calculated from the force-time data obtained from tests of four hydrated and four dehydrated equine leg bones. The ratio of hydrated versus dehydrated energy absorption capacities varied from 0.84 to 3.78. Averaging the individual ratios for the different types of bone yielded a value of 2.00. This might imply that the material properties deteriorate by a factor of two after a bone is dehydrated.

IMPACTOR GEOMETRY EXPLORATORY TESTS - Exploratory studies were conducted using several different impactor geometries. It is likely that different levels of fracture severity would result from varying the impactor shape. Minimization of the fracture damage to the vascular and neurological system is an obvious program goal. The intent of these tests was to produce some comparative data with regard to fracture damage versus impactor geometry. Four different impactors were used: (1) a 1970 metal Chevrolet bumper, (2) a 7.62-centimeter diameter pipe, (3) a 4.1275-centimeter diameter pipe, and (4) a flat plate with a height of 7.62 inches.

The 4.1275-centimeter pipe, the 7.62-centimeter pipe, and the Chevrolet bumper all produced very similar fractures during tibia (in vitro) testing. Both experimental and clinical comminuted fractures often are characterized by a butterfly wedge indicating tension failure of the bone on the side (posterior) opposite of the impact. The similarity in damage from these three impactors probably exists because each impactor produces a single-point loading condition. The only difference among the damages produced by the two pipes



and the Chevrolet bumper was observed during the intact human leg tests. The legs wrap around the impactors while being displaced and conform to the impactor geometry. In the case of the bumper, this spreads the load over a greater surface area and usually results in more skin lacerations and foot damage.

Although few impact tests have been conducted using the flat plate, there seems to be an interesting difference in the resultant damage. The frequency of comminuted fractures is still about the same, however, the bone edges and the butterfly wedge do not seem to be as sharp or jagged using the flat plate. The loading condition that the flat plate induces to the bone is basically two-point. The resulting different bending behavior might be the reason for the more rounded edges in the fracture region.

**FEMUR LATERAL IMPACT** - A series of tests was conducted to obtain preliminary data regarding fracture type and the breaking strength of femurs under typical side impact loading conditions. Twelve femurs were impacted with the 4.1275-centimeter pipe and one femur with the flat plate. The average failure force for the femurs impacted with the pipe was 2,528 N compare to 2,525 N for the nine tibias discussed earlier. The breaking force for the femur impacted by the plate was 4,572 N. This force value is probably larger because of the two-point loading condition discussed previously. The side impacts were in the lateral-medial (l-m) direction which is almost always the case for clinical injuries. Two of the pipe impact tests and the plate impact test produced wedges in which

failure was initiated on the compression side. This is in contrast to most of the tibias, where failure began on the tension side. Failure in the femurs may have been initiated on the compression side instead of the tension side because of the difference in geometry.

INITIAL HUMAN TIBIA TESTS - Because of the obvious importance of the tibia in determining the dynamic response of the lower leg to impact, tests were conducted to identify the ultimate failure force and force-deflection characteristics of the human tibia removed from the leg. Three separate series of test conditions were utilized in evaluating the strength of this long bone which was simply supported at each end. The first of this series of three was designed to provide reference data concerning the characteristics of the instrumentation system as well as to provide information on the behavior of this bone under low speed impact. The second series of low speed impact tests was intended to reflect only the effect of using a 4.1275-centimeter pipe as the impacting object rather than having direct impact by the transducer. The third series was intended to provide information on the effect of impact speed in that the only difference between the second and third series was that the third series was conducted at a target speed of 7.62 m/s rather than at 0.9 to 1.8 m/s. The specific conditions of the first series involved the direct impact, anterior-posterior (a-p), of the force transducer with the tibial bone at approximately midshaft, using nine specimens, and employed an impact speed of between 0.6 and 1.5 m/s. The second series, also involving nine specimens and an a-p impact, used a

velocity range of from 0.9 to 1.8 m/s and employed a 4.1275-centimeter pipe impactor with the force transducer mounted on the side opposite impact. The last series involved six specimens, impacted by the 4.1275-centimeter pipe in the a-p direction with a velocity of 7.62 m/s. The results of these three series of tests are summarized in Table 1.

**TABLE 1. Ultimate Failure Force for Embalmed Human Tibias Impacted with Pipe and Transducer at Varying Speeds**

Test Condition	Ultimate Failure Force (M)	
	Mean	Standard Deviation
Transducer Impact @ 0.6-1.5 m/s	1555	654
Pipe Impact @ 0.9-1.8 m/s	1046	650
Pipe Impact @ 7.3-7.9 m/s	2451	282

Although the reason for the difference between the direct transducer impact and the pipe impact at low speed is not obvious, the most probable explanation is that the structure supporting the force transducer may have inadvertently contacted the specimen. It appears as if there is little difference in the ultimate failure force of the specimens under low and high speed impacts although this cannot be validated because of the large variance in the data and the small sample size.

**SIMPLY SUPPORTED LEG** -The next activity in this research involved impacting intact legs in a manner analogous to that of the simply supported bone. Here, the intact leg was mounted from a steel rod passing through the lower condyle of the femur with the heel against a very rigid steel shape. The

impacts were delivered with the 4.1275-centimeter steel pipe at approximately the distal 1/3 of the tibia and with a striking velocity of 7.62 m/s. Based on five specimens, the average peak force was 2331 N while the standard deviation was 358 N. It is unlikely that there is a statistically significant difference between the impact strength of the tibia within the intact leg and that of the bare tibia, at least not at 7.62 m/s. However, the sample size is still quite small.

Review of the force transducer data as well as of the high speed films provides considerable insight into the role the soft tissue plays in maintaining leg integrity during impact and following bone fracture. In essence, the portion of the limb distal to the fracture must be accelerated by means of tensile forces delivered through the soft tissue around the area of the fracture. Unquestionably, much of the internal soft tissue damage attendant to this type of impact must be related to the stretching and bending in the immediate proximity of sharp bone fragments and the splintered bone shaft.

**TIBIA TESTS FOR ULTIMATE FAILURE STRENGTH** - It is known that the strength of bone varies markedly depending on the age, sex, and state of health of the individual and on the size, dimensions, and structure of the bone. Those variables can be classified as either material properties or geometric conditions. Post-test examination of some bone specimens will result in their exclusion from the data base because of obvious gross deterioration from certain bone diseases. Even with these exclusions, bone material properties seem to have a wide range of variance. This variability makes comparative testing of

impact response and alternative bumper designs difficult. It would be convenient if such variability could be accounted for strictly in terms of fundamental “structural” differences with mechanical properties being included as parameters that do not vary over large ranges. To evaluate this possibility, a series of nine tibia (anterior-posterior, a-p loading) impact/fracture tests was conducted in which the dimensions of each bone were well characterized and the impact forces were measured as functions of time up to failure. An attempt is made here to correlate the data in terms of (1) a bending stress, (2) an energy absorption capacity, and (3) an average cortex thickness. The intention was to search for parameters that would normalize geometric parameters and leave only the material properties.

**BENDING STRESS** - The maximum bending stress in a simply supported beam with a transverse force,  $F$ , imposed at the center is (Beer and Russell, 1981)

$$\sigma_{\max} = \frac{|M|_{\max} c}{I} = \frac{FLc}{2I} \quad , \quad [1]$$

where  $I$  is the moment of inertia with respect to the centroid,  $L$ , is the beam length (from support to support), and  $c$  is the distance from the centroid to the beam edge on the side opposite the applied force. For the situation of a-p loading on the tibia, these parameters are illustrated in Figure 1 in an idealized cross-sectional view:

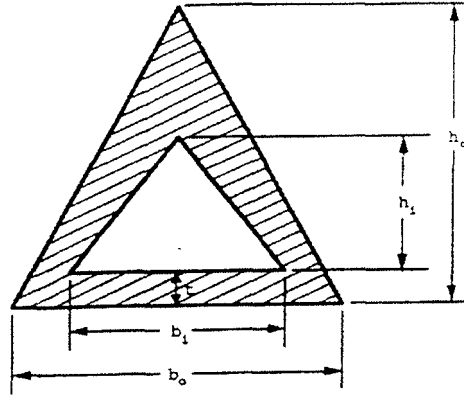


**FIGURE 1.** Idealized cross-sectional view of the human tibia.

For analysis, the tibia is idealized as a hollowed-out triangular region with the outer triangle having dimension  $b_o$ ,  $h_o$ ; the inner triangle having dimensions  $b_i$ ,  $h_i$ , with a varying cortex thickness,  $t$ , (six measurements were recorded at different circumferential locations). With this idealization, the centroid distance,  $c$ , is

$$c = \frac{\frac{1}{6}b_o h_o^2 - \frac{1}{6}b_i h_i^2 - \frac{1}{2}b_i h_i t}{\frac{1}{2}b_o h_o - \frac{1}{2}b_i h_i} \quad [2]$$

The moment of inertia,  $I$ , with respect to the centroid is

$$I = \left[ \left( \frac{1}{36} \right) b_o h_o^3 + \left( \frac{1}{2} \right) b_o h_o d_o^2 \right] - \left[ \left( \frac{1}{36} \right) b_i h_i^3 + \left( \frac{1}{2} \right) b_i h_i d_i^2 \right], \quad [3]$$

where  $d_o$  is the distance between the centroid of the outer triangle and the centroid of the “annular” cortex region, and  $d_i$  is the distance between the centroid of the inner triangle and that of the annular cortex region. Equations [1],

[2], and [3] were used along with the measured force value at the instant of failure to calculate the maximum bending stresses for the nine tibia tests. The values are shown in Table 2 and on Figure 2. Inspection of Table 2 and Figure 2 indicates that the bending stress appears to be a relatively good correlational parameter having an average value of  $270 \times 10^6$  pascals with a range of  $126 \times 10^6$  to  $486 \times 10^6$  pascals. The five points that group around an average value of  $204 \times 10^6$  pascals seem to be well correlated by their bending stress. These tests all exhibited very similar force versus time curves, whereas the other four plots showed peculiarities.

**TABLE 2. Ultimate Strength of the Embalmed Human Tibia Submitted to Anterior-Posterior Impact Loading**

Tibia Specimen Number	Ultimate Failure Force (N)	Ultimate Bending Stress (E- 6 N/m <sup>2</sup> )	Energy Absorption Capacity (J/m <sup>3</sup> )	Average Cortex Thickness (mm)
1	4887	379.25	59,358	7.67
2	1969	186.54	23,123	7.73
3	4957	486.17	29,345	6.81
4	2217	212.68	11,001	6.16
5	1979	193.18	14,535	5.94
6	1299	222.50	21,543	4.21
7	751	125.62	13,198	3.99
8	1340	207.27	19,307	4.07
9	3330	417.01	22,236	6.03

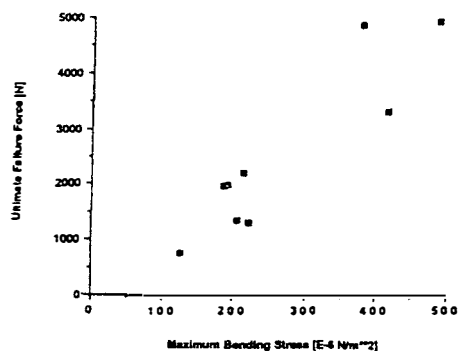


**FIGURE 2.** Ultimate failure force versus maximum bending stress for nine embalmed human tibias.

ENERGY ABSORPTION CAPACITY - Force versus time data obtained for the bone impact tests were used to estimate the energy absorbed by bone up to the point of failure per unit cortex volume.

The relationship derived for the energy absorption capacity is

$$\frac{U}{V} = \frac{v_o \int_0^{t_f} F dt - KE}{V},$$

where U = internal energy absorbed to time  $t_f$ ,  
 $v_o$  = impactor velocity,  
 $t_f$  = time from instant of contact to failure,  
F = impact force measurement ,  
t = time,  
V = cortex volume between support points,  
and KE = the kinetic energy of the bone specimen, at the instant of failure.

The volume was obtained by immersing the tibias (with removed condyles above L and removed marrow) into a beaker of water and measuring the displacement. The kinetic energy was estimated by assuming a linear velocity profile from  $v_o$  at the specimen midshaft down to  $v = 0$  at each end support location. A mean cross-sectional area,  $A_{cs}$ , for each tibia was estimated from measurements of the cortex thickness at several circumferential positions. Consequently, the kinetic energy was estimated from

$$KE = \frac{\bar{A}_{cs} \rho}{g_c} \int_0^L v_y^2 dy$$

where  $v_y$  = local transverse vel. at position  $y = v_o(1-y/L)$ ,  
y = longitudinal direction with zero at the midshaft,  
 $\rho$  = bone density = avg. value of  $1900 \text{ kg/m}^3$  (Cowin, 1989),  
 $g_c$  = proportionality coefficient =  $1 \text{ (kg-m)/(N-s}^2\text{)}$ ,  
and L = length from midshaft of specimen to point at which specimen contacts support.



In each case, the kinetic energy proved to be negligible compare to the energy absorption capacity. The calculated strain energy densities for the nine tibias are shown in Table 2 and are plotted on Figure 3. The data point at force equal to 4887 N and an energy absorption capacity of 59,358 J/m<sup>3</sup> is believed to be specious. The force-time plot for that point is the only one in which the force value decreased momentarily before rupture and it was observed that the cart structure shifted in the guide rails during impact. The time to rupture was also unusually long for this test compared to the others. Disregarding this test it is seen that on Figure 3 energy absorption capacity seems to be relatively constant even though the breaking force varied over a wide range. For a force range from 751 N to 4957 N, the energy absorption capacity ranges only from 11,001 J/m<sup>3</sup> to 29,345 J/m<sup>3</sup>. The average energy absorption capacity for the eight tibias is 19,286 J/m<sup>3</sup>.

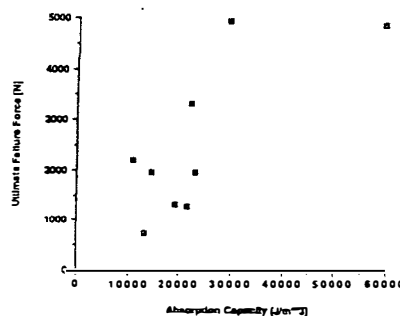


**FIGURE 3.** Ultimate failure force versus energy absorption capacity for nine embalmed human tibias.

The measured force at the instant of failure for each bone specimen versus the mean cortex thickness is plotted on Figure 4. It is seen that cortex thickness is a fairly good correlating parameter for the breaking force.

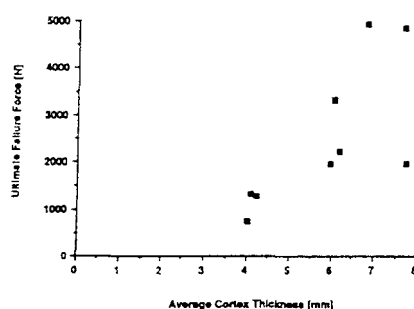


**FIGURE 4.** Ultimate failure force versus average cortex thickness for nine embalmed human tibias.

A series of high-speed impact tests was completed in which twenty-one embalmed intact legs were fractured with an impactor velocity of approximately 7.5 m/s. The fractured legs were then subjected to a second impact under the same support conditions. The measured average breaking force for legs from the first impacts, causing fracture, was 5992 N. The average value for the second impacts after fracture was 2925 N.

The difference between the two averages, 3067 N, is most likely the force required to break the tibias without any influence of the soft tissue mass. This speculation was supported when seventeen “bare” tibias were tested separately and their average breaking force value was 3022 N. An important deduction might follow that the soft tissue mass behind the tibia in the human leg does not provide structural support that raises the breaking force limit of the tibia.

## DISCUSSION

The research has demonstrated that fractures can occur without entrapment (crushing injury). The fractures can occur from just the inertial

restraint of the tibia from the upper thigh and foot. The elastic motion resulting in fracture occurred before significant rigid body motion.

Although the data are preliminary, x-ray data and dissection indicate that the mechanism of fracture depends on impact velocity.

Additional observations may be noted: (1) The horse bone tests confirmed the belief that dehydration of bone decreases its strength and causes increased brittleness, but more tests are needed; (2) the mechanism of internal soft tissue damage can be attributed to the stretching and bending of the soft tissue in the proximity of sharp bone fragments, and; (3) with the exception of the femur tests, it can be stated that failure under impact loading is usually initiated on the tension side of the bone. The femur data might be explained by the different geometric configuration and the fact that the femur impacts were lateral-medial as compared to anterior-posterior for the tibias. (4) Impactor shape affects fracture patterns. Distributing the impact load over more points or a larger area seems to lessen the sharp edges on the fractured areas of the bone, consequently decreasing the soft tissue damage. Note, however, that as the load is spread over a larger area, more rigid body motion could occur to the whole body which might result in other injuries (e.g. head injury).

For the series of nine tibia tests, the ultimate failure strength proved to be a good material property correlational parameter. The sample size is small, so there is a relatively large standard deviation, but it appears from Figures 2 and 3 that the ultimate bending stress and the energy absorption capacity are relatively

constant with only a slight increase at higher force values. Also, the average cortex thickness seems to be an excellent indicator of ultimate breaking force.

Recent experiments explored the effect that the soft tissue mass of the lower leg has on the tibia with regard to breaking strength. Twenty-one embalmed legs were fractured with an impactor velocity of approximately 7.5 m/s. The broken legs were then subjected to a second impact under the same support conditions. After comparison of data to that of impact tests using “bare” tibias it appears as if the soft tissue does not play a role other than contributing additional mass. The attachment of the muscles and soft tissue does not seem to raise the strength limit of the tibia.

Conducting the necessary tests and gathering all the data needed to fully understand the response of the human leg during impact loading is a large task. Our work is just beginning to lay the groundwork for continued research.

## BIBLIOGRAPHY

- Kress, T.A., et al. “Determination of Lower Limb Failure Modes and Tissue Damage by Impact Loading.” Proc. of the VI International Cong. on Exp. Mech. Bethel, CT: The Society for Experimental Mechanics, Inc., 1(1988).
- Beer, P. Ferdinand and Russell E. Johnston Jr. Mechanics of Materials. New York, NY: McGraw-Hill, Inc., 1981.
- Cowin, S. C. Bone Mechanics. Boca Raton, Florida: CRC Press, Inc., 1989.

**PART 3**  
**GENERAL IMPACT BEHAVIOR OF THIGHS AND FEMURS**

## ABSTRACT

Research was performed in an attempt to better define tolerance levels (magnitude of loading that yields a specific degree of injury) of the human thigh. The objectives of this study are to ultimately provide data to be used in the enhancement of crash dummy biofidelity and the development of artificial bone for a frangible experimental dummy (FrED®).

For this study, sixty-eight femurs and twenty-two intact lower limbs from embalmed human cadavers have been subjected to dynamic impact loading. The bones and limbs were mounted in one of two different configurations that simulate: 1. Standing- Specimens were simply-supported with the long axis placed perpendicular to the plane of impact and the direction of impact was either anterior-posterior (a-p) or lateral-medial (l-m). 2. Sitting- Specimens were suspended by cord with the long axis parallel to the plane of impact. Mass was placed at the proximal end of these bones or limbs to emulate constraints imparted by the pelvis and other upper-body components. The impact points in this configuration were the condyles of the femurs or the flexed knee of the intact legs.

The impact apparatus consists of an accelerator that propels a cart headed by a pipe/or plate instrumented with a force transducer. This provided a data record of the transient (ms) relationship of the force (kN) applied to the specimen during impact. The gross response of the thigh to dynamic impact was recorded by standard 30 frames/s VHS video. Several impacts were also captured on a Kodak Ektapro high-speed video system at 1,000 frames/s. Additional data were collected from radiographs and photographs.

The femur appears stronger when impacted in the a-p direction than the l-m direction. Also, soft tissue damage was masked due to the fixation process,

and it was concluded that the soft tissue did not play a role in affecting fracture outcome.

## **INTRODUCTION**

This research project is the result of a collaborative effort between anatomists at the University of Louisville School of Medicine and Biomedical Engineers from the University of Tennessee Engineering Institute for Trauma and Injury Prevention.

Progress made since the introduction of the research in 1986 has been significant and includes the design and installation of a state-of-the-art impact testing laboratory; the completion of impact tests using human legs, animal legs, and simulated leg structures; and development of a basic understanding of the response of the human leg to impact loading. Other contributions include appropriate biological and structural material testing, development efforts for a computer-based simulation of lower leg response to impact loading, clinical studies of accidents involving traumatic leg injury, statistical studies of traumatic injuries, whole body vibration research, underwater impact injury studies, head impact tolerance and experimental injury research, various accident reconstruction projects, causal mechanism analyses of human injury, and other biomechanical laboratory experimentation.

This section presents some results for the purposes of understanding fracture behavior of the human femur and thigh during impact loading.

## **MATERIALS AND METHODS**

Human cadavers were bequeathed to the University of Louisville School of Medicine for the purposes of research and education. Use of cadaver

specimens for this research project was authorized by the Human Tissue Use Committee in the Department of Anatomical Sciences and Neurobiology at the University of Louisville Health Sciences Center in Louisville, Kentucky, U.S.A.

Lower limbs and femurs were collected from dissection laboratories after completion of medical and dental gross anatomy courses. At least six months prior to this study, the cadavers were embalmed via femoral artery injection of a fixative composed of 20% Isopropyl Alcohol, 20% Propylene Glycol USP, 4% Formaldehyde (Formalin), 4% Phenol and 52% warm water.

Radiographs were made of the intact lower limb specimens, then the limbs and femurs were transported to the test facility.

All specimens were tested at the Impact Biomechanics Laboratory, a special facility in the Department of Industrial Engineering at the University of Tennessee, Knoxville, Tennessee, U.S.A. The testing apparatus consisted of a pneumatic-powered accelerator which propelled an impact cart. The impact cart was headed by an instrumented pipe or plate. Specimens were mounted in a variety of configurations in an impact zone.

Accelerator & Cart - The accelerator consisted of a piston that was powered by compressed air. A ram on the end of the piston contacted the cart throughout its stroke of approximately 1.5 m. The impact cart is constructed of aluminum and steel and weighs approximately 50 kgs. It was guided into the specimen impact zone by a rail system. The cart travels free of the ram for less than a meter and trips a photovoltaic cell/timer apparatus which measures time to travel a given distance. This allows for the calculation of cart velocity just prior to impact. The change in velocity ( $\Delta v$ ) of the cart between the end of the ram stroke and the end of the impact has been measured at less than 4% during most impacts.



Impactor & Instrumentation - Heading the cart was one of two different instrumented impactors. Used most often was the laboratory standard 10 cm section of steel pipe with a 4.13 cm outside diameter. The other impactor was a steel plate measuring 2.5 cm by 10 cm. Both were mounted in the same fashion - by slide pins on the front of the cart. When contacting a specimen, the pipe or plate was freely able to impinge on a quartz force transducer, model 208A03 (commercially available through PCB Piezotronics). The transducer was coupled with a Hewlett Packard 3562A signal analyzer. The analyzer recorded and stored a plot of force versus time for each impact.

Specimen Mounting - The thighs and femurs were mounted in one of two test configurations that simulated a standing or seated individual. To simulate standing, the specimen was simply supported with the long axis placed perpendicular to the plane of impact. The specimens were mounted such that either the lateral or anterior surface of the midshaft was impacted. Thus, the direction of impacts were anterior-posterior or lateral-medial.

In the tests simulating a seated person, the lower limb or femur was suspended by cord with the long axis placed parallel to the impact plane. The impact occurred at the knee of the intact lower limbs and at the condyles of the femur. A mass was placed at the proximal end of the specimen in order to simulate the inertial constraints imparted by the pelvis and other upper body components (see Figure 1).

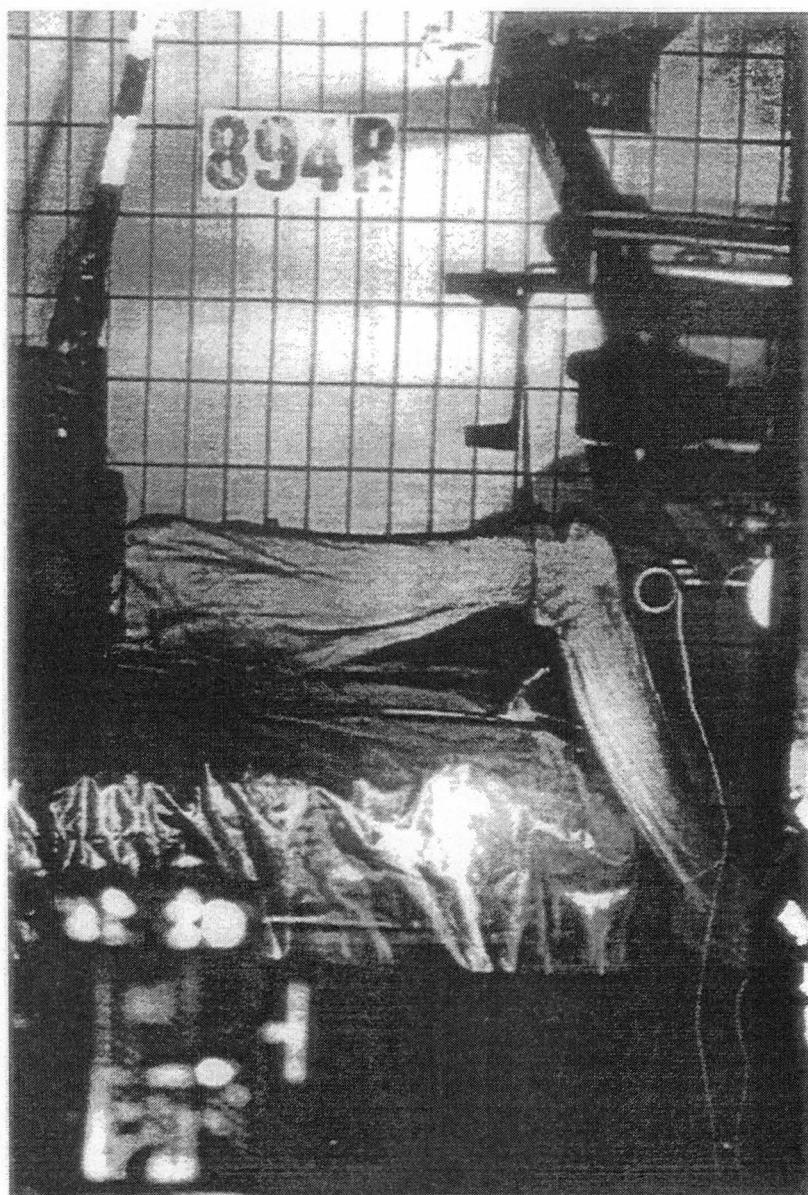


**FIGURE 1.** Test set-up for axial (or longitudinal) impact of intact human cadaver thighs. Note the instrumented impact pipe lined up to strike the knee. Cylinder holding clay is situated at the hip.

For the bone impacts, the mass placed at the head of the femur was modified to include a simulated acetabular cup. Additionally, a Hybrid III crash dummy foot was suspended from the distal femur in an effort to address the constraints due to the leg.



**TABLE 2. Dynamic Response Characteristics of the Human Thigh to Impact Loading**

n	Impact Direction	Impactor	Average Force $\mu$ (kN)	Standard Deviation $\sigma$ (kN)	Average Velocity (m/s)	Fracture Classifications	Remarks (Raw data notes for researchers)
4	AX Knee	Pipe	8.82	1.45	7.5	(n=4) 50% Comminuted patella only. 50% Comminuted fractures of femur, tibia and patella.	No additional mass behind the hip.
1	AX Knee	Pipe	4.50	na	7.5	(n=1) Fractures of the neck and condyles.	38 kg mass behind the hip.
1	AX Knee	Plate	11.07	na	7.5	(n=1) Comminuted patella. Femur not fractured.	11 kg mass behind the hip.
4	AX Knee	Pipe	10.24	1.47	7.5	(n=4) 75% Comminuted patella and distal femur. 25% Comminuted patella only.	11 kg mass behind the hip.
2	AX Knee	Pipe	8.07	4.06	7.5	(n=2) Both had comminuted femur, tibial condyles & patella.	18 kg mass behind hip.
4	A-P Thigh	Pipe	5.81	1.78	7.5	(n=6) 16.7% Neck fractured. 50% Oblique 50% Wedge formation 16.7% Transverse	919L & 879L had false force triggers. Percentages > 100 due to multiple fractures per specimen.
6	L-M Thigh	Pipe	6.17	1.81	7.5	(n=6) All comminuted. 1 fracture of femoral neck.	

Note: All intact specimens were embalmed and impacted midshaft while simply-supported, unless noted otherwise.

## DISCUSSION

Area under the force-time curve for each a-p impacted femur was determined. The average value is 2658 N-ms. The value for the l-m loaded femurs was 2254 N-ms. The a-p loaded bone, therefore, does not absorb much more energy than the l-m loaded bone, although the strength is much greater in the a-p direction. Note that the average breaking force in the a-p direction is 5,697 N as compared to 3,053 N for impacts in the l-m direction.

Most of the fractures in the a-p tests were comminuted. Interestingly, however, few produced tension or compression wedges. The vast majority of the comminuted fractures were side wedges. The side wedges were equally

dispersed as lateral and medial wedges. Approximately one-fourth of the fractures were oblique, and one was a shatter.

The axial impacts of intact thighs produced severely comminuted fractures although the neck (or hip) was rarely involved. Two-thirds of the comminuted fractures involved the patella with shaft of the femur, whereas the remaining impacts resulted in fractured patellas alone. The radiograph depicted in Figure 2 shows a relatively common fracture pattern seen in this study. There are comminuted fractures of the patella, femoral condyles and distal femoral shaft.

Extensive dissection was performed on the intact thighs and it was clear that fixation drastically stiffened the soft tissues making them highly resistant to strain and failure.

Almost all perpendicular impacts to the intact thigh (a-p and l-m) resulted in comminution of the femur and wedge formation was prevalent.



**Figure 2.** Lateral X-ray view of the comminuted knee. Arrow indicates point of impact.

## CONCLUSIONS

In consideration of the data, it is apparent that the femur is stronger and stiffer when impacted in the a-p direction than when impacted in the l-m direction. Bone is non-homogeneous, anisotropic and has properties that vary according to location on the bone. This directional change in properties, therefore, should be expected.

Bone develops in such a way that it is stronger in areas encountering greater stress. Since normal body activities (running, jumping, etc.) apply a moment to the femur similar to three-point loading in the a-p direction, this strength increase in the a-p direction is understandable.

No notable effects of age vs. strength or of age vs. stiffness were evident. While it is acknowledged that the bones of a 20-year-old would, on average, be stronger than 80-year-old bones, no data from this study supports that assumption as the specimens ranged in age from 53 to 89 years old.

Comparison of the fracture data of the bare femur versus the femur with all its associated soft tissue yielded no noticeable differences. In other words, the contributory role of embalmed soft tissues in affecting fracture outcome is minimal.

**PART 4**  
**IMPACT RESPONSE OF THE FEMUR**

## ABSTRACT

This paper presents some of the results of a research project entitled "Dynamic Response of the Human Leg to Impact Loading." A test facility was developed for laboratory experimentation that simulates leg impacts during automobile, pedestrian, motorcycle, and bicycle accidents. Analyses and discussions are presented for several experiments designed to study the mechanical behavior of the human femur subjected to impact loading.

About 100 bones have been broken in the specially designed laboratory as part of this research. The testing was divided into four categories: (1) femurs subjected to bending loads, (2) femurs under torsional loads, (3) femurs under axial loads, and (4) fresh tissue impact loadings.

The femur appears stronger when impacted in the anterior-to-posterior (a-p) direction than when impacted in the lateral-to-medial (l-m) direction. The fractures produced by the a-p impacts provide interesting clinical information. It was found that even very small torsional preloads can greatly diminish the femurs breaking strength. Axially loading the femur allowed mapping of the stress along the femur to accurately predict fracture locations.

Femur and intact thigh tests are continuing and these results will be supplemented in the future. This paper presents the implications of the first designed series of tests.



## INTRODUCTION

The work reported on in this paper is part of a research project entitled "Dynamic Response of the Human Leg to Impact Loading," being jointly conducted by the University of Tennessee and the University of Louisville. The intent of the research project is to describe and quantify the dynamic response of the human leg to impact loadings as encountered when pedestrians or cyclists are struck by automobiles. The approach has been to develop a test facility that simulates collisions between automobiles and pedestrians, motorcycles, or bicycles. The facility was designed so that it would produce leg injuries comparable to those normally seen in a clinical setting.

Progress made since the introduction of the research in 1986 has been significant and includes the design and installation of a state-of-the-art impact testing laboratory; the completion of impact tests using human legs, animal legs, and simulated leg structures; and development of a basic understanding of the response of the human leg to impact loading. Other contributions include appropriate biological and structural material testing, development efforts for a computer-based simulation of lower leg response to impact loading, clinical studies of accidents involving traumatic leg injury, statistical studies of traumatic injuries, whole body vibration research, underwater impact injury studies, head impact tolerance and experimental injury research, various accident reconstruction projects, causal mechanism analyses of human injury, and other biomechanical laboratory experimentation.

This paper presents some results for the purposes of understanding fracture behavior of the human femur during impact loading.

## **METHODOLOGY**

The biomechanics test facility discussed in the introduction was used for the experiments. The impact machine used for most of the tests will be referred to in this paper as the crash simulator. The three principle parts of the crash simulator are the accelerator and cart, the specimen holding device, and the force measurement system.

The simulator is a pneumatically-powered machine used to simulate a car/motorcycle or car/pedestrian collision. A cart of significant mass (50 kilograms) is propelled down a rail system where it impacts a test specimen (e.g. a human bone, a human leg, an animal bone or an artificial bone). The cart is instrumented with a force measurement system enabling the user to obtain dynamic force information during impact.

A 4.1275-centimeter (1 5/8-inch) pipe or a 7.62 x 20.32 x 0.3175 centimeter (3 x 8 x 1/8 inch) plate mounted on the cart serves as the impacting surface. Data from each test using the crash simulator is obtained via a force transducer mounted on the impact cart. The transducer is mounted in such a way that during impact it "feels" the same reaction that the test specimen does. The pipe or plate is held on by slide pins which allow all of the force to be transferred to the force transducer. The force transducer is manufactured by PCB Piezoelectronics,

model number 208A04. The sensitivity of the transducer is 1.16 kilonewtons per volt.

The signal from the force transducer passes through a PCB Power Unit and then to a Hewlett-Packard 3562a Dynamic Signal Analyzer where the force versus time history of the event is recorded.

For this study, four different types of tests using the crash simulator were conducted on the femur. These tests involved utilizing four separate support/specimen holding structures: simply-supported (pinned-pinned) bone loaded in the a-p direction; simply-supported bone loaded in the l-m direction; simply-supported bone with a torsional preload; and axially loaded bone.

Ninety-four bones were obtained for use in this study. Eighty of the bones were embalmed femurs with soft tissue removed. The other 14 bones were fresh, cryogenically frozen long bones from two recently deceased persons. Demographic information was available for some of the bones. The fresh frozen bones were thawed in a saline water bath just prior to testing.

A key objective of this study was to understand the mechanical behavior of the femur during impact, therefore a number of different loading conditions were applied to the bones. These different conditions can be described by dividing them into four types of tests: 1) bending, 2) torsional, 3) axial, and 4) fresh tissue tests.

In all tests except the low strain rate axial tests and the steady state torsional tests, the crash simulator was used. Data was recorded in the form of a

force-time plot, an example of which is shown in **Figure 1**.

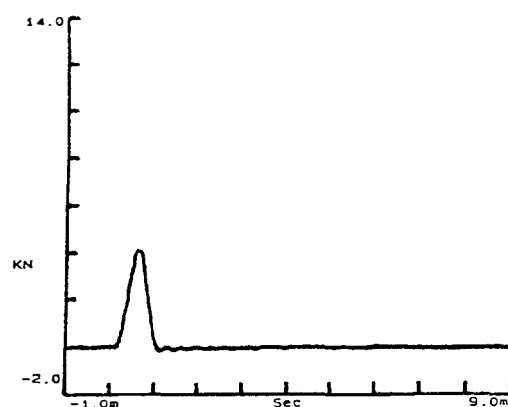


**FIGURE 1.** Sample force-time plot produced by crash simulator during impact.

The breaking force, the amount of time from impact initiation to fracture, and the area under the curve were obtained from each force-time curve. The breaking force was used to calculate, among other things, the ultimate stress. The time measurement allows for the calculation of displacement since there is a constant velocity through impact. The area under the curve is directly related (by the reciprocal of the volume) to the amount of energy absorbed during impact and is used strictly for comparison with other tests.

Prior to testing, certain anatomical measurements were made on the bones. Following testing, cortical thickness measurements were taken.

Protocol, justification and procedure for each test is detailed below.

### **Test Series I: Breaking Strength of Femur**

An automobile impact onto the side of a motorcycle is primarily a lateral-medial type of impact.

Lateral-medial loadings of bare femurs were accomplished using the crash

simulator at a speed of approximately seven meters per second. A "simple support, I-m loading" holding device was developed and used for these tests. Twelve femurs were tested.

The breaking force was determined for each bone from the force-time plot. The breaking forces for the twelve bones were averaged to determine a bone tolerance level. Kress (1989) reported good correlation between breaking strength and cortical thickness of long bone impact tests. First and second order curves were fit to the femur data.

Using the breaking force and the anatomical measurements taken for each bone, the ultimate bending stress can be approximated using beam theory.

The formula for calculating bending stress is

$$\sigma_{b(max)} = M_{(max)}c/I$$

where  $\sigma_b$  = bending stress, M = bending moment, c = distance from centroid to edge of beam, and I = moment of inertia.

For a simply-supported beam loaded in the center, the maximum moment is

$$M_{(max)} = PL/4$$

where P = breaking force and L = distance between supports.

For the femur calculations, the shaft will be considered a perfect cylinder with an outer radius,  $r_o$ , and an inner radius,  $r_i$ , with

$$r_i = r_o - t$$

where t is the cortical thickness. The cortical thickness is measured at six points at midshaft and averaged. Other researchers have supported this method (Viano

and Khalil, 1976; and Moore, 1985). This distance from a centroid to edge of bone,  $c$ , is simply  $r_o$ , and  $I$  is given by

$$I = [\pi/4](r_o^4 - (r_o - t)^4).$$

In addition to bending stress, Young's modulus can be approximated using beam theory. The equation for maximum deflection of this beam

$$\delta_{(max)} = PL^3/48EI$$

can be written as

$$E = PL^3/48\delta I$$

where  $E$  = Young's modulus and  $\delta$  = maximum deflection.

The maximum deflection is found by multiplying time of contact until fracture occurs by striker velocity, since there is no significant change in the striker velocity through the event. This calculation only gives an approximation for Young's modulus because the equation used is only valid for uniform cross-sectional bodies.

The area under the force-time curve is calculated to represent the relative energy absorption. The types of fractures that occurred were recorded.

Anterior-posterior loading of the femur is a common occurrence. It is most often associated with airborne bodies. Testing the femur in this direction was also of academic interest, because bone is non-homogeneous, anisotropic, and has complex, varying geometry.

Much of the procedure for this type of test was the same as for lateral-medially loaded femurs except that a "simple-support, a-p loading" holding device

was used and 32 femurs were tested.

Demographic information was available for these bones, making it possible to study age effects on the fracture behavior of the bone. In addition, this testing allowed for a comparison to be made between the behavior of left and right femurs of the same person.

### **Test Series II: Torsional Strength of Femur**

Six femurs were available for determination of the maximum, slowly-applied torque to produce failure. Gradually increasing torsional forces were applied until the bones fractured.

The maximum torsional stress is calculated as (remember the femur shaft is being considered as a hollow circular cylinder)

$$\tau_{(max)} = T_{(max)} c/J$$

where  $\tau$  = shear stress,  $T$  = torque,  $c$  = distance from centroid to outer edge of bone ( $r_o$ ), and  $J$  = polar moment of inertia,

$$J = [\pi/2](r_o^4 - (r_o - t)^4).$$

It is suspected that the legs of motorcycle riders undergo multiple loading configurations when suffering a collision.

To begin to understand the effects of these multiple loads, combined torsion and bending tests were performed. A torsional preload was placed on a simply-supported femur. The femur was then impacted at high-speed in the lateral-medial direction with the crash simulator.

To best understand the effect of the torsional preload, matched pairs of

femurs were used. The right femur was struck in the l-m direction with no torsional preload. The left femur was struck similarly but with a torsional preload.

### **Test Series III: Compressive Strength of Femur**

Although several researchers have investigated the compressive strength of the entire thigh, few, if any, have loaded a whole, bare femur in the axial direction at low (steady-state) and high speeds (7.6 meters per second). Eighteen bones were tested under such conditions.

A materials testing machine was employed to test nine bare, embalmed femurs in axial compression to failure. Cups simulating the acetabulum and the tibial plateau were designed to fit the machine and allow a distributed load on the condyles and head of the femur. The only data measured was the breaking forces. Video and photographic documentation allowed for the analysis of fractures.

Using the breaking force and the anatomical measurements, breaking strength can again be approximated using beam theory. Due to the geometry of the femur, an axial load is not truly an axial load. A bending element is also involved. The stress when bending and axial loads are involved is given by

$$\sigma_x = (\sigma_x)_{centric} + (\sigma_x)_{bending} = P/A \pm Mc/I$$

where P = force, A = cross-sectional area, M = bending moment, c = distance from centroid, and I = moment of inertia.

If axially loaded, the centric effect on the femur is completely compressive. However, the bending effect will impose compression on the medial side and



tension laterally. Therefore the stress in the bone is given by

$$\sigma_x = P/A + Mc/I \text{ (medial) and } \sigma_x = P/A - Mc/I \text{ (lateral)}.$$

It should be noted that these calculations are approximations.  $Mc/I$  does not hold when  $E_t$ , tension, does not equal  $E_c$ , compression. The  $E$ 's are close enough in the bone (four percent according to Evans, 1951), however, that this does not significantly change the results. Also, it should be noted that the neutral axis is not the same as the centroidal axis.

Stresses were calculated at three cross-sections on the bone: at midshaft, just below the greater trochanter, and at the neck of the femur (see **Figure 2**). The cross-section of minimum moment of inertia was chosen at each area.

The breaking force,  $P$ , and cross-sectional areas are taken directly from measurements. The bending moment,  $M$ , is equal to  $Pd$  ( $M = Pd$ ) where  $d$  = moment arm. A hollow cylinder cross-section is assumed as before.

In order to examine high speed loading of the femur in the axial direction, nine femurs have been impacted in the crash simulator. The axial loading, specimen holding device was used. The flat plate impactor was used instead of the pipe.

Measurements and calculations for these tests were the same as for the statically loaded bone.

#### **Test Series IV: Fresh Tissue Testing**

The type of preservation technique used on the tested bones affects the properties of the bones. In an effort to begin to examine these effects, 14 fresh

bones were tested in the crash simulator. These bones were cryogenically frozen just after death and were wet-thawed shortly before testing.

Breaking force and area-under-curve data were obtained for each bone. Anatomical measurements were not taken due to the disease risks of the bones utilized.

## **RESULTS AND DISCUSSION**

Results from 94 bone-breaking tests are presented. Embalmed, bare femurs have been broken at high speeds (approximately 7 m/s) in the lateral-medial, anterior-posterior, and axial directions. Bone fracture tests have also been performed for steady-state force application in the axial direction and in torsion. Other conditions have included impacting in the lateral-medial direction while the bones are subjected to a torsional preload and a series of fresh bone tests.

### **Test Series I: Breaking Strength of Femur**

Twelve femurs have been impacted in the crash simulator in the lateral-medial direction. Their average cortex thickness was 0.00691 meters and average breaking force was 3053 Newtons (N). Anatomical measurements were not available for three of the bones, and force signals were not obtained for three bones. Linear regression was used to develop a relationship between breaking force and average cortex thickness, and the correlation coefficient was 0.61. The second order correlation coefficient improves to 0.82. The least squares relationship is

$$\text{Breaking Force (N)} = -22 + 52 \times \text{cortex}^2 \text{ (mm)}.$$

The ultimate bending strength and Young's modulus were calculated by the method described in the methodology section. The average breaking force was 3053 Newtons; the average bending strength was 147 Megapascals; and the average Young's modulus was 30 Gigapascals. These values compare favorably to values found in previous literature.

The average area under the force-time curve is 2236 N-ms. This value is difficult to interpret. It is, however, related to the amount of energy absorbed during impact and can be compared to other area under force-time curve calculations.

Six of the twelve fractures were comminutions (see **Table 1**). Most of the comminutions produced tension wedges, that is the fracture started on the tension side of the bending bone. Oblique and spiral fractures occurred. The spiral fractures were probably caused by the specimen holding device which also served as a torsional delivery system. Its configuration alone may have encouraged a spiral fracture. One bone that had severe osteoporosis shattered upon impact.

**TABLE 1. Types of Fractures Occurring in L-M Loaded Femurs**

Fracture Type	Number	Percentage %
Comminution		
Tension Wedge	5	41.7
Compression Wedge	1	8.3
Oblique	3	25.0
Spiral	2	16.7
Shatter	1	8.3

Effects of impact direction on the properties of the bone were investigated by turning the femurs 90 degrees and striking them in the anterior-posterior direction. The crash simulator was used to break 32 femurs in this manner. Anatomical measurements, support distance, and breaking force data for all of the bones tested were recorded. The average cortex thickness was 0.00739 meters and the average breaking force was 5697 Newtons. The linear regression between breaking force and cortex thickness had a linear correlation coefficient of 0.40. The second order correlation was 0.42 only improving the relation slightly. Therefore the linear regression polynomial curve fit equations for these tests will not be provided.

The ultimate bending stress and Young's modulus were calculated. The average bending stress was 284 Megapascals, and the average Young's modulus was 88 Gigapascals.

Ages of specimens ranged from 53 to 89 years old. Ultimate Bending Stress and Young's Modulus were compared and the scatter of data indicated no real age dependence in this range of age.

The breaking stress of right and left matched pairs of femurs (two femurs belonging to the same individual) were compared. The result, surprisingly, is that the left bone is roughly eight percent stronger on average than the right bone. However, a closer examination of the data reveals that two sets of bones had the left one much stronger than the right (for whatever reason). Discarding these two sets from the averaging results in virtually equal strength for right and left bones.

Area under the force-time curve for each bone was determined. The average value is 2658 N-ms. The value for the l-m loaded femurs was 2254 N-ms. The a-p loaded bone, therefore, does not absorb much more energy than the l-m loaded bone, although the strength is much greater in the a-p direction.

Seventy-one percent of the fractures in this a-p test were comminuted (see **Table 2**). Interestingly, however, few produced tension (3) or compression (2) wedges. The vast majority (17) of the comminuted fractures were side wedges. The side wedges were equally dispersed as lateral and medial wedges. Eight fractures were oblique, and one was a shatter.

**Table 2. Types of Fractures Occurring in A-P Loaded Femurs**

Fracture Type	Number	Percentage %
Comminution		
Tension Wedge	3	9.6
Compression Wedge	2	6.5
Oblique	17	54.8
Spiral	8	25.8
Shatter	1	3.2

### **Test Series II: Torsional Strength of Femur**

Six femurs were loaded in torsion at low strain rates. The average cortex thickness, support distance and maximum torque for each bone is presented in **Table 3**. The linear relation, with a correlation coefficient of 0.90, between maximum torque and cortex thickness is given by

$$\text{Maximum Torque (N-m)} = 6 + 15 \times \text{cortex (mm)}.$$

Using a polynomial curve fit improves the relation to 0.92. The least squares fit is

$$\text{Maximum Torque (N-m)} = 49 + 1.2 \times \text{cortex}^2 \text{ (mm)}.$$

**TABLE 3. Independent Variables and Torque Data on Femurs Loaded in Torsion at Low Strain Rates**

Bone	Cortex Thickness (meters)	Support Distance (meters)	Maximum Torque (N- m)
1	.00564	.381	96.0
2	.00758	.381	154.6
3	.00628	.318	113.8
4	.00894	.356	115.9
5	.00959	.387	145.0
6	.00201	.330	<u>24.4</u>
Average			108

Ultimate torsional stress was calculated. The average breaking torque of 108 N-m is slightly lower than Yamada's (1971). If, however, bone six is removed from the average, the breaking torque comes up to 125 N-m. Bone six was highly osteoporotic.

The torsional strength of 28 MPa is also lower than Yamada's value of 45 MPa. This is attributed to our use of embalmed (and perhaps older) bones rather than fresh, wet bones used by Yamada.

Five of the six femur fractures were spiral. The osteoporotic bone six shattered.

The question of combined loads on the femur was investigated by loading six bones in torsion and in bending. A torsional preload was placed on the bones, which were then impacted in the lateral-medial direction by the crash simulator.

Cortex thickness, support distance, amount of preload and breaking force are shown in **Table 4**. Notice that two different torque levels were used.

**TABLE 4. Independent Variables and Torque Data for Femurs Loaded in L-M Bending with Torsional Preload**

Bone	Cortex Thickness (meters)	Support Distance (meters)	Torsional Preload (N-m)	Breaking Force (N)
RPFTU1L	.00611	.41	20.2	3657
RPFTU2L	.00586	.33	10.1	1355
RPFTU3L	.00702	.33	10.1	3335
RPFTNO2L	.00598	.33	10.1	1684
RPFTU4L	.00810	.34	20.2	1234
RPFTU5L	.00743	.36	20.2	1806

All six bones used in these tests were the matching pairs to the six bones tested in the lateral-medial direction without a torsional preload. The average breaking force with no torsional preload was 2549 Newtons. The average with a preload was 2179 Newtons.

After data manipulation, it was determined that on the average, a 14 percent torsional preload decreases the breaking force 14 percent. Interestingly, spiral fractures are present in 50 percent of these preloaded bones.

### **Test Series III: Compressive Strength of Femur**

Nine femurs were loaded at low strain rates in the axial direction using a materials testing machine. The output from the machine is a force reading.

From the ultimate load and anatomical measurements, stresses can be calculated. Since fractures under these loading conditions occur most frequently at three locations (midshaft, sub-trochanter, and neck), stress calculations at all

three of these cross-sections were made for each bone.

The six calculated stress values for each bone were recorded on figures as illustrated generally in **Figure 2**. There were two calculated values (lateral and medial) for each of the three locations. Stresses on the lateral side of the bone are tensile and are compressive on the medial sides. Based on the stresses, predictions were made for the fracture location. On eight of the nine femurs the prediction is correct. Bone #881R was the only incorrectly predicted fracture. On this test the cup holding the head of the femur was impinging its neck leading to fracture at that site. In all cases the compressive stress is approximately 1.5 times greater than the tensile. 77.8% of the fractures occurred on the neck, 11.1% were sub-trochanteric, and 11.1% were simultaneous neck and shaft fractures.

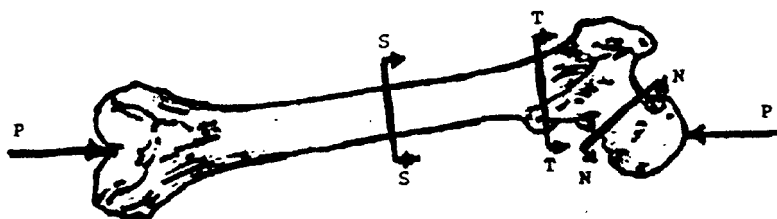


**FIGURE 2.** Diagram of axially loaded femur showing cross-sections of stress calculation: S=shaft, T=trochanter, N=neck.

High speed axial impacts of the bare femur were of interest next. Nine bones were struck in this matter; six provided good force data.

Stresses were calculated, mapped, and examined on these bones as previously done. In these cases, all predictions for fracture locations were correct. The only minor exception was a concomitant shaft fracture along with the



predicted neck fracture in bone #862L. Such concomitant fractures are common clinically (Chapman, 1984). Once again, the compressive stresses are 1.5 times greater than the tensile. 66.7% of the fractures were in the neck, 16.7% were sub-trochantric, and 16.7% were in the shaft.

#### **Test Series IV: Fresh Tissue Testing**

Fourteen cryogenically-frozen, fresh long bones were broken to help understand the effects of embalming on the properties of the bone.

**Table 5** presents the results of these tests. When compared to the embalmed data, breaking force values appear to increase 44 percent for fresh femurs and 78 percent for fresh tibias. Energy absorption also increases for fresh bones. There is, however, too little data to make definitive conclusions.

**TABLE 5. Results from A-P Impact of Fresh Long Bones of Two Individuals**

Cadaver Number	Bone	Breaking Force (N)
105	Femur (right)	9482
	Femur (left)	10017
	Tibia (right)	6620
	Tibia (left)	5542
	Fibula (right)	930
	Fibula (left)	772
	Humerus (right)	5285
	Humerus (left)	4469
98	Femur (right)	7228
	Femur (left)	6065
	Tibia (right)	4988
	Tibia (left)	4313
	Fibula (right)	1129
	Fibula (left)	895

## Summary of Recorded and Calculated Response Characteristics

**Table 6** presents a summary of the test conditions and recorded data for all of the different tests that have been performed to date utilizing the femur.

**Table 7** contains some calculated response characteristics from data obtained in selected femur tests.

If a discrepancy is noticed between certain n values, it should be noted that some of the data, due to their specious nature, were excluded from calculations.

**TABLE 6. Summary of the Response Characteristics of the Human Femur**

n	Impact Direction	Impactor	Average Force (kN)	Standard Deviation (kN)	Average Velocity (m/s)	Fracture Classifications	Remarks
2	A-P D ½	4.13 cm Pipe	4.22	0.49	7.5	(n=2) 50% Tension Wedge 50% Comminuted	Impacted distal third.
2	A-P	4.13 cm Pipe	1.00	0.64	Static	(n=2) 50% Tension Wedge 50% Comminuted	Manual Push.
4	A-P	4.13 cm Pipe	8.20	1.86	6.6	(n=4) 50% Oblique 50% Transverse	Cryogenic Fresh. Thawed for test.
30 26*	A-P -	4.13 cm Pipe (Pre-1) -	5.76 5.78	1.93 1.41	7.5 7.5	(n=32) 40.65 Comminuted 15.6% Oblique 12.5% Segmental 21.9% Side Wedge 6.3% Compression Wedge 3.1% Tension Wedge	*Specious values for #798L, 796R, 720L & 551L, excluded in "n=26." #776L & 779L, had no $\mu$ recording.
2	A-P	70mm Snub	0.98	0.27	7.5	(n=2) Both Comminuted Longitudinal Segments.	Drop-tower Impactor (DRI).
2	Pure Torsion	Pre-torque Device	58.1 N-m	53.7 N-m	Static	(n=2) Both Spiral Fractures.	Failed during pre-torque for "Pipe (Pre-T)" setup.
6 5*	Pure Torsion -	S-S Torsion -	108.3 N-m 125.1 N-m	46.4 N-m 24.1 N-m	Static Static	(n=6) All Spiral Fractures.	*Specious value of #6 was excluded in "n=5."
4 3*	L-M -	4.13 cm Pipe (Pre-1) -	2.86 2.13	1.70 1.06	7.0 6.8	(n=4) 75% Segmental 25% Oblique	Pre-torque of 20.14 N-m. *Specious value of #695R was excluded in "n=3."
4 3*	L-M -	4.13 cm Pipe (Pre-1) -	2.70 1.57	2.72 1.84	6.8 6.8	(n=6) 66.7% Spiral 33.3% Comminuted	Pre-torque of 10.06 N-m. #689 R & U7L had no recording of force. *Specious value of #U6L was excluded in "n=3."
2	L-M P½	4.13 cm Pipe	5.60	1.63	7.5	(n=3) 33.3% Tension Wedge 33.3% Oblique 33.4% Comminuted	Impacted proximal third. #997L had no recording of force.
17	L-M	4.13 cm Pipe	3.16	1.89	7.1	(n=18) 27.8% Oblique 27.8% Segmental 16.7% Tension Wedges 11.1% Other Wedges 11.1% Compression Wedges 5.6% Comminuted	#698L had no recording of force.
1	L-M	10 cm Plate	4.57	na	7.5	(n=1) Compression Wedge	
10 8*	Axial -	10 cm Plate -	7.11 7.06	2.32 1.73	6.8 6.6	(n=10) 80% Involved Hip 40% Involved Shaft 20% Involved Knee	*Specious values for #557L & 4L were excluded in "n=8."
9 7*	Axial -	Materials Testing Machine	5.27 5.01	2.47 1.44	Static Static	(n=9) 80.9% Neck Fractures 11.1% Subtrochanteric Fracture.	Compression testing of whole femur. *Specious values for #859R & 812 R were excluded in "n=7."

**TABLE 7. Some Calculated Dynamic Response Characteristics from Selected Data of the Human Femur**

FEMUR (Avg. Cortex Thickness = 5.75 mm)						
12	L-M	4.13 cm Pipe	3.05	7.6	41.7% comminuted (tension wedge most prevalent)	Bending Strength = 147 MPa Young's Modulus = 30 GPa Energy = 2,236 N-ms
30	A-P	4.13 cm Pipe	5.70	7.5	70.9% comminuted (side wedge most prevalent)	Bending Strength = 284 MPa Young's Modulus = 88 GPa Energy = 2,658 N-ms
5	Pure Torsion	S-S Torsion	125.1 N-m	Static	All spiral fractures	Torsional Stress = 26 MPa
9	Axial	Materials Testing Machine	5.27	Static	88.9% Neck Fractures 11.1% Subtrochantric fractures	Compressive Stress = 125 MPa Tensile Stress = 79 MPa Compressive Strength is 1.5 times > tensile strength
6	Axial	10 cm Plate	6.46	7.6	80% Involved Hip 40% Involved Shaft 20% Involved Knee	Compressive Stress = 174 MPa Tensile Stress = 121 MPa

Note: All bones and intact specimens were embalmed and impacted while simply-supported, unless noted otherwise.

## CONCLUSIONS

This paper has presented data on the impact response of the human femur under several loading conditions. The data presented are important, because of the role they can play in the quantification of the damage to hard and soft tissue under loading conditions similar to those which occur when an automobile impacts a human leg. The data provides insight into protection mechanism design and input for computer and physical models. The results of each test series are discussed below.

### Test Series 1: Breaking Strength of Femur

From the data, it is apparent that the femur is stronger and stiffer when impacted in the anterior-posterior direction than when impacted in the lateral-medial direction. Bone is non-homogeneous, anisotropic and has properties that vary according to location on the bone (Evans, 1951). This directional change in properties, therefore, should be expected.

Bone develops in such a way that it is stronger in areas encountering greater stress. Since normal body activities (walking, running, etc.) put a moment on the femur similar to three-point loading in the a-p direction, this strength increase in the a-p direction can be expected.

No notable effects of age vs. strength or of age vs. stiffness were evident. While it is acknowledged that 20-year-old bones on the average would be stronger than 80-year-old bones, no such statement can be made for the age span of the specimens in this study (53 to 89 years old).

Mather (1968) showed that the left and right femurs absorbed the same amounts of energy when impacted. It was further shown in this report that left and right matched pairs have essentially equal properties (with only a few exceptions). This finding adds validity to many past experiments involving testing of matched pairs of bones. Comments about the resultant fractures from bending impact tests may be of interest. The lateral-medial impacts produced wedges that occurred on the lateral and medial sides. The anterior-posterior impacts also produced wedges occurring on the lateral and medial sides. Kress (1989) stated that a vast majority of clinically seen femur impacts occur in the l-m direction. With these additional findings, however, it is possible that a-p impacts may actually be mislabeled clinically as l-m impacts.

## **Test Series II: Torsional Strength of Femur**

Low strain rate torsional tests were performed to develop a relationship between ultimate torque and cortical thickness. This relationship permitted the

calculation of "percentage of maximum torque" values that established torsional preloads.

The tests clearly showed that even a small torsional preload reduced the breaking strength of the femur significantly. It also showed that a small torsional load (as compared to the impact load) can still result in a spiral fracture of the femur.

### **Test Series III: Compressive Strength of Femur**

True axial loading in compression should produce only compressive stresses. However, in these axial experiments on the femur, tensile stresses resulting from bending could actually be the fracture initiators.

From the process of mapping out the stress on the bone, predicting the fracture, and showing the actual fracture location, it is obvious that bone geometry is the critical parameter in determining fracture location. In 14 out of 15 tests, the cross-section under the greatest calculated stress was the fracture site. Predictions were easy to make and extremely accurate.

A majority of the fractures (80 percent) occurred at the neck of the femur. This number appears high when compared to clinical studies where 50 percent of automobile accident victims (Daffner et al., 1988) and 17 percent of motorcycle victims (Deaner et al., 1975) with broken femurs have neck fractures. But when you consider age of the bones studied (the average age was 64.9 years), 80 percent neck fractures is not surprising. Osteoporosis attacks the femur in a disproportionate manner. The neck of the femur tends to lose bone at a higher

disproportionate manner. The neck of the femur tends to lose bone at a higher rate than the rest of the femur (Hofeldt, 1987). As evidence of this, the three youngest bones tested broke at the shaft.

Fung (1984) reported a compressive strength in bone that is approximately 1.5 times greater than its tensile strength. Viewing the figures of mapped out stresses on the femur, it can be seen that the compressive stress on the medial side of the femur is always approximately 1.5 times the tensile stress on the lateral side of the femur.

The impact breaking strength was 39 percent greater than the breaking strength at very slow rates of load application. This change is significant and is almost exactly the change predicted by McElhaney (1966). This indicates that high-speed impact tests are necessary for studying automobile-motorcycle collisions.

The average breaking load for the slowly loaded bone was 5274 Newtons and for the impacted bones was 6464 Newtons. Present automobile design regulations dictate that a force of 10,000 Newtons may not be exceeded when a knee impacts a dashboard at 6.6 meters per second (Krishnaswamy, 1991). Results from this research indicate that this level might be high. Only one femur had a breaking tolerance higher than 10,000 Newtons.

More tests need to be performed in this area. Since a preponderance of neck fractures occur when using femurs of the elderly, young bones need to be tested. This is not as important in the other tests (l-m, a-p, torsion), since the bone

however, the neck of old bones fracture before the shaft fracture threshold can be measured.

#### **Test Series IV: Fresh Tissue Testing**

Findings from this research, based on results from a small sample size, indicate that there is a significant change between fresh and embalmed properties.

The fresh human femurs were 43.9 percent stronger than the embalmed femurs and absorbed 79.8 percent more energy. The difference in breaking strength for the tibias was even greater.

This conclusion must be viewed carefully. Only 14 fresh bones were tested. Also, these fresh bones came from individuals younger than the average embalmed bone donor.

More fresh tissue testing needs to be performed, and anatomical measurements need to be taken on the fresh tissue tested. This will help determine the exact difference between fresh and embalmed tissue.

## BIBLIOGRAPHY

- Chapman, Michael W. "Concomitant Ipsilateral Fractures of the Hip and Femur." The Multiply Injured Patient with Complex Fractures, Meyers, Marvin H., Editor, Philadelphia: Lea and Febiger, 1984.
- Daffner, Richard H., et al. "Patterns of High-Speed Impact Injuries in Motor Vehicle Occupants." Journal of Trauma, 28(1988), pp. 498-501.
- Deaner, R.M., and V.H. Fitchett. "Motorcycle Trauma." Journal of Trauma, 15(1975), pp. 678-681.
- Evans, F.G., and M. Lebow. "Regional Differences in Some of the Physical Properties of Human Femur." J. Applied Physiol., 2(1951), pp. 563-572.
- Fung, Y.C. Biomechanics - Mechanical Properties of Living Tissues. New York: Springer-Verlag, 1981.
- Hofeldt, Fred. "Proximal Femoral Fractures." Clinical Orthopaedics and Related Research, 1987, pp. 12-18.
- Kress, Tyler A. "Mechanical Behavior of Lower Limbs in Response to Impact Loading: Facility Development and Initial Results." Master of Science Thesis in Engineering Science, The University of Tennessee, Knoxville, 1989.
- Krishnaswamy, Prakash, et al. "Crash Codes Pave the Way to Safer Vehicles." Mechanical Engineering, 113(1991), pp. 60-62.
- Mather, B. S. "Variation with Age and Sex in Strength of the Femur." Med. and Biol. Engr., 6(1968), pp. 129-132.
- McElhaney, James H. "Dynamic Response of Bone and Muscle Tissue." Journal of Applied Physiology, 21(1966), pp. 1231-1236.
- Moore, Keith L. Clinically Oriented Anatomy. Baltimore: Williams and Wilkins, 1985.
- Tucker, Guy V. "The Mechanical Behavior of the Human Femur Subjected to Impact Loading." Master of Science Thesis in Engineering Science, The University of Tennessee, Knoxville, 1991.
- Viano, D.C., and T.B. Khalil. "Investigation of Impact Response and Fracture of the Human Femur by finite Element Modeling." Proceedings Mathematical Modeling Biodynamic Response to Impact. Society of Automotive Engineers, Inc., 760773, 1976, pp. 53-60.



## **PART 5**

### **AN IMPACT RESPONSE COMPARISON OF UNEMBALMED VS. EMBALMED LEGS**

## ABSTRACT

Intact legs from nine cadavers were collected for dynamic impacting to emulate motor vehicle trauma. Bequeathed cadavers arrived at the University of Louisville School of Medicine within 48 hours of expiration (all post-rigor mortis). Cadavers were screened for HIV and Hepatitis B virus. One leg was immediately removed and frozen at 0° C until thawed for testing. The other leg remained with the cadaver to be embalmed by standard femoral artery injection with 20% Isopropyl Alcohol, 20% Propylene Glycol, 4% Formalin (37% Formaldehyde Solution), 4% Phenol and 52% Warm Water. The embalmed legs were removed from the cadavers after a minimum of 7 weeks. Pre-test radiographs were made and the legs were transported to the University of Tennessee Engineering Institute for Trauma and Injury Prevention. Just prior to testing, a hole was drilled in the femur and a rod was inserted from side to side. The leg was placed upright in the test zone and a weight of over 50 kgs. was applied to the rod (simulating upper body mass). An athletic shoe was placed on the foot and the foot was set on a concrete block. Additionally, for most tests, there was an attempt to pressurize the vasculature by use of a crude embalming pump. The impacting apparatus consisted of a 50 kg. cart propelled by a pneumatic accelerator to approximately 7.7 m/s into the anterior of the leg midway between the knee and the ankle. The cart was headed by a steel pipe of nearly 4.75 cm. diameter. The pipe was coupled to a force transducer which

relayed impact force data to a Hewlett Packard 3562A computer signal analyzer system. Testing was captured on VHS video, 35 mm still photos and 16 mm color high speed film shot at 1,000 frames per second. Post-test analyses included radiographs and thorough dissection.

## **INTRODUCTION**

Several test subjects are available to researchers in the study of human trauma biomechanics. These include animals, surrogates (crash dummies), cadavers, and occasionally combinations thereof. Studies may be performed on live, anaesthetized animals but their anatomy, and the way in which it behaves dynamically, is often significantly different from humans. Although surrogate technology is progressing rapidly, the ability to directly infer the extent of injury (i.e. traumatized anatomy) is still insufficient.

Several issues must be considered when determining the proper experimental design. Will the subject be easy to instrument? Will results be consistent from test to test? Is the subject representative of human geometry? Is it sufficiently deformable or frangible, etc.? Cost is also an important consideration but specimen biofidelity may be paramount. Is the subject going to yield an accurate picture of actual human trauma? In order to have valid trauma data, it is important to determine the amount of damage done by certain events. Cadaver use may be superior to the use of animals or surrogates in maintaining

biofidelity but many drawbacks still exist:

1) Most bequeathed cadavers are the remains of persons who were of great age and of generally declining health. It can be argued, however, that safety designs that mitigate trauma for these specimens would likely be beneficial to almost any member of society (excluding some important different design challenges with regard to the small bodies of infants and children). In other words, if we can protect the most feeble members of our society then it stands to reason that the more stout persons will also be protected.

2) Cadaveric specimens lack the normal physiologic internal pressures of living persons including vascular pressure and normal turgor of the tissues, cells and the extracellular fluid. Shortly after death the decay process begins and cells quickly begin to deteriorate. This can be temporarily arrested to some degree by prompt freezing, but thawing brings about a return of the decay process.

3) Kinematics of a flaccid human cadaver may differ from those of a live person. However, this may be of little consequence during high speed dynamic experimentation. In such testing the velocities associated with the impact are high enough that human responses such as bracing, deflecting, and tensing have minimal effect on resultant injuries. So, the flaccid nature of the cadaver is not a major drawback as long as the mass/inertial effects of various body components are properly modeled or accounted for.

If the cadaver is deemed the appropriate model for experimentation, then the next consideration is whether to use unembalmed or embalmed tissue. Unembalmed or fresh tissue may be a pathogenic biohazard putting handlers at risk for AIDS, hepatitis, etc. Fixing the tissues as is done in the embalming process makes handling nearly risk free. Therefore, embalmed tissue has considerable advantages over unembalmed tissue in terms of its safety, ease of handling, and storage. It is assumed, however, that the biofidelity of embalmed tissue is less than that of unembalmed.

## **OBJECTIVE**

The objective of this study was to determine how the traumatized anatomy of embalmed human cadaver legs differs from that of unembalmed legs. The legs were impacted in experiments that simulate trauma due to motor vehicle accidents. Every effort was made to make the specimens as "life-like" as possible in hopes that the dynamic response would be similar to that of a live standing or walking human struck in the leg by an object of relatively large mass (automobile, motorcycle, etc.). Testing conditions accounted for: 1) the constraints of the upper body mass, 2) friction between the foot and the pavement, and 3) pressurization of the vasculature.

The extreme variability between human cadavers was accounted for by making the study self-controlled in that, for each cadaver, one leg was left

unembalmed and the other was embalmed. Therefore, age, sex and overall physical condition could essentially be "factored out" allowing for a more meaningful comparison of the collected impact data.

## **METHODOLOGY**

Cadavers are generously bequeathed to the University of Louisville Medical School for the expressed purpose of research and education. Many of the cadavers are preserved and dissected in a gross anatomy course for dental students. The lower limbs are not studied in this course, and therefore, the limbs are available for research pending committee and departmental approval. Approval was granted for ten such cadavers to be used in this study. The cadavers are usually received by the medical school within 48 hours of expiration (post-rigor mortis).

Upon arrival, cadavers were evaluated by a two-step screening process for inclusion in this study. First, an attempt was made to enter an equal number of males and females all of whom were ambulatory and did not appear to suffer a prolonged death. Ten suitable specimens were identified. The second phase of screening involved the collection of blood serum which was tested for the presence of hepatitis B surface antigens (HBV) and human immunodeficiency virus (HIV) antibody. Unfortunately, one of the ten tested positive for HBV and was immediately rejected and cremated. Thus nine pairs of legs were available

for this study (see **Table 1**).

For each cadaver, one leg was sectioned from the body, bagged in plastic and securely placed in a freezer at 0° Celsius. The other leg remained with the body which was embalmed, bagged and stored for at least seven weeks. Embalming was achieved through femoral artery perfusion of a relatively standard preservative solution consisting of 20% isopropyl alcohol, 20% propylene glycol, 4% formalin (37% formaldehyde solution), 4% phenol and 52% warm water.

Just prior to departure for testing, the embalmed legs were removed from the cadavers and taken to a special radiology suite along with the frozen unembalmed mates. Pre-test radiographs were made in order to rule out recent fractures or the presence of prosthetic devices. After checking the X-ray films, the specimens were transported to a unique dynamic impactor facility at the University of Tennessee in Knoxville, TN, USA. The facility is housed within the Department of Industrial Engineering and operated by the Engineering Institute for Trauma and Injury Prevention. The unembalmed and embalmed legs were each subjected to the same test scenario.

Upon arrival at the test facility, the frozen specimens were allowed to thaw for at least twenty-four hours. Immediately prior to testing, the specimens were removed from their plastic bags and a hole was drilled from side-to-side in the

**TABLE 1. Specimen Data**

Specimen Number	Age and Sex	Cause of Death <sup>2</sup>	Left or Right	Embalmed or Unembalmed	Time (months) Embalmed or Frozen
295	74-F	Lung Cancer and Pulmonary Disease	R	E	4½
			L	U	4
300 <sup>1</sup>	92-M	Cardiac Arrest and Diabetes Mellitus	R	E	4
			L	U	3½
301	94-F	Pneumonia and Dehydration	L	E	4
			R	U	3½
306	75-M	Small Cell Lung Cancer	L	E	3½
			R	U	3
308	79-M	Acute Myocardial Infarction	L	E	3
			R	U	2½
310	91-F	Urosepsis and Dehydration	R	E	3
			L	U	2½
312	43-F	Liver Failure and Cervical Cancer	L	E	2½
			R	U	2
314	76-M	Myocardial Infarction and old Stroke	R	E	2¼
			L	U	1¾
316	91-M	Adenocarcinoma and Colon Cancer	R	E	2¼
			L	U	1¾

Notes: <sup>1</sup> All specimens were Caucasian except for 300 which was African-American.

<sup>2</sup> Causes of death are listed as noted on the death certificate.

distal femur at the level of the condyles. A rod was passed through the hole and the leg was placed upright in the impact zone of the test machine. A weight of over 50 kgs. was applied to the rod in an effort to simulate the upper body mass.



The foot of the specimen was placed in an athletic shoe and set on a concrete surface. Additionally, for most tests, an attempt was made to pressurize the vasculature by using a crude embalming machine to infuse the vessels with a sugar water solution via cannulation of the popliteal or femoral artery (depending on where the specimens were sectioned at the thigh). The machine registered a pressure of between 2 and 3 psi (A resting systolic blood pressure of 120 mm Hg is equivalent to about 16 KPa which is roughly 2.3 psi). Two of the embalmed legs (301L and 314R) could not be adequately pressurized presumably due to the presence of fixed blood in the vessels. In one case (308L), an abnormal branching pattern of the femoral artery resulted in numerous small arteries, none of which would accept the pressurization cannula. Although the veins were of sufficient size, any attempt to pressurize them would have been futile due to the presence of natural one-way valves designed to prevent the flow of blood down the leg. **Figure 1** (on p.5) shows a specimen in the test set-up.

Every effort was made to ensure that the set-up conditions for each specimen remained consistent. This was a difficult task due to the soft and highly flexible nature of the unembalmed specimens. In this photo a stack of weights is seen at center top. The bar supporting those weights is connected to a harness that straddles the leg and is connected from side-to-side by a rod through the femoral condyles. The various riggings seen restrict movement of the weights after impact. The foot was placed in a shoe on one or two concrete blocks depending on specimen length. Note the plastic tubing on the left leading to the top of the specimen. This is the tube used in an attempt to pressurize the vasculature with a sugar water solution. The impact cart will strike the specimen as it runs from right to left in this photo. The small up-turned lamp in the center of the photo is part of the timing mechanism for cart velocity determination.

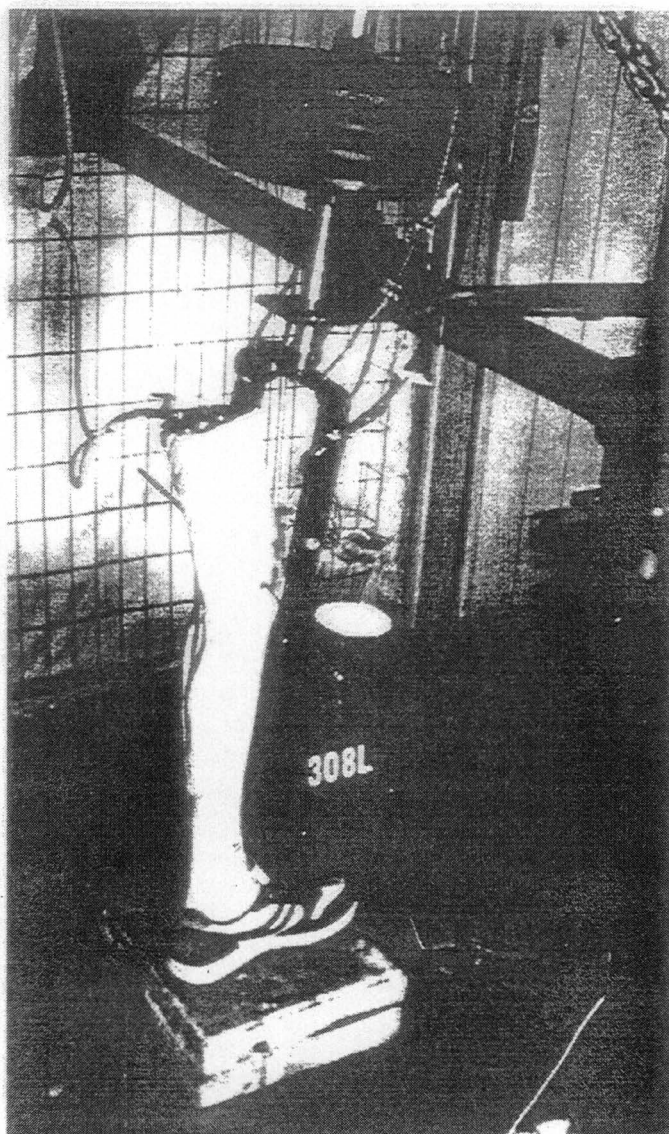


**FIGURE 1.** Test set-up.

The specimens were impacted on the anterior mid-leg by a 50 kg impact cart. The cart is propelled by a pneumatic-based accelerator to a velocity of approximately 7.7 m/s (range = 7.15 to 7.94). The accelerator consists of a pressurized cylinder with a piston and ram system. The ram pushes the rail-guided cart through a stroke of approximately 1.5 m, then the cart travels freely for about 0.5 m before impacting the specimen.

The leading or striking edge of the cart consists of a steel pipe measuring 4.75 cm in diameter. The pipe is mounted to the cart transversely by two slide pins that enable the pipe to freely impinge on a piezoelectric quartz force transducer (PCB Series 208A). The signal from the force transducer is transmitted through an amplifier and on to a Hewlett Packard 3562A signal analyzer. A record of force versus time is stored for each test (system error led to no trigger of the analyzer on test 295R). Testing was also recorded with 35 mm still photography and on standard VHS video at 30 frames/s. Most of the tests were filmed with a 16 mm rotating prism high speed camera at 1,000 frames/s on color 400 ASA film for tungsten lighting.

After testing, the legs were x-rayed again and then carefully dissected. All damage was noted and photographed. Vessel integrity was determined by pressurization with a syringe. Remains were returned to the University of Louisville School of Medicine for proper cremation and burial.

## RESULTS

Mid-shaft tibial cortex thickness, peak force and cart velocity data are listed for each test in **Table 2**. Dissection results indicating damage to the skin, muscles, vessels and bone are summarized in **Table 3**.

**TABLE 2. Test Data**

Specimen <sup>1</sup>	Avg. / Smallest Cortex Thickness (mm)	Peak Force (kN)	Cart Velocity (m/s)
295Re	4.33 / 1.97	No Trigger	7.08
295Lu	4.93 / 2.10	5.95	7.94
300Re	6.74 / 4.33	6.80	7.15
300Lu	6.56 / 3.53	7.80	7.62
301Le	6.24 / 3.36	4.78	7.30
301Ru	4.13 / 2.90	4.18	7.87
306Le	7.79 / 4.61	8.46	7.30
306Ru	7.49 / 4.81	6.21	7.84
308Le	7.89 / 4.25	8.46	7.71
308Ru	7.74 / 4.79	7.43	7.69
310Re	4.15 / 2.48	5.03	7.48
310Lu	5.34 / 3.05	3.75	7.84
312Le	6.29 / 4.11	5.32	7.51
312Ru <sup>2</sup>	8.41 / 5.27	5.69	7.76
314Re	7.85 / 5.13	7.56	7.59
314Lu <sup>2</sup>	7.02 / 4.29	6.29	7.41
316Re	6.56 / 4.41	7.51	7.50
316Lu <sup>2</sup>	8.31 / 7.38	8.16	7.35

Notes: <sup>1</sup> The specimen number is listed followed by designations for left (L) or right (R) and embalmed (e) or unembalmed (u).

<sup>2</sup> These specimens did not fracture.

**TABLE 3. Damage Summary (Dissection Results)**

Leg <sup>1</sup>	Laceration <sup>2</sup>		Muscles & Ligaments Damaged <sup>3</sup>	Vessels <sup>4</sup>	Bone Fractures <sup>5</sup>
295Re	4	20.5	5% TA	Fib V	Bad Comm >15 pcs
295Lu	2	34.0	60% Gas & Sol, 100% EHL & TP, 50% FDL & FHL, 10% FiB	None	Bad Comm >6 pcs w. Protrusion
300Re	1	1.5	10% FDL	None	Mild Comm Trans
300Lu	1	7.5	50% FDL, 20% TA, 20% Gas, 30% Sol, 50% FHL, 5% FiB	P. Tib A & Vs	Mild Comm Obl
301Le	6	13.5	50% Gas, 40% Sol, 33% FHL, 50% FDL,	Part of Saph V	Comm >15 pcs w. Protrusion
301Ru	2	19.5	50% Gas, 50% Sol, 30% FHL, 90% TP	Fib A & Vs	Mild Comm Trans
306Le	0	0	<5% TA	A. Tib. A	Mild Comm Trans
306Ru	1	1.5	10% TA, 10% Gas,, 10% FHL, 5% TP	Fib Vs	Mild Comm Trans
308Le	2	3.5	2 cm vertical tear in Gas	None	Mild Comm Trans
308Ru	1	1.5	10% Gas & Sol, 30% FHL, 50% FDL, 5% FiB	P. Tib A	Mild Comm Trans = Large Segs
310Re	1	13.0	10% FDL, 10% TP, 75% FHL, 5% TA	None	Comm >6 pcs w. Protrusion
310Lu	2	13.5	30% FDL, 10% TP, 75% FHL, 30% Gas & Sol	Fib A & Vs	Mild Comm Obl w. Protrusion
312Le	0	0	50% Gas, 50% Sol, 5% FHL	None	Comm w. Tension Wedges
312Ru	0	0	Knee ligaments & all muscles were OK	None	None
314Re	1	1.5	<5% TA	None	Mild Comm
314Lu	0	0	Knee ligaments & all muscles were OK	None	None
316Re	1	1.5	10% Sol, 10% FDL	Fib A & V	Mild Comm Trans
316Lu	0	0	Knee ligaments & all muscles were OK	None	None

Notes: <sup>1</sup> The specimen number is listed followed by a designation for left (L) or right (R) and embalmed (e) or unembalmed (u).

<sup>2</sup> The number of skin lacerations is listed, followed by the total linear distance those cuts travel (cm).

<sup>3</sup> The percent values represent an estimate of the horizontal tear length as it relates to total width of the particular muscles listed.

Muscle key: Gas= Gastrocnemius, Sol= Soleus, T= Tibialis, Fi= Fibularis, A= Anterior, P= Posterior, F= Flexor, E= Extensor, D= Digitorum, H=Hallucis, L=Longus, B= Brevis.

<sup>4</sup> Artery (A) and Vein (V) damage key: P.= Posterior, A.= Anterior, Tib= Tibial, Fib= Fibular, Saph= Saphenous.

<sup>5</sup> Fracture descriptions: Comm = Comminuted, Trans= Transverse, Obl= Oblique, Seg= Segmental.

Three of the unembalmed legs did not fracture. For the purposes of the discussion in the following paragraph, these and their respective matches will be excluded in order to generalize findings with respect to the six pairs that fractured.

The fractured **unembalmed** specimens showed considerably more soft tissue damage than their fractured embalmed match (see **Figures 2 and 3**). Lacerations to the skin and superficial fascia were judged to be greater in five of the six pairs. Muscle damage was greater for the unembalmed leg in all six cases and vessel damage was greater in four of the six. Oddly enough, the nervous system appeared to escape serious injury as there was virtually no gross damage to any of the nerves. It is important to note that no microscopic analysis was performed; since nerve components are often injured by "stretching" or "pinching," it is quite probable that damage was present but went undetected. The comparison of the osteologic data is more complex. The damage was similar in half of the matched pairs, but the other half appeared to show greater comminution of the embalmed legs. Further review of the post-test radiographs may lead to a more clear picture regarding bone damage.

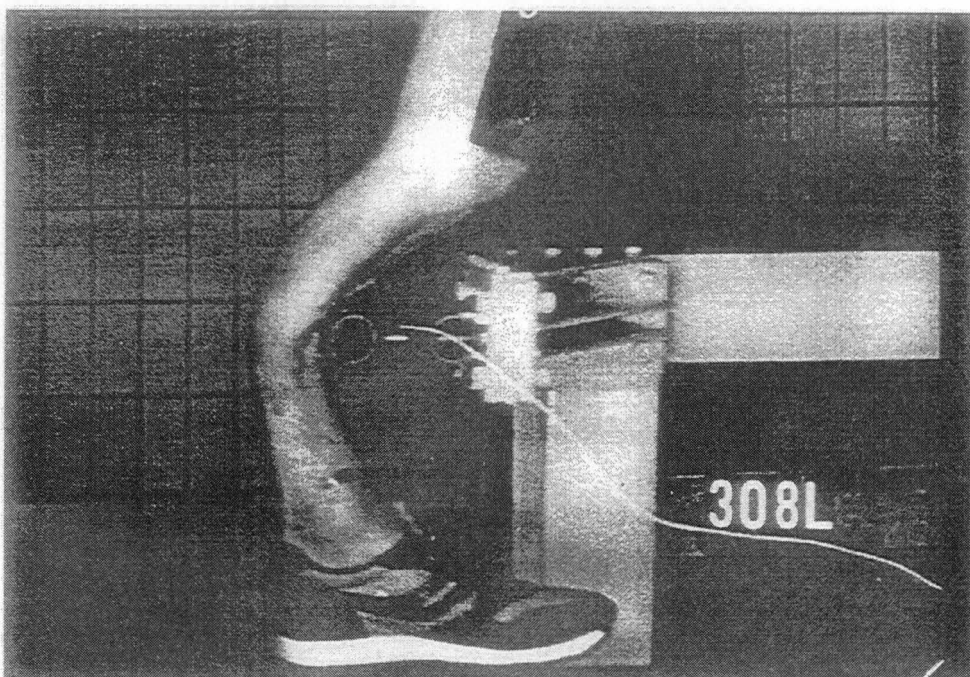


**FIGURE 2.** Embalmed leg 308L. Note the wrapping of this embalmed leg around the impacting pipe. The only lacerations on this specimen were small vertical tears at the interface of the pipe and the shin bone.

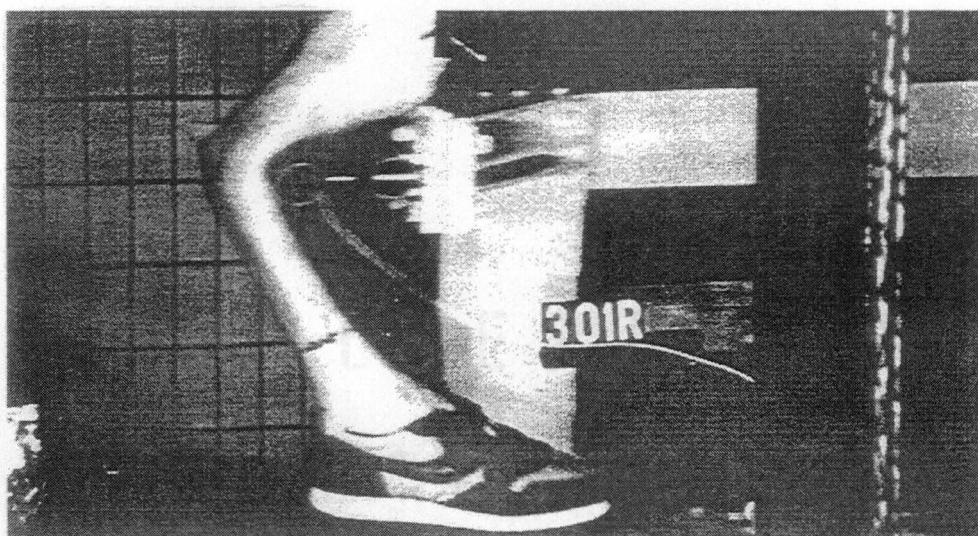


**FIGURE 3.** Unembalmed leg 301R. This unembalmed leg also wraps around the impacting pipe, but notice the tibia protruding from the posterior aspect of the leg. Overall soft tissue damage was generally greater in the unembalmed specimens.

To reasonably compare the effects of the embalming process on anatomical damage, other experimental variables between matched pairs need to be as similar as possible. As mentioned earlier, matched pairs were selected for use in this study to "factor out" variables associated with differences between humans and careful attention was directed to each test set-up in order to maintain consistency (Unfortunately, set-up differences were evident in the last three tests of unembalmed legs. See **Discussion** section for more detail.). The same impact cart and velocity were used in all tests. Presumably, this would result in similar impact input (forces, accelerations, etc.) to each specimen. The inputs were similar for each test as indicated by the recorded force-time plots. Sample plots from an unembalmed and an embalmed specimen are shown in

**Figure 4.**

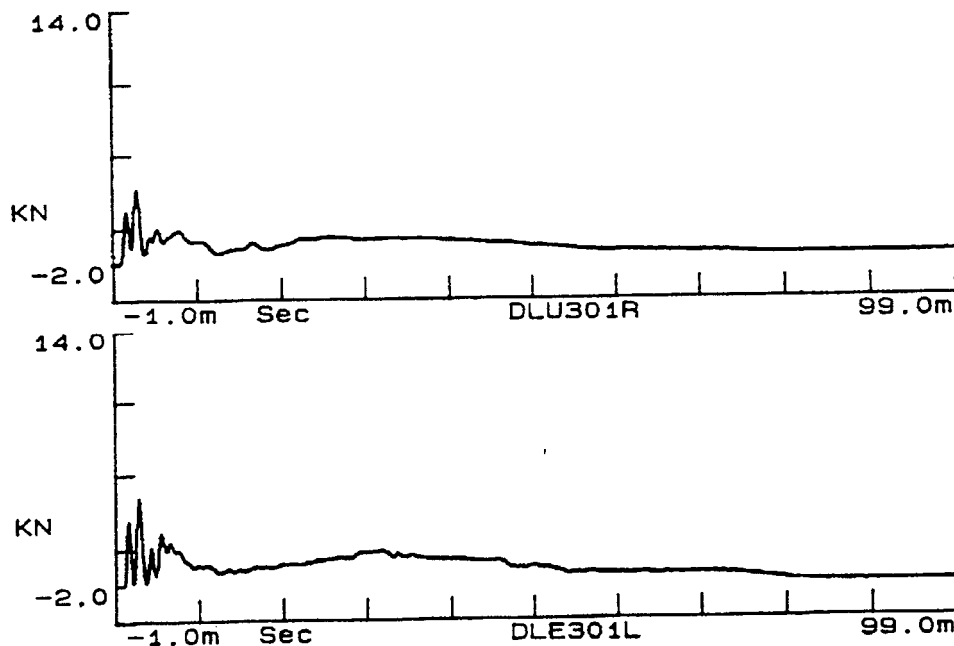


**FIGURE 4.** Sample force plots (specimens 301Ru and 301 Le).



## DISCUSSION

Dissection data clearly indicates that soft tissue damage to fractured embalmed legs was much less than that seen in fractured unembalmed legs. Specifically, damage was greater to the skin, the superficial fascia, muscles and blood vessels; however, the nerves were an exception. In some cases, blood vessels were punctured and large muscle masses were torn for several centimeters, but, to the naked eye, nerves defiantly remained intact. The immediate question is whether this defiance accurately models the live human response to anterior mid-leg trauma. This question is addressed in the following two paragraphs.

1. Perhaps live nerves are rarely transected in mid-leg anterior impacts and the lack of damage seen in this study is appropriate. If so, then the resistance to laceration may be explained by several mechanisms: a) The anatomy of the lower limb may afford nerves a tremendous amount of protection from anterior impacts to the mid-leg. Most of the large nerves are situated posterior to the bones of the leg; therefore, fractures would absorb much of the energy of impact prior to involvement of the nerves. b) Transection may not be the most common mechanism of injury. Stretching is often cited as the cause of central nervous system injuries such as diffuse axonal injury (DAI). Compression of the brain is the primary cause of concussions. Maybe peripheral nerves of the leg are most often injured in similar manners without being torn.

2. If nerve transection is commonly seen after "real-world" anterior mid-leg impacts then there may be factors which were not, or could not be accounted for: a) Live nerves may simply be more fragile than those of a cadaver. b) Perhaps when all of the components of the leg have their normal turgor, the nerves are put in a more precarious position. c) Nerve transection may occur secondary to the impact. This would include violent motion of the fractured limb immediately after impact or improper splinting/transport, etc. It may also include the human body's post-traumatic responses. Nerves may be impaired due to inflammatory processes or vascular compromise, but transection may occur during contraction of the musculature immediately after impact. This natural mechanism may result in laceration of the nerves as they are pinched between sharp bone fragments. It is believed that differences in the set-up resulted in a slightly different test configuration for the three unembalmed legs that did not fracture. One of these three is shown in **Figure 5**. Films show that these legs were not positioned as upright as the previous ones. Instead, these legs may have been flexed such that an acute angle was formed with the concrete (i.e. the knee was tilted forward). In addition to absorbing the impact in a different manner, this tilt introduced more freedom of movement of the leg with respect to the knee during impact. This would be consistent with medical observations regarding the laxity of intracapsular knee ligaments while the leg is flexed. This was verified in the high speed films. Because of this variation in test set-up the inertial constraints were altered resulting in no fractures.

*Leg 316L. This was the last unembalmed leg to be tested and the third in a row that did not fracture. Note that there is no wrapping around the impactor and some posterior translation at the knee is evident.*

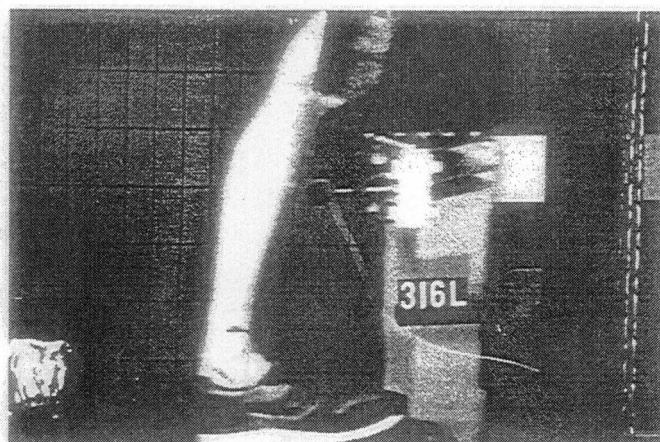


**FIGURE 5.** Impact resulting in no fracture.

## **PART 6**

### **FRACTURE PATTERNS OF LONG BONES**

## **ABSTRACT**

A primary objective of this experimental investigation was to further understand relationships among loading characteristics as they affect the resultant fractures of human long bones (tibia, femur, humerus, and fibula). Numerous human cadaver long bones were loaded in controlled laboratory conditions with varying test parameters such as loading direction, specimen choice, impact velocity, and test method. Data presented in this section focus on the resultant fracture patterns for the tibia and femur tests. Observations were made based on these data and on the authors' general knowledge with respect to fracture behavior. These comments draw upon a decade of laboratory experience of dynamically loading human cadaver long bones.

## **INTRODUCTION**

All persons are at risk for fractures, especially to the long bones. This is true for young persons, who generally may otherwise be healthy, and older persons, in which osteoporotic and arthritic changes can increase the seriousness of such fractures. Most fractures heal successfully, but many result in significant loss of function and permanent disability. Some of the complications are directly related to the fracture itself, but others are associated with accompanying effects of the fracture. The fractured bone may pierce the skin creating an open wound possibly resulting in infection, or may lead to other injuries involving the surrounding neurologic, vascular, and connective tissues.

The primary sources of such injuries are the jagged edges of the fractured components and displaced bone fragments. Potential post-traumatic impairments may include arthritis, chronic pain, decreased weight-bearing capacity, limited range of motion, and osteodeformities.

An understanding of long bone failure mechanisms and fracture patterns is helpful in characterizing the resultant injuries. Also, more knowledge with respect to failure mechanisms can facilitate development of better “systems” or “environments” to minimize severity of injuries.

Breaking strength and fracture patterns of long bones have been studied quite extensively with good documentation dating as far back as the 19th century. Messerer (1880) tested 500 bones from 90 cadavers of both sexes and various ages. He found that the cracking or tearing of the bone generally occurred on the convex (tension) side of the bone. In bones exhibiting significant bend there was crushing on the concave (compression) side, at the point of application of the load, before a tearing or tension fracture occurred. The significance of tensile stresses as the cause for bone failure was further emphasized by Evans and Lissner (1948) through stresscoat studies. Mechanical property studies over the years have shown that bone is weaker in tension than in compression. Rauber (1876) was one of the first researchers to discover that when a bone is subjected to increasing amounts of equal tensile and compressive forces it fails in tension first. Kress and Porta (1993) have

found that the human femur seems to be approximately 1.5 times stronger in compression than tension, even during dynamic loading conditions.

A fracture, or break in the surface of a bone, can range from a simple crack to complete rupture of the bone structure with fragmentation. Injury severity, as it relates to fractures, depends on three primary parameters: fracture location, degree of displacement of the broken bone or associated fragments, and nature of the surrounding soft tissues and skin. These parameters are variable depending on the specific loading situation.

Long bone fractures occur to the diaphysis (shaft) and/or the epiphyses (articular regions). The shaft is usually discussed in terms of three equal subdivisions of the bone's length. The third closest to the torso is described as "proximal", the middle third is simply "the middle third," and the third furthest from the torso is described as "distal."

Open fractures, as opposed to closed, involve damage to the overlying skin and, naturally, the adjacent soft tissue structures. These fractures usually result in increased blood loss, decreased healing rates, and greater risk of infection. This increased risk of infection is supported by Dellinger et al (1988) in a study of 240 patients. Roth et al (1986) reviewed infectious morbidity in 838 patients and found that infection was prevalent 8% more often with open fractures as compared to closed.

Comminuted (i.e. bone is broken into more than two pieces) is another type of fracture that can cause significant soft tissue damage. Varying degrees

of comminution manifest as relatively simple wedges or segmental fractures to more complex longitudinal split or massively fragmented fractures (as illustrated in Figure 1). Also shown in Figure 1 are the common non-comminuted fracture patterns: transverse, oblique, and spiral. Other descriptions of fractures (e.g. impacted, avulsion, greenstick, etc.) will not be discussed due to the scope of this section.

## **OBJECTIVE**

An intent of this experimental investigation was to further understand relationships among loading characteristics (e.g. direction of applied force, dynamic vs. static, torsional vs. bending) as they affect the resultant fractures of human long bones. This understanding should be useful as an aid for evaluating the effectiveness of any protective or mitigative devices or strategies. It should also be helpful in identification of all of the associated resultant injuries from a fracture. Perhaps this information could be a useful tool for accident reconstruction purposes and furthering progress with respect to emergency management for the affected individual.



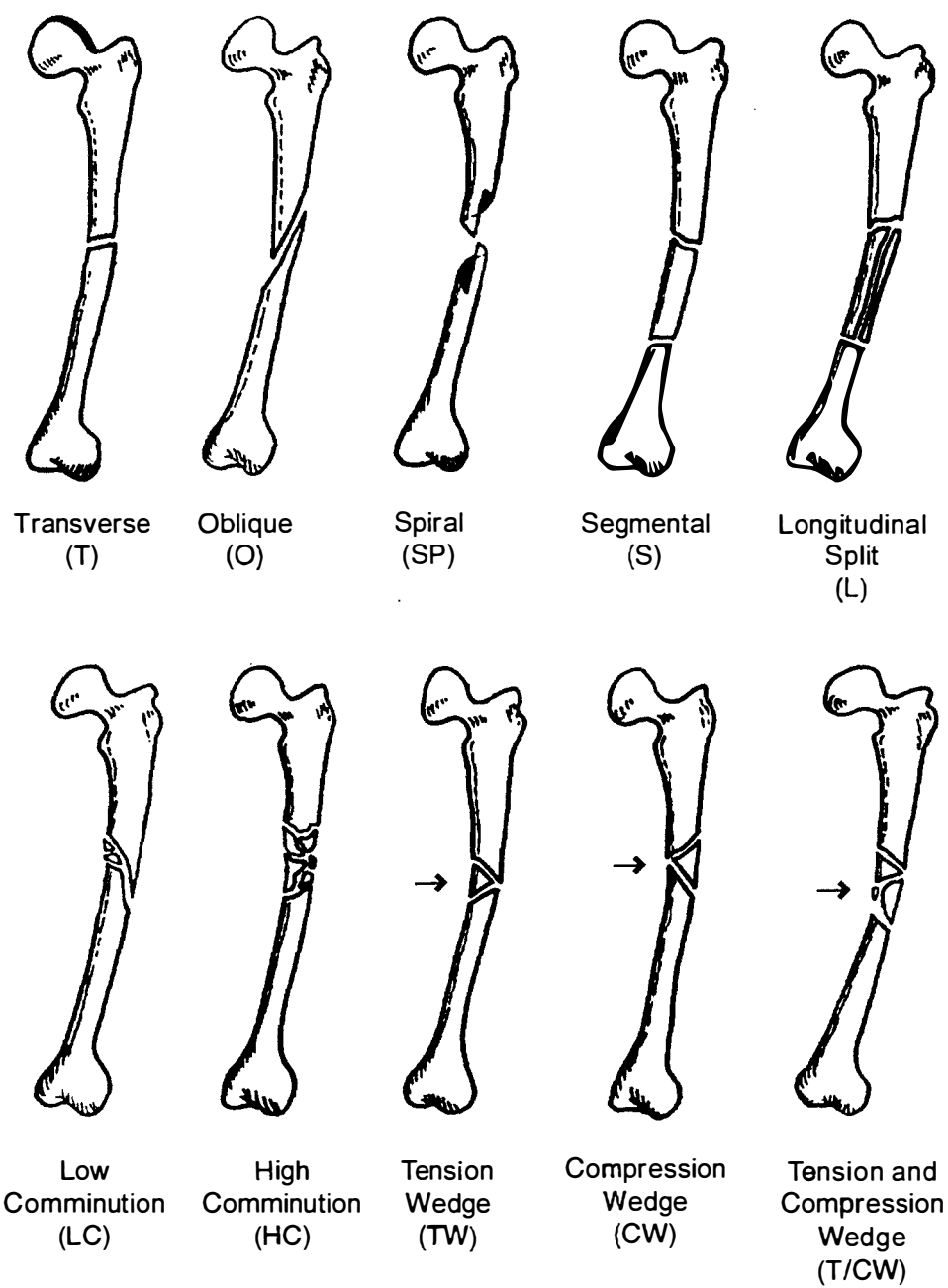


**FIGURE 1.** Fracture patterns (legend notation in parenthesis).

## EXPERIMENTAL METHOD

A total of 558 bone fracture tests are being reported on in this section. Most of the results and discussion focus on a narrowed field of these tests consisting of 253 tibias and 136 femurs. As detailed in Table 1, the specimens were obtained from a geriatric population (on the average) consisting of both males and females. All bare bones were tested in a pin-pin setup and the intact leg tests were mostly pin-inertial (foot hanging freely) or pin-friction (shoed foot on concrete block). The pin-pin setup supported the bare bones at their ends (epiphyseal aspects) and were impacted at midshaft.

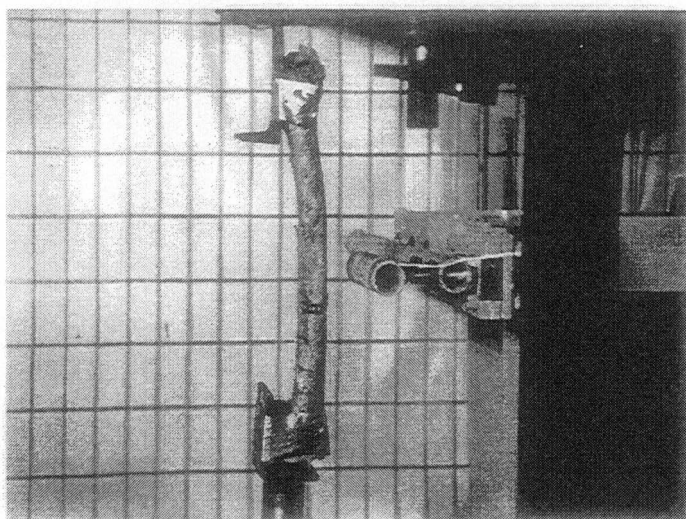
Two general setups were used for the experiments. Figure 2 shows a test setup that consists of a pneumatic-based accelerator which propels a wheeled cart toward the mounted specimen. The accelerator consists of a piston assembly inside of a pneumatic chamber that is pressurized in order to achieve target velocities. For most tests the pressure was 0.34 MPa (50 psi) yielding a cart velocity of approximately 7.5 m/s. A ram connected to the piston pushed an aluminum and steel impact cart (50 kgs) throughout its stroke of approximately 1.5 meters. Then the cart separated from the ram and traveled along a railway for less than a meter before striking the specimen. In that stretch, it was timed by a photovoltaic cell/timer apparatus allowing for calculation of the velocity before impact.

Heading the cart is an instrumented 10-cm steel impactor pipe with an outside diameter of 4.13 cm. It is mounted to the front of the cart via slide pins.

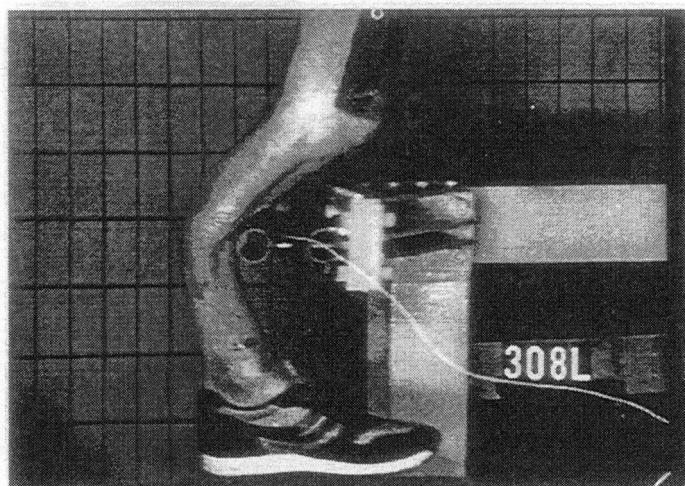
When contacting a specimen, the pipe was freely able to impinge on a piezoelectric quartz force transducer (PCB Piezotronics model 208A03), thereby producing a measured force equal to that which is delivered to the specimen. The transducer signal was recorded on a Hewlett Packard 3562A signal analyzer allowing storage of a force vs. time plot for each impact. However, for the purposes of this section, discussion will focus on the resultant fracture data.

The second setup consists simply of a swinging pipe approach as shown in Figure 3. This “swinging pipe” is the same instrumented pipe that is mounted to the cart in the other setup.

After impact each specimen was examined (intact legs were also x-rayed and dissected) in order to categorize the fracture pattern. Ten patterns were observed as shown in Figures 1 and 4. The results have been grouped into logical categories as illustrated by the fifteen data charts in Figures 5 and 6. These correspond, respectively, with the first fifteen rows of Table 1. Note that all the fracture data from the swinging pipe tests (Figure 3) could be classified into four categories (Figure 6). Considering that all of these tests were of bare bones, the data may be indicating a lower incidence of comminution as compared with the intact specimens.



(a)



(b)

**FIGURE 2.** Wheeled cart set-up. (a) shows simply-supported bare bone, and (b) shows impact of intact leg.

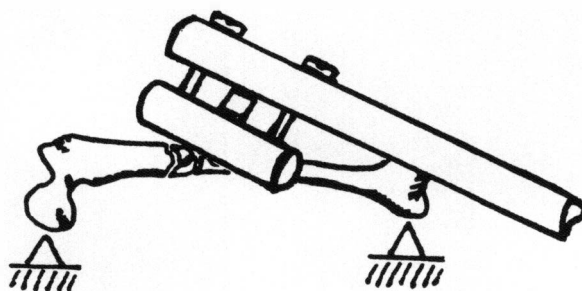


**FIGURE 3.** Sketch Showing "Swinging Pipe" Approach.

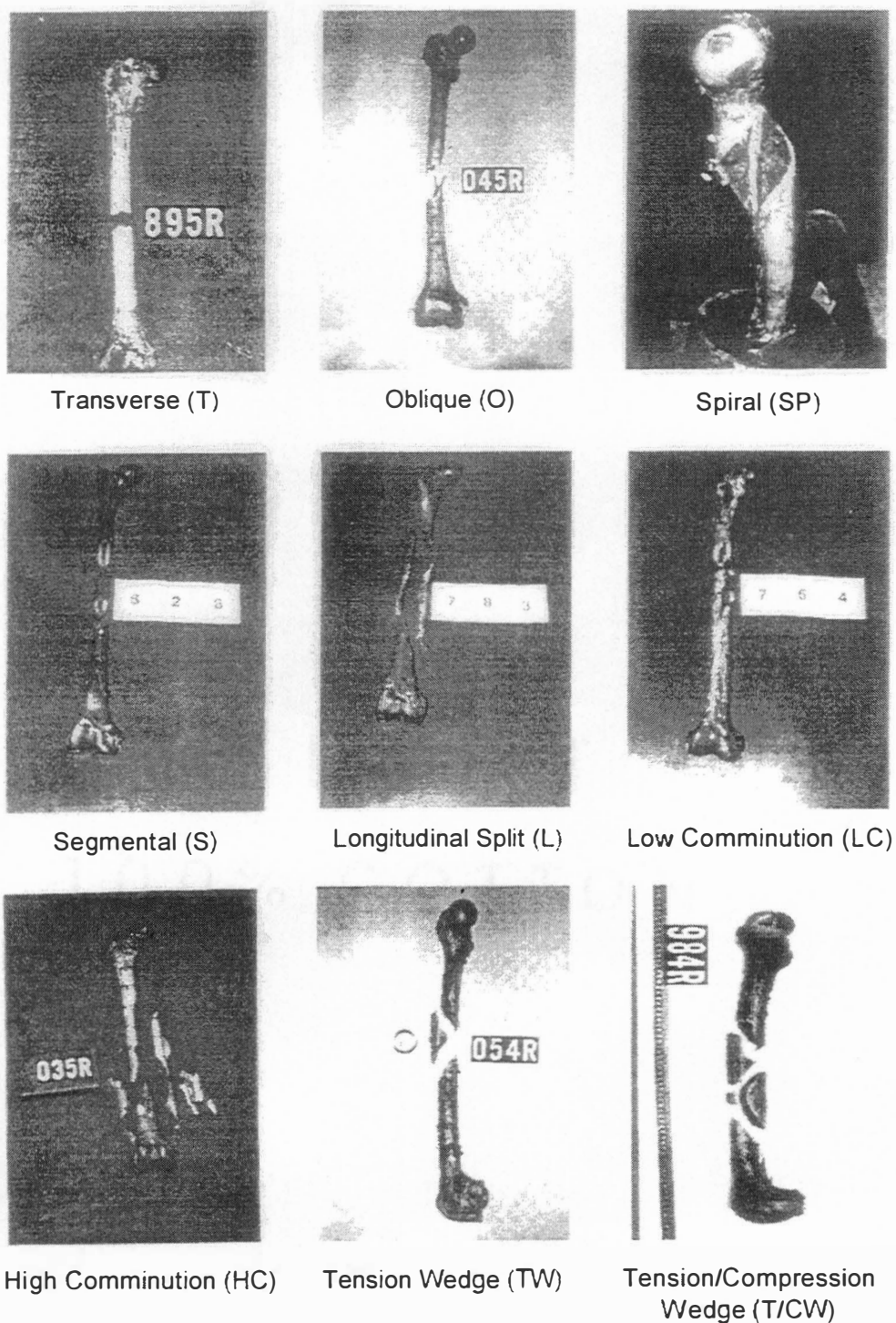


**FIGURE 4.** Photographs of actual test specimens showing fracture patterns.

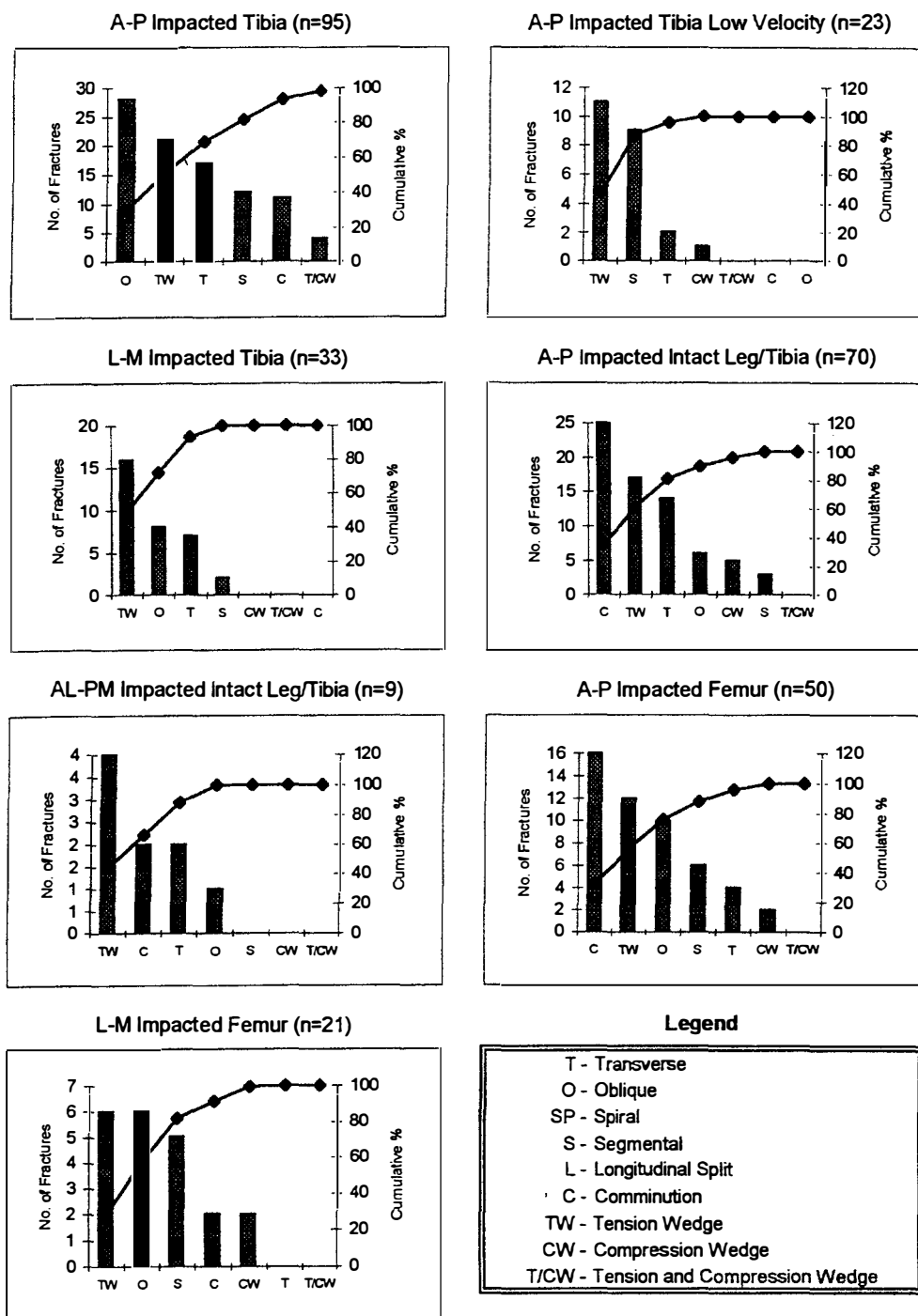
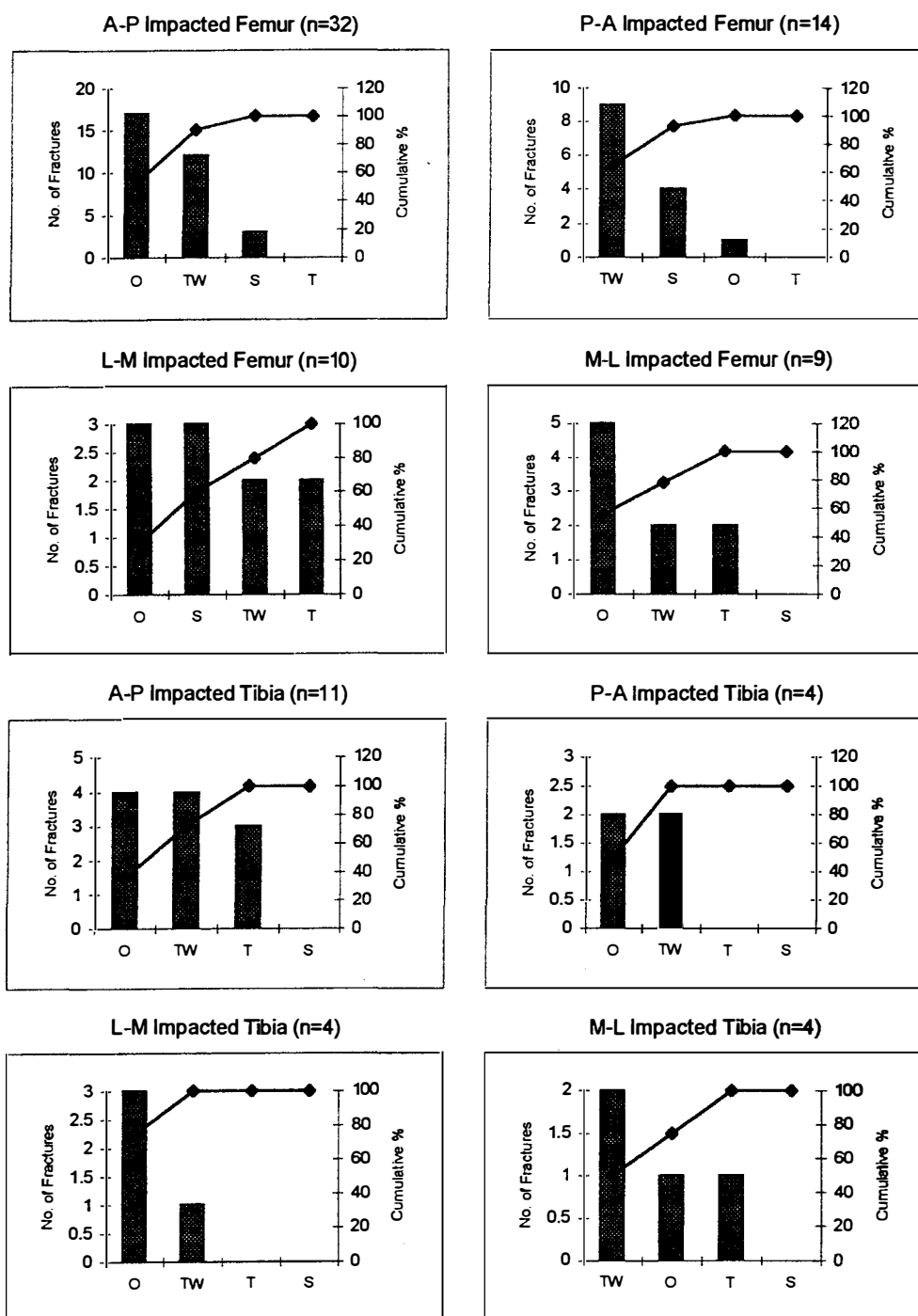


FIGURE 5. Fracture patterns from impacts using apparatus in figure 2.



**FIGURE 6.** Fracture patterns from impacts using apparatus in figure 3.

## RESULTS

All of the observed patterns were produced by transverse loading of the shafts of the long bones, except for the spiral fracture which resulted only from pure torsion or from the existence of pre-torsional loading. The photographs in Figure 4 are of actual test specimens and illustrate the different patterns in the same respective order as Figure 1. A compression wedge type fracture is not included in the photographs, because it has the same appearance as a tension wedge (just rotated 180°). Figures 5 and 6 show the frequencies of occurrence of these patterns resulting from various experimental impacts. These data and other data are tabulated at the end of this section as an appendix. Each chart in Figures 5 and 6 represents a different combination of the test parameters that include loading direction, specimen choice (tibia, femur, or intact leg), impact velocity, and test method. As noted in the figures, the direction of impact was anterior-to-posterior (A-P), posterior-to-anterior (P-A), lateral-to-medial (L-M), medial-to-lateral (M-L), or at a 45° offset angle laterally from the anterior side to the posterior/medial side (AL-PM). All impacts in Figure 5 were at a speed of approximately 7.5 m/s except for the indicated low velocity data which were at approximately 1.2 m/s. Figure 6 contains data from the swinging pipe test series in which 88 bones were fractured all at a velocity estimated to be about 5.0 m/s. This speed was approximated by digitizing twelve of the test films.



## OBSERVATIONS AND CONCLUSIONS

(1) It appears reasonable to combine the data from varying loading directions (A-P, P-A, L-M, AND M-L). In other words, the resultant fracture types seem to be extremely similar regardless of the direction of the impact.

(2) Intact leg impacts promote more comminution type fractures than bare bone impacts. It is believed that the impactor continues to impart forces and energy on the intact leg bones because of the containment provided by the surrounding soft tissue. Also, the inertial constraints of the foot mass and upper leg/body components cause a wrap-around effect that results in increased comminution as the specimen stretches around the impactor.

(3) Embalmed intact leg fractures exhibit greater comminution than unembalmed. The embalment process causes significant increase in stiffness of the soft tissue containment.

(4) It is reasonable to assume that transverse, oblique, segmental, and tension wedge fractures are all just different manifestations of tensile failure. Even high comminution fractures probably originate as tensile fractures but get further fragmented due to other influences.

(5) Compressive wedge type failures are extremely rare in long bones. This is expected as human bone is approximately 1.5 times stronger in compression than it is in tension.

(6) Although the femur is stronger and has a different cross-sectional geometric shape, its fracture patterns as a result of transverse loading are generally the same as those for the tibia.

(7) The most common fracture pattern is the tension wedge and is followed closely by the oblique fracture.

(8) Transverse and oblique fractures generally have jagged edges.

(9) Spiral fractures have the “smoothest” break edge, perhaps indicating that it follows some pre-existing engineering structural line. Wedge fracture lines tend to follow curved paths similar to the spiral fracture path.

(10) Tensile wedge fractures clearly originate at a location directly opposite of the point of impact and the wedge segment radiates back through the bone initially forming a  $90^\circ$  vertex angle (propagates  $45^\circ$  from the horizontal both superiorly and inferiorly) indicating possible transition along the lines of principal stress (transition from purely tensile to shear). Refer to the illustration of the tension wedge in Figure 1 in which the arrow indicates the direction of impact. A previous report by Levine (1986) stated the opposite of what this illustration shows. He stated that the butterfly occurs on the side in which the bone is in tension implying that the “base” of the “triangle wedge” occurs on the opposite side of the impact. This is not correct for almost all cases as indicated in Table 1. Levine’s work describes a compression wedge, which is an extremely uncommon pattern for long bones.

(11) The only bare bones with high comminution were those that were extremely osteoporotic or loaded axially at high speeds (e.g. a knee impact).

(12) Because of the high incidence of tension wedges, this fracture pattern can be used as an indicator of the direction of impact.

(13) Many oblique fractures also have tensile wedge patterns that are not detected by x-ray. Note the appearance of these lines in a specially treated bone in Figure 7.

(14) The fracture patterns of low speed impacts (1.2 m/s) are very similar to those of high speed (7.5 m/s) with the exception that high comminution is not observed in the low speed fractures. This is somewhat of a unique observation because it has been commonly thought that the butterfly wedge results only from high speed impacts.

(15) Spiral fractures only appear when the bones are subjected to torsional loads. Furthermore, if long bones are loaded in pure torsion then spiral fractures will result 100% of the time. Previous researchers, Kramer et al (1973), reported that the absence of spiral fractures from transversely loading long bones of geriatric humans was due to the fact that older people have more brittle bones. This is not the case. A transverse load is simply not a causal mechanism of a spiral fracture.

(16) Approximately two out of three spiral fractures of the femur were located at the proximal third.

(17) A torsional loading direction is herein defined as being “clockwise” if the top is held and the bottom is twisted in the clockwise direction (looking up). Contrary to popular belief, a clockwise torsional load will result in the spiral portion of the fracture being oriented like a right-hand screw (see Figure 8). For example, the spiral fracture illustrated in Figure 1 would have been loaded torsionally in the counterclockwise direction. This interesting observed fracture behavior is indicative that the bone is failing in tension rather than shear when loaded in torsion.

(18) Segmental fractures are much more prevalent in femurs than tibias.

(19) Transverse loading to the tibia/fibula most often results in a segmental fracture of the fibula.

(20) Surfaces of eight bones were videographically scanned and stored in the computer prior to their impact tests. Post-test examination of the fractures and stored computer images provided no evidence of the presence of surface stress risers that could have caused fracture or crack propagation.

(21) Fractures resulting from 7.5 m/s impacts can be quite serious, that is causing significant injury. This conjecture is also supported by research pertaining to pedestrian injury and vehicle design by Pritz and Hassler (1975).

(22) Pritz and Hassler also reported no noticeable differences in injury severity associated with cylindrical impactor radius changes from 1-inch to 4-inches. This is consistent with the findings in this study.

(23) Comminuted fractures can occur without entrapment (crushing injury). For 7.5 m/s impacts of intact legs, the inertial restraint of the tibia from the upper thigh and foot is sufficient enough to result in comminuted fractures without any additional support. For low speed tests (static and 1.2 m/s), simply-supported legs have resultant bone fractures comparable to inertially supported legs at high speeds.

(24) Age changes in bone can exist, although these changes do not seem to significantly affect fracture patterns (except when compared to babies or small infants). Such changes can include mineral mass, volume, density, and mechanical properties. During dynamic loading situations when ultimate strength is exceeded, bone basically fails as a brittle material (young or old). So, the fractured patterns do not vary too much, unless severe osteoporitic changes have occurred. Such osteoporosis can increase the incidence of high comminution (shatter).

(25) For impact loading of the long bone shaft, arthritic changes did not seem to affect the resultant fracture pattern of the entire bone. In other words, a fair supposition would be that arthritis only affects failure patterns when they involve joints.

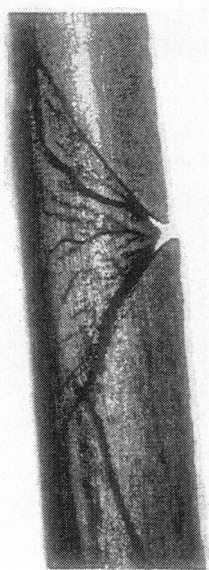


**FIGURE 7.** Fractured bone after special treatment showing tensile wedge stress fractures.

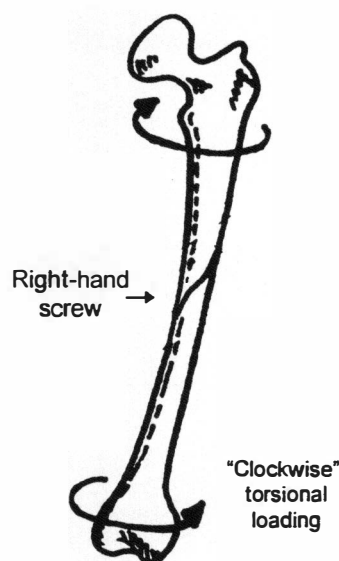


**FIGURE 8.** Relationship between torsional loading direction and resultant spiral fracture direction.

## BIBLIOGRAPHY

- Cowin, S.C. *Bone Mechanics*. CRC Press, Inc. New York, New York: 1989.
- Dellinger, E.P., et al. "Risk of Infection After Open Fracture of the Arm or Leg." *Arch Surg*. Volume 123: Nov 1988.
- Evans, F.G. *Stress and Strain in Bones*. Charles C. Thomas Publisher. Springfield, Illinois: 1957.
- Evans, F. G. and Lebow, M. "The Strength of Human Compact Bone as Revealed by Engineering Technics." *Am. J. Surg*. Volume 83, pp. 326-331: 1952.
- Evans, F. G. and H.R. Lissner. "Stresscoat Deformation Studies of the Femur Under Vertical Static Loading." *Anat. Rec*. Volume 101, pp. 225-241: 1948.
- Frost, H.M. *The Laws of Bone Structure*. Charles C. Thomas Publisher. Springfield, Illinois: 1964.
- Gustilo, R.B. *The Fracture Classification Manual*. Mosby Year Book: 1991.
- Heckman, J.D. "Fractures." *Clinical Symposia*. Volume 43, Number 3. Ciba-Geigy: 1991.
- Kramer, M., K. Burow, and A. Heger. "Fracture Mechanism of Lower Legs Under Impact Load." SAE technical paper #730966. Society of Automotive Engineers, Inc.: 1973.

- Kress, T.A. Mechanical Behavior of the Human Lower Limb to Impact Loading: Facility Development and Initial Results. Masters Thesis. University of Tennessee. Knoxville, Tennessee: 1989.
- Kress, T.A., et al. "Automobile/Motorcycle Impact Research Using Human Legs and Tibias." Rider-Passenger Protection in Motorcycle Derivative Vehicles in Traffic Accidents. SAE International Congress and Exposition. Detroit, Michigan: 1990.
- Kress, T.A., et. al. "Determination of Lower Limb Failure Modes and Tissue Damage by Impact Loading." Proceedings of the 6th International Congress on Experimental Mechanics. Portland, Oregon: 1987.
- Kress, T.A., D.J. Porta, et al. "Human Femur Response to Impact Loading." Proceedings of the International Research Council on Biokinetics of Impacts. Netherlands. pp. 93-104: 1993.
- Levine, R.S. "An Introduction to Lower Limb Injuries." Biomechanics and Medical Aspects of Lower Limb Injuries. SAE technical paper #861922. Society of Automotive Engineers, Inc. pp. 23-29: 1986.
- Messerer, O. *Über Elasticität und Festigkeit der menschlichen Knochen.* Stuttgart, Cotta. pp. 1-100: 1880.
- Pike, J.A. *Automotive Safety: Anatomy, Injury, Testing, & Regulation.* Society of Automotive Engineers, Inc.: 1990.
- Porta, D.J., T.A. Kress, P.M. Fuller, and J.N. Snider. "Impact Studies of Embalmed Human Cadaver Thighs and Femurs." Proceedings of the 14th International Technical Conference on the Enhanced Safety of Vehicles (ESV). Munich, Germany. Volume 1, pp.. 299-304: 1994.
- Porta, D.J., T.A. Kress, et al. "Dynamic Impacting of Embalmed Versus Unembalmed Human Cadaver Legs." Proceedings of the 22th Annual International Workshop on Human Subjects for Biomechanical Research. Fort Lauderdale, Florida. pp. 135-144: 1994.
- Porta, D.J., T.A. Kress, et al. "Biomechanics of Impacting Human Cadaver Thighs." *The Anatomical Record.* San Diego, California. Supplement Number 1. p.96: 1993.
- Pritz, H.B., et al. "Experimental Study of Pedestrian Injury Minimization Through Vehicle Design." SAE technical paper #750166. Society of Automotive Engineers, Inc.: 1975.
- Rauber, A.A. "Elasticität und Festigkeit der Knochen." Leipzig, Wilhelm Engelmann. iv, pp. 1-75: 1876.
- Roth, A.I., et al. "Infectious Morbidity in Extremity Fractures." *Journal of Trauma.* Volume 26, Number 8: 1986.
- Snider J.N., J.F. Wasserman and T.A. Kress. "The Response of the Human Lower Leg to Impact Loading." Proceedings of the International Research Council on the Biokinetics of Impacts, Bergisch-Gladbach (FRG): 1988.

**APPENDIX**

The following table summarizes the data collected with regard to the dynamic response characteristics of human long bones. As mentioned earlier, the seven charts contained in Figure 5 correspond to the first seven rows of this table, and the next eight rows correspond to the data in the charts for Figure 6.



**TABLE 1. Summary Data of the Dynamic Response Characteristics of Human Long Bones**

Impact Plane & Specimen	Impactor	Male Mean Force kN (Std. Dev.)	Female Mean Force kN (Std. Dev.)	Average Velocity m/s (Std. Dev.)	n	Fracture Classifications	Cadaver Information (%Sex - Avg Age)
A-P Tibia	Pipe	4.85 (2.08)	3.60 (1.72)	7.5 (0.35)	95	29.5% Oblique      22.1% Tension Wedge      20.0% Transverse 12.6% Segmental      11.6% Comminuted      2.1% Compression Wedge 2.1% Tension/Compression Wedge	52.4% M - 69.6 47.6% F - 74.6
A-P Tibia (Low Vel)	Pipe	2.21 (0.91)	1.86 (0.85)	1.5 (0.59)	23	47.8% Tension Wedge      39.1% Segmental      8.7% Transverse 4.4% Compression Wedge	52.3% M - 77.0 47.7% F - 82.3
L-M Tibia	Pipe	4.07 (1.22)	2.91 (1.31)	7.7 (0.28))	33	48.5% Tension Wedge      24.2% Oblique      21.2% Transverse 6.1% Segmental	42.4% M - 74.3 57.6% F - 78.9
A-P Intact Leg/Tibia	Pipe	6.96 (2.62)	5.08 (2.51)	7.3 (1.41)	70	35.7% Comminuted      24.3% Tension Wedge      20.0% Transverse 8.6% Oblique      7.1% Compression Wedge      4.3% Segmental	50.0% M - 76.7 50.0% F - 75.8
AL/PM Intact Leg/Tibia	Pipe	8.45 (0.57)	4.11 (1.16)	7.3 (0.22)	9	44.4% Tension Wedge      22.2% Comminuted      22.2% Transverse 11.2% Oblique	37.5% M - 82.7 62.5% F - 72.0
A-P Femur	Pipe	5.70 (2.68)	4.58 (1.45)	7.4 (0.46)	50	32.0% Comminuted      24.0% Tension Wedge      20.0% Oblique 12.0% Segmental      8.0% Transverse      4.0% Compression Wedge	52.3% M - 69.2 47.7% F - 72.6
L-M Femur	Pipe	5.48 (1.17)	3.05 (2.12)	7.5 (0.35)	21	28.6% Tension Wedge      28.6% Oblique      23.8% Segmental 9.5% Comminuted      9.5% Compression Wedge	28.6% M - 71.0 71.4% F - 76.8
A-P Femur	Pipe	2.67 (1.67)	2.10 (1.38)	5.0 <sup>1</sup>	32	53.1% Oblique      37.5% Tension Wedge      9.4% Segmental	32.3% M - 75.4 67.7% F - 75.8
P-A Femur	Pipe	2.48 (0.69)	1.45 (0.65)	5.0 <sup>1</sup>	14	64.3% Tension Wedge      28.6% Segmental      7.1% Oblique	42.9% M - 83.5 57.1% F - 79.5
L-M Femur	Pipe	4.75 (4.07)	3.14 (na)	5.0 <sup>1</sup>	10	30.0% Oblique      30.0% Segmental      20.0% Transverse 20.0% Tension Wedge	88.9% M - 69.3 11.1% F - 73.0
M-L Femur	Pipe	2.29 (1.25)	1.61 (1.08)	5.0 <sup>1</sup>	9	44.4% Oblique      33.3% Transverse      22.3% Tension Wedge	75.0% M - 76.3 25.0% F - 81.0
A-P Tibia	Pipe	2.96 (1.79)	1.35 (0.32)	5.0 <sup>1</sup>	11	36.4% Tension Wedge      36.4% Oblique      27.2% Transverse	54.5% M - 75.0 45.5% F - 70.6
P-A Tibia	Pipe	na	1.12 (0.78)	5.0 <sup>1</sup>	4	50.0% Tension Wedge      50.0% Oblique	100.0% F - 84.0
L-M Tibia	Pipe	1.02 (0.35)	na	5.0 <sup>1</sup>	4	75.0% Oblique      25.0% Tension Wedge	100.0% M - 68.3

Notes: <sup>1</sup> A velocity of 5.0 m/s is an estimate based on video analysis of pipe swing speeds

<sup>2</sup> These femurs were subjected to a pre-torque of 10.06 or 20.14 N-m during impact

<sup>3</sup> Sex was unknown for this group, data was placed in the column for Males out of convenience.

**TABLE 1. (continued)**

Impact Plane & Specimen	Impactor	Male Mean Force kN (Std. Dev.)	Female Mean Force kN (Std. Dev.)	Average Velocity m/s (Std. Dev.)	n	Fracture Classifications	Cadaver Information (% Sex - Avg Age)
M-L Tibia	Pipe	1.89 (na)	1.72 (0.66)	5.0 <sup>1</sup>	4	50.0% Tension Wedge      25.0% Oblique      25.0% Transverse	25.0% M - 85.0 75.0% F - 82.3
Torsion of Humeri	na	56.05 N-m (19.20)	11.96 N-m (3.75)	na	6	100% Spiral Fractures	66.7% M - 74.5 33.3% F - 77.0
Torsion of Tibia/fibulas	na	91.96 N-m (51.09)	na	na	4	100% Spiral Fractures	100% M - 76.3
Torsion of Femurs	na	106.72 N-m (23.78)	96.68 N-m (39.36)	na	33	100% Spiral Fractures	63.0% M - 72.8 37.0% F - 78.0
A-P Fibula	Pipe	2.15 (1.27)	0.93 (0.68)	7.4 (0.63)	25	Most were Segmental or Comminuted	80.0% M - 74.5 20.0% F - 60.8
P-A Humerus	Pipe	4.88 <sup>3</sup> (0.58)	na <sup>3</sup>	6.9 (0.21)	2	50.0% Tension Wedge      50.0% Oblique	Unknown
A-P Tibia	Plate	4.20 (2.11)	4.21 (1.67)	7.5 (0.12)	25	32.0% Tension Wedge      28.0% Segmental      20.0% Comminuted 8.0% Oblique      8.0% Compression Wedge      4.0% Transverse	56.5% M - 67.0 43.5% F - 68.6
L-M Fibula	Pipe	1.15 (0.52)	0.57 (0.28)	7.8 (0.29)	21	Mostly Wedge, Oblique and Segmental	52.4% M - 72.5 47.6% F - 78.4
L-M FemurPre-Torque <sup>2</sup>	Pipe	3.03 <sup>3</sup> (1.83)	na <sup>3</sup>	6.9 (0.25)	10	40.0% Spiral      30.0% Segmental 20.0% Comminuted      10.0% Oblique	Unknown
Axial Femur	Plate	8.38 (1.94)	6.20 (1.83)	6.8 (0.94)	10	Fractures of the Neck in 80%, Shaft in 40% and Knee in 20% (Percentages are >100 due to multiple fractures per specimen)	50.0% M - 63.8 50.0% F - 67.0
Axial Femur	MTS	5.42 (3.02)	4.99 (1.22)	Static	9	88.9% Neck Fracture      11.1% Subtrochanteric Fracture	66.7% M - 66.5 33.3% F - 71.7
Axial Intact Knee	Plate	9.47 (1.78)	8.46 (na)	7.5 (0)	5	60.0% Fracture of Patella only 40.0% Comminuted Fractures of Patella, Tibia and Femur	80.0% M - 88.5 20.0% F - 73.0
Axial Intact Knee	Pipe	9.87 (1.42)	8.37 (3.37)	7.5 (0)	7	85.7% Comminuted Fractures of Patella, Tibia and Femur 14.3% Fracture of Patella only	28.6% M - 89.0 71.4% F - 75.4
A-P Intact Thigh	Pipe	8.23 (na)	5.00 (0.93)	7.5 (0)	6	50.0% Wedge      50.0% Oblique      16.7% Transverse 16.7% Neck Fracture (Percentages are >100 due to multiple fractures per specimen)	50.0% M - 81.3 50.0% F - 87.0
L-M IntactThigh	Pipe	6.98 (2.20)	5.37 (1.20)	7.5 (0)	6	100% Comminuted.7% Neck Fracture (Percentages are >100 due to multiple fractures per specimen)	50.0% M - 81.3 50.0% F - 87.0

## **PART 7**

### **IMPACT RESPONSE OF THE FRONTAL BONE AND FACE**

## ABSTRACT

In a frontal collision, often the kinematics are such that vehicle occupants contact interior components causing fractures of the frontal bone and the periorbital region. Few studies of impact to cadaver supraorbital rims resulting in frontal bone/facial fractures discuss tolerance levels, the relationship between force data and anatomical consequences in human tissue.

In this study, twenty frozen human cadaver heads, ages ranging from 59 to 101, were sectioned from the body at various levels between the fifth cervical vertebra and the foramen magnum. Once thawed, they were impacted in order to induce fractures that are consistent with those seen in a clinical setting. Specific impact targets were the areas of the supraorbital rims, frontal sinuses, and junctions with the nasal and ethmoid bones. An impact cart was propelled to a mean velocity of 7.16 m/s ( $s = 0.55$  m/s) to strike the supraorbital portion of the unrestrained head. The cart was fitted with a 4.13-cm diameter impacting pipe instrumented with a force transducer coupled with a signal analyzer in order to record force-time behavior during impact.

Testing was recorded on standard VHS video and analyses were made on data from palpation, photography, computed tomography (CT) scans, and selected anthropometric measurements. These data are discussed as they relate to the force recorded during impact. Average peak force values and calculated absorbed energies are presented and discussed as they pertain to impact response of the frontal bone/facial skeleton.

The presence of skeletal injury to the cranium and face is better indicated by the energy absorption value rather than the tolerance level. It was also noted that severe to critical injury will almost always result from the type of impact defined in this section.

## **INTRODUCTION**

The general mechanism of injury during a frontal motor vehicle crash is fairly well understood. In such a crash, a motor vehicle rapidly decelerates a fraction of a second before the occupant(s). This differential deceleration results in a collision (the so-called "second impact") between the occupant and the interior of the vehicle.

Tolerance data of unembalmed human heads may be valuable to engineers designing frontal crash protection or automobile interior components. Such data would also be useful for biofidelity enhancement in the development of frangible face components for dummy head forms. Melvin (1989) states that further research is needed to understand the load sharing ability of facial bones and to establish tolerable values for such loading.

This study had two major goals: 1) to produce upper facial fractures consistent with those seen in a clinical setting, and 2) to compile preliminary tolerance data with regard to the force measured during impact.

The target impact area was the upper third of the face, specifically the supraorbital rims and the naso-orbital-ethmoid complex. This particular region

can be injured when occupant kinematics result in the head striking the windshield, the steering wheel, the instrument panel, a pillar support, the back of the front seat or any forward interior structure. Refer to Huelke and Compton (1983) for a more thorough discussion regarding facial injury causation.

There are relatively few reported experiments of intact unembalmed human cadaver heads in which the supraorbital rims have been the dynamic loading area. It is believed that this study is one of the largest involving this type of impact. In fact, Melvin (1989) reported that there are no response data for the supraorbital region.

## **MATERIALS AND METHODS**

Producing facial fractures consistent with those seen in a clinical setting was the primary goal of this study. The sponsor's main objective was to use the fractured specimens in a course instructing maxillofacial surgeons in the reparation of complex facial trauma. Twenty frozen, unembalmed human cadaver heads ranging in age from 59 to 101 years (8 M and 12 F) were used for this study. All specimens had been retrieved fresh over a period of seven months. Each was frozen immediately after death and thawed prior to testing. The heads were also examined grossly and radiographically for signs of prior facial trauma. Specimen #11 may have had a previous nasal fracture. Specimen #15 showed signs of a craniotomy, and specimen #20 had an edematous right eye.

A trauma research team composed of biomedical engineers and human anatomists was enlisted by maxillofacial physicians to produce fractures consistent with those seen in actual trauma - especially those observed due to frontal motor vehicle crashes. The laboratory setting provided a safe and controlled environment for fracture generation and the collection of data. Immediately prior to impact, numerous anthropometric measurements were recorded including specimen weight, orbital indices (height/width), head circumference at the brow, and several widths between paired facial bones. This data is included in Table 1.

The testing apparatus consisted of a pneumatic-based accelerator which propelled a wheeled impact cart toward the mounted head.

Accelerator & Cart - The accelerator is basically a piston assembly in a chamber of compressed air. The chamber was pressurized to 0.3447 MPa (50 psi) for most of the tests in order to achieve a target velocity of approximately 7.5 m/s (actual mean velocity of all tests was 7.16 m/s;  $s = 0.55$  m/s). A ram connected to the piston pushed the aluminum and steel impact cart (50 kgs) throughout its stroke of approximately 1.5 meters. Then the cart separated from the ram and traveled along a railway for less than a meter before striking the head. In that stretch, it was timed by a photovoltaic cell/timer apparatus allowing for calculation of the velocity. The change in velocity of the cart ( $\Delta v$ ) from before to after impact was negligible.

Impactor & Instrumentation - Heading the cart was an instrumented 10-cm steel impactor pipe with an outside diameter of 4.13 cm. It is mounted to the front of the cart via slide pins. When contacting a specimen, the pipe was freely able to impinge on a piezoelectric quartz force transducer, model 208A03 (commercially available through PCB Piezotronics), thereby producing a measured force equal to that which is delivered to the specimen. The transducer was coupled with a Hewlett Packard 3562A signal analyzer. The analyzer recorded and stored a plot of force vs. time for each impact.

Specimen Mounting - The heads were sectioned from the cadaver at various levels of the cervical spine ranging from the C-5 intervertebral disc to the foramen magnum. In order to position them for a supraorbital strike, a bag of clay served as a cradle or a pedestal (refer to Figure 1) depending on the length of the remaining neck of each specimen. Plastic was taped to the inferior portion of the head/neck in order to control fluid loss, etc. The cart was decelerated by contacting bales of wood fiber and the head was caught in a plastic and foam nest.





**FIGURE 1. Mounting of head.** The head was mounted on a bag of clay. Plastic and foam nest in lower left of photo will secure specimen after impact. Also notice "posterior tilt" of this specimen as mounted.

Specimen Examinations - Immediately after each impact, the heads were manually examined for laceration and fracture determination was made via palpation by maxillofacial surgeons. In tests 3a, 5a, 5b, 6a, 8a and 8b, **no** fracture was evident and the heads were remounted and impacted at progressively higher velocities until fracture was obvious. All testing and laboratory examinations were recorded on standard 30 frames/s VHS video. Additionally, 35-mm still photography was used to document pretest and post-test conditions of the heads. Upon completion of testing, damage to all 20 heads was radiographically documented using CT scans. The scans were evaluated by maxillofacial surgeons and judged to be comparable to clinical trauma. A summary of the diagnoses is given in Table 2.

## RESULTS

Known cadaver data and test measurements are in Table 1 which is continued on the following page. Table 2 contains the clinical diagnoses as determined from axial and coronal CT scans. Discussion and selected computations are included in the section following the tables.

**TABLE 1. Cadaver Data and Test Measurements**

Test	1	2	3a, 3b	4	5a, 5b, 5c	6a, 6b, 6c	7	8a, 8b, 8c	9	10
History (Age, Race, Gender)	76WF	70WM	75WM	87WM	87WM	57WM	63WM	86WF	64WF	75WF
Cause of Death	Cerebral Edema	Prostate Cancer	Prostate Cancer	Prostate Cancer	Prostate Cancer	Respiratory Failure	Rupt. Aortic Aneurysm	Ventricular Fibrillation	Cardiac Arrhythmia	Natural
Circumference @ Brow (cm)	52.5	59.5	57.5	55.0	56.0	69.0	58.0	54.5	56.0	55.5
Left Max. Orbit Height (mm)	no data	34.1	37.5	37.4	33.9	33.4	33.7	31.7	37.8	32.5
Left Max. Orbit Width (mm)	no data	41.8	38.2	37.1	38.3	35.2	37.4	35.0	38.5	37.3
Left Orbital Index (Ht/W)	no data	0.816	0.982	1.008	0.885	0.949	0.901	0.906	0.982	0.871
Right Max. Orbit Height (mm)	29.3	33.6	36.3	37.3	34.5	32.3	31.5	31.5	36.6	33.2
Right Max. Orbit Width (mm)	37.0	41.3	38.2	37.0	36.4	35.6	38.5	45.1	37.8	37.3
Right Orbital Index (Ht/W)	0.792	0.814	0.950	1.008	0.948	0.907	0.818	0.698	0.968	0.890
Avg. Orbital Index (Left+Right)/2	no data	0.815	0.966	1.008	0.916	0.928	0.860	0.802	0.975	0.881
Inter-Orbital Width (mm)	26.4	28.7	28.4	28.1	25.2	25.5	26.4	20.3	23.6	24.6
Temporal-Temporal Width (mm)	110.0	118.2	116.0	113.0	105.8	121.6	118.6	107.2	110.5	116.8
Zygomatic-Zygomatic Width (mm)	109.3	128.9	118.4	121.3	109.7	118.4	112.4	112.2	116.5	119.2
Parietal-Parietal Width (mm)	134.5	149.0	142.6	143.0	145.8	154.4	135.7	140.2	149.2	145.2
Weight as Tested (kg)	3.66	4.25	4.31	3.52	3.40	4.42	4.25	3.20	3.97	3.69
Peak Force (kN) Multiple values indicate additional tests of same specimen until fracture.	4.88	10.88	9.81 No Trigger	4.78	8.22 11.08 11.04	8.09 10.94 8.44	6.07	11.36 11.26 7.06	6.86	9.08
Velocity (m/s) Multiple values indicate additional tests of same specimen until fracture.	7.19	7.10	6.13 6.37	6.43	6.19 6.31 7.47	6.46 7.22 7.77	7.22	6.55 7.32 8.35	7.89	7.25
Specimen Cross-section Level	C-3	C-4	C-5	C-5	C-1	C-2	C-2	C-1	C-1	C-2
Head Movement R=Rotational T=Translational	T	T	R, T	T	R, R, R	R, R, R	R	R, R, T	T	T

TABLE 1. (continued)

Test	11	12	13	14	15	16	17	18	19	20
History (Age, Race, Gender)	69BM	86WF	78WF	89WM	82WF	75WF	74WF	93WF	101WF	73WF
Cause of Death	Renal Failure	Brain Stem Infarction	Rupt. Aortic Aneurysm	Pulmonary Edema	Myocardial Infarction	Myocardial Infarction	Cerebrovascular Accident	Coronary Artery Disease	Pulmonary Edema	Intestinal Infarction
Circumference @ Brow (cm)	56.0	54.4	56.0	56.5	54.0	58.0	54.0	54.0	52.5	58.0
Left Max. Orbit Height (mm)	35.8	36.9	33.1	35.6	30.5	35.2	31.2	33.7	35.7	35.1
Left Max. Orbit Width (mm)	40.8	37.4	36.4	38.1	34.2	35.0	34.7	35.4	34.3	37.4
Left Orbital Index (Ht/W)	0.877	0.987	0.909	0.934	0.892	1.006	0.899	0.952	1.041	0.939
Right Max. Orbit Height (mm)	34.1	34.6	32.3	35.4	33.7	34.8	30.3	33.4	34.8	38.7
Right Max. Orbit Width (mm)	37.6	36.0	34.6	38.5	33.4	35.0	34.1	35.6	32.2	n/a
Right Orbital Index (Ht/W)	0.907	0.961	0.934	0.919	1.009	0.994	0.889	0.938	1.081	n/a
Avg. Orbital Index (Left+Right)/2	0.892	0.974	0.921	0.927	0.950	1.000	0.894	0.945	1.061	n/a
Inter-Orbital Width (mm)	30.7	21.6	28.8	22.1	26.0	24.1	25.1	27.2	26.7	24.4
Temporal-Temporal Width (mm)	118.5	114.7	126.4	111.6	111.4	112.0	111.7	107.8	110.9	120.3
Zygomatic-Zygomatic Width (mm)	117.4	112.2	121.6	118.1	112.7	116.0	108.9	109.7	113.0	124.3
Parietal-Parietal Width (mm)	140.3	130.7	137.7	137.3	128.9	140.8	137.3	144.7	136.4	137.4
Weight as Tested (kg)	4.48	3.46	3.18	3.97	3.49	4.31	3.29	3.40	3.63	3.77
Peak Force (kN)	7.88	8.06	7.07	7.45	9.33	8.46	7.73	6.61	10.39	9.89
Velocity (m/s)	7.47	7.50	7.47	7.41	7.32	7.47	7.41	7.35	7.32	7.53
Specimen Cross-section Level	C-5	C-1	Foramen Magnum	C-2	Foramen Magnum	C-2	C-2	C-2	C-2	C-2
Head Movement R=Rotational T=Translational	T	T	T	T	T	T	R	T	T	T

TABLE 2. Clinical Diagnoses from Axial and Coronal CT Scans

Specimen	NOE <sup>1</sup>	Sinus <sup>2</sup>	Le Fort <sup>3</sup>	AIS <sup>4</sup>	Additional Notes
1	✓n	✓	I, II, III	3	Hypoplastic frontal sinus
2	✓	✓		4	Orbital roofs fractured
3	✓	✓		4	Massively depressed frontal bone with linear fractures; Maxilla and temporal bones also fractured
4	✓	✓		4	Orbital roofs, zygoma and angular processes fractured
5	✓	✓		4	Hypoplastic frontal sinus; Orbital roofs and maxilla fractured
6	✓n	✓		4	Hypogenesis of the frontal sinus
7	✓	✓		4	Orbital roofs fractured
8	✓n	✓	III	4	Several fractures of the frontal bone
9	✓	✓		4	Orbital roofs and maxilla fractured
10	✓	✓	II	4	Hypoplastic frontal sinus; Orbital roofs fractured
11	✓	✓	I, II	4	Orbital roofs fractured and linear fractures of the frontal bone; Possible previous nasal fracture
12	✓	✓		4	Orbital roofs fractured
13	✓	✓	II	4	Orbital roofs and right orbital wall fractured
14	✓	✓	I, II	4	Segmental maxillary fracture
15	✓	✓a		4	Old craniotomy or previous skull fracture
16	✓	✓	I, II, III	4	Nondisplaced fractures of frontal bone
17	✓	✓		4	Several fractures to the right maxilla and angular process
18	✓	✓		4	Orbital roofs and maxillary fractures
19	✓	✓a	II	4	Hypoplastic frontal sinus; Right orbital roof, temporal and zygomatic bones fractured
20	✓n	✓a		3	Segmental fracture of the maxilla; Edematous right eye

Notes: <sup>1</sup>NOE - ✓ = Comminuted fractures of the nasal, orbital and ethmoid bones including the cribriform plate.  
 ✓n = Naso-orbito-ethmoid fracture with no cribriform plate involvement noted.

<sup>2</sup>Sinus - ✓ = Comminuted fractures of the frontal sinuses with anterior and posterior table involvement.

✓a = indicates that only the anterior table was involved in the fracture.

<sup>3</sup>Le Fort - A grading system of facial fractures: Class I is a horizontal segmented fracture of the lower maxilla. Class II Le Fort fractures cause the complete separation of the maxilla (or maxilla and nasal bones) from the other facial bones.

This results in a large pyramidal-shaped segment of bone. Le Fort III indicates the complete separation of the maxilla and other large facial bones from the base of the cranium (craniofacial disjunction).

<sup>4</sup>AIS - The value listed is the maximum anatomical injury rating according to 1990 Abbreviated Injury Scale published by the Association for the Advancement of Automotive Medicine (1= Minor, 2= Moderate, 3= Serious, 4= Severe, 5= Critical, and 6= Maximum).

## DATA EVALUATION AND DISCUSSION

Virtually all of the specimens exhibited a large transverse laceration to the forehead in the region of the supraorbital rims and/or bridge of the nose. This was also true on the four specimens that required additional impacts to produce a definite fracture. In most cases, fracture of the naso-orbital-ethmoid complex and the frontal sinus were obvious. Additionally, there were fractures of the base of the skull, specifically the orbital roofs and cribriform plate of the ethmoid bone. Facial impacts causing basilar skull fractures are not uncommon in motor vehicle trauma (Huelke, 1988 and Myklebust, 1988).

Refer to Table 2 for a detailed breakdown of the fracture data. It is believed that the assigned AIS values are conservative for two reasons. 1) The use of cadavers prohibits the evaluation of blood loss and physiologic parameters such as loss of consciousness, etc. 2) The grading is based solely on palpation and CT scan analyses of the skeletal tissues. A value of AIS 5 or 6 can only be assigned for injury to internal organs (brain, brain stem, or major intracranial vessels). Also, measurements of maximum skull depression and depth of penetrating injury were not recorded.

Post-test radiography indicated that the majority of the impacts resulted in severe facial trauma including comminuted fractures of several skull bones. During the experiment, on-site assessments by palpation indicated that four heads did not fracture upon first impact (tests 3a, 5a, 6a and 8a; average velocity = 6.33 m/s). Fractures were also not evident in three of these upon

second impact (tests 5b, 6b and 8b; average velocity = 6.95 m/s), thus warranting a third test. Energy calculations from measured force-time data might refute the conjecture that test 6b resulted in no fracture.

The specimen mounting technique was not precisely controlled. Analyses of the videotape and force-time plots gave clues as to the reasons for non-fractures. It appears that the impacted heads that did not fracture were initially mounted with a posterior tilt. Note that the specimen in Figure 1 is angled counterclockwise from the vertical. The impact to these tilted heads was more of a glancing blow causing the head to rotate downwards (posteriorly) away from the impacting pipe as illustrated in Figure 2. Most of the heads that fractured at first impact were struck with the forehead nearly perpendicular to the plane of impact. The videotape clearly shows these heads contacted the impacting pipe for a greater period of time than the tilted heads.

In reviewing the Table 1 data, velocity might appear to be the only determining factor for fracture generation. The average velocity for the tests in which fractures occurred was 7.42 m/s ( $s = 0.37$  m/s;  $n=19$ ). Test 3b resulted in fractures, but was excluded from the velocity average because force-time data was not obtained. The six non-fracture tests had an average velocity of 6.49 m/s ( $s = 0.43$  m/s). Test 6b was excluded from all averages and calculations due to the previously discussed conflicting results (palpation vs. energy calculation) regarding the presence of a fracture. Even though the difference between average velocities of fracture versus non-fracture impacts was approximately 1

m/s, there may be other contributing factors relating to the occurrence of fractures. Note that upon review of the videotape, rotational and translational head motions were observed (see Figures 2 and 3 below).

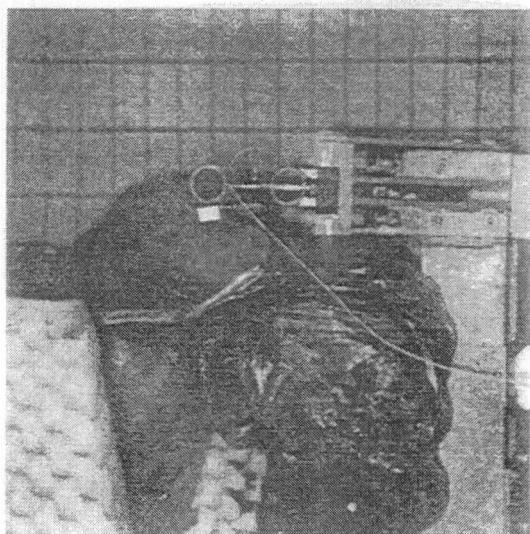


**FIGURE 2.** Rotational movement of impacted head.

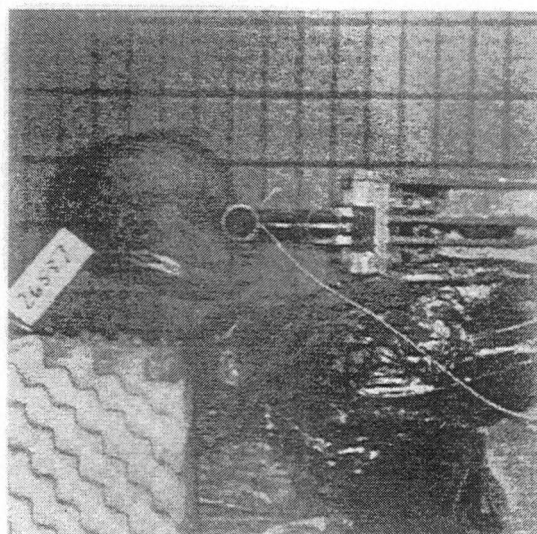


**FIGURE 3.** Translational movement of impacted head.

The combined effect of lower cart velocity and head rotation was evident in the tests resulting in non-fracture. Head rotation occurred for three reasons: 1) the aforementioned "posterior tilt," 2) striking the head above its center of gravity (especially in those sectioned at more inferior cervical levels), and 3) the clay mounting structure/neck interface may have acted as a fulcrum.

The fractured heads "wrapped" around the impacting pipe causing their continued motion to be more translational (see Figure 3).

In many of these cases, the pedestal of clay was analogous to a golf tee in that it allowed translation as opposed to the fulcrum effect.

In order to conclusively support this observation, the force-time curves for all 26 (no force-time data was obtained for test 3b) tests were integrated to determine the maximum head velocity. Assuming all of the force was converted to kinetic energy of the head, velocity is obtained by using the formula below:

$$v = \frac{g_c}{m} \int F dt ,$$

where  $v$  = velocity of the head,

$g_c$  = the proportionality coefficient relating force to mass & acceleration,

$m$  = mass of the head,

$F$  = measured force, and

$t$  = measured time.

This equation is a form of Newton's Second Law (force is proportional to the product of mass and acceleration). Figures 4 and 5 show sample curves of a non-fracture and a fracture impact, respectively. The non-fracture impacts produce smoother force-time curves as similarly reported by previous researchers (e.g. Hodgson et al, 1966-1967). For each of the non-fracture impacts, the calculated velocity fell far short of the cart velocity - indicating, conclusively, that the contact between the head and the impactor was lost early.

By contrast, the same integral for those impacts that caused fracture, showed a final velocity in excess of the cart velocity - indicating continued contact throughout a more significant travel distance of the cart.

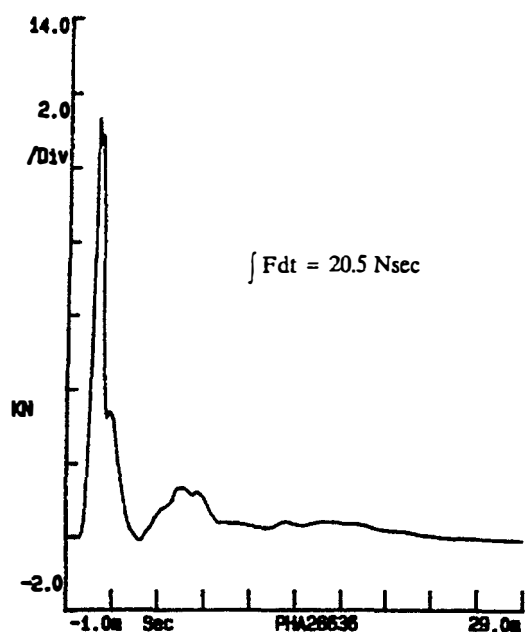


FIGURE 4. Force-time plot of test 8a: non-fracture.

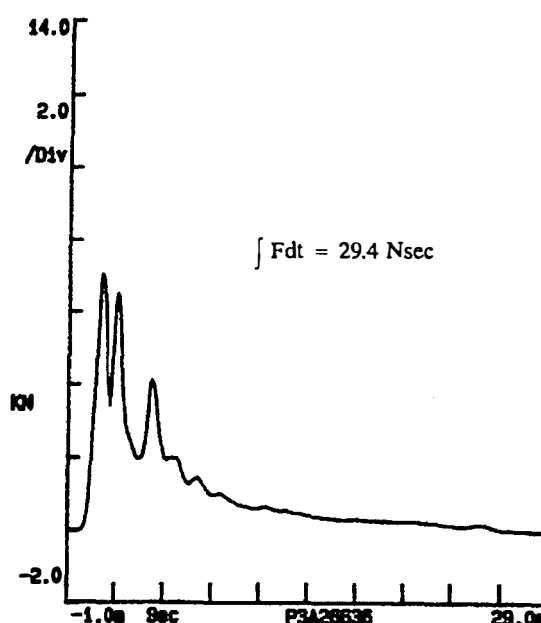


FIGURE 5. Force-time plot of test 8c: fracture.

This "excess velocity" is not an actual incremental increase in the speed of the head, but is proportional to the energy absorbed by the head to cause strain and failure. Consider the following equation:

$$E = W - KE = v \int Fdt - \frac{mv^2}{2g_c},$$

where  $E$  = energy absorbed by the head and facial bone structures in strain and failure,  
 $W$  = work done on the head by the cart,  
 $KE$  = maximum kinetic energy of the head,  
 $v$  = velocity of the cart,  
 $F$  = measured force,  
 $t$  = measured time,  
 $m$  = mass of the head, and  
 $g_c$  = proportionality coefficient relating force to mass & acceleration.



This equation implicitly assumes negligible change in cart velocity during impact (verified by digitization) and that the final velocity of the fractured heads is, at most, the velocity of the cart.

Calculated values for E, W and KE for each test can be found in Table 3. The average energy absorbed, E, for the impacts that caused fractures is 155.1 Nm ( $s = 62.5$  Nm;  $n=19$ ) and only 78.3 Nm ( $s = 12.8$  Nm;  $n=6$ ) for non-fracture impacts. It may be of interest to note that the average E of the impacts that caused fractures involving the heads that were subjected to multiple strikes is 145.7 Nm ( $s = 32.8$  Nm;  $n=3$ ). This value is significantly larger than the average 78.3 Nm of energy absorbed for the non-fracture impacts.

There is a stand-out energy value from an impact causing fracture. Specifically, the E value for test 19 is only 79 Nm. Perhaps degenerative changes associated with advanced age account for this failure at relatively low energy. The cadaver in this test was the oldest specimen - 101 years.

The peak force values from force-time data of the impacts causing fractures ( $n=19$ ) were averaged,  $F_{avg} = 8.00$  kN ( $s = 1.82$  kN), to provide a tolerance level indicating the force threshold at which fracture begins. This value is comparable to the frontal bone tolerance levels reported by Nahum (1975). It is important to note that the 8.00-kN tolerance value reported here is dependent on methodology parameters including impactor geometry, impact angle and location, and human-to-human variation. Force application time is also a critical parameter in all of the tests. This is evident in that the average peak force value

for the heads that did not fracture (n=6) was 9.97 N (s = 1.51 N).

Nahum (1975) reported lower tolerance values for females as compared to males. However, no noticeable difference was detected in the means in this study. The average male fracture tolerance value is 8.1 kN (n=7) and the female value is 8.0 kN (n=12). Mean absorbed energy values for the fractured male and female specimens were 153.1 Nm (n=7) and 156.2 Nm (n=12) respectively.

**TABLE 3. Calculated Energy Values**

Test	Work, W (Nm)	Kinetic Energy, KE (Nm)	Energy, E (Nm)
1	221	95	126
2	202	107	95
<b>3a<sup>nf</sup></b>	<b>153</b>	<b>81</b>	<b>72</b>
4	176	73	103
<b>5a<sup>nf</sup></b>	<b>152</b>	<b>65</b>	<b>87</b>
<b>5b<sup>nf</sup></b>	<b>151</b>	<b>68</b>	<b>83</b>
5c	216	95	121
<b>6a<sup>nf</sup></b>	<b>189</b>	<b>92</b>	<b>97</b>
6c	316	133	183
7	294	110	184
<b>8a<sup>nf</sup></b>	<b>134</b>	<b>69</b>	<b>65</b>
<b>8b<sup>nf</sup></b>	<b>152</b>	<b>86</b>	<b>66</b>
8c	245	112	133
9	279	124	155
10	188	97	91
11	426	125	301
12	292	97	195
13	232	89	143
14	260	109	151
15	285	94	191
16	268	120	148
17	207	90	117
18	215	92	123
19	176	97	79
20	414	107	307
AVG (n=19)	-	-	155.1 (s = 62.5)
<b>AVG<sup>nf</sup> (n=6)</b>	-	-	<b>78.3 (s = 12.8)</b>

Note: <sup>nf</sup>values in bold are data from non-fracture impacts

## CONCLUSIONS

1) Frontal bone/facial fractures similar to those seen in motor vehicle trauma may be successfully produced in the laboratory setting.

2) Impact to the supraorbital rims, given the other methodological conditions, at speeds near 7.2 m/s will almost always cause severe to critical injury.

3) The occurrence of skeletal injury to the cranium and face is better indicated by the energy absorption value rather than the tolerance level. Energy accounts for the total time that force is applied to the head, whereas tolerance level is only a peak force value at a specified time (at which the first fracture just begins).

## REMARKS

Data analyses beyond the scope of this section may provide additional useful information.

It is anticipated that tolerance levels will be specified as they pertain to certain fracture events that occur after the onset of the first fracture. Hopefully, this can be accomplished by a more detailed comparison of the CT data with the force-time curves.

Although extensive anthropometric data has been collected and presented in this section, most of it was not examined as it may relate to injury causation. If significant correlations or trends exist, they will be noted and

investigated further.

## BIBLIOGRAPHY

- Hodgson, V.R., et al. "Response of the Facial Structure to Impact." Proceedings of the 8<sup>th</sup> Stapp Car Crash Conference. pp. 229-250. Wayne State University Press, Detroit, MI, USA. 1965.
- Hodgson, V.R., et al. "Injury to Facial Bones." Proceedings of the 9<sup>th</sup> Stapp Car Crash Conference. pp. 145-163. University of Minnesota, Minneapolis, MN, USA. 1966.
- Hodgson, V.R., et al. "Tolerance of the Facial Bones to Impact." The American Journal of Anatomy. 120(1), 1967.
- Huelke, Donald F., et al. "Basilar Skull Fractures Produced by Facial Impacts - Case Histories and a Review of the Literature." SAE Paper No. 881711. Society of Automotive Engineers, Warrendale, PA, USA. 1988.
- Huelke, Donald F. and Charles P. Compton. "Facial injuries in automobile crashes." Journal of Oral and Maxillofacial Surgery, 41:241-244, 1983.
- Huelke, Donald F. and James H. Harger. "Maxillofacial Injuries: Their Nature and Mechanisms of Production." Journal of Oral Surgery. 27:451-460, 1965.
- Melvin, John W. "Facial Bone Injury Biomechanics Research." Report No. GMR-6825. General Motors Research Laboratories, Warren, MI, USA. 1989.
- Myklebust, Joel, et al. "Steering Wheel Induced Facial Trauma." SAE Paper No. 881712. Society of Automotive Engineers, Warrendale, PA, USA. 1988.
- Nahum, Alan M. "The Biomechanics of Maxillofacial Trauma." Clinics in Plastic Surgery. 2(1):59-64, 1975.
- Swearingen, J.J.P. "Tolerances of the Human Face to Crash Impact." Report No. AM 65-20. Federal Aviation Agency, Civil Aeromedical Research Institute, Oklahoma City, OK, USA. 1965.

## **PART 8**

### **IMPACT RESPONSE OF THE SPINE**

## **ABSTRACT**

A drop-tower experiment involving dynamic axial loading of human cadaver spines was performed to provide information to support the hypothesis that the common mechanisms behind vertebral column failure under axial loading is the inertial effects of the torso mass. Six specimens, each consisting of a portion of the basilar skull, the entire spine, the pelvis, and the proximal third of the thighs, were raised to varying heights and allowed to drop freely and impinge upon an aluminum impact plate that actuated a force transducer. The injury results were documented through pre- and post-test x-rays and dissection. All injuries occurred in the mid-thoracic region and the conclusion is that the major mechanisms causing injury is the inertial effects of upper body mass.

## **INTRODUCTION**

It is well understood and documented that axial loading of the spine through contact with the head results in fractures to the cervical region. Diving injuries and spear-tackling football injuries are often fractured cervical vertebrae. On the other hand, resultant injuries can be quite different if the axial load is transmitted through the pelvic region (via contact with the ischial tuberosities). If an individual is loaded in this fashion (e.g. bottoming out while seated in a vehicle or falling from a height and landing rear first), failure of the vertebral column at the region near the bottom of the rib connections (i.e. thoracic-12 vertebrae) is expected. These failure patterns are clearly related to the inertial

effects of the torso mass. A drop-tower experiment involving dynamic axial loading of human cadaver spines was performed to provide auxiliary information to support the hypothesis that the common mechanisms behind vertebral column failure under axial loading is the inertial effects of the torso mass.

## **METHODOLOGY**

To test the hypothesis of this experiment, six specific anatomical specimens were dissected from embalmed cadavers and used in a drop-tower apparatus. Each specimen consisted of a portion of basilar skull, the entire spine, the pelvis, and the proximal third of the thighs. Four of the six specimens had an accelerometer-instrumented, 5.5 kilogram, magnesium dummy head attached. The head was attached with large hose clamps to the sectioned basilar skull and contained a uniaxial accelerometer at the center of gravity.

The experimental apparatus consisted of a 3-meter drop-tower/guide rail with the upright specimen attached at its basilar skull end. The specimens were raised to varying heights and allowed to drop freely upon an aluminum impact plate that actuated a force transducer.

The experimental matrix is shown in Table 1 on the following page.

**TABLE 1. Experimental Matrix**

Specimen #	Drop Height (cm)	Calculated Impact Velocity (m/s) (mph in parenthesis)	Dummy Head
1	130	1.6 (3.6)	Yes
2	130	1.6 (3.6)	Yes
3	225	2.1 (4.7)	Yes
4	315	2.5 (5.6)	Yes
5	295	2.4 (5.4)	No
6	265	2.3 (5.1)	No

## RESULTS

Pre- and post-test x-rays were taken of all specimens. Each specimen was also dissected in order to fully characterize the injury results as summarized in Table 2.

**TABLE 2. Primary Injury Results**

Specimen #	Fractured Vertebral Bodies	Involved Disks
1	T4,T5	T3/T4, T4/T5
2	T8,T9	T7/T8, T8/T9, T9/T10, T10/T11, T11/T12
3	T6	T6/T7
4	T4, T5	T4/T5, T5/T6
5	None	None
6	None	None

## DISCUSSION

As the drop height and final impact velocity were increased, the measured forces increased and the resultant injuries were more severe. The major



observation was that all of the injuries occurred in the mid-thoracic region. The vertebral column injuries usually involved two adjacent vertebrae and included impacted vertebral body fractures, disk ruptures and tears, and tears/lacerations in longitudinal ligaments. It is important to note that the specimens with minimal upper mass (no head) had no detectable injury. The conclusion is that the major mechanisms causing injury is the inertial effects of the upper mass.

## BIBLIOGRAPHY

- L. Douglas Baughman, "Development of an Interactive Computer Program to Produce Body Description Data." AFAMRL Technical Report No. AFAMRL-TR-83-058, July, 1983.
- Robert J. Bauze, Gordon M. Ardran, "Experimental Production of Forward Dislocation in the Human Cervical Spine." The Journal of Bone and Joint Surgery, Vol. 60-B, No. 2, May, 1978, pp. 239-245.
- T. Belytschko, J. Williams, M. Rencis, "Injury Mechanisms in Pilot Ejection." AAMRL Technical Report No. AAMRL-TR-85-019, July, 1985.
- Ali Erkan Engin, "Analysis of the Kinematic Properties Data of the Shoulder Complex During Forced Motion." AFAMRL Technical Report No. AFAMRL-TR-83-067, August, 1983.
- David E. Goldman, Henning E. Von Gierke, "The Effects of Shock and Vibration on Man." Naval Medical Research Institute No. 60-3, January 8, 1960.
- W. Goldsmith, J. L. Sackman, G. Ouligian, M. Kabo, "Response of a Realistic Human Head-Neck Model to Impact." Journal of Biomechanical Engineering, Vol. 100, February, 1978, pp. 25-33.
- T. Hallel (Huller), L. Naggan, "Parachuting Injuries: A Retrospective Study of 83,718 Jumps." The Journal of Trauma, Vol. 15, No.1, January, 1975, pp. 14-19.
- Voigt R. Hodgson, L. Murray Thomas, "Mechanisms of Cervical Spine Injury During Impact to the Protected Head." SAE Paper 801300, 1980.
- Tin-Kan Hung, Guan-Liang Chang, William W. Feng, Maurice S. Albin, "Studying Animals to Understand Spinal Cord Injuries." SOMA, April, 1987, pp. 40-44.
- A. I. King, "Biomechanics of the Spline and Pelvis." SAE Paper, January, 1973.

- David H. Laananen, "Passenger Response in Transport Aircraft Accidents - A Simulation." SOMA, Vol. 2, No. 1, April, 1987, pp. 18-25.
- James McElhaney, Richard G. Snyder, John D. States, M. Alexander Gabrielsen, "Biomechanical Analysis of Swimming Pool Neck Injuries." SAE Paper 790137, 1979.
- Shigeo Naito, Shigeru Sugiyama, "Drop Test Simulation Model for Motorcycles." SAE Technical Paper 930227, March 1-5, 1993.
- Roger W. Nightingale, Barry S. Myers, James h. McElhaney, William J. Richardson, Brian J. Doherty, "The Influence of End Condition on Human Cervical Spine Injury Mechanisms." SAE Paper 912915, 1991.
- David Orne, Y. King Liu, "A Mathematical Model of Spinal Response to Impact." Journal of Biomechanics, Vol. 4, No. 1-D, pp. 49-71.
- K. Mothiram Patil, M. S. Palanichamy, Dhanjoo N. Ghista, "Dynamic Response of Human Body Seated on a Tractor and Effectiveness of Suspension Systems." SAE Paper 770932, 1977.
- D. C. Reid, L. Saboe, "Spine Fractures in Winter Sports." Sports Medicine, Vol. 7, No. 6, 1989, pp. 393-399.
- David C. Reid, Linda A. Saboe, D. Gordon Allan, "Spine Trauma Associated with Off-Road Vehicles." Sports Medicine, Vol. 16, No. 6, June, 1988, pp. 143-152.
- Richard D. Rink, "Injuries of the Vertebral Column and Spinal Cord." Anatomy and Biomechanics of Trauma, April 28-29, 1992, pp. 78-94.
- T. Scalea, A. Goldstein, T. Phillips, S. J. A. Scalafani, T. Panetta, J. McAuley, G. Shaftan, "An Analysis of 161 Falls from a Height: The 'Jumper Syndrome'." The Journal of Trauma, Vol. 26, No. 8, August, 1986, pp. 706-712.
- Albert B. Schultz, "Biomechanics of the Human Spine and Trunk." Handbook of Bioengineering, McGraw-Hill, New York.
- A. B. Schultz, D. N. Warwick, M. H. Berkson, A. L. Nachemson, "Mechanical Properties of Human Lumbar Spine Motion Segments - Part I: Responses in Flexion, Extension, Lateral Bending, and Torsion." The Journal of Biomechanical Engineering, Transactions of the ASME, Vol. 101, February, 1979, pp. 46-52.
- Dennis F. Shanahan, George R. Mastroianni, "Spinal Injury in a U.S. Army Light Observation Helicopter." Aviation, Space, and Environmental Medicine, January, 1984.
- Alexander Vasilakis, Thomas Vargish, Keith N. Apelgren, Walter H. Moran Jr., "All Terrain Vehicles (ATVs): A Recreational Gamble." American Surgeon, Vol. 55, No. 3, March, 1989, pp. 142-144.

**PART 9**

**BIOMECHANICAL EFFECTIVENESS OF A SAFETY DEVICE:  
THE AIR BAG**

## **ABSTRACT**

The air bag system is described in terms of four basic elements: the crash sensors and controls, the inflator, the air bag itself, and the diagnostic circuitry. A general discussion of these elements is provided and a review of air bag related injuries is also presented which includes data from various sources such as the University of Michigan Transportation Research Institute, National Highway Traffic and Safety Administration, Transport Canada, and the Insurance Institute for Highway Safety. The most frequently occurring accident type is the frontal collision and has been the main focus of safety efforts with regard to restraint systems. Air bags are an effective injury prevention device, however their deployment can introduce new injury mechanisms. Air bags save lives and decrease the severity of major injuries in exchange for increasing the number of minor injuries. Certain risk factors exist during an accident involving air bag deployment including occupants sitting in close proximity to the air bag module (often small women) and unbelted occupants who move forward early in a crash or during precrash braking. The body regions most frequently injured are the head and neck, followed by the upper extremities, and then the lower extremities. Abrasions, contusions, and lacerations are identified as the injuries most often observed. Among the most severe air bag induced injuries are those to the eye, but these occur infrequently. From the review of injuries related to air bags, it appears that deployment of untethered air bags, closeness to air-bag

module or proximity to the steering wheel, and high velocity of deployment (high capacity inflator) are potential causal mechanisms.

## INTRODUCTION

Air bags have been rapidly assimilated into new motor vehicles. In fact, slightly over 90 percent of all 1994 model-year cars are equipped with a driver-side air bag, and over half of these also have passenger bags. U.S. law requires all new cars to have both driver and front passenger air bags by 1998 (and trucks by 1999).

It is reasonable to assume that by the year 2000 as many as a half million air bag deployments will occur annually. This extrapolates into over 200,000 injuries induced by air bag deployment using present-day injury rates as reported by the Insurance Institute for Highway Safety Administration.

Air bags are an effective injury prevention device in that they reduce the number of resulting deaths, and mitigate major injuries. However, there is a safety "trade-off", because air bags actually increase the total number of resulting injuries from vehicle collisions. Current air bag design and deployment characteristics introduce new injury mechanisms that increase the occurrence of minor injuries in medium speed accidents (change in velocity of 16-32 km/h).

This section presents a discussion of relevant design features of air bag systems and their deployment. Of course, these features and their design optimization are critical considerations as they relate to induced injuries. A

significant review of the extent and type of induced injuries is included after the design discussion.

## **AIR BAG SYSTEMS**

The air bag system can be described in terms of four basic elements: the crash sensors and controls, the inflator, the air bag itself, and the diagnostic circuitry. If the diagnostic circuitry is in proper working order to ensure deployment readiness, it is the design details of the other three elements that are critical with regard to injury effects.

Most of today's systems are equipped with several electromechanical ball-in-tube or spring-mass sensors mounted in front areas of the vehicle. These sensors are damped and are wired with an arming sensor which is set to a 1- to 2-g preload to prevent incidental detonation from jolts unrelated to an accident. Generally, the sensors are designed to activate air bag deployment whenever a sudden deceleration occurs in the automobile's forward motion that is approximately equivalent to a 16 to 19 km/h crash into a solid barrier. For most collisions, the sensors start the deployment process 15 to 20 msec after initial impact causing a pyrotechnic squib to ignite a gas generant (sodium azide) in the 18-23 msec time frame. Consequently, 21 to 27 msec after impact, the burning sodium azide produces nitrogen gas that expands into a nylon air bag which blows through a polyurethane sheath (or steering wheel cover). The actual inflation procedure, which consists of the nitrogen gas exiting its aluminum

vessel and surging into the air bag, takes about 20 to 40 msec. This allows the driver, who has moved forward about 125 to 150 mm, to contact the fully inflated bag around 45 to 50 msec into the event. The bag deflates during the 80 to 100 msec time span after the impact through vent holes placed in the back of the bag directed away from the driver. Figure 1 illustrates a typical timeline of the events associated with air bag deployment and driver movement.

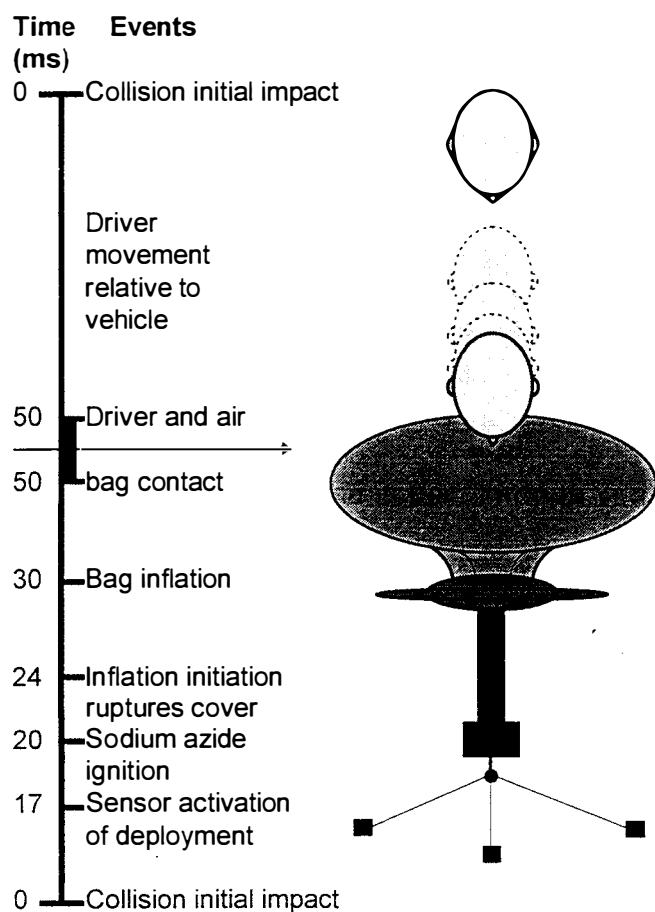


**FIGURE 1.** Example of typical timeline for air bag deployment process and driver movement.

In summary, the present day air bag deployment design criterion is 125 mm - 30 ms. This is based on the estimation that the bag is fully inflated in about 30 ms and restraint begins when the occupant has traveled 125 mm forward relative to the passenger compartment.

A variety of sensor (e.g. electromechanical, all-electronic or all-mechanical) and inflator designs exist in which the critical features are timing and speed. With respect to inflating the bag, timing and speed are obviously relevant for occupant protection, but inadvertent deployment has to be avoided and the hot nitrogen gas needs to be vented properly in order to avoid contact with skin while "decelerating" the occupant. "Safer" alternatives are being considered including sophisticated systems that differentiate between low- and high- severity crashes and inflators that do not involve pyrotechnic materials. Future inflators may consist of hybrid systems containing pressurized argon gas that when heated will expand to fill the air bag. Allied-Signal and Atlantic Research Corp. developed the hybrid inflator technology.

Timing and speed are important to ensure that the bag is fully expanded when the occupant first contacts it. This is to avoid high-speed bag/occupant interactions that could cause "slapping" injuries.

Most of today's air bags are made of nylon 6,6 in 420, 630 or 840 denier. Abrasive-resistant nylon (polyamide) provides a high strength-to-weight ratio, ages well, and adheres to coatings that are often used to enhance the bag's slip coefficient for smooth and rapid deployment. Another attribute of nylon is its



good elongation characteristics. This allows for uniform stress distribution along perimeter seams. These characteristics allow the forces to be widely distributed, enhancing fracture resistance at the highest stress points.

Having a diameter of about 610 to 710 mm, the circular-shaped driver-side air bag is much smaller and inflates more rapidly than the rectangular-shaped passenger-side unit. The driver-side bag has less time and distance to travel before contact with an occupant, since the bag is mounted closer to the driver via the steering column. As a result, the passenger units are typically three to five times larger. Smaller driver-side bags, often called face bags, are used in many vehicles in Europe and Japan because 9 out of 10 of the drivers wear seat belts making them more likely to be positioned for optimal protection.

A major evolutionary change in air bag design came with the introduction of the internal tethering systems for improved deployment control. Adding tethers inside the air bag limits intrusion of the air bag into the normal driver space during deployment, therefore reducing the risk of inflation-induced injuries to the driver. Tethering also allows for a more rapid lateral expansion, increasing protection effectiveness for out-of-position occupants. At full deployment, tethered bags extend 250-330 mm towards the driver and untethered bags extend 380-510 mm.

An air bag's diagnostic system serves three primary functions. It first evaluates the entire system when the key is placed into the ignition. Secondly, it continues to monitor the system periodically during operation. Finally, as a

backup power source it contains storage capacitors that are continuously charged by the battery . These capacitors can remain active for several seconds even after battery failure. They provide the charge needed to ignite the squib in the inflator module. These functions are coordinated through a microprocessor that informs the operator of any malfunctions.

Almost all air bag systems are designed to deploy in crashes equivalent to hitting a solid barrier at 16-19 km/h. This deployment threshold feature relates to frontal crash severity. Some engineers argue that this threshold may be too low causing unnecessary deployments and that additional efforts should be directed towards addressing issues such as side, rear, and rollover accidents.

Air bag systems incorporate a wide variety of features such as deployment thresholds, inflation speeds, material choices, folding patterns, tethering, and gas ventilation. There should be an "optimal" design for safety purposes, however an air bag's effectiveness is strongly dependent on vehicle crush characteristics, occupant anthropometrics, and occupant positioning.

## **REVIEW OF AIR BAG INDUCED INJURIES**

Air bags are definitely one of the best automobile safety devices ever to be developed. They have been extremely effective in preventing deaths and serious injuries. Researchers from the Insurance Institute for Highway Safety reported on about 18,000 driver crash deaths during 1985-1992 stating that there were fewer deaths in front and front-angle crashes in air bag-equipped

cars. The National Highway Traffic and Safety Administration's National Accident Sampling System (NHTSA's NASS) shows a steady decline in serious injuries from accidents during 1988-1993. This may be indicative that the air bag system is effective.

The Office of Defects Investigations at the National Traffic Safety Administration handles consumer complaints. They have received some complaints about injuries from air bags. Air bags restrain occupants in collisions, but they may cause some injuries as they perform this restraint function. This does not mean that air bags are ineffective. They save lives and decrease the severity of major injuries in exchange for increasing the number of minor injuries. In low severity crashes, the deployment of the air bag may expose occupants to risk, introducing them to air bag induced injuries. There are some conditions in which the driver seems to be particularly vulnerable. An unbelted occupant can move forward too far and/or be out-of-position during a crash. Even if belted, sitting too close to the air bag module can lead to more severe injuries. It is often found that small or elderly women sit close to the steering wheel.

Most air bag induced injuries occur while the bags are still inflating. Although seat belts do not eliminate the occurrence of occupant contact with the bag during inflation, they are crucial in holding occupants in place as much as possible so that air bags can work properly. Air bags are supplemental restraint systems that are designed to work in conjunction with seat belts. See Table 1 comparing resultant injuries from different restraint combinations.

**TABLE 1. AIS Rating of Most Severe Injury as a Percentage of Drivers in Each Category of Restraint**

Injury Severity	Restraint Use and Type			
	None	Belt Only	Air Bag Only	Air Bag + Belt
AIS = 1	73.8%	84.4%	79.4%	83.0%
2	17.9	12.0	11.7	14.5
3	5.4	2.7	7.4	1.8
4	1.3	0.51	1.0	0.50
5+	1.57	0.43	0.58	0.16

Source: Malliaris AC, Digges KH, Debloss JH: Injury Patterns of Car Occupants Under Air Bag Deployment. SAE Paper 950867, International Congress and Exposition, Detroit, Michigan, 1995.

While air bags are saving lives, the acceptable trade-off is increased abrasions, contusions, and lacerations. The body regions most frequently injured by the air bag are the head and neck, followed by the upper extremities, the trunks, and then the lower extremities. (see Table 2 in which Malliaris reports on data from NHTSA's NASS files).

**TABLE 2. Most Severely Injured Body Region as a Percentage of Drivers in Each Category of Restraint**

Body Region	Restraint Use and Type			
	None	Belt Only	Air Bag Only	Air Bag + Belt
Head/Neck	66.3%	52.5%	47.2%	47.9%
Trunk	14.8	24.3	17.0	21.7
Upper Xtrem	7.5	8.9	17.9	22.6
Lower Xtrem	11.4	14.4	18.0	7.9

Source: Malliaris AC, Digges KH, Debloss JH: Injury Patterns of Car Occupants Under Air Bag Deployment. SAE Paper 950867, International Congress and Exposition, Detroit, Michigan, 1995.

Among the most severe air bag induced injuries are those to the eye, but these occur infrequently. According to a study conducted by Transport Canada, the vast majority (94%) of the injuries sustained by drivers were confined to AIS

1 severity level. About 4.5% were AIS 2 and 1.5% were AIS 3 or greater. One of the great advantages of the air bag, even without a safety belt, is the reduction in critical and untreatable injuries (AIS 5). Transport Canada presents a closer look at the injuries in accidents with air bag deployment. This is reproduced in Table 3, which shows the percentages and severities of injuries by body region.

**TABLE 3. Distribution of Individual Injuries Sustained by Belted Drivers in Collisions Which Resulted in the Deployment of an Air Bag System**

Body Region	Anatomic Structure	AIS1 (%)	AIS2 (%)	AIS3 (%)	Total (%)
Head	Head	0.55	1.10	0.55	2.20
	Skin	1.37	0.27	-	1.65
Face	Organs	0.82	-	-	0.82
	Skeletal	0.82	-	-	0.82
	Skin	24.73	-	-	24.73
Neck	Skin	2.47	-	-	2.47
Thorax	Organs	-	0.27	0.27	0.55
	Skeletal	1.10	0	0	1.10
	Skin	8.24	0	0	8.24
Abdomen	Organs	-	0.27	-	0.27
	Skin	2.75	-	-	2.75
Spine	Organs	7.14	-	-	7.14
	Skin	0.27	-	-	0.27
Upper Extremity	Organs	0.82	-	-	0.82
	Skeletal	2.47	1.65	0.55	4.67
	Skin	27.75	-	-	27.75
Lower Extremity	Organs	0.27	-	-	0.27
	Skeletal	1.65	1.10	-	2.75
	Skin	10.71	-	-	10.71
Total		94.0	4.7	1.4	100.0

Source: Dalmotas DJ, Hurley RM, German A: Air Bag Deployments Involving Restrained Occupants. SAE Paper 950868, International Congress and Exposition, Detroit, Michigan, 1995.

The University of Michigan Transportation Research Institute and other organizations have compiled data for a large number of collisions involving air bag deployment. They found that the primary air bag associated injuries are erythema, abrasions, lacerations, and contusions to the face, arms, wrist, and upper-chest. A special NHTSA investigation in 1993 reported data that are summarized in Table 4, which adds insight into the types and locations of injuries sustained from air bags.

**TABLE 4. Type and Location of Occupant Injuries Caused by Air Bags**

	Head/Neck/Face	Chest	Upper Extremity	Other	Total
Abrasion	116	16	91	2	<b>225</b>
Contusion	35	31	44	4	<b>114</b>
Laceration	34	0	15	0	<b>49</b>
Burn	7	0	30	1	<b>38</b>
Other	8	0	3	0	<b>11</b>
<b>Total</b>	<b>200</b>	<b>47</b>	<b>183</b>	<b>7</b>	<b>437</b>

Our familiarity with the literature together with case data from various sources has provided insight about some specific injury details and resulted in the development of Table 5. The intent of this table is to provide a characterization of air bag induced injuries with regard to their causal mechanisms. Most of these injury data are for drivers and relate the type of injury to the collision conditions that led to the injury. Data are summarized about four primary body regions: head/face, neck, upper extremities, and trunk. The lower extremities are not in the path of the deploying air bag and are generally only injured if the occupant is unbelted or if significant interior compartment crumple or intrusion occurs.

**TABLE 5. Characterization of Air bag Induced Injuries**

Body Region: Head/Face		
Injury	Risk Factor	Mechanism of Injury
Abrasion and/or Laceration	Deployment of untethered bag (as opposed to tethered) Closeness to air bag module Unbelted driver	Individual contacts the central portion of the bag causing more localized pressure Surface of inflating air bag moving at high velocity "slaps" occupant Individual contacts the bag
Contusion	Untethered air bag or improper use of seat belt	Air bag impacts driver's face
Burn	Poor location of exhaust ports or unbelted occupant Burn through the front of the nylon bag Sodium azide residue in the driver compartment from incomplete burning	Gases escaping through the exhaust ports Hot gases directly contacting the face through burn holes or tears in bag Highly alkaline residue contacts individual eye
Nasal Fracture	Foreign objects or body parts between air bag and occupant	Individual or object strikes self (e.g. hand/arm gets impacted by air bag and directed toward the face)
Body Region: Neck		
Injury	Risk Factor	Mechanism of Injury
Cervical Sprain	Unbelted driver	Force of impact between unrestrained driver and the inflating air bag
Cervical Fracture	Sitting too "close" and/or too "high" above the air bag module	Inflating air bag expanding upward hyperextends neck
Body Region: Upper Extremities		
Injury	Risk Factor	Mechanism of Injury
Abrasion and/or Laceration	Occupant moves deflated air bag out of the way with arm High capacity inflator Proximity to the air bag	Skin contact with metal inflator after deployment High velocity air bag fabric impacting perpendicular to the skin surface Deploying air bag snags on jewelry, which in turn scuffs the skin
Contusion	Proximity to the air bag	Deploying air bag can slide along the forearm, slap the forearm, or push the forearm/hand into the face
Burn	Location of vent ports or unbelted occupant	Exhaust gas or powder residue contact with skin
Fracture of fingers, hand or forearm, sprains to wrist	Closeness to air bag module at the time of deployment	Upper limb is accelerated by the inflating bag and impacts instrument panel, rear view mirror, or windshield; also could impact other body region (e.g. face or chest)
Body Region: Trunk		
Injury	Risk Factor	Mechanism of Injury
Intrathoracic fractures and ruptures	High speed collision, unbelted driver	Torso interaction with the air bag
Erythema on anterior abdominal wall	Unbelted and sitting too high	Contact with the air bag

Among the most severe air bag induced injuries are those to the eye, but their occurrences are extremely rare. NHTSA investigated 436 air bag induced injuries and only 28 of these involved the occupant's eyes. 25 of the 28 were classified as minor injuries (IIHS, 1993). Even though they do not occur often, air bag induced ocular injuries should be a serious concern because of the possibility of permanent impairment and because, even under favorable

conditions, such as the presence of a fastened three-point belt, a severe ocular injury can occur. Rimmer and Shular (1991) documented a serious air bag induced eye injury that occurred to a belted 26-year old male. Some injuries can be serious enough to require surgery such as detached retinas or ruptured globes. In a 1994 study conducted by Werner and Sorenson, data were collected from 1,654 severe frontal crashes. This study documented one retinal detachment, one scleral laceration, and one corneal laceration. Eyeglasses can also be an added risk factor, because of the potential for breakage. Gault et al (1995) reported on three such cases in which the visual prognosis from the injury was poor. Table 6 lists some different eye injuries and suggests possible causes or conditions that could lead to these injuries.

**TABLE 6. Suggested Causation of Some Eye Injuries Related to Air Bags**

<b>Eye Injury</b>	<b>Possible Cause of Injury</b>
Corneal abrasion	Seam of the air bag brushing across the driver's face
Periorbital damage	Impact on out of position head; broken glasses
Corneal endothelial cell loss	Impact of the air bag during inflation (driver positioned very near the air bag module)
Chemical keratitis	Incomplete combustion of the inflation material (about 70g of sodium azide)
Minor blunt trauma (contusions)	Blunt trauma to the eye associated with air bag impact
Hyphemas (internal eye bleeding)	High pressure blunt trauma to the eye associated with air bag impact
Moderate conjunctival injection	Air bag inflates and bursts - showering the occupant with a fine powder
Retinal detachment	The air bag striking the occupant's face at high velocity



A common risk factor is the driver's closeness to the air bag module. If the driver is too close he/she will contact the air bag during the inflation and expansion process. This can be quite serious because peak leading edge velocities of air bags can range from 171 to 328 km/h as reported by Powell and Lund (1995).

Because of the serious nature of eye injuries, safety engineers may need to examine the injury causal mechanisms as they relate to the air bag in order to optimize design. For this section, some of NHTSA's NASS files, dating from 1984-1994, were reviewed. Only twenty-five cases with air bag induced eye injuries were identified in the files. Collision and injury information was extracted from each of these case files and compiled into Appendix H. An attempt was made to list causal mechanisms associated with each injury while also providing information about the occupant and the collision itself.

Review of other clinical cases has identified at least one fatal case associated with the injury sustained from an air bag deployment. The closed-head fatal injury of cerebral edema and extensive intracranial hemorrhages occurred to a belted 157.5 cm tall female who was sitting close to the air-bag at the time of its deployment.

Air bag induced injuries are an acceptable tradeoff in comparison to the injuries incurred in the absence of an air bag. There are unusual circumstances that do lead to serious injury because of the air bag's presence but the odds are

overwhelmingly greater for reducing the seriousness of an injury if an air bag is present.

## **DISCUSSION**

The review of numerous publications associated with air bag induced injuries has led to the identification of causal mechanisms. It is clear that tethering the bags is a significant design improvement. Abrasions are less likely to occur when a tethered bag is present because the probability of occupant contact with the bag before complete inflation is reduced. Generally speaking, the closer the occupant is to the air bag module the more significant are the abrasions and other injuries, but even more so if the bag is untethered.

Vehicle and air bag manufacturers are continuing to refine their air bag system designs for improved safety. Some refinements include using improved folding patterns and special fabric coatings to allow deployment to be "smoother". Other design efforts have included altering deployment thresholds and bag inflation pressures.

A group of Canadian researchers recommends different thresholds for deploying air bags depending on whether or not occupants are belted. Belted occupants may sustain injuries from air bags in crashes of low severity in which they would otherwise be uninjured. In these cases, the deployment threshold should be higher. The researchers suggest a lower deployment threshold for unbelted occupants because the chance of significant injury is greater.

Sullivan (1992) produced a report for NHTSA characterizing the average peak deployment velocity of an air bag as 232 km/h with a maximum velocity of 340 km/h. The report states "the possibility of injuries during air bag inflation can be reduced by reducing bag size and inflation speed". The report also states that a large portion of the reported injuries are to smaller occupants who tend to be seated closer to the steering wheel than most other occupants.

It appears that deployment of untethered air bags, closeness to the air bag module or proximity to the steering wheel and high velocity of deployment (high capacity inflator) are the most significant factors associated with induced injuries. It is recommended that occupants in vehicles with air bags sit as far from the steering wheel, or module, as is comfortable to minimize the possibility of contact with the air bag before full inflation.

## **BIBLIOGRAPHY**

- Ashley SA: Automotive Safety is in the Bag. Mechanical Engineering 116:58, 1994
- Augenstein JS, Digges KH, Lombardo LV, et al: Occult Abdominal Injuries to Airbag-Protected Crash Victims: A Challenge to Trauma Systems. J Trauma 38:502, 1995
- Aylward WG, Cooling RJ, Leaver PK: Trauma-Induced Retinal Detachment Associated with Giant Retinal Tears. Retina 13:136, 1993
- Barr CC: Prognostic Factors in Corneoscleral Lacerations. Arch Ophthalmol 101:919, 1983
- Bayley GS, Handman D, Lee C, Lee CS, et al: Experimental Measurements of Deploying Pressure Distribution on a Passenger-Side Air-Bag Door. SAE Paper 950339, International Congress and Exposition, Detroit, Michigan, 1995
- Bradley EK: What You Should Know Before Entering the Air Bag Business. Automotive Technology International, p95, 1994

- Braude LS: Protective Eyewear Needed With Driver's-Side Air Bag? *Arch Ophthalmol* 110:1201, 1992
- Burgess AR, Dischinger PC, O'Quinn TD, et al: Lower Extremity Injuries in Drivers of Airbag-Equipped Automobiles: Clinical and Crash Reconstruction Correlations. *J Trauma* 38:509, 1995
- Campbell JK: Automobile Air Bag Eye Injuries. *Nebr Med J*, September, p306, 1993
- Canavan YM, Archer DB: Anterior Segment Consequences of Blunt Ocular Injury. *Br J Ophthalmol* 66:549, 1982
- Classe JG, Semes LP: Types of (eye) Injuries. *Assessing Blunt Ocular Trauma* 3:117, 1992
- Crouch ET: Evolution of Air Bag Components and Materials. *Automotive Engineering* 102:99, 1994
- Dalmotas DJ, German A, Hendrick BE, et al:  
Airbag Deployments: The Canadian Experience. *J Trauma* 38:476, 1995
- Dalmotas DJ, Hurley RM, German A: Air Bag Deployments Involving Restrained Occupants. *SAE Paper 950868*, International Congress and Exposition, Detroit, Michigan, 1995
- Blacksin MF: Patterns of Fracture After Air Bag Deployment. *J Trauma* 35:840, 1993
- Fischer K: Passenger Air Bag System Tailoring Algorithm. *SAE Paper 950874*, International Congress and Exposition, Detroit, Michigan, 1995
- Freedman EL, Safran MR, Meals RA: Automotive Airbag-Related Upper Extremity Injuries: A report of Three Cases. *J Trauma* 38:577, 1995
- Fukagawa K, Tsubota K, Kimura C, et al: Corneal Endothelial Cell Loss. *Ophthalmology* 100:1819, 1993
- Gault JA, Vichnin MC, Jaeger EA, Jeffers JB: Ocular Injuries Associated with Eyeglass Wear and Airbag Inflation. *J Trauma* 38:494, 1995
- Goffstein R, Burton TC: Differentiating Traumatic From Nontraumatic Retinal Detachment. *Ophthalmology* 89:361, 1982
- Graul TA, Ruttum MS, Lloyd MA, et al: Trabeculectomy for Traumatic Hyphema with Increased Intraocular Pressure. *Am J Ophthalmol* 117:155, 1994
- Gross KB, Koets MH, D'Arcy JB, et al: Mechanism of Induction of Asthmatic Attacks Initiated by the Inhalation of Particles Generated by Airbag System Deployment. *J Trauma* 38:521, 1995
- Han DP: Retinal Detachment Caused by Air Bag Injury. *Arch Ophthalmol* 111:1317, 1993
- Horsch J, Lau I, Andrzejak D, Viano D, et al: Assessment of Air bag Deployment Loads. *SAE Paper 902324*, International Congress and Exposition, Detroit, Michigan, 1990
- Huelke DF: An Overview of Air Bag Deployments and Related Injuries. *Case Studies and Lit. Review. SAE Paper 950866*, International Congress and Exposition, Detroit, Michigan, 1995

- Huelke DF, Moore JL: Field Investigations of the Performance of Air Bag Deployments in Frontal Collisions. *Accid Anal and Prev* 25:717, 1993
- Huelke DF, Moore JL, Compton TW, et al: Upper Extremity Injuries Related to Airbag Deployments. *J Trauma* 38:482, 1995
- Huelke DF, Moore JL, Ostrom M: Air Bag Injuries and Occupant Protection. *J Trauma* 33:894, 1992
- Hussey B, Rink LM: Predictive Techniques for Airbag Inflator Exit Properties. SAE Paper 950344, International Congress and Exposition, Detroit, Michigan, 1995
- Insurance Institute for Highway Safety Report: Air Bags: Chronology, April, 1993
- Insurance Institute for Highway Safety Report: Air Bags 28:1, 1993
- Insurance Institute for Highway Safety Report: Air Bag Effectiveness 30:1, 1995
- Ito K, Ishikawa, Sakamoto K, et al: A Driver-Side Airbag System Using a Mechanical Firing Microminiature Sensor. SAE Paper 950346, International Congress and Exposition, Detroit, Michigan, 1995
- Jagger G, Vernberg K, Jane JA: Air Bags: Reducing the Toll of Brain Trauma. *Neurosurgery* 20:815, 1987
- Jones IL, Warner M, Stevens JD: Mathematical Modeling of the Elastic Properties of Retina: A Determination of Young's Modulus. *Eye* 6:556, 1992
- Joondeph BC, Young TL, Saran BR: Multiple Scleral Ruptures After Blunt Ocular Truma. *Am J Ophthalmol* 108:744, 1989
- Kallieris D, Stein M, Mattern R: The Performance of Active and Passive Dirver Restraint Systems in Simulated Fronal Collitions. In 38th Stapp Car Crash Conference Proceedings. Ft. Lauderdale, Florida, Society of Automotive Engineers, 1994, pp165-175
- Keshavaraj R, Tock RW, Nusholtz GS: A Novel "Blister-Inflation" technique for Evaluating the Thermal Aging of Airbag Fabrics During Deployment. SAE Paper 950341, International Congress and Exposition, Detroit, Michigan, 1995
- Keshavaraj R, Tock RW, Nusholtz GS: Comparison of Contributions to Energy Dissipation Produced with Safety Airbags. SAE Paper 950340, International Congress and Exposition, Detroit, Michigan, 1995
- Keshavaraj R, Tock RW, Nusholtz GS: Modeling of Biaxial Deformation of Airbag Fabrics Using Artificial Neural Nets. SAE Paper 950343, International Congress and Exposition, Detroit, Michigan, 1995
- Klove EH, Oglesby RN: Special Problems and Considerations in the Development of Air Cushion Restraint Systems. SAE Paper 720411, 2nd International Conference on Passive Restraints, Detroit, Michigan, 1972
- Kratzke SR: Regulatory History of Automatic Crash Protection in FMVSS 208. SAE Paper 950865, International Congress and Exposition, Detroit, Michigan, 1995

- Kuhn F, Morris R, Witherspoon CD, et al: Air Bag: Friend or Foe? Arch Ophthalmol 111:1333, 1993
- Kuhn F, Morris R, Witherspoon CD, et al: Ocular Injuries in Motor Vehicle Crashes. Ophthalmology 100:1280, 1993
- Larkin GL: Airbag-Mediated Corneal Injury. Am J of Emerg Med 9:444, 1991
- Lau IV, Horsch JD, Viano DC, et al: Mechanism of Injury from Air Bag Deployment Loads. Accid Anal Prev 25:29, 1993
- Leshner MP, Durrie DS, Stiles MC: Corneal Edema, Hyphema, and Angle Recession After Air Bag Inflation. Arch Ophthalmol 111:1320, 1993
- Libertiny GZ: Air Bag Effectiveness - Trading Major Injuries for Minor Ones. SAE Paper 950871, International Congress and Exposition, Detroit, Michigan, 1995
- Lund AK, Ferguson SA: Driver Fatalities in 1985-1993 Cars with Airbags. J Trauma 38:469, 1995
- Malliaris AC, Digges KH, DeBlois JH: Evaluation of Air Bag Field Performance. SAE Paper 950869, International Congress and Exposition, Detroit, Michigan, 1995
- Malliaris AC, Digges KH, DeBlois JH: Injury Patterns of Car Occupants Under Air Bag Deployment. SAE Paper 950867, International Congress and Exposition, Detroit, Michigan, 1995
- Marsh IV JC: Airbags: Education and Experience. Automotive Engineering, September, p29, 1993
- Melvin JW: Injury Assessment Reference Values for the CRABI 6-month Infant Dummy in a Rear-Facing Infant Restraint with Airbag Deployment. SAE Paper 950872, International Congress and Exposition, Detroit, Michigan, 1995
- Mishler KE: Hyphema Caused by Air Bag. Arch Ophthalmol 109:1635, 1991
- Nanda SK, Mieler WF, Murphy ML: Penetrating Ocular Injuries Secondary to Motor Vehicle Accidents. Ophthalmology 100:201, 1993
- Patrick LM, Nyquist GW: Airbag Effects on the Out-of-Position Child. SAE Paper 720442, International Congress and Exposition, Detroit, Michigan, 1972
- Powell MR, Lund AK: Leading Edge Deployment Speed of Production Airbags. SAE Paper 950870, International Congress and Exposition, Detroit, Michigan, 1995
- Reed D: Father of the Air Bag. Automotive Engineering, February, p67, 1991
- Reed MP, Schneider LW, Burney RE: Investigation of Airbag-Induced Skin Abrasions. SAE Paper 922510, International Congress and Exposition, Detroit, Michigan, 1992
- Reed MP, Schneider LW, Burney RE: Laboratory Investigations and Mathematical Modeling of Airbag-Induced Skin Burns. In 38th Stapp Car Crash Conference Proceedings. Ft. Lauderdale, Florida, Society of Automotive Engineers, 1994, pp177-190

- Reinfurt DW, Green AW, Campbell BJ, et al: Survey of Attitudes of Drivers in Air Bag Deployment Crashes. *Journal of Safety Research* 25:147, 1994
- Rimmer S, Shuler JD: Severe Ocular Trauma From a Driver's-Side Air Bag. *Arch Ophthalmol* 109:23, 1991
- Rosenblatt MA, Freilich BF, Kirsch D: Air Bag-Associated Ocular Injury. *Arch Ophthalmol* 111:1318, 1993
- Rosenblatt MA, Freilich BF, Kirsch D: Air Bags: Trade-Offs. *N Engl J Med* 325:1518, 1991
- Ruan JS, Prasad P: Head Injury Potential Assessment in Frontal Impacts by Mathematical Modeling. SAE Paper 942212, International Congress and Exposition, Detroit, Michigan, 1994
- Rutledge R: Injury Severity and Probability of Survival Assessment in Trauma Patients Using a Predictive Hierarchical Network Model Derived from ICD-9 Codes. *J Trauma* 38:590, 1995
- Sanke RF: Blunt Ocular Trauma. *Am Fam Physician* 29:159, 1984
- Sastry SM, Copeland RA, Mezgebe H, et al: Retinal Hemorrhage Secondary Airbag-related Ocular Trauma. *J Trauma* 38:582, 1995
- Sastry SM, Paul BK, Bain L, et al: Ocular Trauma Among Major Trauma Victims in a Regional Trauma Center. *J Trauma* 34:223, 1993
- Schreck TM, Rouhana SW, Santrock J: Physical and Chemical Characterization of Airbag Effluents. *J Trauma* 38:528, 1995
- Scott IU, John GR, Stark WJ, et al: Airbag-Associated Ocular Injury and Periorbital Fractures. *Arch Ophthalmol* 111:25, 1993
- Shokoohi F: Airbag Sensor Fire Time - Occupant Performance Criterion. SAE Paper 950873, International Congress and Exposition, Detroit, Michigan, 1995
- Smally AJ, Binzer A, Dolin S, et al: Alkaline Chemical Keratitis: Eye Injury From Airbags. *Ann Emerg Med* 21:1400, 1992
- Smock WS, Nichols II GR: Airbag Module Cover Injuries. *J Trauma* 38:489, 1995
- Sullivan LK, Kossar JM: Air Bag Deployment Characteristics. National Highway Traffic Safety Administration DOT HS 807 869, February, 1992
- Tanavde AS, Khandelwal H, Lasry D, et al: Airbag Modeling Using Initial Metric Methodology. SAE Paper 950875, International Congress and Exposition, Detroit, Michigan, 1995
- Viano DC: Restraint Effectiveness, Availability and Use in Fatal Crashes: Implications to Injury Control. *J Trauma* 38:538, 1995
- Vinger PF, The Eye and Sports medicine. In Duane's Clinical Ophthalmology. Philadelphia, Pennsylvania, JB Lippincott Company, 1994, pp1-94
- Vos TH, Goetz GW: Inflatable Restraint Systems: Helping Save Lives on the Road. TRW Space and Defense Quest, Winter, 1989/1990
- Walz FH, Mackay M, Gloor B: Airbag deployment and Eye Perforation by a Tobacco Pipe. *J Trauma* 38:498, 1995

- Wang JT: On Airbag Inflator Grade Designation-A Five Index Grading System. SAE Paper 950345, International Congress and Exposition, Detroit, Michigan, 1995
- Wedrich A, Velikay M, Binder S, et al: Ocular Findings in Asymptomatic Amateur Boxers. *Retina* 13:114, 1993
- Werner JV, Sorenson WW: Survey of Airbag Involved Accidents, Analysis of Collisions Characteristics, and System Effectiveness, and Injuries. SAE Paper 940802, International Congress and Exposition, Detroit, Michigan, 1994
- Whitacre MM, Pichard WA: Air Bag Injury Producing Retinal Dialysis and Detachment. *Arch Ophthalmol* 111:1320, 1993
- Wong AD, Cooperberg PL, Ross WH, et al: Differentiation of Detached Retina and Vitreous Membrane with Color Flow Doppler. *Radiology* 178:429, 1991
- Yoganandan N, Pintar FA, Reinartz J, et al: Human Facial Tolerance to Steering Wheel Impact: Biomechanical Study. *Journal of Safety Research* 24:77, 1993



**PART 10**

**BIOMECHANICAL EFFECTIVENESS OF A SAFETY DEVICE:  
A BOAT MOTOR CAGE-TYPE PROPELLER GUARD**

## ABSTRACT

The intent of this research was to describe and quantify the nature and extent of impact injuries inflicted on a swimmer's leg when struck by a particular cage-type propeller guard on a boat outboard motor. A specific objective was to determine a threshold velocity above which the injury would be considered to be sufficiently severe enough to result in loss of leg function.

An outboard motor fitted with the cage-type prop guard was towed at various speeds on a platform attached to a centrifuge arm. The prop guard was impacted onto embalmed human cadaver legs which were positioned stationary underwater and connected to upper-body components of a Hybrid III test dummy.

Measurements were made of: 1) the position and velocity of the impactor as it struck the cadaver legs, 2) high-speed motion pictures of the external response of the legs and attached Hybrid III components (via high-speed motion pictures and video), and 3) acceleration and force (from some of the tests). Post-impact analysis of the test legs included detailed radiographs, careful dissection, and evaluation of fractures to the tibia and fibula. Specific tissue responses evaluated were bone fracture and fragmentation patterns.

The resultant fractures were considered to be conservative (less severe) than what would actually occur in "real-world" impacts because of reasons discussed in the report. Six out of seven of the legs tested resulted in comminuted fractures so severe that loss of leg function would be expected. The seventh

impact, at the lowest velocity of 10.4 mph, resulted in a transverse fracture from which full recovery would be likely.

It was concluded that for the loading condition and population studied in this series of tests, the specific prop-guard cage is not an effective device in preventing severe leg injury at boat velocities greater than or equal to about 13 mph.

Follow-up studies could be conducted using "fresher", embalmed, full human cadavers to confirm the findings and answer other questions of interest.

## INTRODUCTION

Tests were performed at the Center for Research in Special Environments at the State University of New York in Buffalo, New York, to take advantage of an existing facility conducive to underwater impact tests.

The facility includes an 8-foot deep water tank with a circumference of 200 feet. The tank surrounds a centrifuge which has a 31.7-foot arm. The purpose of the tests was to study the effects of a specific cage-type guard (see **Figure 1**) on injury severity to the human leg. A specific objective was to determine a threshold velocity above which the injury would be considered sufficiently severe to result in loss of leg function.

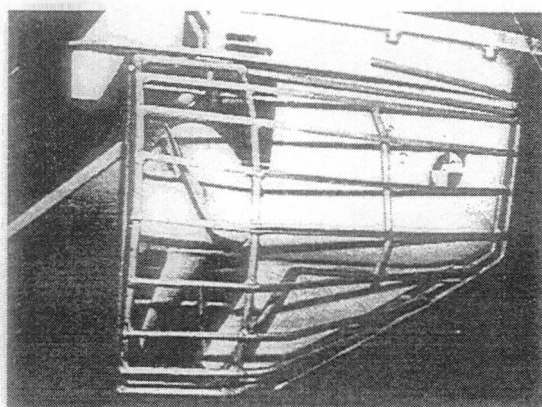


**FIGURE 1.** Photograph of cage-type guard mounted on propeller in which the forward direction of travel for the boat is to the right.

The cage-type guard, shown in Figure 1, is made of 5/16 inch diameter steel wire rods welded together in such a fashion that the "impact" end forms a wedge that makes a transition to a cylindrical section covering the propeller.

## **METHODOLOGY**

A total of eight embalmed human cadaver legs (sectioned at mid-thigh region and connected to the Hybrid III upper-body components) were used for the study. Ball-and-socket metal "hip joints" were the connective links between the cadaver legs and the Hybrid III components. The joints were connected to the femurs of each leg by the use of surgical cement and then attached to the Hybrid III in a manner such that the Hybrid remained "waterproofed." The legs were impacted with the prop-guarded motor towed at various speeds beginning at 21.0 mph. The speed was systematically decreased until a "threshold" velocity was determined. The threshold velocity is that speed above which injury is so severe that loss of leg function would result. Table 1 shows the conditions for all the tests.

For seven of the eight legs tested in Buffalo the following were the fixed conditions:

- 1) impactor: cage-type prop guard (see Figure 1),
- 2) object impacted: embalmed human cadaver leg connected to Hybrid III torso,
- 3) position of leg: horizontal to water surface and completely submerged,
- 4) impact location: proximal one-third of tibia, and
- 5) impact direction: anterior-to-posterior.

**TABLE 1. Test Conditions and Resultant Fractures**

Test #	Impactor	Velocity (mph)	Accelerometer	Fracture Description
L1	CGM <sup>1</sup>	21.0	No	Comminution <sup>2</sup>
L2	CGM	21.0	No	Comminution
L3	CGM	17.2	No	Comminution
L4	CGM	17.2	Yes	Comminution
L5	CGM	13.6	Yes	Comminution
L6	CGM	13.6	Yes	Comminution
L7	CGM	10.4	Yes	Transverse <sup>3</sup>
L8 <sup>4</sup>	PIPE	17.2	Yes	Non-applicable
L8M <sup>5</sup>	PIPE	17.2	Yes	Non-applicable

Notes: <sup>1</sup>CGM: Cage-Guarded Motor

<sup>2</sup>Comminution: Comminution fractures of the proximal tibia and fibula; for more detailed description of osteology, see Appendix C.

<sup>3</sup>Transverse: Transverse fractures of the proximal tibia and fibula; for more detailed description of osteology, see Appendix C.

<sup>4</sup>L8: This test included a force transducer.

<sup>5</sup>L8M: This test was a second impact to the leg used in test L8. Test conditions were the same, except that fracture had already occurred from test L8. The purpose of this special test was to independently measure the forces required to accelerate the mass without including the force to fracture the bone.

Photographs were made of the legs before and after the tests, and high-speed motion pictures were made of the impacts. X-rays were taken of the legs prior to and after testing and extensive dissection work was performed to evaluate the nature and extent of injury.

Accelerometers were placed inside four of the seven legs near the point of attachment to the Hybrid III components. This allowed the researchers to obtain acceleration data for possible future empirical calculations. A special test was required to relate the acceleration data to the applied force. For this special test, the impactor was a pipe structure previously used during in-air tests at the University of Tennessee laboratory. This pipe structure included a transducer for direct measurement of the force.

## **INSTRUMENTATION AND SPECIMEN EVALUATION**

Each leg was characterized before and after impact by utilizing x-rays, still photography, and various anthropometric measurements. Post-impact evaluation included dissection with particular attention directed toward bone fracture and fragmentation.

The instrumentation system employed during the impacts provided a time base, impactor position and velocity, and the external leg response to the impact (via high-speed photography).

Accelerometers and a force transducer were used as outlined in the Methodology section of this report. The data acquisition system that recorded the signals was a Hewlett Packard 3562A analyzer.

Nominal impact velocities were established by presetting the values on a PC computer that was programmed to generate an analog control voltage. This system was calibrated after completion of all tests by the procedure outlined in Appendix B.

## RESULTS

The results for all the tests are summarized in **Table 1** (page 6) and more detailed results are presented in Appendices C and D. Examination of the post-test x-rays reveals that velocities at 13.6 mph and higher all produced comminuted fractures of both the tibia and fibula that are judged to be severe enough that loss of leg function would result. The post test x-ray of the leg impacted at 10.4 mph reveals less severe transverse fractures of the tibia and fibula. Consequently, the threshold velocity is judged to fall within the range of 10.4 mph to 13.6 mph. Additional tests are needed to provide a statistically justifiable technical basis for this result.

The expected vascular and neurological damage was not observed during post-test dissection of the legs. It is believed that this lack of effect was due to the "leather-like" condition of the soft tissue as a result of long-term storage and fixation. Unfortunately, most of the cadaver legs available for this study were all

embalmed at various times ranging from about three to seven years ago; the tissue had changed to the point that soft tissue damage could only be inferred from the extent of bone damage. Tests to confirm this are being conducted in-air at the University of Tennessee laboratory using legs in a similarly deteriorated state at test conditions that are known to produce extensive vascular and neurological damage to "fresher" legs. Results support the above conjecture that extensive vascular and neurological damage should have occurred. These results and additional comments intended to clarify or supplement this work is included in Appendix G. This was presented in the form of a report addendum after the main tests and analysis were completed.

The long-term storage and fixation apparently did not affect the bone strength adversely as it did the soft tissue. Behavior of the bone was realized to be comparable to that of a "fresher" population as supported in Appendix E. Therefore, the resultant fracture data are considered to be valid and representative.

## **DISCUSSION AND RECOMMENDATIONS**

As shown in Appendix C, six out of seven of the resultant fractures from the leg tests were comminuted with multiple fragmentation. It is important to note that these fractures or resultant injuries are considered to be "conservative" (or less severe) than what would be expected in "real-life" situations, because:



- 1) during the tests, all of the legs pulled loose  
at the hip connection limiting the inertial  
constraints imposed by the upper-body  
Hybrid III parts,
- 2) the direction of impact of the tibia is the  
"toughest" direction of the bone for a  
transverse load, and
- 3) the proximal region of the tibia is stronger  
than the midshaft and distal areas.

It is the judgment of the researchers that, for the loading condition and population studied in this project, the prop-guarded cage was not effective in preventing extensive injury to the leg at boat velocities greater than or equal to 13.6 mph. Above this speed, the observed damage was so severe that complete loss of leg function would be expected.

A total of seven tests is not enough to establish statistical significance of these results, however the researcher's opinion is that these results would be reproducible in subsequent tests.

It would be useful to conduct tests with legs that have "fresher" soft tissue. This would allow the researchers to confirm the inference that the soft tissue injury would result in loss of leg function as discussed in this report.

Additional tests should use entire intact cadavers instead of sectioned legs connected to Hybrid III dummy components. This would provide more realistic constraints during the impacts.

Six out of the seven cadaver legs tested were pulled loose at the hip connection to the test dummy. Although attachment of the cadaver leg to the test dummy may have different hip failure characteristics than an intact cadaver, the delivered forces are very comparable. There may be a need to examine post-impact forces experienced by the hip with and without the cage-type guard. These researchers speculate that more severe hip injuries will occur more often when a cage-type guard is used.

It would be desirable for future tests to utilize a cadaver population that is somewhat younger to relate better to real-life situations. Appendix F outlines the cadaver information for the legs used in this study. The average age at time of death for seven of the cadavers was approximately 75 years.

## **APPENDICES**

- Appendix A: Research Overview of “Dynamic Response of the Human Leg to Impact Loading”
- Appendix B: Velocity Report of Centrifuge from the Center for Research in Special Environments at the State University of New York
- Appendix C: Post-test Dissection and X-ray Data
- Appendix D: Dissection Measurements: Cortical Thicknesses and Weights
- Appendix E: Characteristics of Tested Tibias
- Appendix F: Cadaver Information
- Appendix G: Addendum to Biomechanical Effectiveness of a Safety Device: A Boat Motor Cage-type Propeller Guard
- Appendix H: Causal Mechanisms of Air Bag Induced Eye Injuries from Actual Cases

## **Appendix A**

### **Research Overview of “Dynamic Response of the Human Leg to Impact Loading”**

## CONTENTS

OVERVIEW .....	3
TABLE 1: Types of Tests Conducted Through July 1993 for JAMA Research Program at The University of Tennessee and The University of Louisville .....	9
TABLE 2: Summary of the Dynamic Response Characteristics of the Human Tibia, Fibula, Femur and Intact Lower Limb to Impact Loading .....	10
TABLE 3: Dynamic Response Characteristics of the Human Tibia .....	17
TABLE 4: Dynamic Response Characteristics of the Human Femur .....	26
TABLE 5: Dynamic Response Characteristics of the Intact Human Lower Limb .....	31
TABLE 6: Some Calculated Dynamic Response Characteristics from Selected Data of the Human Tibia and Femur .....	39

## OVERVIEW

This report summarizes the activities and findings from the research project entitled "Dynamic Response of the Human Leg to Impact Loading." The intent of this research has been to describe and quantify the dynamic response of the human leg to impact loading such as that encountered when a pedestrian or cyclist is struck by an automobile. The information resulting will be valuable as a guide for designing safer vehicles and protective systems.

Research was initiated in 1986 and significant progress has been made at the University of Tennessee and the University of Louisville. This progress includes the design and installation of a state-of-the-art impact testing laboratory; the completion of significant impact tests using human legs, animal legs, and simulated leg structures; and development of a basic understanding of the response of the human leg to impact loading. Other contributions include appropriate biological and structural material testing, development efforts for a computer-based simulation of lower leg response to impact loading, evaluation of an alternative leg impact response measurement system, and participation in supporting research and related information exchanges.

This research has established that the majority of lower leg fractures observed with cyclists are not a result of a "crushing injury" as previously thought, but rather involve the leg fracturing when the accelerating forces produced by the striking object exceed the leg's structural strength.

In general, the response of the human lower leg to impact loading has been found to depend not only on the basic strength of the tibia and fibula, but also upon the mass distribution and post

fracture deformation of the entire leg. Other factors which influence the lower leg's response to impact include the configuration of external structures which may inadvertently serve to support the limb during impact, the specific location of the impact on the leg, and the impacting object's configuration and velocity.

The researchers have been involved in a variety of activities that have contributed to the establishment of expert knowledge and understanding of human body dynamics. Some include: 1) clinical studies of accidents involving traumatic leg injury, 2) statistical studies of traumatic injuries, 3) whole body vibration research, 4) underwater impact injury studies, 5) head impact tolerance and injury research (laboratory tests), 6) various accident reconstruction projects, 7) causal mechanism analyses of human injury, and 8) other biomechanical laboratory experimentation.

A key focus of the experimentation has been high speed impacts of human leg bones and intact legs. Other tests have included the use of animal and artificial bone specimens.

**Table 1** gives an overview of the types of tests conducted to date. Some of the more significant findings and relative comments are summarized below.

- 1) The impact testing facility met all design criteria and is set up for use in a functional biomechanics laboratory.
- 2) Fractures can occur without entrapment (crushing injury). For high speed tests the inertial restraint of the tibia from the upper thigh and foot is sufficient enough to result

in comminuted fractures without any additional support. For low speed tests, simply-supported legs have resultant bone fractures comparable to inertially supported legs at high speeds.

- 3) Early findings from a small sample size of intact goat legs indicated no significant difference in breaking force values between the embalmed legs and the fresh legs. However, recent tests with the human femur has shown significant differences in both the breaking force and energy absorption capacity. Sample size and specimen variability still leave these comparison data questionable.
- 4) If monitored and tailored properly, the plastination process offers the potential to be an effective way to restore or maybe preserve the properties of specimens. An important secondary observation from these tests is that the plastination process may significantly aid the development of molds for researchers interested in constructing analogue human leg structures.
- 5) The tests confirmed the belief that dehydration of bone (without embalmment) changes its strength and causes increased brittleness.
- 6) Impactor shape affects fracture patterns. Distributing the impact load over more points or a larger area seems to lessen the sharp edges on the fractured areas of the bone, consequently decreasing the soft tissue damage. Note, however, that as the load is spread over a larger area, more rigid body motion may occur to the whole body which could result in other injuries (e.g. head injury).
- 7) A variety of tests have been conducted to characterize the behavior of the human intact leg, tibia, fibula, femur, humerus, knee, hip, and ankle under impact loading conditions.



Table 2 lists average numerical characteristics derived from these tests. Tables 3, 4, and 5 are a comprehensive "breakdown" of the same data that is summarized and presented in Table 2. Some additional response characteristics of the tibia and femur were calculated from measured data and are presented in Table 6. Note: Test results have shown that the smallest measured cortex thickness around the tibia cross-section is a good correlation parameter for breaking force. Also, for axially loaded femurs, calculated maximum bending stress values are good fracture location predictors.

- 8) Analogue structure tests resulted in the current synthetic human bone choice to be a fiber-reinforced polyamide. The "best bone" to date consists of a composite mixture of 65-70% nylon 6-6, 30% short glass fibers, and 0-5% salt. The hollow cylindrical-shaped (3/4" I.D. and 1" O.D.) bone can be used as a replaceable test specimen in the Hybrid III dummy. Polyamide data under static and dynamic loading conditions sufficiently resembles those of bone to warrant additional testing and work. However, research emphasis has been to continue human tissue testing and not develop the synthetic test specimens.
- 9) Soft tissue mechanical property tests provided values for creep, relaxation, stress and strain for both embalmed and fresh canine muscle (extensor digitorum longus). These tests were performed on an Interlaken Materials Testing Machine. The obtained data is valuable information for developing computer models and for preparing high-speed tests. The comparative tests showed that embalmed specimens exhibited significantly different stress-strain behavior than fresh specimens. Consequently, embalmed specimens should not be used to develop the property data. Creep/relaxation data indicated that standard

structural models may be appropriate for muscle and tendon, however, stress-strain behavior indicated that the tendon model should be viscoelastic in nature. Vibrational tests are in process in order to further evaluate the viscoelastic properties. The modulus of elasticity values were consistent with literature data, but the effects of strain rate are yet to be resolved.

- 10) During alternative simulant leg tests, impact location was the condition that was varied by Dynamic Research, Inc. (DRI) researchers. Two simulant leg structures (MATD composite dummy leg and TRRL honeycomb leg) were tested and their data was compared with human leg tests. Force values and dissection results of the human leg tests were comparable to data obtained in the University of Tennessee/University of Louisville (UT/UL) laboratories. Also, a key conclusion of the DRI researchers was that the honeycomb leg is inappropriate for evaluation of rider protection.
- 11) An analytical finite element model was developed for the human tibia subjected to impact loading. In an attempt to verify the finite element analysis, the computational model (matching the experimental test conditions) was executed for dry, embalmed human tibias. Fracture force data and fracture propagation trends were investigated in these tests. Results show that the finite element model agrees with the general trends shown experimentally. With the development of an accurate constitutive model of the tibia and better experimental verification, the finite element method may prove to be a valuable tool in injury prediction and in the design of injury mitigating devices.
- 12) In addition to the finite element analysis, efforts are well underway for the development of a fuzzy logic based computer model. The hope is that this model will be able to consistently indicate whether a leg under certain given conditions (controlled as input to

the model) will break and if so, what kind of fracture exists. Experiments are ongoing in order to collect data for input into the model so that the underlying hypotheses and membership functions may be validated.

- 13) A comprehensive research plan and a new portable experimental apparatus has been developed in order to determine mechanical properties (such as creep and relaxation) of embalmed, unembalmed and in vivo dog muscle. The study is proceeding.
- 14) Research work and laboratory set-up in Europe is well underway for impact experimentation on the legs of unembalmed human cadavers. The research program should gain international attention because of its uniqueness (cooperation between Americans, Dutch, Germans, and the Japanese). Testing is scheduled to begin soon, but is pending upon discussions with JAMA.
- 15) An internal proposal, "Impact Tolerance of Embalmed vs. Unembalmed Human Cadaver Legs," has been submitted to the University of Louisville School of Medicine Research Committee for approval. The intent is to conduct a series of impact tests designed to provide data relevant for injury comparison of embalmed versus unembalmed human legs. The specific aim of the study is to determine how the embalmment procedure affects human tissue susceptibility to traumatic injury.

This effort (the "Dynamic Response of the Human Leg to Impact Loading" project) has resulted in the development of the world's largest database of its kind with respect to the characterization of the human leg's dynamic and fracture behavior. The research program has been unique and gained worldwide attention for its contribution to the field of impact biomechanics. The collected mechanical and dynamic behavior data will certainly be valuable to vehicle designers, medical doctors, biomedical engineers, anatomists, and others.

**TABLE 1: Types of Tests Conducted Through July 1993 for JAMA Research Program at The University of Tennessee and The University of Louisville**

TYPE OF TEST	SPECIMEN(S) USED
1) Facility Development and Performance	Variety
2) Crushing/Inertia	Human Intact Leg, Goat Intact Leg
3) Effect of Embalming	Human Intact Leg, Goat Intact Leg
4) Effect of Plastination	Dog Bone
5) Effect of Dehydration	Horse Bone, Dog Bone
6) Impactor Geometry and Impactor Material	Human Intact Leg, Human Tibia, Human Femur
7) Dynamic Response	Human Intact Leg, Human Tibia, Human Fibula, Human Femur, Human Humerus, Human Knee, Human Hip, Human Ankle
8) Analogue Structures	Wood, Bakelite, Polyurathane, PRL Synthetics, Nylon Composite
9) Soft Tissue Mechanical Properties	Dog Muscle and Tendon
10) Effectiveness of Alternative Simulant Leg Structures (Performed Cooperatively with Dynamic Research, Inc.)	Human Intact Leg, Human Tibia, Human Femur, MATD Composite Dummy Leg, TRRL Honeycomb Leg
11) Validation of Finite Element Computer Model Development	Human Tibia
12) Development of Fuzzy Logic Computer Model	Human Intact Leg
13) Mechanical Property Evaluations for Embalmed, Unembalmed, and In Vivo Canine Muscle	Embalmed Dog Muscle, Unembalmed Dog Muscle, In Vivo Dog Muscle
14) Fresh Tissue Research ("on hold" until further discussions with JAMA)	Unembalmed Human Whole Body
15) Unembalmed Versus Embalmed Tissue Study (this is future work pending approval through the university)	Unembalmed Human Intact Leg, Embalmed Human Intact Leg

**TABLE 2: Summary of The Dynamic Response Characteristics of  
The Human Tibia, Fibula, Femur and Intact Lower Limb to Impact Loading**

Results from Impact Biomechanics Research at the University of Tennessee & the University of Louisville  
(Sponsored by the Japan Automobile Manufacturers Association)

All bones and intact specimens were embalmed and impacted midshaft while simply-supported, unless noted otherwise.

n	Impact Direction	Impactor	Average Force (kN)	Standard Deviation (kN)	Average Velocity (m/s)	Fracture Classifications	Remarks
TIBIAS							
4	A-P Tibia	Pipe	5.37	0.98	7.6	(n = 4) 50.0% Oblique 25.0% Segmental	25.0% Tension Wedge UT Fresh Tissue Bank.
4	A-P Fibula	Pipe	0.93	0.15	6.9	(n = 4) 50.0% Segmental 25.0% Oblique	25.0% Comminuted UT Fresh Tissue Bank.
2	P-A Humerus	Pipe	6.85	0.21	6.9	(n = 2) 50.0% Tension Wedge	50.0% Oblique UT Fresh Tissue Bank.
8 7*	A-P Tibia "	Transducer "	150 125	0.75 0.27	1.2 1.2	(n = 8) 50.0% Segmental 37.5% Wedges 12.5% Transverse	* 2nd "n" figured after dropping specious value of 6681.- high force value.
1	A-P P's Tibia	Pipe	nt.	na	7.8	(n = 1) Medial Wedge.	
1	A-P Tibia	Pipe	1.20	na	7.9	(n = 1) Comminuted.	Strain gauge applied.
13	A-P Tibia	Pipe Low v <sub>a</sub>	2.38	0.80	1.4	(n = 13) 46.1% Tension Wedges 7.7% Compression Wedges	38.5% Segmental 7.7% Transverse
2	A-P Tibia	Pipe Low v <sub>b</sub>	0.425	0.02	2.8	Tension Wedges in Both.	Low P's, Analyzer setting?

10

n	Impact Direction	Impactor	$\mu$ Force (kN)	$\sigma$ (kN)	v (m/s)	Fracture Classifications			Remarks
26	A-P Tibia	Pipe III v	2.37	1.64	7.8	(n=24)	33.3% Oblique 8.3% Compression Wedges 8.3% Transverse 8.3% Tension & Compression Wedges	29.2% Tension Wedges 8.3% Segmental 4.3% Comminuted	* Specious Force values for #679L, 592R and the 2 ?L's not included in 2nd "n." (651L was nt)
22*	"	"	2.23	1.36	7.5				
6	A-P Tibia	Polymer Plate	2.49	0.73	7.6	(n=6)	50.0% Tension Wedges 16.7% Segmental	33.3% Oblique	
8	A-P Tibia	10 cm Plate	2.91	1.00	7.4	(n=8)	50.0% Tension Wedges 12.5% Compression Wedge	25.0% Segment 12.5% Transverse	
57	A-P Tibia & Fibula	Pipe	4.82	1.78	7.4	(n=58)	25.9% Transverse 15.5% Tension Wedge 13.8% Segmental	24.1% Oblique 15.5% Comminuted 5.2% Side Wedges	* Values for 828L, 760L, 783L, & 926R excluded in 2nd "n." (754R nt)
53*	"	"	4.76	1.51	7.4				
21	A-P Fibula	Pipe	1.84	1.27	7.5	Most were segmented or comminuted.			Same impact as above. * Specious values for #865R, 984L and 992L excluded in 2nd "n." (812L, 880L, 881L/R, 997L/R and 111L F were nt).
18*	"	"	1.57	0.66	7.5				
1 <sub>a</sub>	A-P Tibia & Fibula	Pipe	6.77	na	7.5	(n=1)	Oblique.	Matched pair hit while inertially supported. a- 2 hits-No Fx., added boot-Fx. b- Fx. first hit, no boot.	
1 <sub>b</sub>	"	Pipe	5.59	na	7.3	(n=1)	Oblique.		
11	A-P Tibia & Fibula	2.5 cm Plate	5.73	1.45	7.5	(n=11)	45.5% Comminuted 9.1% Compression Wedge	36.5% Segmental 9.1% Tension Wedge	* Specious values for #926L, 002L & R excluded in 2nd "n."
8*	"	"	6.52	0.61	7.5				
27	L-M Tibia & Fibula	Pipe	2.92	1.94	7.7	(n=31)	41.8% Tension Wedges 22.6% Transverse 6.5% Side Wedges	22.6% Oblique 6.5% Segmental	* Specious values for #889L, 880R and 034R excluded in 2nd "n." (884R, 871L, 034L, 972R & 962R were nt)
24*	"	"	3.74	1.23	7.7				
1	L-M T/F, Foot	Pipe	2.17	na	7.6	(n=1)	Oblique.		Intact foot attached to Tibia/fibula.

n	Impact Direction	Impactor	$\mu$ Force (kN)	$\sigma$ (kN)	v (m/s)	Fractures	Remarks
21	L-M Fibula	Pipe	0.85	0.49	7.7	Mostly Wedges, Segments and Obliques.	Same impact as above.
20*	"	"	0.78	0.35	7.7		* 859R excluded in 2nd "n." (nt: 877L, 889L, 884R, 906R, 871R, 880R, 870R, 034L/R, 972R & 962R)
FEMURS							
2	A-P Dist Femur	Pipe	4.22	0.49	7.5	(n=2) 50% Tension Wedge 50% Comminuted	
2	A-P Femur	Pipe	1.00	0.64	Static	(n=2) 50% Tension Wedge 50% Transverse	TAK Machine
4	A-P Femur	Pipe	8.2	1.86	6.6	(n=4) 50.0% Oblique 50.0% Transverse	UT Fresh Tissue Bank
30	A-P Femur	Pipe	5.76	1.93	7.5	(n=32) 40.6% Comminuted 15.6% Oblique	* Specious values for #798L/R, 720L and 551L excluded in 2nd "n." (776L & 779L were nt)
26*	"	"	5.78	1.41	7.5	12.5% Segmental 21.9% Side Wedge 6.3% Compression Wedge 3.1% Tension Wedge	
2	A-P Femur	70mm Snub	0.98	0.27	7.5	(n=2) Both Comminuted Longitudinal Segments.	DRI Vertical Impactor.
2	na	Torque	58.05 N-m	53.67 N-m	Static	(n=2) Both Spiral Fractures.	Failed during pre-torque.
6	na	S-S Torsion	108.3 N-m	46.4	Static	(n=6) All Spiral fractures.	* Specious value of #6 excluded in 2nd "n."
5*	"	"	125.1 N-m	24.1 N-m	Static		
4	L-M Femur	Pipe (Pre-T)	2.86	1.70	7.0	(n=4) 75% Segmental 25% Oblique	* Specious value of 695R excluded in 2nd "n." Pre-torque of 20.14 N-m.
3*	"	"	2.13	1.06	6.8		
4	L-M Femur	Pipe (Pre-T)	2.70	2.72	6.8	(n=6) 66.7% Spiral 33.3% Comminuted	* Specious value of U6L excluded in 2nd "n." Pre-torque of 10.06 N-m.
3*	"	"	1.57	1.84	6.8		

n	Impact Direction	Impactor	$\mu$ Force (kN)	$\sigma$ (kN)	v (m/s)	Fractures	Remarks
2	L-M Pys Femur	Pipe	5.60	1.63	7.5	(n = 3) 33.3% Tension Wedge 33.4% Comminuted	33.3% Oblique (997L was nt)
17	L-M Femur	Pipe	3.16	1.89	7.1	(n = 18) 27.8% Oblique 16.7% Tension Wedges 11.1% Compression Wedges	27.8% Segmental 11.1% Other Wedges 5.6% Comminuted (698L was nt)
1	L-M Femur	10 cm Plate	4.57	na	7.5	(n = 1) Compression Wedge	
10 8*	AX Femur "	10 cm Plate "	7.11 7.08	2.32 1.73	6.8 6.6	(n = 10) 80% Involved Hip 40% Involved Shaft 20% Involved Knee	* Specious values for 557L and 4L were excluded in 2nd "n." Percentages > 100 due to multiple fractures per specimen.
9 7*	AX Femur "	Materials Testing Machine	5.27 5.01	2.47 1.44	Static Static	(n = 9) 88.9% Neck fractures. 11.1% Subtrochanteric fracture.	
INTACT SPECIMENS							
2	L-M Ankle	Pipe	5.14	0.02	4.7	(n = 2) Fractures of both Maleoli, Calcaneus and Talus.	Approx 36 kg. mass medially.
1	L-M Ankle	Pipe	11.17	na	11.8	(n = 1) Fractures of all both maleoli and all tarsal bones, with a cavitating fracture of Calcaneus and Talus.	Same as above.
2	L-M Heel	Pipe	4.35	1.23	4.0	(n = 2) Calcaneus and Tarsals crushed.	Same as above.
1	L-M Leg	3" Pipe	na	na	7.6	(n = 1) No tibial fracture. Cominuted Fibula.	Inertial support.
2	L-M Leg	Pipe	4.76	0.00	7.5	(n = 2) 1-Tibial Tension Wedge 2-No Tibia fx.	



n	Impact Direction	Impactor	$\mu$ Force (kN)	$\sigma$ (kN)	v (m/s)	Fractures	Remarks
5	A-P D½ Leg	3" Pipe	na	na	7.4	(n = 5) 40.0% Cominuted, 40.0% Transverse, 20.0% No Frx.	Inertial support.
6	A-P Leg	3" Pipe	na	na	7.3	(n = 6) 33.3% Tension wedge 33.3% Transverse 16.7% Cominuted 16.7% No Frx.	Inertial support.
5	A-P Leg	Car Bumper	na	na	7.3	(n = 5) 40.0% Transverse 40.0% Tension wedge, 20.0% Cominuted	Inertial support.
1	P-A Leg	Pipe	2.28	na	8.7	(n = 1) Cominuted segment.	Inertial support.
2	A-P D½ Leg	Pipe	1.78	0.48	9.2	(n = 2) Both cominuted.	
2	A-P Leg	Pipe	1.19	0.31	2.4	(n = 2) Both cominuted wedges.	
12	A-P Leg	Pipe	4.01	3.23	7.7	(n = 13) All were cominuted. 38.5% had wedge formation (2 Compression, 2 Tension and 1 Lateral).	(995L was nt)
9	A-P Leg	Pipe	$\mu = 6.23$ $\mu_{SI} = 3.26$ $\mu_d = 2.97$ ***** $\mu = 6.23$	$\sigma = 1.70$ $\sigma_{SI} = 1.24$ $\sigma_d = 1.32$ ***** $\mu = 1.82$	7.3 7.2 <sub>SI</sub>	(n = 9) 44.4% Tension Wedges 33.3% Segmental 11.1% Compression Wedge 11.1% Transverse	Inertial Support. Legs impacted again after fracture to determine forces related to soft tissue (SI).
8*	"	"	$\mu_{SI} = 2.66$ $\mu_d = 3.23$	$\mu_{SI} = 1.02$ $\mu_d = 1.14$			* Specious value for #577L was excluded in "n=8."

n	Impact Direction	Impactor	$\mu$ Force (kN)	$\sigma$ (kN)	v (m/s)	Fractures	Remarks
8	A-L Leg	Pipe	$\mu = 5.19$ $\mu_{S1} = 2.55$ $\mu^d = 2.65$ ..... $\mu = 4.11$	$\sigma = 2.20$ $\sigma_{S1} = 0.86$ $\sigma_d = 1.80$ ..... $\sigma = 1.04$	7.3 7.3 <sub>S1</sub>	(n=9) 33.3% Medial Wedges 22.2% Transverse 22.2% Comminuted 11.1% Oblique 11.1% Tension Wedge	Inertial Support. Legs impacted again after fracture to determine forces related to soft tissue (ST).  S28L did not fracture and was excluded. S77R was nt.  * Specious values for S17R and 742R were excluded from "n=6."
6*	"	"	$\mu_{S1} = 2.35$ $\mu_d = 1.76$	$\sigma_{S1} = 0.90$ $\sigma_d = 0.76$			
2	A-P Leg	TA Plate	5.70	0.85	1.70	(n=2) 50.0% Tension Wedge 50.0% na	Testing of Fuzzy Logic Model. 10 cm Bumper with Air Springs. Friction in the form of a 20 kg superior to inferior vector was applied. The velocity listed is the average of the minimum forces required to induce a definite fracture ( $\sigma=0.51$ )
1	A-P Leg	TA Plate	1.49	na	6.3	(n=1) Comminuted Wedge.	Same as above but with foam padding on bumper.
1	A-P Leg	TA Plate	3.29	na	7.9	(n=1) Transverse.	Same as above, but without foam.
1	A-P Leg	TA Plate-b	6.24	na	8.0	(n=1) Oblique.	Used 4 cm plate and maintained friction. (no foam, no air springs)
1	A-P Leg	TA Plate	1.14	na	5.2	(n=1) Comminuted.	Regular 10 cm plate. No friction, no air springs and no foam.
1	A-P Leg	TA Plate	1.67	na	4.9	(n=1) na.	Same as above, with friction.
1	P-A Leg	TA Plate	1.14	na	2.8	(n=1) na.	10 cm plate with airsprings, no friction, no foam.

n	Impact Direction	Impactor	$\mu$ Force (kN)	$\sigma$ (kN)	v (m/s)	Fractures	Remarks
2	A-P 1/3 Leg	Pipe	3.17	1.32	7.5	(n=2) Both comminuted.	Inertial Support.
4	AX Knee	Plate	8.82	1.45	7.5	(n=4) 50.0% Comminuted Patella only. 50.0% Comminuted fractures of Femur, Tibia and Patella.	No additional mass behind hip.
1	AX Knee	Pipe	4.50	na	7.5	(n=1) Fractures of the neck and condyles.	38 kg mass behind hip.
1	AX Knee	Plate	11.07	na	7.5	(n=1) Comminuted patella. Femur not fractured.	11 kg mass behind hip.
4	AX Knee	Pipe	10.24	1.47	7.5	(n=4) 75.0% Comminuted Patella and distal Femur. 25.0% Comminuted Patella only.	11 kg mass behind hip.
2	AX Knee	Pipe	8.07	4.06	7.5	(n=2) Both had comminuted Femur, Tibial Condyles & Patella.	18 kg mass behind hip.
4	A-P Thigh	Pipe	5.81	1.78	7.5	(n=6) 16.7% Neck fractured. 50.0% Oblique 50.0% Wedge formation. 16.7% Transverse.	9191. & 8791. had false force triggers. Percentages > 100 due to multiple fractures per specimen.
6	L-M Thigh	Pipe	6.17	1.81	7.5	(n=6) All comminuted. 1 fracture of Femoral Neck.	

**TABLE 3: Dynamic Response Characteristics of the Human Tibia**

Direct Results from Impact Biomechanics Research at  
the University of Tennessee & the University of Louisville  
(Sponsored by the Japan Automobile Manufacturers Association)

All bones were embalmed specimens and impacted midshaft while simply-supported, unless noted otherwise in "Remarks" column.

Date	Body #	Direction	Impactor	Force (kN)	v (m/s)	Fractures (Cortex Measures Avg/Smallest mm.)	Remarks
11/10/87	?R	A-P P½	Pipe	nt	7.8	Medial Wedge. (Tibia, T-5)	JE-87-23. d = 36.8 cm. P½
02/05/88	?R	A-P	Pipe	1.20	7.9	Comminuted. (T-4)	Strain gauge. JE-88-31 (51)
11/21/89	105L	A-P	Pipe	5.54	8.4	Tension Wedge.	Fresh Tibia. UT Tissue Bank.
"	105R	A-P	Pipe	6.62	nt	Segmental.	Fresh Tibia. d = 39.5 cm
"	98R	A-P	Pipe	4.99	7.1	Oblique.	Fresh Tibia. d = 33.0 cm
"	98L	A-P	Pipe	4.31	7.1	Oblique.	Fresh Tibia. d = 33.0 cm
02/05/88	Fresh	A-P	Pipe	nt	7.9	Segmental. (T-2)	Fresh JE-88-32
11/21/89	105L	A-P	Pipe	0.77	8.4	Comminuted.	Fresh Fibula.
"	105R	A-P	Pipe	0.93	4.6	Oblique.	Fresh Fibula. d = 39.5 cm
"	98L	A-P	Pipe	0.90	7.3	Segmental.	Fresh Fibula
"	98R	A-P	Pipe	1.13	7.1	Segmental.	Fresh Fibula
11/21/89	105L	P-A	Pipe	4.47	6.7	Oblique.	Fresh Humerus. d = 31.8 cm
"	105R	P-A	Pipe	5.29	7.0	Tension wedge.	Fresh Humerus. d = 31.8 cm

Date	Body #	Direction	Impactor	Force (kN)	v (m/s)	Fractures (Cortex Measures Avg/Smallest mm.)	Remarks
02/04/88	668L	A-P	Transducer	3.26	1.2	Large Segment. (T-7)	JE-88-08 (11L)
"	653L	A-P	Transducer	1.58	1.2	Large Segment. (T-3)	JE-88-20 (32L)
"	604L	A-P	Transducer	1.14	1.2	Large Segment with Tension Wedge. (T-3)	JE-88-22 (27L)
"	600L	A-P	Transducer	1.09	1.3	Large Segment. (T-4)	JE-88-33 (29L)
"	551R	A-P	Transducer	0.98	1.2	Lateral Wedge. (T-2)	JE-88-26 (551R)
"	566L	A-P	Transducer	1.05	1.2	Transverse. (T-3)	JE-88-27 (566L)
"	656L	A-P	Transducer	1.66	1.0	Tension Wedge. (T-6)	JE-88-07 (10L)
"	619L	A-P	Transducer	1.27	1.4	Comminuted Wedge. (T-5)	JE-88-18 (26L)
02/04/88	600R	A-P	Pipe- Low $v_a$	1.80	1.2	Tension Wedge. (T-5)	JE-88-15 (29R)
"	631L	A-P	Pipe	2.67	1.2	Comminuted Tension Wedge. (T-4)	JE-88-16 (25L)
"	631R	A-P	Pipe	2.78	1.9	Comminuted Segmental. (T-3)	JE-88-17 (25R)
"	598L	A-P	Pipe	3.43	1.2	Large Segment. (T-4)	JE-88-19 (13L)
"	656R	A-P	Pipe	3.42	0.9	Large Segment with Tension Wedge. (T-4)	JE-88-21 (10R)
"	619R	A-P	Pipe	2.71	1.4	Medial Wedge or Segment. (T-4)	JE-88-06 (26R)
"	668R	A-P	Pipe	2.83	1.3	Transverse. (T-3)	JE-88-10 (11R)
"	531R	A-P	Pipe	2.10	2.3	Tension Wedge. (T-6)	JE-88-25 (531R)
"	553L	A-P	Pipe	0.95	1.0	Compression Wedge. (T-4)	JE-88-28 (52)
"	534L	A-P	Pipe	1.80	2.3	Tension Wedge. (T-12)	JE-88-29 (534L)
"	553R	A-P	Pipe	1.23	2.6	Tension Wedge. (T-8)	JE-88-30 (553)
"	604R	A-P	Pipe	2.01	1.5	Comminuted Segment. (T-3)	JE-88-34 (27R)
"	653R	A-P	Pipe	3.19	1.2	Comminuted Segment with Tension Wedge. (T-5)	JE-88-35 (32R)
11/10/87	?R	A-P	Pipe Low $v_b$	0.44	2.4	Tension Wedge. (T-4)	JE-87-24. d = 34.3 cm
"	?R	A-P	Pipe	0.41	3.1	Tension Wedge. (T-3)	JE-87-26. d = 30.5 cm

Date	Body #	Direction	Impactor	Force (kN)	v (m/s)	Fractures (Cortex Measures Avg/Smallest mm.)	Remarks
02/05/88	587L	A-P	Pipe- Hi v	1.05	7.5	Compression Wedge. (T-2)	JE-88-09 (20L)
"	606R	A-P	Pipe	1.63	7.5	na. (T-5)	JE-88-11 (19R, fmf)
"	651L	A-P	Pipe	nt	7.5	Oblique. (T-2)	JE-88-12 (01= 28L)
"	610L	A-P	Pipe	0.83	7.8	Oblique Comminuted. (T-2)	JE-88-13 (33L)
"	616L	A-P	Pipe	1.49	7.4	Oblique. (T-4)	JE-88-14 (23L)
"	606L	A-P	Pipe	1.52	7.9	Tension Wedge. (T-9)	JE-88-23 (19L)
"	616R	A-P	Pipe	1.40	7.4	Oblique. (T-5)	JE-88-24 (23R)
"	651R	A-P	Pipe	1.16	7.4	Oblique. (T-2)	JE-88-36 (28R)
11/10/87	7L	A-P	Pipe	0.67	7.8	Transverse Comminuted. (T-4)	JE-87-22. d = 37.5 cm
"	7L	A-P	Pipe	0.50	7.8	Large Segment. (T-3)	JE-87-25. d = 33.0 cm
06/20/89	693L	A-P	Pipe	4.89	7.4	Tension Wedge. (T-7.67/4.79)	Kress M.S.
"	693R	A-P	Pipe	1.97	7.4	Tension Wedge. (T-7.73/4.63)	
"	648R	A-P	Pipe	4.96	7.4	Tension & Compression Wedges.(T-7.28/5.07)	
"	698L	A-P	Pipe	2.23	7.1	Tension Wedge. (T-6.16/4.24)	SEM?
"	698R	A-P	Pipe	1.98	7.4	Oblique. (T-5.94/3.87)	
"	630L	A-P	Pipe	1.30	7.4	na. (T-4.21/2.15)	
"	630R	A-P	Pipe	0.75	7.4	Segment. (T-3.99/1.85)	
"	623L	A-P	Pipe	1.34	7.4	Tension Wedge. (T-4.07/1.76)	
"	623R	A-P	Pipe	3.33	7.4	Transverse. (T-5.58/3.64)	
07/23/89	679R	A-P	Pipe	5.63	7.3	na. (T-7.08/5.02)	
"	592R	A-P	Pipe	5.69	7.4	Compression Wedge? (T-7.85/6.15)	
"	627R	A-P	Pipe	1.62	7.4	Large Tension Wedge. (T-5.22/3.87)	
"	746R	A-P	Pipe	4.00	7.4	Tension Wedge. (T-5.76/3.68)	
"	704R	A-P	Pipe	3.88	7.4	Tension & Compression Wedges. (T-6.52/4.41)	
"	622R	A-P	Pipe	1.19	7.6	Comminuted. (T-2.90/1.67)	

Date	Body #	Direction	Impactor	Force (kN)	v (m/s)	Fractures (Cortex Measures Avg/Smallest mm.)	Remarks
07/23/89	No2R	A-P	Pipe	2.09	7.3	Oblique. na	
"	No17R	A-P	Pipe	4.54	7.4	Oblique distal 1/8. (T=6.57/4.55)	
07/21/89	664L	A-P	Polymer Plate	3.61	7.6	Tension Wedge. (T=7.88/4.77)	
"	679L	A-P	P-Plate	2.29	7.6	Oblique. (T=7.71/5.92)	
"	592L	A-P	P-Plate	2.41	7.6	Tension Wedge & Segment. (T=7.87/5.73)	
"	627L	A-P	P-Plate	1.35	7.6	Comminuted Oblique. (T=4.23/2.35)	
"	746L	A-P	P-Plate	2.56	7.6	Tension Wedge. (T=5.80/3.71)	
"	724L	A-P	P-Plate	2.70	7.6	Segment. (T=5.60/3.97)	
07/21/89	724R	A-P	10 cm Plate	2.96	7.4	Segment. (T=4.97/3.55)	
"	664R	A-P	10 cm Plate	3.22	7.3	Tension Wedge. (T=6.62/4.27)	
"	No17L	A-P	10 cm Plate	1.46	7.4	Tension Wedge & Oblique. (T=7.61/4.75)	
"	704L	A-P	10 cm Plate	3.44	7.2	2 Large Segments. (T=6.29/4.25)	
"	662L	A-P	10 cm Plate	1.31	7.2	Jagged Transverse. (T=2.78/1.72)	
"	No2L	A-P	10 cm Plate	3.13	7.4	Compression Wedge.	
6/28/89	747L	A-P	10 cm Plate	3.76	7.4	Tension Wedge.	d = 31.8 cm
"	747R	A-P	10 cm Plate	4.01	7.6	Tension Wedge.	d = 31.8 cm
01/26/91	760R	A-P	Pipe	3.61	4.8	Tibia- Side Wedge, fibula- 2 segments (T=6.76/4.44)	Tibias & fibulas from here on, unless noted otherwise.
"	779R	A-P	Pipe	6.50	7.0	T-Oblique f-segment. (T=7.58/3.75)	
"	756R	A-P	Pipe	2.45	7.0	Oblique. (T=6.83/3.73)	
"	781R	A-P	Pipe	3.21	nt	T-Transverse f-segment. (T=7.13/4.39)	
"	723R	A-P	Pipe	4.50	6.9	Transverse. (T=7.68/5.61)	

Date	Body #	Direction	Impactor	Force (kN)	v (m/s)	Fractures (Cortex Measures Avg/Smallest mm.)	Remarks
01/26/91	754R	A-P	Pipe	nt	6.8	Transverse. (T= 7.23/3.68)	
"	752R	A-P	Pipe	3.15	7.2	Oblique. (T=9.09/5.20)	
"	798R	A-P	Pipe	7.26	7.8	Comminuted Tension Wedge. (T=9.19/5.22)	
"	783R	A-P	Pipe	6.03	7.2	T-Oblique f-segment. (T=8.88/5.33)	
"	738R	A-P	Pipe	6.44	7.4	T-Tension Wedge f-comminuted. (T=6.86/4.25)	
"	778R	A-P	Pipe	5.55	7.4	T-Comm Transverse f-segment. (T=6.07/3.35)	
"	828R	A-P	Pipe	5.98	7.6	T-Tension Wedge f-Comminuted. (T=8.90/5.23)	
"	776R	A-P	Pipe	2.43	7.1	Oblique. (T=4.73/2.63)	
"	720R	A-P	Pipe	5.83	7.5	T-Transverse f-segment. (T=7.97/3.98)	
"	U1R	A-P	Pipe	3.47	7.5	T-Transverse f-comminuted TW. (T=5.96/4.17)	
"	798L	A-P	Pipe	6.82	7.5	T-Transverse f-segment. (T=8.34/4.13)	
"	781L	A-P	Pipe	5.83	7.6	Transverse. (T=6.46/4.08)	
"	752L	A-P	Pipe	3.79	7.4	Tension Wedge. (T=8.57/3.78)	
"	779L	A-P	Pipe	7.37	7.5	Tension Wedge. (T=6.32/2.98)	
"	754L	A-P	Pipe	3.81	7.5	T-Transverse f-TW. (T=7.42/4.81)	
"	828L	A-P	Pipe	10.12	7.4	Segment. (T=8.10/4.65)	
"	778L	A-P	Pipe	7.46	7.4	T-Transverse f-segment. (T=6.29/4.27)	
"	760L	A-P	Pipe	1.96	7.4	T-Transverse f-segment. (T=6.24/3.93)	
"	783L	A-P	Pipe	8.60	7.5	Comminuted. (T=8.17/4.70)	
"	709L	A-P	Pipe	5.18	7.5	T-Transverse f-segment. (T=6.32/4.17)	
"	776L	A-P	Pipe	3.58	7.4	Comminuted TW. (T=5.79/2.20)	
"	756L	A-P	Pipe	2.33	7.6	Comminuted. (T=8.01/3.61)	
"	723L	A-P	Pipe	4.71	7.4	T-Transverse f-segment. (T=7.14/5.08)	
"	738L	A-P	Pipe	7.49	7.7	T-Tension Wedge f-segment. (T=6.75/3.73)	
"	720L	A-P	Pipe	6.45	7.6	T-Oblique f-segment. (T=7.49/3.76)	



Date	Body #	Direction	Impactor	Force (kN)	v (m/s)	Fractures (Cortex Measures Avg/Smallest mm.)	Remarks
03/10/92	812L	A-P	Pipe	4.21/na	7.5	T-Oblique f-segment. (T=9.16/7.91)	Tibias & Fibulas, Cooper Corts.
"	859L	A-P	Pipe	5.36/1.94	7.5	Comminuted Segments. (T=8.39/5.71)	
"	888L	A-P	Pipe	7.01/2.17	7.5	Tension Wedges. (T=9.07/6.45)	
"	888R	A-P	Pipe	5.38/0.96	7.5	Segments. (T=9.32/6.15)	
"	880L	A-P	Pipe	3.99/na	7.5	Comminuted Segments. (T=6.34/4.65)	
"	881R	A-P	Pipe	2.87/na	7.5	T-Oblique f-segment. (T=8.26/5.28)	
"	881L	A-P	Pipe	3.22/na	7.5	Comminuted segments. (T=7.95/4.87)	
"	997R	A-P	Pipe	2.92/na	7.5	Oblique. (T=6.72/4.86)	
"	997L	A-P	Pipe	2.64/na	7.5	Oblique. (T=6.92/4.43)	
11/14/92	895L	A-P	Pipe	3.62/1.39	7.4	Side Wedge. (T=7.86/3.97, f=4.59/3.48)	Tibias with fibulas
"	870L	A-P	Pipe	3.35/0.75	7.4	Large Segment. (T=6.60/3.67, f=3.84/2.74)	
"	902L	A-P	Pipe	5.19/1.92	7.3	Comminuted. (T=9.33/5.55, f=4.88/3.54)	
"	867L	A-P	Pipe	3.93/1.23	7.4	Comminuted. (T=6.75/4.24, f=4.80/2.92)	
"	812R	A-P	Pipe	5.65/2.64	7.6	Comminuted. (T=7.45/4.22, f=4.45/3.83)	
"	862L	A-P	Pipe	4.64/2.62	7.5	Oblique. (T=7.25/4.39, f=4.76/2.98)	
"	862R	A-P	Pipe	4.39/1.70	7.6	Comminuted. (T=7.61/4.70, f=3.97/2.81)	
"	865L	A-P	Pipe	3.30/1.74	7.5	Comminuted. (T=7.30/3.93, f=4.61/2.30)	
"	865R	A-P	Pipe	4.16/0.24	7.6	Comminuted. (T=7.42/4.76, f=4.92/3.72)	
"	883R	A-P	Pipe	4.60/1.81	7.5	Small Wedge. (T=8.06/4.81, f=4.50/4.09)	
"	868L	A-P	Pipe	4.97/0.90	7.4	Large Segment. (T=6.09/4.18, f=4.02/3.65)	
"	868R	A-P	Pipe	4.24/2.23	7.4	Tension Wedge. (T=6.46/4.24, f=3.94/2.89)	
"	882R	A-P	Pipe	4.40/1.84	7.3	Tension Wedge. (T=6.73/3.35, f=4.24/2.70)	Plastic condyles
"	902R	A-P	Pipe	4.72/1.49	7.3	Tension Wedge. (T=7.88/4.52, f=4.60/3.43)	
"	U1L	A-P	Pipe	3.36/0.50	7.8	Oblique. (T=6.22/4.76, f=3.68/3.39)	
"	984L	A-P	Pipe	7.53/4.54	7.6	Transverse. (T=9.65/6.13, f=5.48/4.75)	Some muscle still attached.

Date	Body #	Direction	Impactor	Force (kN)	v (m/s)	Fractures (Cortex Measures Avg/Smallest mm.)	Remarks
11/14/92	926R	A-P	Pipe	1.78/0.51	7.7	Oblique. (T=5.79/2.73, f=3.33/3.13)	
03/10/92	111.	A-P	Pipe	4.69/na	7.5	T-oblique f-segment. (T=6.88/3.87)	DRI comparison
"	992L	A-P	Pipe	6.95/5.56	7.5	Segment. (T=9.33/5.16)	DRI comparison
09/05/91	011R	A-P	70 mm Snub	nt	7.6	Comm Longitudinal. (T=4.42/2.61, f=2.51/1.98)	By DRI Vertical Impactor @ UofL. E=1450 j, Mass=52 kg, poor plot
"	992R	A-P	70 mm Snub	2.62	7.6	T-Comm, f-27 cm seg. (T=7.40/5.06, f=6.21/4.57)	By DRI Vertical Impactor @ UofL. E=1450 j, Mass=52 kg, poor plot
1 & 2/93	929L	A-P	2.5 cm Plate	7.00	7.5	Comminuted. (T=8.19/4.23)	F.F.M. Validation Tests. Potted t
"	984R	A-P	2.5 cm Plate	7.02	7.5	Comminuted Segments. (T=9.51/5.41)	"
"	955L	A-P	2.5 cm Plate	6.91	7.5	Comminuted. (T=6.12/3.91)	"
"	971R	A-P	2.5 cm Plate	6.22	7.5	Segment. Crack propagated P-A. (T=7.04/4.45)	"
"	926L	A-P	2.5 cm Plate	3.51	7.5	Comminuted Segment. Crack P-A. (T=3.99/2.24)	"
"	991R	A-P	2.5 cm Plate	5.85	7.5	Comminuted. Crack Med-dist-ant. (T=8.25/5.72)	"
"	977R	A-P	2.5 cm Plate	6.03	7.5	Comm Comp Wedge? Crack P-A. (T=7.84/4.85)	"
"	977L	A-P	2.5 cm Plate	5.78	7.5	Comminuted. Crack A-P. (T=7.06/6.02)	"
"	002L	A-P	2.5 cm Plate	3.38	7.5	Comminuted Tension Wedge. (T=4.73/3.25)	"
"	002R	A-P	2.5 cm Plate	4.00	7.5	Segment. (T=5.25/3.28)	"
"	955R	A-P	2.5 cm Plate	7.34	7.5	Comminuted. (T=5.91/3.20)	"
05/02/93	007L	A-P	Pipe	6.88, 6.79, 6.64/5.71	23.8, 25.0, 24.6	No fx with first 2 impacts. T-Oblique, f-Segment with Tension Wedge. (T=7.76/4.81, f=4.08/3.63)	INERTIAL. 2 impacts to bare bone then added 1 kg boot.
"	007R	A-P	Pipe	5.59	24.0	T-Oblique, f-comm. (T=7.34/4.72, f=4.18/3.88)	Inertial set-up. No boot.

Date	Body #	Direction	Impactor	Force (kN)	v (m/s)	Fractures (Cortex Measures Avg/Smallest mm.)	Remarks
03/11/92	859R	L-M	Pipe	4.90/2.37	7.5	Oblique. (T=7.66/5.53)	Tibias & Fibulas. Porta Corts
"	877L	L-M	Pipe	2.30/na	7.5	Oblique. (T=7.55/3.75)	
"	898R	L-M	Pipe	3.60/1.52	7.5	T-Tension Wedge f-segment. (T=8.25/5.14)	
"	889L	L-M	Pipe	1.15/na	7.5	Large Wedge. (T=4.67/2.66)	
"	906R	L-M	Pipe	2.71/na	7.5	Oblique. (T=6.87/4.24)	
"	884R	L-M	Pipe	nt	7.5	Segment. (T=6.59/4.45)	
"	871R	L-M	Pipe	nt	7.5	Comminuted Tension Wedge. (T=3.69/2.34)	
"	880R	L-M	Pipe	1.33/na	7.5	Tension Wedge. (T=6.98/5.10)	
"	875R	L-M	Pipe	2.71/0.45	7.5	Comminuted Transverse. (T=7.74/4.61)	
"	870R	L-M	Pipe	2.43/na	7.5	Transverse. (T=8.34/4.95)	
11/14/92	925R	L-M	Pipe	4.26/0.48	8.6	Segment. (T=9.42/5.01, f=4.69/3.94)	Tibias & fibulas. Porta Corts
"	034L	L-M	Pipe	nt	7.4	na. (T=7.90/3.47, f=3.70/3.25)	
"	961L	L-M	Pipe	3.32/0.54	8.5	Oblique. (T=5.96/3.71, f=3.26/2.45)	Red marrow
12/03/92	034R	L-M	Pipe	1.52/<1	7.2	Transverse. (T=5.56/2.12, f=4.13/1.95)	Tibias & fibulas. Porta corts
"	929R	L-M	Pipe	3.84/0.75	7.8	Oblique. (T=7.11/3.72, f=6.32/3.78)	Perio held all together.
"	972R	L-M	Pipe	nt	7.4	T-TW f-segment. (T=8.13/4.54, f=6.00/4.25)	Med rotated 50°
"	979R	L-M	Pipe	4.88/1.10	7.6	T/f Tension Wedges! (T=8.89/6.25, f=6.02/4.29)	**
"	979L	L-M	Pipe	4.89/1.17	7.8	T/f Tension Wedges! (T=9.21/5.90, f=6.66/5.55)	** Saved wedges.
"	024L	L-M	Pipe	4.49/1.32	7.9	T/f Tension Wedges. (T=7.62/4.02, f=5.60/4.63)	Med rotated 45°, predicted plot!
"	024R	L-M	Pipe	5.62/0.89	7.8	Jagged Transverse. (T=7.36/4.01, f=5.32/3.91)	
"	988L	L-M	Pipe	4.55/1.11	7.9	Jagged Transverse. (T=8.15/5.91, f=5.14/3.41)	
"	988R	L-M	Pipe	5.88/0.70	7.9	Transverse. (T=10.82/8.08, f=4.43/4.20)	
"	950L	L-M	Pipe	5.75/0.96	7.8	Comminuted TW. (T=10.41/7.20, f=7.46/4.82)	Abn sect anat, pulled medially.
"	950R	L-M	Pipe	5.04/0.94	7.6	T-Oblique, f-seg. (T=9.92/5.55, f=6.78/5.12)	

Date	Body #	Direction	Impactor	Force (kN)	v (m/s)	Fractures (Cortex Measures Avg/Smallest mm.)	Remarks
12/03/92	022L	L-M	Pipe	3.27/0.66	7.8	Comminuted TW. (T=6.73/4.15, f=4.31/3.12)	
"	022R	L-M	Pipe	2.25/0.87	7.6	T-Jagged Trans, f=TW. (T=6.48/4.08, f=5.86/4.85)	
"	023L	L-M	Pipe	2.21/0.33	7.8	Oblique (S-P to L-A). (T=6.16/3.81, f=3.40/2.17)	
"	023R	L-M	Pipe	3.00/0.26	7.8	Comm TW, f-oblique. (T=7.40/5.11, f=3.77/2.73)	
"	962L	L-M	Pipe	2.96/0.24	7.7	TW, f-segment. (T=6.94/4.37, f=3.75/2.29)	Dark bone
"	962R	L-M	Pipe	nt	7.7	Comm TW, f-oblique. (T=6.54/4.09, f=4.02/3.26)	
"	974L	L-M	Pipe	2.49/0.52	7.5	T-SW, f-oblique. (T=7.66/4.74, f=6.27/4.28)	Horiz fxs, possible nicks?
"	895R	L-M	Pipe	2.46/0.73	7.5	TW, f-dual 6" seg. (T=7.18/3.56, f=4.75/4.17)	
12/05/92	362R	L-M	Pipe	2.17/0.45	7.6	Longitudinal Obliques. (T=5.46/2.51, f=5.16/3.61)	T/f with intact foot! INERTIAL.

**TABLE 4: Dynamic Response Characteristics of the Human Femur**

Direct Results from Impact Biomechanics Research at  
the University of Tennessee & the University of Louisville  
(Sponsored by the Japan Automobile Manufacturers Association)

All bones were embalmed specimens and impacted midshaft while simply-supported, unless noted otherwise in "Remarks" column.

Date	Body #	Direction	Impactor	Force (kN)	v (m/s)	Fractures (Cortex Measures Avg/Smallest mm.)	Remarks
03/05/92	553R	A-P D $\frac{1}{2}$	Pipe	4.57	7.5	Comminuted Tension Wedge.	Impacted distal third.
"	516L	A-P D $\frac{1}{2}$	Pipe	3.87	7.5	Comminuted.	Impacted distal third.
12/05/92	895R	A-P	Pipe	0.54	Static	Jagged Transverse. (Avg/Smallest) 7.16/5.53	TAK Machine.
"	531R	A-P	Pipe	1.45	Static	Tension Wedge & Long Comm. 7.56/4.40	TAK Machine.
11/21/89	98R	A-P	Pipe	7.23	nt	Transverse.	Fresh Tissue Bank @ UT. d=40.5 cm
"	98L	A-P	Pipe	6.07	6.8	Oblique.	Fresh Tissue Bank @ UT. d=40.5 cm
"	105L	A-P	Pipe	10.02	8.2	Transverse.	Fresh Tissue Bank @ UT. d=44.5 cm
"	105R	A-P	Pipe	9.48	4.8	Oblique.	Fresh Tissue Bank @ UT. d=44.5 cm
11/21/89	U8R	A-P	Pipe	6.40	7.5	Small Commination.	
01/27/91	783R	A-P	Pipe	7.81	7.6	Comminuted. Avg cortex = 9.30	Tucker M.S.
"	756R	A-P	Pipe	3.19	7.6	Comminuted. 6.98	3-TW 2-CW 17-SW 8-Obi 1-Com
"	723R	A-P	Pipe	4.82	7.4	Lateral Wedge. 7.44	=29? incl 3/15?
"	738R	A-P	Pipe	5.48	7.7	Comminuted Long Segments. 4.54	
"	752R	A-P	Pipe	6.05	7.8	Least comminuted. 8.68	
"	781R	A-P	Pipe	3.66	7.8	Medial Wedge. 5.88	
"	798R	A-P	Pipe	8.91	7.4	Tension and Compression Wedges. 7.85	

Date	Body #	Direction	Impactor	Force (kN)	v (m/s)	Fractures (Cortex Measures Avg/Smallest mm.)	Remarks
01/27/91	778R	A-P	Pipe	4.09	7.1	Medial Wedge. 7.01	
"	754R	A-P	Pipe	6.38	7.9	Mild Commminution. 8.91	
"	720R	A-P	Pipe	7.63	7.5	Mild Commminution. 9.95	
"	760R	A-P	Pipe	4.42	7.5	Comminuted. 6.59	
"	828R	A-P	Pipe	6.75	7.5	Segment. 8.16	
"	779R	A-P	Pipe	6.61	7.5	Comminuted. 8.20	
"	U1R	A-P	Pipe	5.21	7.5	Mild Commminution. 8.09	
"	553L	A-P	Pipe	5.06	7.2	Comminuted Long Segments. 8.31	
"	783L	A-P	Pipe	8.21	7.1	Comminuted. 8.24	
"	738L	A-P	Pipe	4.57	7.2	Large Lateral Wedge. 6.70	
"	709L	A-P	Pipe	6.14	7.3	Compression wedge. 6.80	
"	776L	A-P	Pipe	nt	nt	Large Lateral Wedge. 6.29	
"	828L	A-P	Pipe	8.03	7.6	Compression Wedge? 8.89	
"	778L	A-P	Pipe	4.13	7.3	Oblique. 6.89	
"	754L	A-P	Pipe	6.18	7.8	Medial Wedge. 6.85	
"	779L	A-P	Pipe	nt	7.5	Comminuted. 6.02	
"	781L	A-P	Pipe	5.20	7.7	●blique with small wedges. 5.87	
"	723L	A-P	Pipe	6.79	7.0	Oblique. 6.52	Prosthetic Hip.
"	760L	A-P	Pipe	4.00	7.6	Oblique. 5.67	Prosthetic Hip.
"	720L	A-P	Pipe	1.44	7.2	Oblique with small wedge. 7.81	
"	752L	A-P	Pipe	6.24	7.3	Comminuted segment. 7.98	
"	798L	A-P	Pipe	9.95	7.4	Sharp Commminution. 7.98	
03/16/92	551L	A-P	Pipe	2.31	7.5	Sharp Commminution. Avg 6.23/ Smallest 2.63	
"	534L	A-P	Pipe	7.20	7.5	2 Side Wedges. 11.70/9.74	

Date	Body #	Direction	Impactor	Force (kN)	v (m/s)	Fractures (Cortex Measures Avg/Smallest mm.)	Remarks
09/05/91	560R	A-P	70 mm Snub	0.78	7.5	Comminuted Long. Segments. 6.74/5.46	Tested by DRI 52 kg Vertical Impactor @ UoFL. E=1450 j. Poor plots.
09/05/91	584R	A-P	70 mm Snub	1.16	7.5	Comminuted Long. Segments. 8.74/6.81	Tested by DRI 52 kg Vertical Impactor @ UoFL. E=1450 j. Poor plots.
07/18/89	689L	na	Torque	96.0 N-m	Static	Spiral	d = 37.5 cm. Failed during pre-torque.
"	704L	na	Torque	20.1 N-m	Static	Spiral at distal end.	d = 33.0 cm. Failed during pre-torque.
08/01/89	1	na	S-S Torsion	96.0 N-m	Static	Spiral	Ult. Torsional Strain = 28 MPa. d = 38
"	2	na	S-S Torsion	154.6 N-m	Static	Spiral Proximal 1/2	31 MPa. d = 37.5 cm.
"	3	na	S-S Torsion	113.8 N-m	Static	Spiral Proximal 1/2	31 MPa. d = 31.8 cm.
"	4	na	S-S Torsion	115.9 N-m	Static	Spiral Proximal 1/2	23 MPa. d = 35.5 cm.
"	5	na	S-S Torsion	145.0 N-m	Static	Torsional & shear @ Neck.	28 MPa. d = 38.8 cm.
"	6	na	S-S Torsion	24.4 N-m	Static	Spiral to Neck.	15 MPa. d = 33.0 cm.
07/14/89	695R	L-M	Pipe (Pre T)	5.04	7.5	Neck & Oblique shaft.	Torque 10.06 N-m, d = 38.8 cm
07/18/89	U2L	L-M	Pipe (Pre T)	1.36	6.7	Segment. c = 5.86	Torque 10.06 N-m, d = 33.0 cm
"	U3L	L-M	Pipe (Pre T)	3.34	7.0	Segment & Neck. c = 7.02	Torque 10.06 N-m, d = 33.0 cm
"	No2L	L-M	Pipe (Pre T)	1.68	6.8	Segment. c = 5.98	Torque 10.06 N-m, d = 33.0 cm
07/18/89	689R	L-M	Pipe (Pre T)	nt, Low F.	6.6	Spiral with 6 fragments.	Torque 20.14 N-m, d = 37.5 cm
"	U1L	L-M	Pipe (Pre T)	3.66	6.8	Comm. Long. Segs. Avg Cortex = 6.11 mm	Torque 20.14 N-m, d = 33.0 cm
"	U4L	L-M	Pipe (Pre T)	1.23	6.8	Spiral. c = 8.10	Torque 20.14 N-m, d = 34.3 cm
"	U5L	L-M	Pipe (Pre T)	1.81	6.8	Spiral & Segment c = 7.43	Torque 20.14 N-m, d = 35.5 cm
07/19/89	U6L	L-M	Pipe (Pre T)	6.11	6.8	Comminuted.	Torque 20.14 N-m, d = 37.5 cm
"	U7L	L-M	Pipe (Pre T)	nt	6.7	Spiral & Segment. c = 7.43	Torque 20.14 N-m, d = 39.5 cm

Date	Body #	Direction	Impactor	Force (kN)	v (m/s)	Fractures (Cortex Measures Avg/Smallest mm.)	Remarks
03/16/92	549R	L-M P½	Pipe	6.75	7.5	Oblique. Avg 9.85/ Smallest 7.29	
"	997L	L-M P½	Pipe	nt	7.5	Tension Wedge. 6.89/5.09	
"	906R	L-M P½	Pipe	4.44	7.5	Comminuted. 9.23/8.13	
06/28/89	698L	L-M	Pipe	nt	7.5	Comminuted Compression Wedge.	d = 43.2 cm
"	746R	L-M	Pipe	1.29	7.6	Comminuted Compression & Tension Wedges.	d = 40.5 cm
"	17R	L-M	Pipe	1.09	7.1	Tension Wedge. Avg. cortex (c) = 8.00	d = 43.2 cm
07/14/89	U1R	L-M	Pipe	3.93	6.9	Oblique, failed on Anterior. c = 6.73	d = 40.5 cm
"	U2R	L-M	Pipe	1.54	7.0	Oblique. c = 6.20	d = 33.0 cm
"	U3R	L-M	Pipe	4.26	6.7	Segment. c = 8.39	d = 33.0 cm
"	No2R	L-M	Pipe	1.70	6.7	Spiral. c = 6.02	d = 33.0 cm
"	U4R	L-M	Pipe	1.70	6.8	Comminuted Long Segment. c = 7.13	d = 34.3 cm
"	U5R	L-M	Pipe	2.17	6.8	Comminuted Segment. c = 7.79	d = 35.6 cm
"	704R	L-M	Pipe	1.83	6.9	Neck & Segment. c = 5.80	d = 33.0 cm
07/19/89	U6R	L-M	Pipe	5.78	6.8	Oblique.	d = 37.5 cm
11/18/90	747R	L-M	Pipe	5.25	6.8	Oblique.	d = 37.5 cm
"	551R	L-M	Pipe	2.19	7.1	Comminuted.	d = 36.0 cm
03/16/92	884R	L-M	Pipe	2.45	7.5	2 Long Tension Wedges. Avg 6.84/ Smallest 5.55	
"	880R	L-M	Pipe	6.10	7.5	Neck & Oblique distal. 7.20/5.49	
"	877L	L-M	Pipe	6.12	7.5	Neck & Wedge Lat to Post. 6.77/5.76	
"	875R	L-M	Pipe	5.13	7.5	Neck & Compression Wedge distal. 8.50/6.84	
"	871R	L-M	Pipe	1.22	7.5	Comminuted Tension Wedge? 5.61/4.29	
06/28/89	698R	L-M	10 cm Plate	4.57	7.5	Compression Wedge. avg cortex = 7.25 mm	d = 43.2 cm



Date	Body #	Direction	Impactor	Force (kN)	v (m/s)	Fractures (Cortex Measures Avg/Smallest mm.)	Remarks
01/25/91	676L	AX	10 cm Plate	8.59	7.5	Neck & Intercondylar.	Tucker M.S.
"	557L	AX	10 cm Plate	10.94	7.5	G. Trochanteric & Intercondylar.	d = 40.5 cm
"	11L	AX	10 cm Plate	9.25	7.5	Comminuted Compression Wedge & Neck.	d = 41.3 cm
02/16/91	41L	AX	10 cm Plate	3.52	7.5	Comminuted.	Tucker M.S.
"	862L	AX	10 cm Plate	6.62	4.9	Medial Wedge & Neck.	
"	867L	AX	10 cm Plate	4.64	6.9	Medial Wedge.	
"	865L	AX	10 cm Plate	6.66	5.3	Neck.	
"	881L	AX	10 cm Plate	4.92	7.1	Neck.	
"	859L	AX	10 cm Plate	8.80	6.7	Subtrochanteric Oblique.	
"	888L	AX	10 cm Plate	7.15	6.8	Neck.	
03/22/91	859R	AX	Materials Testing Machine (MTM)	10.57	Static	Medial Wedge & Neck.	Static Compression Testing.
"	902R	AX	MTM	4.05	Static	Neck.	
"	812R	AX	MTM	1.85	Static	Subtrochanteric Oblique.	
"	883R	AX	MTM	6.25	Static	Neck.	
"	862R	AX	MTM	6.14	Static	Neck.	
"	865R	AX	MTM	5.05	Static	Neck.	
"	724L	AX	MTM	3.63	Static	Neck.	
"	881R	AX	MTM	3.74	Static	Neck.	
"	880L	AX	MTM	6.18	Static	Medial Wedge & Neck.	

**TABLE 5: Dynamic Response Characteristics of the Intact Human Lower Limb**

Direct Results from Impact Biomechanics Research at  
the University of Tennessee & the University of Louisville  
(Sponsored by the Japan Automobile Manufacturers Association)

All specimens were embalmed and support is noted in "Remarks" column.

Date	Cad #	Plane	Impactor	F (kN)	v (m/s)	Fractures (Cortex Measurements Avg/Smallest mm)	Remarks
05/01/93	013R	L-M ankle	Pipe	5.15, 8.34	3.9, 5.3	Medial & Lateral Malcolli, Talus and Calcaneus. (Tibia- T 7.30/5.24, fibula-f 6.08/5.35)	Approx. 36 kg mass medial to ankle. Inertial support for Ankle Crush.
05/02/93	013L	L-M ankle	Pipe	5.21	4.1	Same fxs. as above. (T-5.65/ 4.85, f-4.05/3.06)	Same as above.
05/02/93	071L	L-M ankle	Pipe	11.17	11.8	Calcaneus, Cuboid, 2 Cuneiforms, Navicular and both maleoli. (T-6.96/4.75, f-4.58/3.16)	Same as above.
05/02/93	958L	L-M heel	Pipe	3.48	4.0	Calcaneus & tarsals crush. (T-2.99/1.71, f-2.39/2.17)	Same as above for Foot Crush.
"	958R	L-M heel	Pipe	5.22	3.9	Calcaneus & tarsals crush. (T-3.47/1.89, f-2.94/2.24)	Same as above.
03/26/87	9R	L-M leg	3" Pipe	na	7.6	T-No fx. f-Simple oblique fx.	JE-87-02, @45° Inertial
03/23/92	009R	L-M Leg	Pipe	4.76	7.5	T-no fx, f-comminuted. (T- 6.42/4.17, f-3.43/2.09)	
12/05/92	974R	L-M Leg	Pipe	4.76	7.5	T-Comminuted Tension Wedge. f-comminuted. (T-6.79/3.42, f-5.04/3.38)	No foot.
03/26/87	1L	A-P D½ Leg	3" Pipe	na	7.5	T/f-Comminuted.	JE-87-06 Inertial
"	2R	A-P D½ Leg	3" Pipe	na	7.3	T/f-Simple Transverse.	JE-87-07 Inertial
"	5L	A-P D½ Leg	3" Pipe	na	7.2	T-Transverse, f-Tension Wedge.	JE-87-08 Inertial
"	10L	A-P D½ Leg	3" Pipe	na	7.4	T/f-Comminuted Transverse.	JE-87-09 Inertial
"	353R	A-P D½ Leg	3" Pipe	na	7.4	No fx.	JE-87-10 Inertial

Date	Cad #	Plane	Impactor	F (kN)	v (m/s)	Fractures (Cortex Measurements Avg/Smallest mm)	Remarks
11/10/87	569R	A-P D½ Leg	Pipe	1.44	10.6	T/f-Comminuted Compression Wedge, 10 cm Lac.	JF-87-27. d = 25.4 cm Inertial
"	569L	A-P D½ Leg	Pipe	2.12	7.8	T/f-Comminuted Transverse, 3 cm Lac.	JF-87-28. d = 22.3 cm Inertial
03/26/87	14R	A-P Leg	3" Pipe	na	13.1	T/f-Comminuted.	JF-87-01 Inertial
"	15R	A-P Leg	3" Pipe	na	7.6	T/f-Comminuted Tension Wedge?	JF-87-03 Inertial
"	11L	A-P Leg	3" Pipe	na	5.3	T/f-Comminuted Tension Wedge?	JF-87-04 Inertial
"	456R	A-P Leg	3" Pipe	na	7.2	No fx.	JF-87-05 Inertial
11/10/87	526R	A-P Leg	3" Pipe	na	2.9	T/f-Comminuted Transverse, 2 cm Lac.	JF-87-16. d = 24.8 cm Inertial
"	539R	A-P Leg	3" Pipe	na	7.4	T/f-Transverse, 6 cm Lac.	JF-87-17. d = 22.3 cm Inertial
03/26/87	8R	A-P Leg	Bumper	na	7.3	T-Comminuted Transverse. f-no fx.	JF-87-11 Inertial
"	3R	A-P Leg	Bumper	na	7.2	T/f-Oblique Comminuted.	JF-87-12 Inertial
"	423R	A-P Leg	Bumper	na	7.3	T-Comminuted Tension Wedge? f-no fx.	JF-87-13 Inertial
"	6R	A-P Leg	Bumper	na	7.2	T/f-Comminuted, Tension Wedge?	JF-87-14 Inertial
"	4R	A-P Leg	Bumper	na	7.3	T-Transverse, f-no fx.	JF-87-15 Inertial
11/10/87	?R	A-P Leg	Pipe	1.41	2.1	T/f-Comminuted Side Wedge, 2 cm Lac.	JF-87-18. d = 30.5 cm Inertial
"	?L	A-P Leg	Pipe	0.97	2.7	T/f-Comminuted Lateral Wedge, 1 cm Lac.	JF-87-19. d = 23.0 cm Inertial
11/10/87	?L	A-P Leg	Pipe	1.45	7.4	T/f-Comminuted Lateral Wedge, 2 cm Lac.	JF-87-20. d = 31.8 cm Inertial
"	?L	A-P Leg	Pipe	2.43	7.7	T/f-Tension Wedge, 2 cm & 9 cm Lac.	JF-87-21. d = 33.0 cm Inertial
02/05/88	?R	A-P Leg	Pipe	2.02	7.5	T/f-Comminuted, 3 Lac > 8 cm, Knee R	JF-88-01. Inertial
"	?L	A-P Leg	Pipe	2.97	7.6	T/f-Comminuted, 1.5 cm Lac.	JF-88-02. Inertial
"	?L	A-P Leg	Pipe	0.82	7.7	T/f-Comminuted, 3 Lac 1 cm.	JF-88-03. Inertial
"	?L	A-P Leg	Pipe	1.54	7.5	T/f-Comminuted Transverse, 1 cm Lac.	JF-88-04. Inertial

Date	Cad #	Plane	Impactor	F (kN)	v (m/s)	Fractures (Cortex Measurements Avg/Smallest mm)	Remarks
02/05/88	2L	A-P Leg	Pipe	1.53	7.5	T/f-Comminuted Transverse, 2 cm Lac.	JB-88-05. Inertial
07/26/89	12L	A-P Leg	Pipe	9.31, 11.08	7.3, 9.3	3" Plate used for 1st impact then Pipe. T/f-Long Comminuted Compression Wedge.	JB-89-21. d=53.4 cm Inertial
"	458L	A-P Leg	Pipe	3.76	7.5	T/f-Comminuted Longitudinal Segments.	JB-89-20. d=60.0 cm Inertial
03/23/92	944L	A-P Leg	Pipe	8.06	7.5	T-Comminuted Tension W.(T-5.75/2.89, f-3.77/2.54)	Inertial support.
03/23/92	995L	A-P Leg	Pipe	nt	7.5	T-Jagged Transverse, f-Tension Wedge (T-7.80/5.23, f-3.68/3.14)	Inertial support.
07/23/89	517L	A-P Leg	Pipe	9.78	7.5	T-Comminuted Compression Wedge, f-comminuted.	JB-89-22. d=50.8 cm Simple
05/02/93	012L	A-P Leg	Pipe	4.43	8.7	T/f-Comminuted. (T-4.70/2.76, f-3.57/2.62)	Inertial support.
05/02/93	012R	P-A Leg	Pipe	2.28	8.7	T/f-Comminuted Segment distal to impact. (T-4.28/3.17, f-3.68/2.61)	Inertial support.
07/30/89	742L	A-P Leg	Pipe	8.36, ST=3.01	7.1, 7.1	T-Comminuted Tension Wedge, f-segment.	2nd Impact for Soft Tissue (ST) JB-89-08. d=47.0 cm Inertial
"	743L	A-P Leg	Pipe	4.53, ST=1.91	7.3, 7.2	T/f-Open Comminuted Tension Wedge (nice X-ray).	JB-89-10. d=45.8 cm Inertial
"	588R	A-P Leg	Pipe	7.01, ST=3.43	7.6, 7.2	T-Open Comminuted Tension Wedge & Distal transverse, f-segment.	JB-89-09. d=45.8 cm Inertial
"	547L	A-P Leg	Pipe	6.57, ST=4.10	7.3, 7.2	T/f-Jagged Transverse.	JB-89-04. d=45.8 cm Inertial
"	111L	A-P Leg	Pipe	4.71, ST=1.84	7.3, 7.3	T/f-Comminuted Segment.	JB-89-01. d=38.8 cm Inertial
"	725L	A-P Leg	Pipe	8.17, ST=4.36	7.3, 7.3	T/f-Large Segment.	JB-89-19. d=42.0 cm Inertial
"	672R	A-P Leg	Pipe	3.38, ST=1.86	6.9, 7.1	T/f-Large Comminuted Segments.	JB-89-14. d=43.2 cm Inertial
07/30/89	577L	A-P Leg	Pipe	10.45, 6.27, ST=5.39	7.1, 7.0, 6.9	No fx until boot added for 2nd impact. T-Cominuted Tension Wedge, f-oblique.	JB-89-15. d=47.0 cm Inertial
"	528R	A-P Leg	Pipe	7.10, ST=3.47	7.5, 7.3	T-Comminuted Compression Wedge, f-no fx.	JB-89-06. d=48.3 cm Inertial

Date	Cad #	Plane	Impactor	F (kN)	v (m/s)	Fractures (Cortex Measurements Avg/Smallest mm)	Remarks
07/26/89	517R	A-L Leg	Pipe	11.05, 8.86, ST = 2.88	7.5, 7.4, 7.5	Not a definite fx until 2nd hit. T/f-Open Comminuted.	JH: 89-18. d = 53.4 cm Inertial
07/30/89	742R	A-L Leg	Pipe	8.04, ST = 3.40	7.2, 7.2	T/f-Comminuted	JH: 89-07. d = 47.0 cm Inertial
"	743R	A-L Leg	Pipe	3.66, ST = 3.09	7.3, 7.3	T-Open Transverse. f-segment.	JH: 89-12. d = 45.8 cm Inertial
"	588L	A-L Leg	Pipe	3.04, ST = 1.73	7.3, 7.3	T/f-Open Comminuted Tension Wedge.	JH: 89-11. d = 45.8 cm Inertial
"	547R	A-L Leg	Pipe	5.99, ST = 3.51	7.2, 7.3	T-Comminuted Medial Wedge. f-segment.	JH: 89-03. d = 45.8 cm Inertial
"	11R	A-L Leg	Pipe	4.13, ST = 1.60	7.3, 7.3	T-Jagged Transverse. f-comminuted.	JH: 89-02. d = 45.8 cm Inertial
"	725R	A-L Leg	Pipe	4.38, ST = 2.81	7.3, 7.3	T/f-Comminuted Medial Wedges.	JH: 89-17. d = 40.7 cm Inertial
"	672L	A-L Leg	Pipe	3.47, ST = 1.35	7.0, 7.1	T-Comminuted Oblique. f-segment.	JH: 89-13. d = 47.0 cm Inertial
"	577R	A-L Leg	Pipe	nt, ST = 5.27	7.0, 7.0	T-Medial Wedge, f-comminuted.	JH: 89-16. d = 47.0 cm Inertial
"	528L	A-L Leg	Pipe	9.97, 7.21, 8.67, 6.54	7.3, 7.5, 7.3, 7.3	No fracture after 4 hits. 2nd was with 1 kg boot.	JH: 89-05. d = 47.0 cm Inertial
03/24/91	059R	A-P P 1/2 Leg	Pipe	4.10	7.5	T/f-Comminuted. (T-4.43/2.48, f-3.87/3.44)	Compare to OMC. Tibial plate. Inertial
03/18/92	582R	A-P P 1/2 Leg	Pipe	2.24	7.5	T/f-Comminuted. (T-4.14/2.14)	Compare to OMC. Inertial support.
04/23/93	755L	A-P Leg	TA Plate	0.64	2.2	No fx. Special 10 cm plate bumper system with Air Springs and foam padding- for this test only.	20 kg superior to inferior vector. Shod foot on concrete block. Testing to validate Fuzzy Logic Model.
"	"	"	"	0.63	2.5	No fx.	"
"	"	"	"	0.80	2.7	No fx.	"
"	"	"	"	0.84	3.0	No fx.	"
"	"	"	"	1.21	4.4	No fx.	"
"	"	"	"	1.38	4.8	No fx.	"
"	"	"	"	1.60	5.7	Fx?	"
"	"	"	"	1.49	6.3	T/f-Comminuted Tension/Lateral Wedge. No soft tissue damage. (T-5.17/3.27, f-2.29/1.74)	"

Date	Cad #	Plane	Impactor	F (kN)	v (m/s)	Fractures (Cortex Measurements Avg/Smallest mm)	Remarks
04/23/93	9911.	A-P Leg	TA Plate	1.29	3.4	No fx. Same 10 cm. bumper system.	20 kg superior to inferior vector. Shoed foot on concrete block.
"	"	"	"	1.90	4.9	No fx.	"
"	"	"	"	2.19	5.8	No fx.	"
"	"	"	"	2.67	6.6	No fx.	"
"	"	"	"	2.76	7.0	No fx.	"
"	"	"	"	3.07	7.1	No fx.	"
"	"	"	"	3.22	7.1	No fx.	"
"	"	"	"	3.77	7.7	Fx?	"
"	"	"	"	3.29	7.9	T-Transverse, f-Oblique. (T-6.73/4.21, f-3.42/2.81)	"
04/23/93	0091.	A-P Leg	TA Plate	2.41	4.9	No fx. Same 10 cm. bumper system.	20 kg superior to inferior vector. Shoed foot on concrete block.
"	"	"	"	2.94	5.9	No fx.	"
"	"	"	"	3.67	6.9	No fx. Slight tear in soft tissue.	"
"	"	"	"	4.11	7.8	No fx.	"
"	"	"	"	3.57	8.2	No fx.	"
"	"	"	"	4.16	8.7	No fx.	"
"	"	"	"	3.89	9.0	No fx.	"
"	"	"	"	4.47	9.5	No fx.	"
"	"	"	"	4.40	9.9	No fx.	"
"	"	"	"	4.64	10.8	Still no fx & little skin damage. Compressor @ max.	"
"	"	"	"	2.57	6.0	Changed to 4 cm plate bumper system. No fx.	"
"	"	"	"	3.50	7.3	No fx.	"
"	"	"	"	3.81	8.8	No fx.	"
"	"	"	"	4.97	9.6	No fx.	"

Date	Cad #	Plane	Impactor	F (kN)	v (m/s)	Fractures (Cortex Measurements Avg/Smallest mm)	Remarks
04/23/93	009L	A-P Leg	TA Plate	5.16	10.1	No fx. Still using 4 cm plate.	"
"	"	"	"	6.26	11.4	No fx.	"
"	"	"	"	7.08	11.6	No fx.	"
"	"	"	"	3.12	7.7	No fx.	"
"	"	"	"	6.24	8.0	No air springs. T/f-Oblique (T-6.09/3.22, f-3.70/3.41)	"
06/15/93	070L	A-P Leg	TA Plate	1.00	2.6	10 cm plate bumper without air springs. No fx.	20 kg superior to inferior vector. No friction.
"	"	"	"	1.39	3.4	No fx.	"
"	"	"	"	1.14	5.2	Comminuted fracture.	"
"	949L	A-P Leg	TA Plate	1.96	3.8	10 cm plate bumper without air springs. No fx.	20 kg superior to inferior vector. Shoed foot on concrete block.
"	"	"	"	1.67	4.9	Fractured.	"
06/15/93	070R	P-A Leg	TA Plate	0.57	2.8	10 cm plate bumper with air springs. No fx.	20 kg superior to inferior vector. No friction.
"	"	"	"	0.80	3.8	No fx.	"
"	"	"	"	1.14	5.0	Fractured.	"
04/27/93	961R	P-A Leg	TA Plate	1.34	5.1	10 cm plate bumper with air springs. T/f-Tension Wedges. (T-3.73/2.12, f-3.77/2.77)	20 kg superior to inferior vector. Shoed foot on concrete block.
06/15/93	949R	P-A Leg	TA Plate	1.20	3.8	10 cm plate bumper with air springs. No fx.	"
"	"	"	"	1.53	4.6	No fx.	"
"	"	"	"	1.79	5.1	No fx.	"
"	"	"	"	1.96	5.5	No fx.	"
"	"	"	"	2.06	6.3	Fractured.	"

Date	Cad #	Plane	Impactor	F (kN)	v (m/s)	Fractures (Cortex Measurements Avg/Smallest mm)	Remarks
05/02/93	995R	AX Knee	Hammer	0.01	Manual	No obvious fracture of patella.	Instrumented Sledge hammer.
"	"	"	Hammer	0.94	Manual	Small crack on posterior.	
"	"	"	Hammer	1.90	Manual	2.5 cm laceration. Small puncture to patella.	
"	"	"	Hammer	2.01	Manual	No additional damage.	
"	"	"	Hammer	1.89	Manual	No additional damage.	Missed Knee, hit proximal tibia.
"	"	"	Hammer	1.94	Manual	Slight increase in posterior crack.	
"	"	"	Pipe	0.36	Manual	No additional damage.	Missed knee, hit below patella.
"	"	"	Pipe	7.41	Manual	Increased crack on posterior side.	Missed knee, hit below patella.
"	"	"	Pipe	10.95	Manual	Fractured patella but incomplete.	
"	"	"	Pipe	11.30	Manual	Complete fracture of proximal portion of patella.	Fxs of Femoral and Tibial Condyles.
03/24/91	727R	AX Knee	Pipe	4.50	7.5	Neck, HBB Fxs of femoral condyles. (F:7.28/6.27)	38.6 kg mass @ hip. Acetab. pre-fx
03/24/91	841R	AX Knee	Plate	8.89	7.5	Comminuted Tibia, Patella & F. (F:4.53/3.02)	No mass behind hip. Previous Hip fx?
"	841L	AX Knee	Plate	10.71	7.5	Comm. F shaft, head & Pat. & t-condyle. (F:5.20/3.22)	Same as above.
03/24/91	906L	AX Knee	Plate	7.22	7.5	Comminuted patella only. (F:9.31/6.53)	Quad tendon cut to bend leg. No mass behind hip.
"	877R	AX Knee	Plate	8.46	7.5	Comminuted patella only. (F:6.89/5.20)	Same as above.
03/18/92	793L	AX Knee	Plate	11.07	7.5	Comminuted patella. Femur not fractured, saved for further study.	Quad Tendon cut to bend leg. 11 kg mass of clay behind hip (1 bag).
03/18/92	008R	AX Knee	Pipe	8.86	7.5	Comminuted patella & distal Femur. (F:5.63/3.81)	Same as above.
"	008L	AX Knee	Pipe	10.87	7.5	Comminuted patella & F condyles. (F:6.49/4.32)	Same as above.
"	025L	AX Knee	Pipe	12.00	7.5	Comminuted patella, HBB F condyles. (F:6.83/5.23)	Same as above. Bumper slid over top.
"	025R	AX Knee	Pipe	9.21	7.5	Comminuted patella. F OK, saved for further study.	Same as above.



Date	Cad #	Plane	Impactor	F (kN)	v (m/s)	Fractures (Cortex Measurements Avg/Smallest mm)	Remarks
03/18/92	894L	AX Knee	Pipe	10.94	7.5	Comminuted F & t condyles & Patella. (F-5.73/4.71)	2 clay bags (18 kg) behind hip.
"	894R	AX Knee	Pipe	5.20	7.5	Comminuted F & t condyles & Patella. (F-5.39/4.19)	Same as above.
03/23/91	919L	A-P Thigh	Pipe	1.69 (f.t.)	7.5	Oblique with small wedge. (F-7.17/5.28)	Simply supported upside down.
"	901L	A-P Thigh	Pipe	8.23	7.5	Jagged transverse. (F-6.92/5.63)	Simply supported upside down.
"	879L	A-P Thigh	Pipe	0.89 (f.t.)	7.5	Compression wedge? (F-7.76/5.67)	Simply supported upside down.
"	860R	A-P Thigh	Pipe	5.29	7.5	Neck, Sub Troch. & Oblique shaft. (F-6.90/5.28)	Simply supported upside down.
"	846R	A-P Thigh	Pipe	5.75	7.5	Comminuted Tension Wedge? (F-5.60/4.38)	Simply supported upside down. Femoral plate present.
"	810R	A-P Thigh	Pipe	3.96	7.5	Oblique. (F-7.14/4.92)	Simply supported upside down.
03/23/91	919R	L-M Thigh	Pipe	4.61	7.5	Comminuted. (F-7.61/5.41)	Simply supported upside down.
"	901R	L-M Thigh	Pipe	7.36	7.5	Comminuted. (F-6.76/4.25)	Simply supported upside down.
"	879R	L-M Thigh	Pipe	8.96	7.5	Comminuted. (F-7.32/5.35)	Simply supported upside down.
"	860L	L-M Thigh	Pipe	4.85	7.5	Comminuted oblique. (F-5.42/3.73)	Simply supported upside down.
"	846L	L-M Thigh	Pipe	4.52	7.5	Neck, Ilium & Compression Wedge in F. (F-6.38/4.15)	Simply supported upside down.
"	810L	L-M Thigh	Pipe	6.74	7.5	Comminuted segment. (F-5.68/3.82)	Simply supported upside down.

**TABLE 6: Some Calculated Dynamic Response Characteristics from Selected Data of the Human Tibia and Femur**

All bones and intact specimens were embalmed and impacted while simply-supported, unless noted otherwise.

n	Impact Direction	Impactor	Average Force (kN)	Velocity (m/s)	Fracture Comments	Response Characteristics
TIBIA (Avg. Cortex Thickness = 6.92 mm)						
9	A-P	4.13 cm Pipe	3.02	7.6	most comminuted	Bending Strength = $344 \times 10^6 \text{ Pa}_3$ Energy Absorption = $19,286 \text{ J/m}^3$
8	A-P	10 cm Plate	2.80	7.6	less sharp fragments than pipe impact	Energy = 3,900 N-ms
6	A-P	Polymer Plate	2.50	7.6	same results as plate impact	Energy = 4,700 N-ms
FEMUR (Avg. Cortex Thickness = 5.75 mm)						
12	L-M	4.13 cm Pipe	3.05	7.6	41.7% comminuted (tension wedge most prevalent)	Bending Strength = 147 MPa Young's Modulus = 30 GPa Energy = 2,236 N-ms
30	A-P	4.13 cm Pipe	5.70	7.5	70.9% comminuted (side wedge most prevalent)	Bending Strength = 284 MPa Young's Modulus = 88 GPa Energy = 2,658 N-ms
5	Pure Torsion	S-S Torsion	125.1 N-m	Static	All spiral fractures	Torsional Stress = 26 MPa
9	Axial	Materials Testing Machine	5.27	Static	88.9% Neck fractures 11.1% Subtrochantric fractures	Compressive Stress = 125 MPa Tensile Stress = 79 MPa Compressive Strength is 1.5 times >tensile strength
6	Axial	10 cm Plate	6.46	7.6	80.0% Involved Hip 40.0% Involved Shaft 20.0% Involved Knee	Compressive Stress = 174 MPa Tensile Stress = 121 MPa

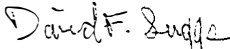
## **Appendix B**


### **Velocity Report of Centrifuge from the Center for Research in Special Environments at the State University of New York**

Centrifuge Velocity Characteristics

State University of New York at Buffalo  
Center for Research in Special Environments

Report by David F. Suggs  
Research Support Specialist  
January 23, 1991

  
David F. Suggs

  
C.E.G. Lundgren, M.D., Ph.D.  
Director, Center for Research in Special Environments

**Objective:**

Measure velocity characteristics of the centrifuge at the Center for Research in Special Environments at the State University of New York at Buffalo when operated in the low speed platform mode.

These measurements will determine actual arm velocity and any degree of variation in speeds used during the propeller guard underwater impact studies conducted at the Center for Biodynamics Research Corporation during December of 1990.

**Method:**

The velocity of the centrifuge is controlled by an IBM type PC computer that is software programmed to generate an analog control voltage proportional to the selected velocity and time base.

Velocity profiles used for the impact testing consisted of three segments: acceleration, steady state, and deceleration. The velocity measurement procedure used the same segments as the impact studies except the time at steady state was increased to allow measurement of time per revolution for ten consecutive rotations of the centrifuge arm. Deviation in arm speed per rotation could then be measured.

Time per revolution was measured by an electronic stopwatch with a photoelectric trigger activated as the centrifuge arm passed by the position detector. Measured and calculated results for each of the six test speeds are compiled in data table #1.

**Conclusions:**

The parameters of the velocity control program were calculated using a 30 foot radius for the motor position at impact. The actual radius at the point of impact was measured to be 31.7 feet. Therefore, as data table #2 summarizes, the velocity at the impact point was slightly greater than the nominal value.

Data table #1 shows an insignificant degree of variation in speed when expressed as the percent difference between each individual time per revolution and the average time per revolution. Of all the speeds measured, the maximum percent difference was 0.24% and the typical value 0.04%. Expressed in mph, the greatest amount of variation was 0.07 mph for the nominal 20.0 mph speed!

Based on these test results it may be concluded that the actual arm velocity of the centrifuge in the low speed platform mode is accurate to within a fraction of a percent for the test speeds listed in table #2.

## State University of New York at Buffalo - Center for Research in Special Environments

Data Table #1 - Centrifuge Velocity Measurements and Calculations

2.5 MPH Nominal - 31.7 ft radius				5.0 MPH Nominal - 31.7 ft radius			
Mi/hr (nominal)	Time/rev measured (sec)	Mi/hr calc	% Diff vs Avg (abs %)	Mi/hr (nominal)	Time/rev measured (sec)	Mi/hr calc	% Diff vs Avg (abs %)
2.5	53.90	2.52	0.06%	5.0	26.62	5.10	0.07%
2.5	53.86	2.52	0.01%	5.0	26.60	5.10	0.00%
2.5	53.88	2.52	0.02%	5.0	26.60	5.10	0.00%
2.5	53.86	2.52	0.01%	5.0	26.60	5.10	0.00%
2.5	53.87	2.52	0.01%	5.0	26.60	5.10	0.00%
2.5	53.86	2.52	0.01%	5.0	26.60	5.10	0.00%
2.5	53.86	2.52	0.01%	5.0	26.59	5.10	0.04%
2.5	53.86	2.52	0.01%	5.0	26.60	5.10	0.00%
2.5	53.85	2.52	0.03%	5.0	26.60	5.10	0.00%
Avg	53.87	2.52	0.02%	Avg	26.60	5.10	0.02%
Max	53.90	2.52	0.06%	Max	26.62	5.10	0.07%
Min	53.85	2.52	0.01%	Min	26.59	5.10	0.00%

7.5 MPH Nominal - 31.7 ft radius				10.0 MPH Nominal - 31.7 ft radius			
Mi/hr (nominal)	Time/rev measured (sec)	Mi/hr calc	% Diff vs Avg (abs %)	Mi/hr (nominal)	Time/rev measured (sec)	Mi/hr calc	% Diff vs Avg (abs %)
7.5	17.59	7.71	0.11%	10.0	13.12	10.34	0.09%
7.5	17.57	7.72	0.00%	10.0	13.11	10.35	0.02%
7.5	17.57	7.72	0.00%	10.0	13.11	10.35	0.02%
7.5	17.57	7.72	0.00%	10.0	13.11	10.35	0.02%
7.5	17.56	7.73	0.06%	10.0	13.10	10.36	0.06%
7.5	17.57	7.72	0.00%	10.0	13.11	10.35	0.02%
7.5	17.57	7.72	0.00%	10.0	13.10	10.36	0.06%
7.5	17.56	7.73	0.06%	10.0	13.10	10.36	0.06%
7.5	17.57	7.72	0.00%	10.0	13.11	10.35	0.02%
Avg	17.57	7.72	0.03%	Avg	13.11	10.35	0.04%
Max	17.59	7.73	0.11%	Max	13.12	10.36	0.09%
Min	17.56	7.71	0.00%	Min	13.10	10.34	0.02%

15.0 MPH Nominal - 31.7 ft radius				20.0 MPH Nominal - 31.7 ft radius			
Mi/hr (nominal)	Time/rev measured (sec)	Mi/hr calc	% Diff vs Avg (abs %)	Mi/hr (nominal)	Time/rev measured (sec)	Mi/hr calc	% Diff vs Avg (abs %)
15.0	8.67	15.65	0.05%	20.0	6.49	20.92	0.24%
15.0	8.67	15.65	0.05%	20.0	6.47	20.99	0.07%
15.0	8.66	15.67	0.06%	20.0	6.48	20.96	0.09%
15.0	8.67	15.65	0.05%	20.0	6.47	20.99	0.07%
15.0	8.66	15.67	0.06%	20.0	6.47	20.99	0.07%
15.0	8.66	15.67	0.06%	20.0	6.48	20.96	0.09%
15.0	8.67	15.65	0.05%	20.0	6.47	20.99	0.07%
15.0	8.66	15.67	0.06%	20.0	6.47	20.99	0.07%
15.0	8.67	15.65	0.05%	20.0	6.47	20.99	0.07%
Avg	8.67	15.66	0.06%	Avg	6.47	20.98	0.09%
Max	8.67	15.67	0.06%	Max	6.49	20.99	0.24%
Min	8.66	15.65	0.05%	Min	6.47	20.92	0.07%

State University of New York at Buffalo - Center for Research in Special Environments

Data Table #2 - Centrifuge Velocity Summary

Nominal MPH	Actual MPH
2.5	2.5
5.0	5.1
7.5	7.7
10.0	10.4
15.0	15.7
20.0	21.0

Sample Calculations - 2.5 MPH Nominal Velocity

Calculate Sec/Rev to MPH

$$\frac{\text{rev}}{\text{sec}} * \frac{\text{ft}}{\text{rev}} * \frac{\text{mi}}{\text{ft}} * \frac{\text{sec}}{\text{hr}} = \frac{\text{mi}}{\text{hr}}$$

$$\frac{1 \text{ rev}}{53.90 \text{ sec}} * \frac{2 * \pi * 31.7}{\text{rev}} * \frac{\text{mi}}{5280 \text{ ft}} * \frac{3600 \text{ sec}}{\text{hr}} = \frac{2.52 \text{ mi}}{\text{hr}}$$

Calculate % Difference

$$\frac{(\text{Time/rev}) - (\text{Avg time/rev})}{\text{Avg time/rev}} * 100\% = \% \text{ Difference}$$

$$\frac{2.520 \text{ sec} - 2.521 \text{ sec}}{2.521 \text{ sec}} * 100\% = 0.06 \%$$

## **Appendix C**

### **Post-test Dissection and X-ray Data**



# Test L-1 Dissection Report

Cad # 13R, Impacted at 20 mph

## Soft Tissue Damage

### Anterior Leg:

**Muscles-** All muscles were intact except: Proximal portion of the Tibialis Anterior was torn horizontally at the level of the tibial fracture.

**Vasculature-** The anterior tibial artery and veins were intact as were the recurrent and muscular branches.

**Nerves-** Though dissected prior to photographing, the Common Fibular nerve and its Superficial and Deep branches were intact throughout the impact zone. Muscular and recurrent branches were also intact.

### Posterior Leg:

**Muscles-** All muscles were intact except: Small tibial bone fragment pierced the proximal portions of the Flexor Digitorum Longus and the Tibialis Posterior.

**Vasculature-** Superficial vessels were unharmed. The Anterior & Posterior Tibial, and the Fibular arteries and veins were intact. Genicular and muscular branches seen were also intact. Tibial Nutrient vasculature was not noted in the impact area.

**Nerves-** The Tibial nerve and its muscular branches were intact.

## Osteology

**Tibia:** Complete (entire circumference) non-displaced comminuted fracture resulting in cavitation of a 4 cm. length on the anterior proximal surface just inferior to the head. Bone fragments were held in place by the periosteum with the exception of the fragment noted above that pierced the deep muscles of the posterior compartment.

**Fibula:** Jagged non-displaced longitudinal fracture at the same level as the tibial fracture.

**Interosseous Membrane:** The membrane was intact on the Tibia, but pulled away from the Fibula for a short distance at the fracture site.

**Measurements:** Impact area is 37.5 cm down from the top of the thigh and 27.5 cm up from the heel. It is a defect roughly 3 cm long x 6 cm wide.

## SUMMARY:

- a) 3 cm. puncture wound to the anterior proximal leg.
- b) Minor muscular damage.
- c) No damage to the major neurovascular components.
- d) Comminuted fractures of the proximal Tibia and Fibula.

Negatives: 52701-1 to 36, 52702-1 to 36, 52820-1 to 21, 52821-1 to 22, 25007-24 & 25.

## Test Leg #1

Cadaver #13-R. Impacted on the proximal third of anterior leg at 20+ mph.

**L1-A)** This is the Anterior View of the impact site, just below the knee (K), after skin and some fascia were removed. There is some minor tearing of the tibialis anterior muscle (M). The tibia (T) shows a comminuted fracture. The fragments are held in place by the periosteum.

**L1-B)** This is the Anterolateral View of the impact site after skin and fascia were removed. The muscles (M) were partially reflected to see the comminuted fracture of the fibula (F). The anterior tibial vessels were intact throughout the impact zone. The artery (A) and interosseous membrane (i) are shown.

**L1-C)** In this deep Posterior View of the leg, all of the superficial muscles were removed. All of the vessels are intact: tibial nerve (N), popliteal artery (A) and its branches, and the vein (V) and its tributaries. A fragment (X) of the tibia (T) is shown piercing some of the deeper muscles but there is no major damage. The comminution of the fibula (F) is clear from this side.

**L1-D)** The completely cleaned Posterior View of the impact zone displays the precise fracture patterns of both the tibia (T) and the fibula (F). The interosseous membrane (i) is intact except at the site of puncture by a tibial fragment (X).



L1-A





L1-B





L1-C





L1-D



X-RAY  
L1 (A-P)





X-RAY  
L1 (L-M)



## Test L-2 Dissection Report

Cad # 602R, Impacted at 20 mph

### Soft Tissue Damage

#### Anterior Leg:

**Muscles-** All muscles were intact except: Proximal, medial portion of the Tibialis Anterior was torn horizontally at the level of the superior tibial fracture cavity.

**Vasculature-** The anterior tibial artery and veins were intact as were the recurrent and muscular branches.

**Nerves-** The Common Fibular nerve and its Superficial and Deep branches were intact throughout the impact zone. Muscular and recurrent branches were also intact.

#### Posterior Leg:

**Muscles-** All muscles were intact except: Small parts of the lateral origin of the Soleus and the most superior origin of the Flexor Hallucis Longus were pulled from the Fibula. Popliteus insertion on the Head of the Tibia was torn at the fracture site.

**Vasculature-** Superficial vessels were unharmed. The Anterior & Posterior Tibial, and the Fibular arteries and veins were intact. Genicular and muscular branches seen were also intact. Tibial Nutrient vasculature was not noted in the impact area.

**Nerves-** The Tibial nerve and its muscular branches were intact.

### Osteology

**Tibia:** Complete (entire circumference) non-displaced comminuted fracture resulting in cavitation of a 3 cm. length on the anterior proximal surface just inferior to the head. Possible Bone Tension Wedge formed with superior extent formed by the posterior head of the Tibia. Longitudinal fracture radiating about 8 cm. inferiorly from the cavity. Fragments were held in place by the periosteum.

**Fibula:** Non-displaced comminuted fracture at the same level as the tibial fracture.

**Interosseous Membrane:** The membrane was intact with the exception of a small tear between the superior extent of the bone fractures.

**Measurements:** The impact area is 40.5 cm down from the top of the thigh and 32.5 cm up from the heel. The area is roughly 2 cm long x 8 cm wide.

---

### SUMMARY:

- a) 10 cm. transverse gash to the anterior proximal leg.
- b) Minor muscular damage.
- c) No damage to the major neurovascular components.
- d) Comminuted fractures of the proximal Tibia and Fibula.

Negatives: 52820-22 to 36, 52821-23 to 36, 28418-1 to 10, 25007-1 to 23.

## Test Leg #2

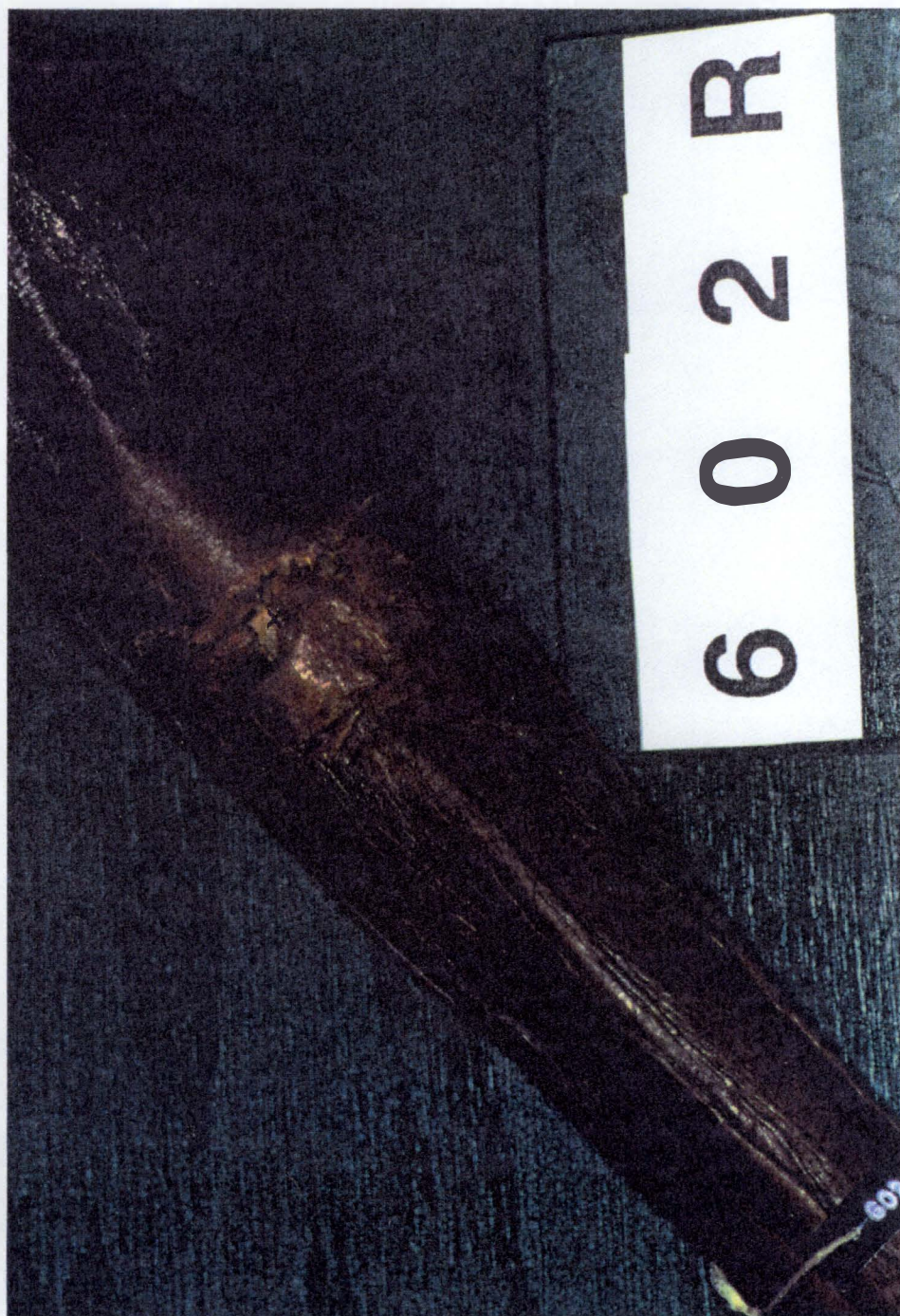
Cadaver #602R. Impacted on the proximal third of the anterior leg at 20 + mph.

L2-A) This is a Pre-dissection View of the anterior leg at the impact site. The skin is torn transversely and a tibial fragment (X) is protruding.

L2-B) In this dissected Anterior View, the comminuted tibia (T) is evident.

L2-C) The deep Anterolateral View of the vessels shows them to be completely intact. The superficial fibular nerve (SN) and deep fibular nerves (DN) are unharmed. The fracturing of the tibia (T) and fibula (F) also had no impact on the anterior tibial artery (A) or veins.

L2-D) The Posterior View of the deep muscles (M) and vessels shows no major damage from the fractured tibia (T) and fibula (F). The popliteal artery (PA) branches into posterior (PTA) and anterior tibial arteries (ATA) at the dissection pin. The posterior tibial artery gives rise to the fibular artery (FA). The common fibular nerve (FN) is seen winding around the head of the fibula. Its branches were reflected previously and therefore visible in this picture.



L2-A





L2-B





C-27

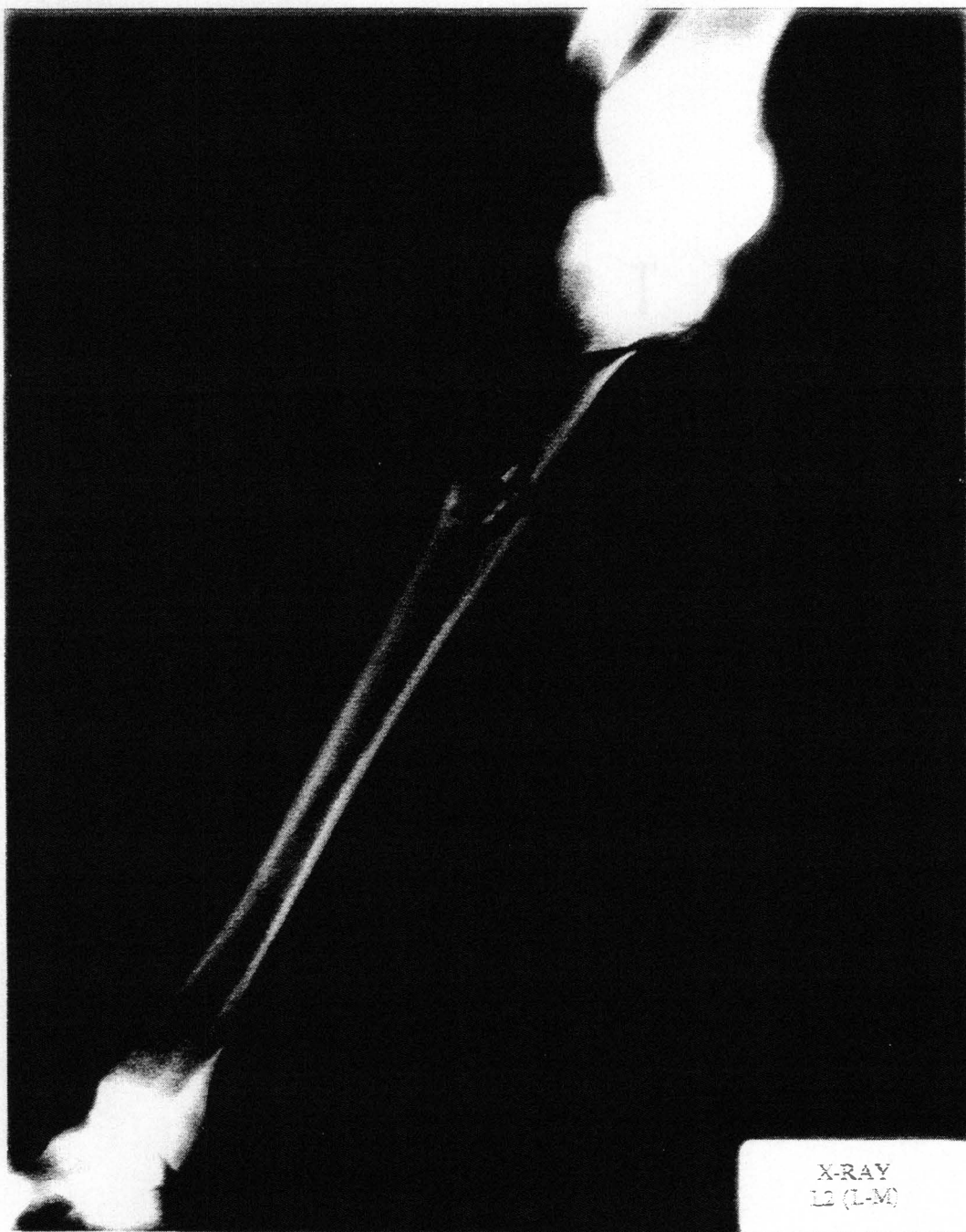




L2-D



X-RAY  
L2 (A-P)





## Test L-3 Dissection Report

Cad # 629L, Impacted at 16.4 mph

### Soft Tissue Damage

#### Anterior Leg:

**Muscles-** All muscles were intact except: Posterior side of the Tibialis Anterior had some small punctures from the shattered Tibia.

**Vasculature-** The anterior tibial artery and veins were intact as were the recurrent and muscular branches.

**Nerves-** The Common Fibular nerve and its Superficial and Deep branches were intact throughout the impact zone. Muscular and recurrent branches were also intact.

#### Posterior Leg:

**Muscles-** All muscles appeared to be intact.

**Vasculature-** Superficial vessels were unharmed. The Anterior & Posterior Tibial, and the Fibular arteries and veins were intact. Genicular and muscular branches seen were also intact. Tibial Nutrient vasculature was intact. Nutrient artery was followed into the marrow.

**Nerves-** The Tibial nerve and its muscular branches were intact.

### Osteology

**Tibia:** Complete (entire circumference) non-displaced comminuted fracture resulting in cavitation of over 20 cm. in length on the anterior proximal surface just inferior to the head, down to the midshaft region. Most badly broken of the 7 test legs. by the posterior head of the Tibia. Longitudinal fracture radiating about 8 cm. inferiorly from the cavity. Fragments were held in place by the periosteum except for a small fragment that punctured the skin on the anterior leg.

**Fibula:** Non-displaced comminuted fracture at the same level as the tibial fracture. There appear to be 2 small tension wedges at opposite ends of the length of the tibial fracture. Fibular head is also comminuted.

**Interosseous Membrane:** The membrane was intact along the shafts of each bone. Small tears were noted between the superior extent of the bone fractures.

**Measurements:** The area of impact is 39 cm down from the top of the thigh and 22 cm up from the heel. The area is roughly 6 cm long x 3 cm wide.

---

### SUMMARY:

- a) Minor scrapes & a small puncture wound anterior leg.
- b) Minor muscular damage.
- c) No damage to the major neurovascular components.
- d) Comminuted fractures of the proximal Tibia and Fibula. It appears that the tibia absorbed most of the impact and the force was not transmitted to the vasculature.

Negatives: 25007-26 to 37, 25797-1 to 36, 25956-1 to 4.

### Test Leg #3

Cadaver #629L. Impacted on the proximal third of the anterior leg at 17 mph.

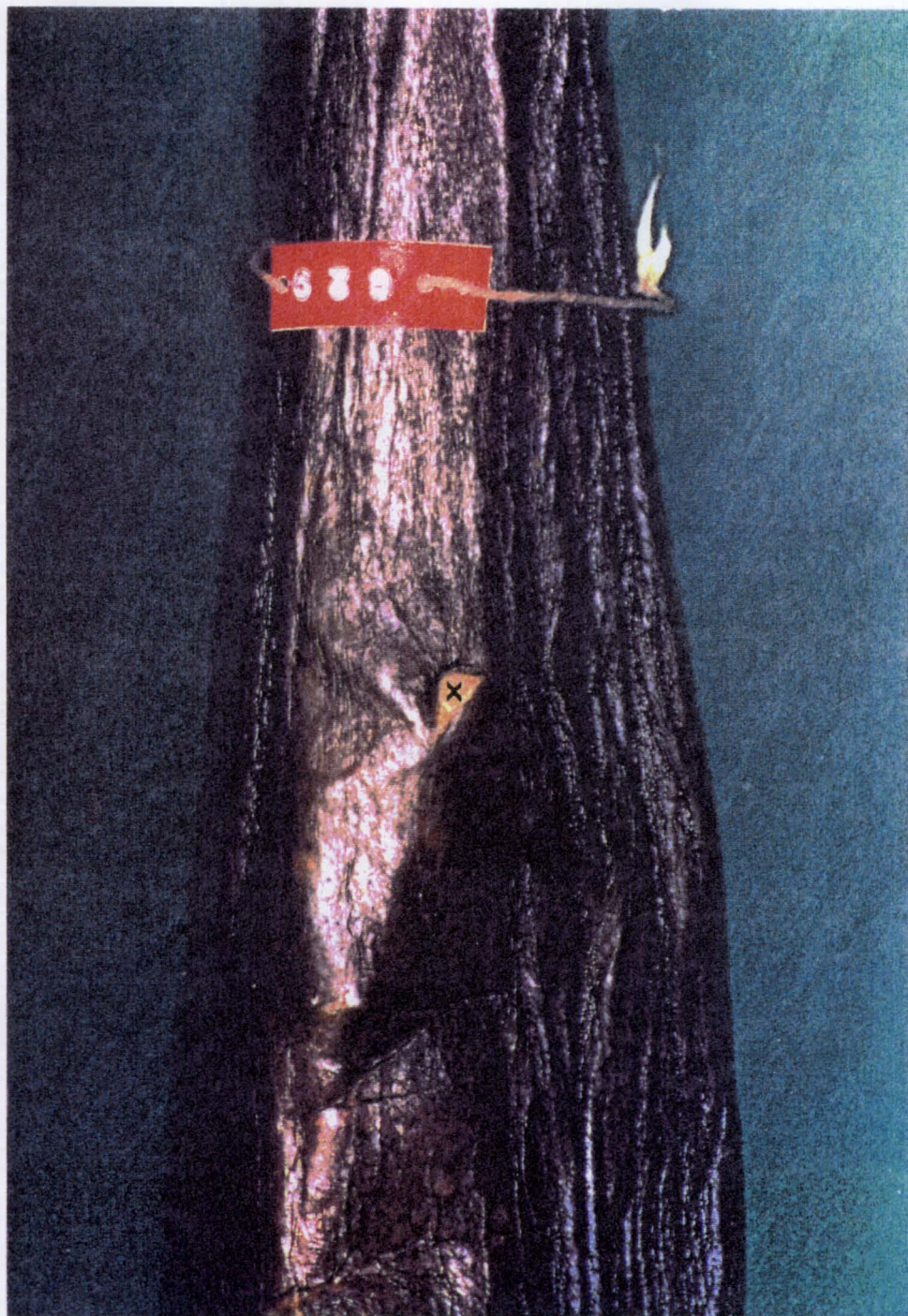
**L3-A)** The Pre-dissection View of this leg gives an indication of the strength of the skin in tissue that has been embalmed for an extensive period of time. Only one shard of a badly comminuted tibia (**X**) pierced the leathery skin.

**L3-B)** An Anterior View, with skin and periosteum removed, shows how extensive the fracture of the tibia (**T**) was in this test.

**L3-C)** This cleaned Anterolateral View clearly shows the fracture patterns of both the tibia (**T**) and fibula (**F**). The superficial fibular (**SN**) and deep fibular nerves (**DN**), as well as the anterior tibial artery (**ATA**), all traverse the impact zone without interruption. The interosseous membrane (**i**) is also intact.

**L3-D)** The Posterior View indicates the posterior tibial artery (**PTA**) and its branches are unharmed by the fracturing of the fibula (**F**) and tibia. The tibial nerve (**TN**) is reflected in this view, but it also escaped injury.

**L3-E)** The cleaned Posterior view gives further evidence of the extensive fracturing of the tibia (**T**) and fibula (**F**).



L3-A





L3-B





L3-C





L3-D





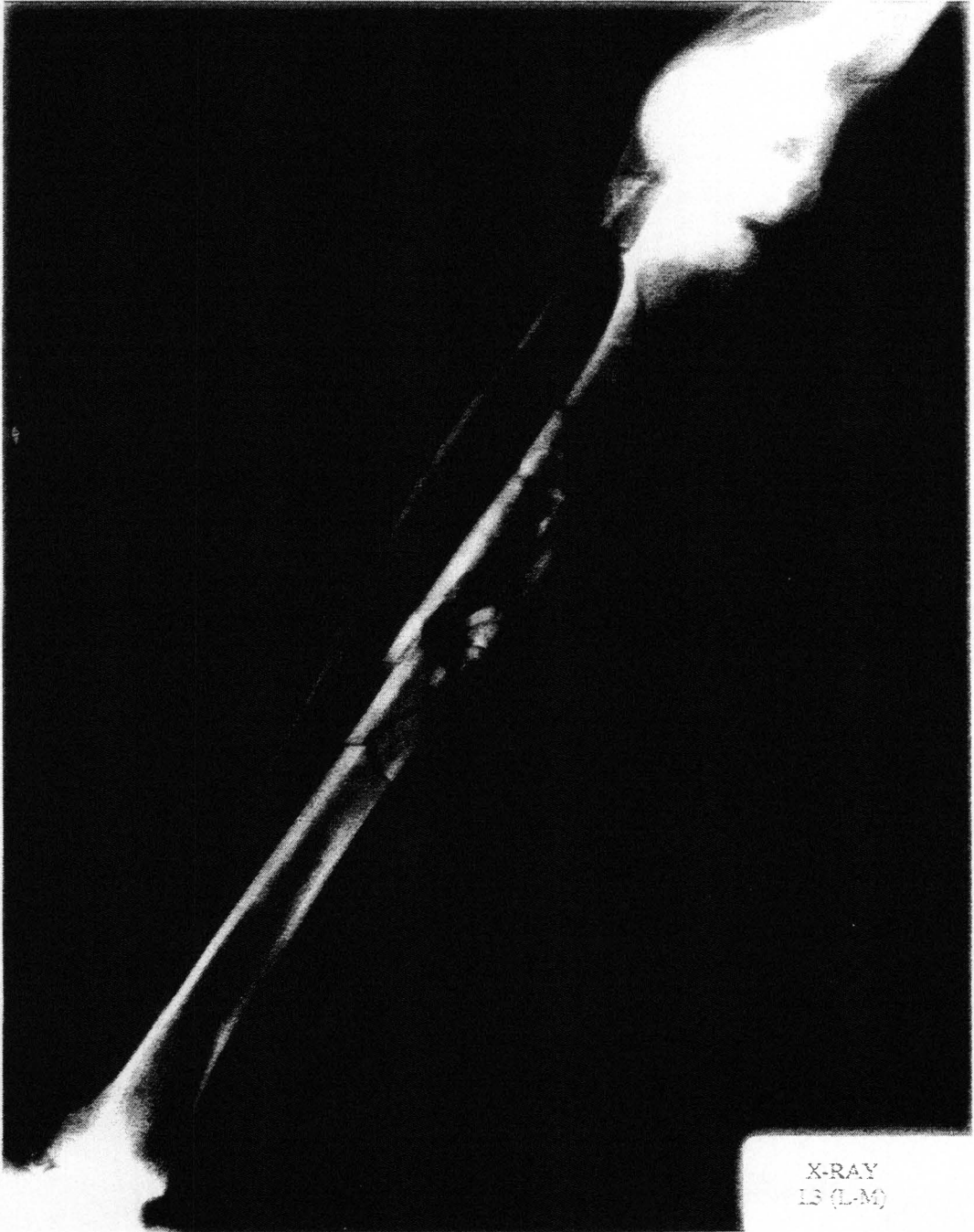
L3-E

LIBERTY  
COTTON



X-RAY  
L3 (A-P)





# Test L-4 Dissection Report

Cad # 646R, Impacted at 16.4 mph

## Soft Tissue Damage

### Anterior Leg:

**Muscles-** All muscles appeared to be intact.

**Vasculature-** The anterior tibial artery and veins were intact as were the recurrent and muscular branches.

**Nerves-** The Common Fibular nerve and its Superficial and Deep branches were intact throughout the impact zone. Muscular and recurrent branches were also intact.

### Posterior Leg:

**Muscles-** All muscles appeared to be intact. Some fragments from the head of the Tibia punctured the Tibialis Posterior and the Popliteus.

**Vasculature-** Superficial vessels were unharmed. The Anterior & Posterior Tibial, and the Fibular arteries and veins were intact. Genicular and muscular branches seen were also intact. Tibial Nutrient vasculature was not noted.

**Nerves-** The Tibial nerve and its muscular branches were intact.

## Osteology

**Tibia:** Complete (entire circumference) non-displaced comminuted fracture resulting in cavitation of 4 cm. in length on the anterior proximal surface just inferior to the head. There appears to be a large Tension Wedge. Fragments were held in place by the periosteum except for a small fragment that punctured the skin on the anterior leg.

**Fibula:** Non-displaced comminuted fracture at the superior extent of the tibial fracture cavity.

**Interosseous Membrane:** The membrane was intact along the shafts of each bone. Small tears were noted between the superior extent of the bone fractures.

**Measurements:** The area of impact is 31 cm down from the top of the thigh and 33.5 cm up from the heel. The area measures 3 cm long x 7 cm wide.

---

## SUMMARY:

- a) Minor scrapes & a small puncture wound anterior leg.
- b) Minor muscular damage.
- c) No damage to the major neurovascular components.
- d) Comminuted fractures of the proximal Tibia and Fibula.

Negatives: 25956-5 to 25.

## Test Leg #4

Cadaver #646R. Impacted on the proximal third of the anterior leg at 17 mph.

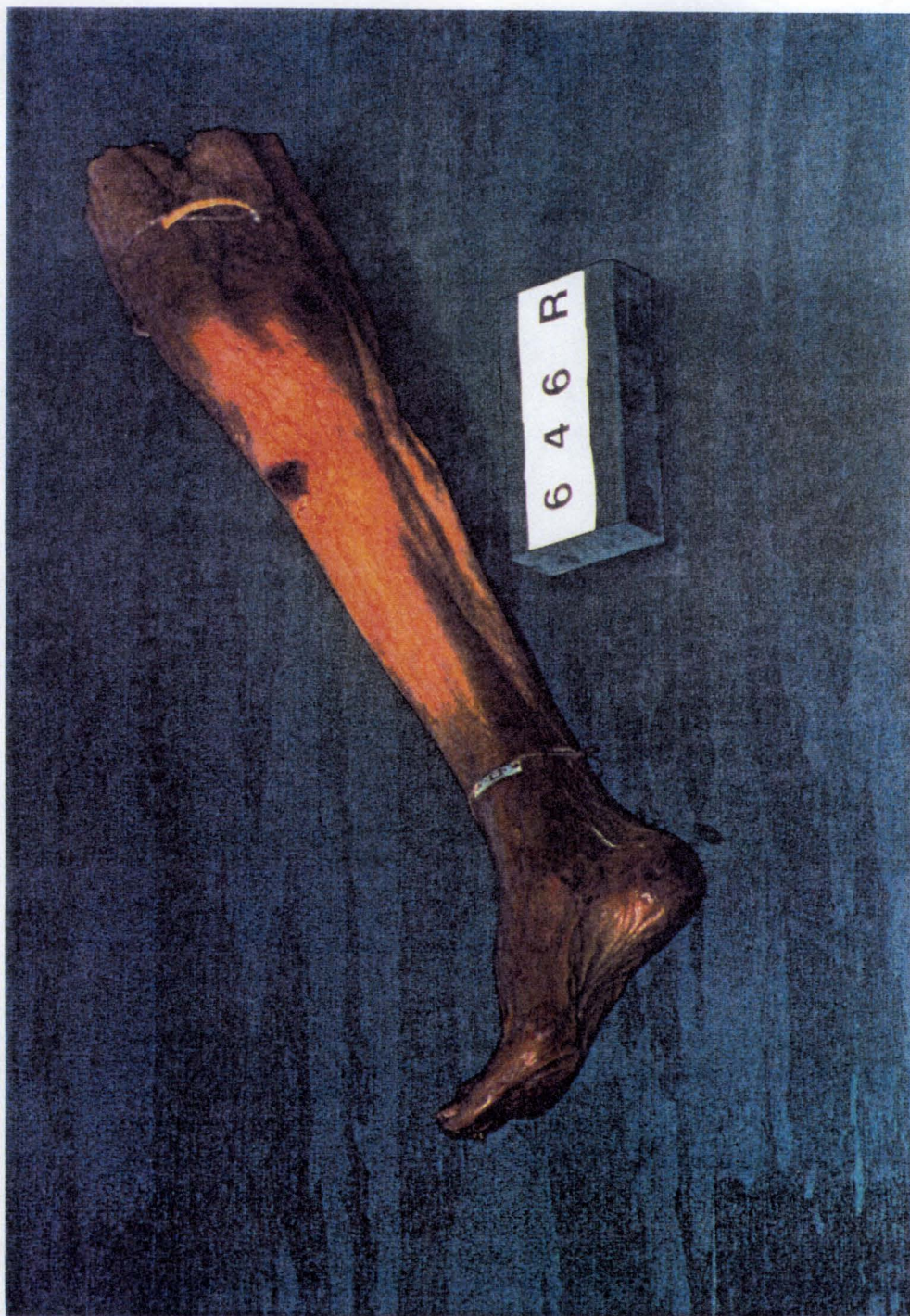
**L4-A)** The Pre-dissection View of this leg shows relatively little damage to the skin on the anterior leg.

**L4-B)** The Anterior View of the dissection reveals the tibial fracture (**T**). A bone fragment is reflected (**X**) to show the fracture pattern within the marrow cavity of the tibia.

**L4-C)** In the Anterolateral View, the fractures of the fibula (**F**) and tibia (**T**) did not harm the anterior tibial artery (**A**) or the superficial (**SN**) and deep (**DN**) fibular nerves. The interosseous membrane (**i**) is clearly intact.

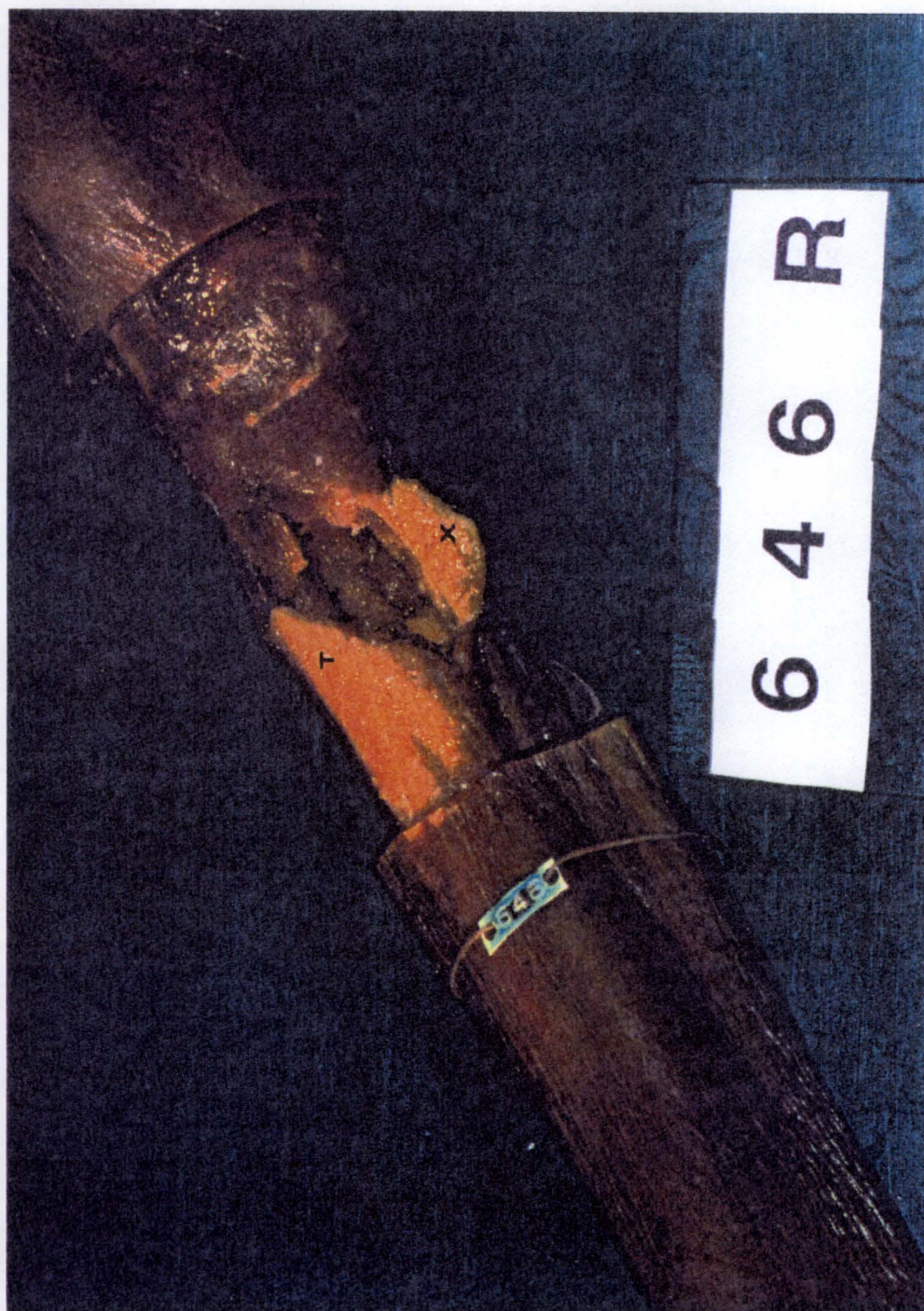
**L4-D)** The Posterior View of the deep vessels shows remarkably little damage for the magnitude of the fractures in the tibia (**T**) and fibula (**F**). The posterior tibial artery and its branches are unharmed. The tendon of the flexor hallucis longus muscle (**M**) is pulled away from the fibula, but there is no transverse damage.

**L4-E)** This cleaned Posterior View of the leg exhibits the gross fracturing of the tibia (**T**) and fibula (**F**).



L4-A





L4-B





L4-C





L4-D

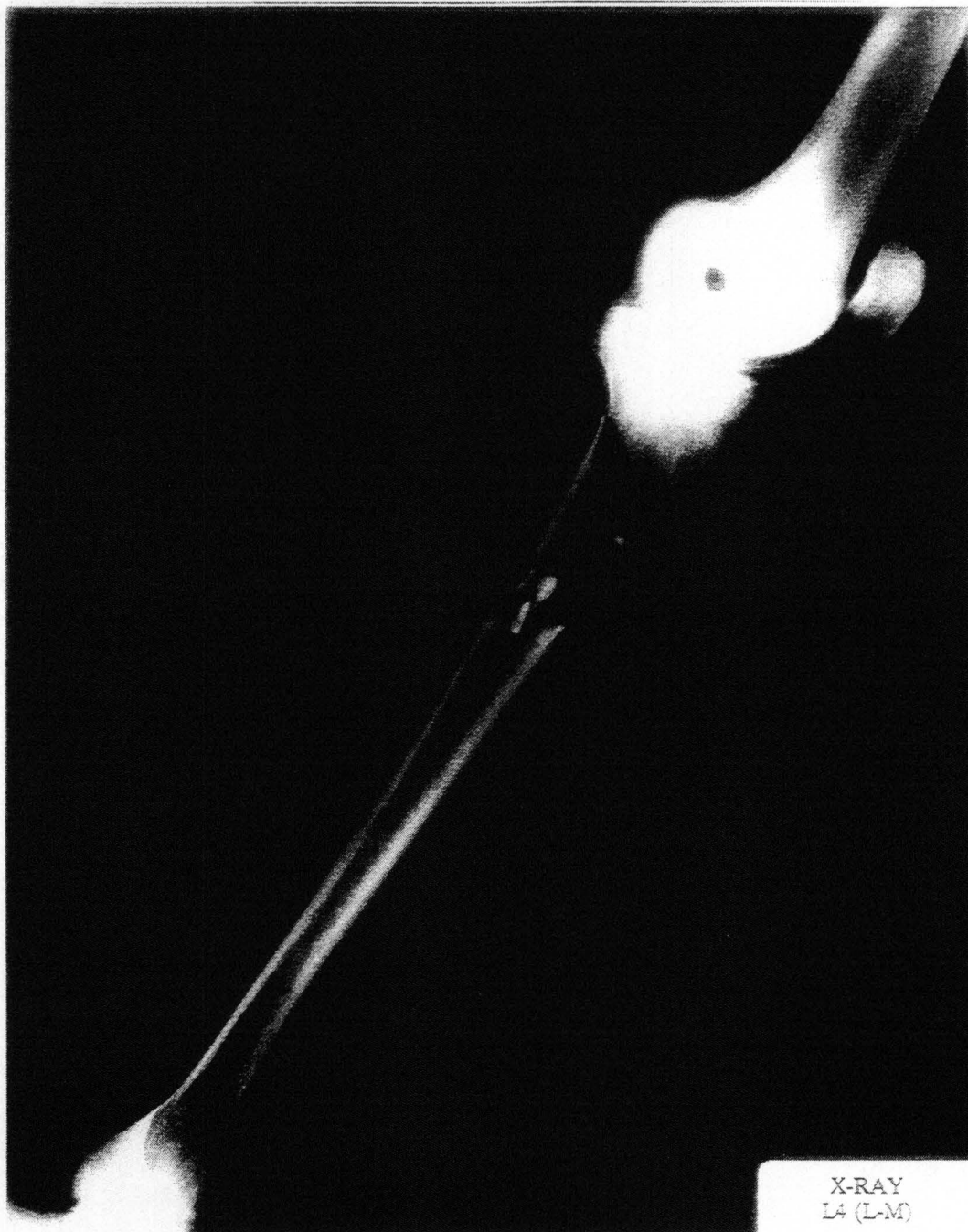




L4-E







X-RAY  
L4 (L-M)

## Test L-5 Dissection Report

Cad # 662R, Impacted at 13 mph

### Soft Tissue Damage

#### Anterior Leg:

**Muscles-** All muscles appeared to be intact.

**Vasculature-** The anterior tibial artery and veins were intact as were the recurrent and muscular branches.

**Nerves-** The Common Fibular nerve and its Superficial and Deep branches were intact throughout the impact zone. Muscular and recurrent branches were also intact.

#### Posterior Leg:

**Muscles-** All muscles were intact except: Some fragments from the head of the Tibia punctured the Tibialis Posterior and the Popliteus. The Popliteus insertion was torn as were small parts of the origins of the Flexor Digitorum Longus, Flexor Hallucis Longus and the Tibialis Posterior.

**Vasculature-** Superficial vessels were unharmed. The Anterior & Posterior Tibial, and the Fibular arteries and veins were intact. Genicular and muscular branches seen were also intact. Tibial Nutrient vasculature was followed into the marrow and found to have been severed within the marrow cavity.

**Nerves-** The Tibial nerve and its muscular branches were intact.

### Osteology

**Tibia:** Complete (entire circumference) non-displaced comminuted fracture resulting in cavitation of 5 cm. in length on the anterior proximal surface just inferior to the head. There appears to be a large Tension Wedge. Fragments were held in place by the periosteum.

**Fibula:** Non-displaced comminuted fracture at the level of the tibial fracture cavity. Head was comminuted as well.

**Interosseous Membrane:** The membrane was intact along the shafts of each bone. Small tears were noted between the superior extent of the bone fractures.

**Measurements:** The area of impact is 42 cm down from the thigh and 40 cm up from the heel. The area measures 5 cm x 5 cm, with no obvious skin defect.

---

### SUMMARY:

- a) Very small puncture wound to anterior leg.
- b) Minor muscular damage.
- c) No damage to the major neurovascular components.
- d) Comminuted fractures of the proximal Tibia and Fibula.

Negatives: 25956-26 to 36, 25953-1 to 21.

## Test Leg #5

Cadaver #662R. Impacted on the proximal third of the anterior leg at 13 mph.

**L5-A)** The Pre-dissection View of the leg shows very little damage to the skin.

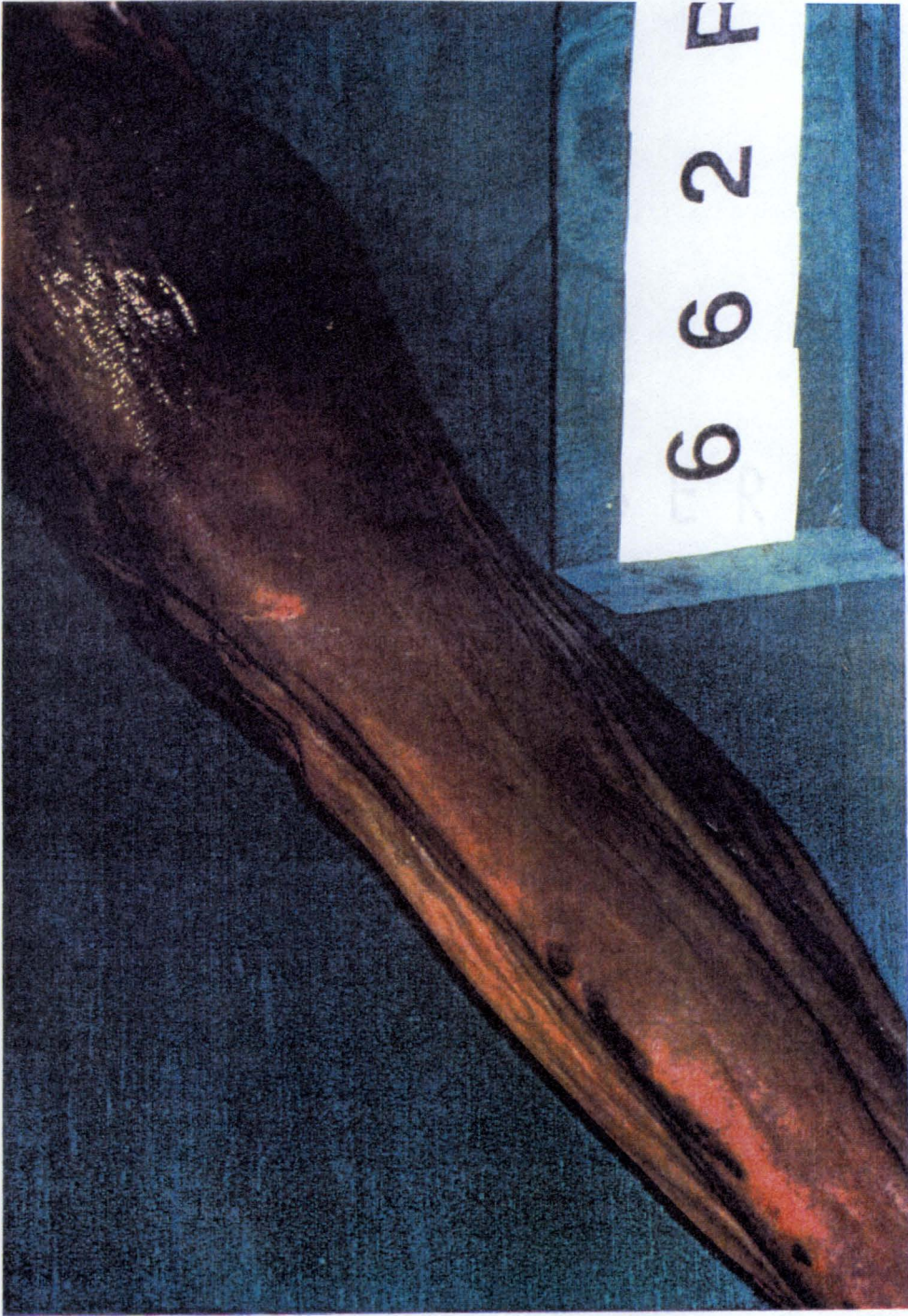
**L5-B)** The Anterior View of the dissection makes clear the comminution of the tibia (**T**). No muscle damage was noted.

**L5-C)** In the Anterolateral View, the tibial (**T**) and fibular (**F**) fractures do not appear to have impinged on the vasculature. The anterior tibial artery (**A**) as well as the superficial (**SN**) and deep fibular nerves (**DN**) are intact.

**L5-D)** The Posterior View clearly shows there is no damage to either the nervous or vascular systems due to the fracturing of the tibia (**T**) or fibula (**F**): The popliteal artery (**PA**) branches into posterior (**PTA**) and anterior tibial arteries (**ATA**) and the posterior gives rise to a fibular artery (**FA**). Even though there is a fracture of the head of the fibula, the common fibular nerve (**FN**) escaped injury.

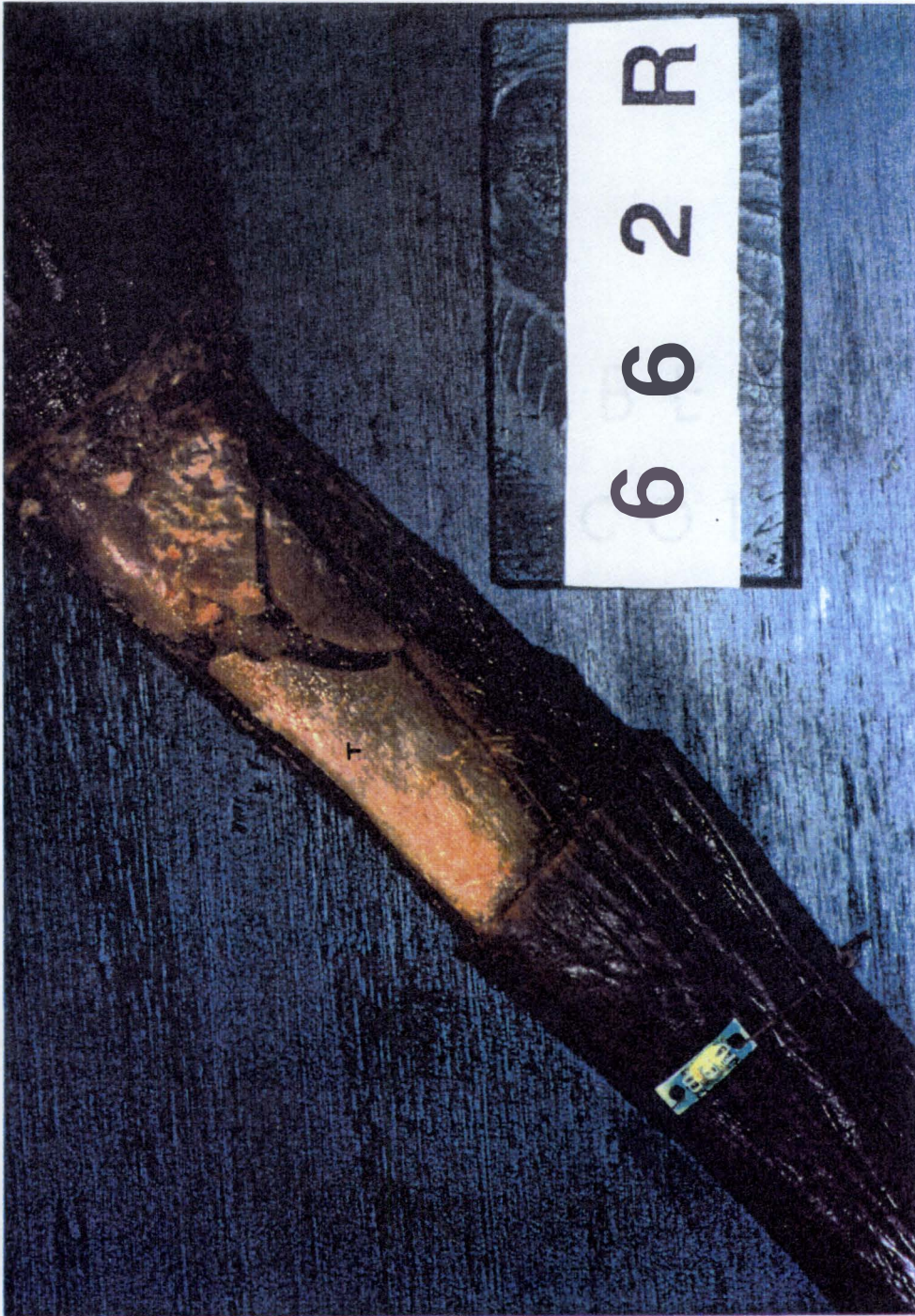
**L5-E)** This completely cleaned Posterior View shows how badly comminuted the tibial (**T**) and fibular (**F**) fractures were in this test. The interosseous membrane (i) shows only minor damage.





L5-A





L5-B





LS-C



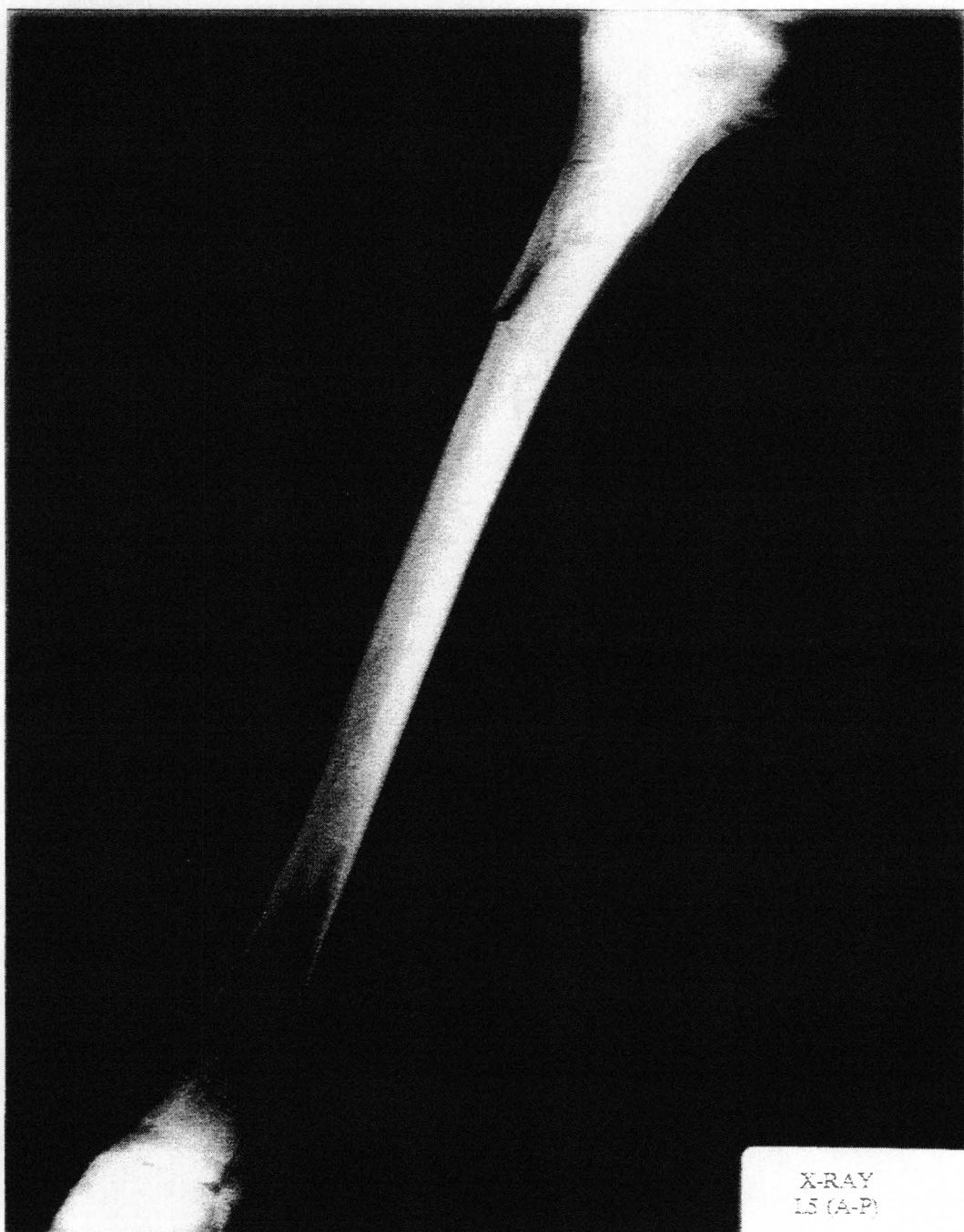


L5-D





LS-E



X-RAY  
L5 (A-P)



X-RAY  
L5 (L-M)



## Test L-6 Dissection Report

Cad # 436L, Impacted at 13 mph

### Soft Tissue Damage

#### Anterior Leg:

**Muscles-** All muscles appeared to be intact.

**Vasculature-** The anterior tibial artery and veins were intact as were the recurrent and muscular branches.

**Nerves-** The Common Fibular nerve and its Superficial and Deep branches were intact throughout the impact zone. Muscular and recurrent branches were also intact.

#### Posterior Leg:

**Muscles-** All muscles were intact except: Some fragments from the head of the Tibia punctured the Tibialis Posterior and the Popliteus.

The Popliteus insertion was torn as were small parts of the origins of the Flexor Digitorum Longus, Flexor Hallucis Longus and the Tibialis Posterior.

**Vasculature-** Superficial vessels were unharmed. The Anterior & Posterior Tibial, and the Fibular arteries and veins were intact. Genicular and muscular branches seen were also intact. Tibial Nutrient vasculature was followed into the marrow and found to have been severed within the marrow cavity.

**Nerves-** The Tibial nerve and its muscular branches were intact.

### Osteology

**Tibia:** Complete (entire circumference) non-displaced comminuted fracture resulting in cavitation of 5 cm. in length on the anterior proximal surface just inferior to the head. There appears to be a large Tension Wedge. Fragments were held in place by the periosteum.

**Fibula:** Non-displaced comminuted fracture at the level of the tibial fracture cavity. Head was comminuted as well.

**Interosseous Membrane:** The membrane was intact along the shafts of each bone. Small tears were noted between the superior extent of the bone fractures.

**Measurements:** The area of impact is 30.5 cm down from the top of the thigh and 29.5 cm up from the heel. The area measures 4 cm long x 9 cm wide.

---

### SUMMARY:

- a) Very small puncture wound to anterior leg.
- b) Minor muscular damage.
- c) No damage to the major neurovascular components.
- d) Comminuted fractures of the proximal Tibia and Fibula.

Negatives: 25956-26 to 36, 25953-1 to 21, 25954-13.

## Test Leg #6

Cadaver #436L. Impacted on the proximal one third of the anterior leg at 13 mph.

**L6-A)** The Pre-dissection View of this leg shows a considerable transverse tear in the skin and fascia.

**L6-B)** The Anterior View of the dissection exhibits a cavitated comminution of the tibia (**T**). No muscle damage was noted.

**L6-C)** In the Anterolateral View of the deep vessels, the cavitation of the tibia (**T**) is evident, as is fracturing of the fibula (**F**). However, the anterior tibial artery (**A**) and the superficial (**SN**) and deep fibular nerves (**DN**) are intact throughout the fracture zone. The interosseous membrane (**i**) is unharmed.

**L6-D)** This Posterior View displays the uninterrupted course of the arterial system near the fracture of the fibula (**F**). The popliteal artery (**PA**) branches into the posterior (**PTA**) and anterior tibial arteries (**ATA**). The posterior gives rise to the fibular artery (**FA**).



L6-A





L6-B



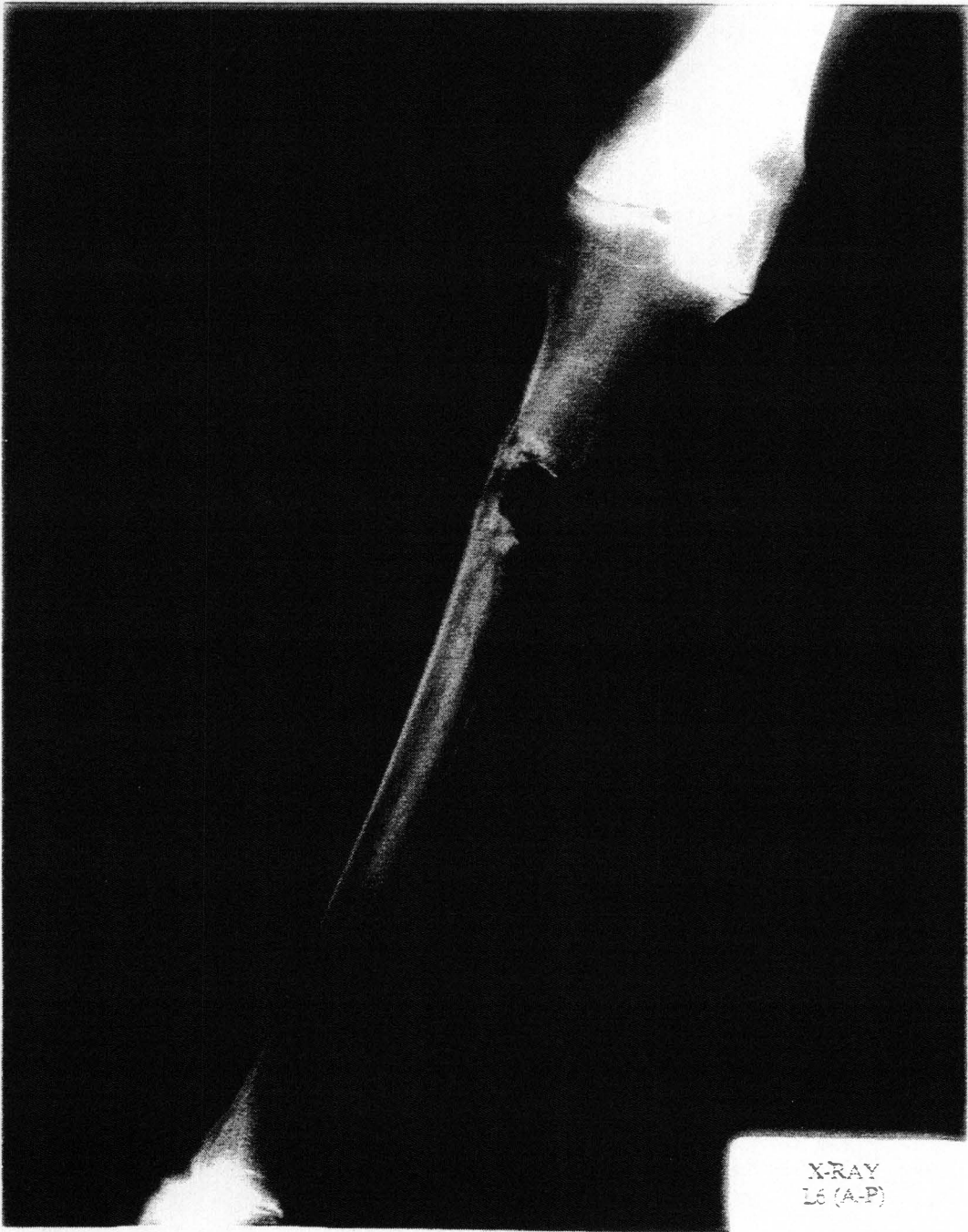


L6-C





L6-D



X-RAY  
L6 (A-P)



X-RAY  
L6 (L-M)

## Test L-7 Dissection Report

Cad # 762R, Impacted at 10 mph

### Soft Tissue Damage

#### Anterior Leg:

**Muscles-** All muscles appeared to be intact.

**Vasculature-** The anterior tibial artery and veins were intact as were the recurrent and muscular branches.

**Nerves-** The Common Fibular nerve and its Superficial and Deep branches were intact throughout the impact zone. Muscular and recurrent branches were also intact.

#### Posterior Leg:

**Muscles-** All muscles appeared to be intact.

**Vasculature-** Superficial vessels were unharmed. The Anterior & Posterior Tibial, and the Fibular arteries and veins were intact. Genicular and muscular branches seen were also intact. Tibial Nutrient vasculature appeared to be intact.

**Nerves-** The Tibial nerve and its muscular branches were intact.

### Osteology

**Tibia:** Simple non-displaced transverse fracture to the anterior proximal shaft of tibia, with a vertically oriented fracture into the head. Fracture was held in place by the periosteum.

**Fibula:** Non-displaced transverse fracture at the level of the tibial fracture.

**Interosseous Membrane:** The membrane was intact along the shafts of each bone.

**Measurements:** The area of impact is roughly 8 cm below the knee. No cavity.

### SUMMARY:

- a) Very small tear in the skin of anterior leg.
- b) No obvious muscular damage.
- c) No damage to the major neurovascular components.
- d) Transverse fractures of the proximal Tibia and Fibula.

Negatives: 25954-11, 12 & 14 to 36.



## Test Leg #7

Cadaver #762R. Impacted on the proximal third of the anterior leg at 10 mph.

**L7-A)** This Pre-dissection View shows virtually no external soft tissue damage to the anterior leg.

**L7-B)** In the Anterior View of the dissection, only a transverse fracture of the tibia (**T**) is seen. Muscles are intact.

**L7-C)** The Anterolateral View of the impact area shows no signs of neurovascular damage. The fractured tibia (**T**) and the non-displaced fracture of the fibula (**F**) did not injure the anterior tibial artery (**A**) or the superficial (**SN**) and deep fibular nerves (**DN**). The interosseous membrane (**i**) is also completely intact.

**L7-D)** The Posterior View of this leg shows that all the vessels are intact regardless of the fractures to the tibia (**T**) and fibula (**F**). The tibial nerve (**N**) is intact throughout the impact zone. The popliteal artery (**PA**) branches into anterior (**ATA**) and posterior tibial arteries (**PTA**). The posterior gives rise to the fibular artery (**FA**). The common fibular nerve (**FN**) winds around the head of the fibula without incident.

**L7-E)** Further cleaning of the Posterior Aspect of this leg shows the fracture patterns of the tibia (**T**) and fibula (**F**). It is particularly interesting to note that the nutrient artery (**NA**) branching from the posterior tibial artery (**PTA**) is intact despite its course directly through the fracture of the tibia. The fibular artery (**FA**) and the anterior tibial artery (**ATA**) are undisturbed by the fracture of the fibula.



L7-A





L7-B





L7-C



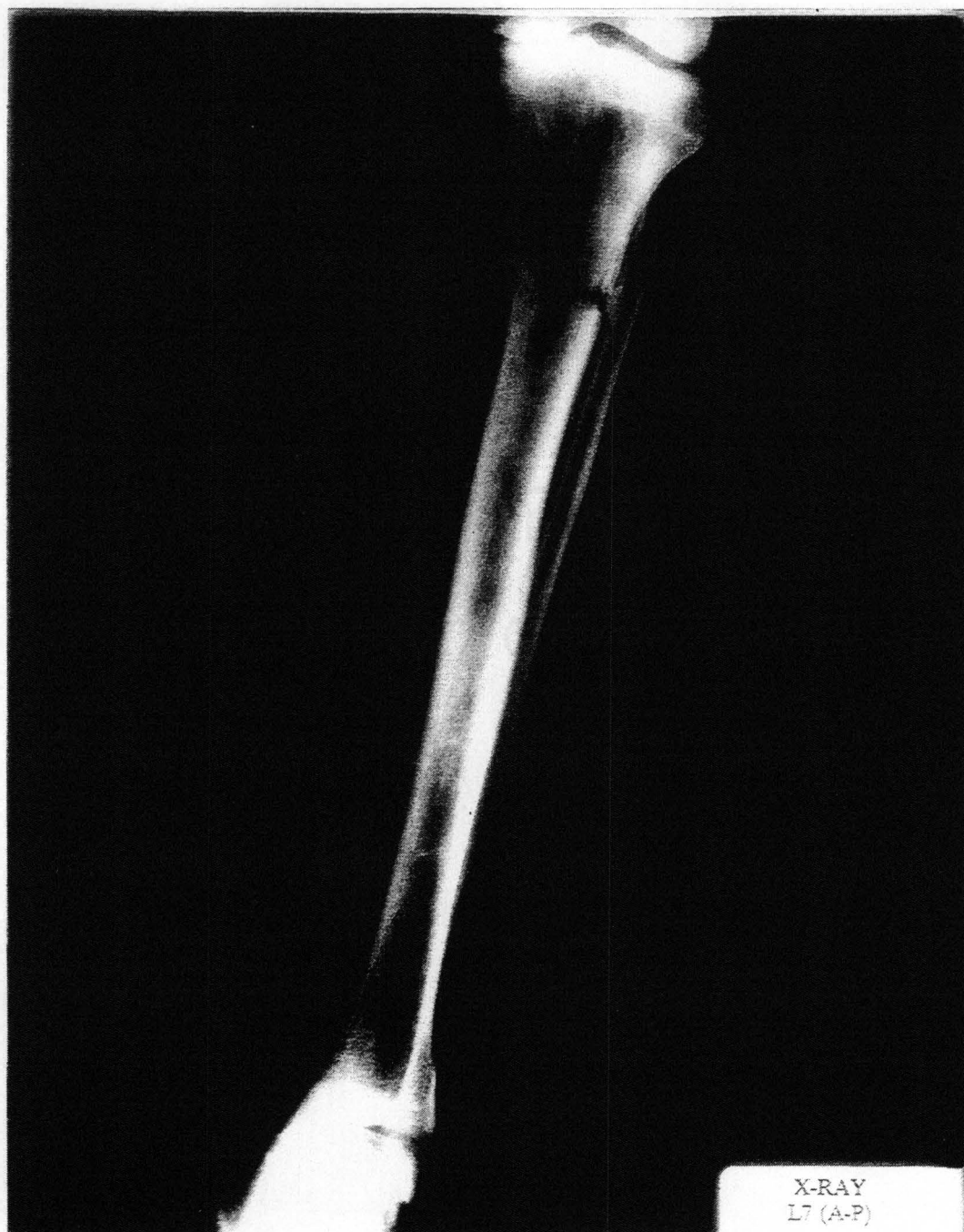


L7-D





L7-E





X-RAY  
L7 (L-M)

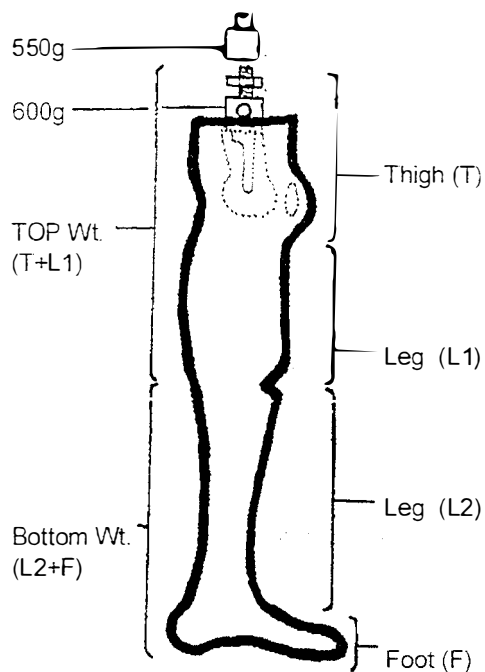
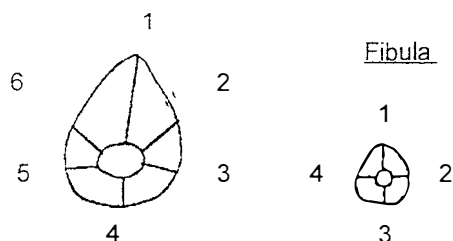


## **Appendix D**

### **Dissection Measurements: Cortical Thicknesses and Weights**

## Dissection Measurements

### Tibia Measuring Points



### CAD # 13R, Test L-1

#### CORTICAL THICKNESSES (cm.)

##### **Tibia:**

1) 1.143      3) 0.410      5) 0.400  
2) 0.330      4) 0.513      6) 0.532

##### **Fibula:**

1) 0.473      3) 0.470  
2) 0.322      4) 0.090

#### WEIGHTS (kg.)

Total= 4.4      Top= 3.2      (T= 3.0, L1= 0.2)  
Bottom= 1.2      (L2= 0.6, F= 0.6)

### CAD # 602R, TEST L-2

#### CORTICAL THICKNESSES (cm.)

##### **Tibia:**

1) 1.510      3) 0.545      5) 0.457  
2) 0.475      4) 0.605      6) 0.482

##### **Fibula:**

1) 0.640      3) 0.347  
2) 0.550      4) 0.130

**WEIGHTS (kg.)** Total= 3.5      Top= 2.3      (T= 2.0, L1= 0.3)  
Bottom= 1.2      (L2= 0.6, F= 0.6)

**CAD # 629L, TEST L-3****CORTICAL THICKNESSES (cm.)****Tibia:**

1) 1.090      3) 0.640      5) 0.550  
 2) 0.455      4) 0.568      6) 0.608

**Fibula:**

1) 0.507      3) 0.410  
 2) 0.303      4) 0.292

**WEIGHTS (kg.)**

Total= 4.3      Top= 3.1      (T= 2.7, L1= 0.4)  
 Bottom= 1.2 (L2= 0.5, F= 0.7)

**CAD # 646R, TEST L-4****CORTICAL THICKNESSES (cm.)****Tibia:**

1) 1.220      3) 0.375      5) 0.403  
 2) 0.815      4) 0.642      6) 0.440

**Fibula:**

1) 0.335      3) 0.303  
 2) 0.200      4) 0.135

**WEIGHTS (kg.)**

Total= 3.7      Top= 2.3      (T= 2.0, L1= 0.3)  
 Bottom= 1.4 (L2= 0.75, F= 0.65)

**CAD # 662R, TEST L-5****CORTICAL THICKNESSES (cm.)****Tibia:**

1) 1.432      3) 0.678      5) 0.565  
 2) 0.460      4) 0.815      6) 0.525

**Fibula:**

1) 0.420      3) 0.435  
 2) 0.415      4) 0.180

**WEIGHTS (kg.)**

Total= 5.40      Top= 3.5      (T=3.1, L1= 0.4)  
 Bottom= 1.9 (L2= 1.0, F= 0.9)

**CAD # 436L, TEST L-6****CORTICAL THICKNESSES (cm.)****Tibia:**

1) 1.060      3) 0.450      5) 0.405  
 2) 0.475      4) 0.655      6) 0.525

**Fibula:**

1) 0.320      3) 0.255  
 2) 0.295      4) 0.137

**WEIGHTS (kg.)**

Total= 3.35      Top= 2.3      (T= 2.0, L1= 0.3)  
 Bottom= 1.05 (L2= 0.8, F= 0.25)

**CAD # 762R, TEST L-7****CORTICAL THICKNESSES (cm.)****Tibia:**

1) 1.423      3) 0.778      5) 0.523  
 2) 0.350      4) 0.670      6) 0.388

**Fibula:**

1) 0.483      3) 0.328  
 2) 0.295      4) 0.225

**WEIGHTS (kg.)**

Total= 4.85      Top= 2.95      (T= 2.6, L1= .35)  
 Bottom= 1.9 (L2= 1.0, F= 0.9)

**CAD # 662L, TEST L-8****CORTICAL THICKNESSES (cm.)****Tibia:**

1) 1.406      3) 0.681      5) 0.601  
 2) 0.506      4) 0.822      6) 0.520

**Fibula:**

1) 0.431      3) 0.429  
 2) 0.410      4) 0.187

**WEIGHTS (kg.)**

Total= 5.40      Top= 3.80      (T=3.0, L1= 0.8)  
 Bottom= 1.6 (L2= 0.7, F= 0.9)



## **Appendix E**

### **Characteristics of Tested Tibias**

Since the soft tissue was a crude representation of the soft tissue of a "fresher" leg, speculation may arise with respect to the bone's condition. The bones appeared to be normal and comparable to those of a fresher population. Long-term storage and fixation effects did not affect the bones adversely as they did the soft tissue. In support of this claim, a direct comparison was made between the average cortex thickness of the tibias in this study to that of a "fresher" population of tibias from a previous study (Japan Automobile Manufacturers Association project data from 1989 Annual Report). See **Table 2** for this comparison.

**TABLE 2**  
**Comparison of Bone Characteristics**

	Average Cortex Thickness (mm) (See Appendix C)	Breaking Strength (N)
Tibias in L1 - L8 legs (in-water tests)	6.64	2,667*
Tibias from "fresher" leg population (in-air test)	5.75	2,401

\*This is not an average value. It is the breaking strength of the tibia from leg L8 only.

The 6.64 mm average cortex thickness of the tibias from this study is a reasonable average compared to the "fresher" population of tibias. It actually is an indicator of stronger bones since 6.64 mm is greater than the 5.75 mm. The special test (introduced in the Methodology section of this report) provides valuable data to establish normality of this population of bones also, even though the soft tissue is so different. Leg L8's average tibial cortex thickness was 7.56 mm. The peak force value measured during impact of test L8 was approximately 5,000 N and the peak force measured from test L8M was approximately 2,333 N. Therefore, the approximate breaking

strength,  $F_{water}$ , of the tibia is equal to:

$$F_{water} = 5,000 \text{ N} - 2,333 \text{ N} = 2,667 \text{ N}.$$

Note that the breaking strength values in **Table 2** are comparable. The breaking strength in water,  $F_{water}$ , was only 266 N greater than that in air,  $F_{air}$ . The cortex thickness of L8, which is greater than that of the "fresher" leg average value, could account for the slight difference.

**Appendix F**  
**Cadaver Information**

## Test Leg / Cadaver Information

<u>Test#</u>	<u>U of L #</u>	<u>MMC/OMC</u>		<u>AGE</u>	<u>SEX</u>	<u>Cause of Death</u>	<u>Date of Death</u>
		<u>Photo #</u>					
L-1	13-R	10-90		*	*	*	*
L-2	602-R	06-90		72	—	Metastatic Cancer	9/17/86
L-3	629-L	05-90		68	—	CA Prostate, ♥-resp arrest	12/31/86
L-4	646-R	04-90		72	—	Pneumonia	3/11/87
L-5	662-R	05-90		84	—	Atherosclerotic ♥ disease	5/17/87
L-6	436-L	08-90		76	—	♥-respiratory arrest	9/04/84
L-7	762-R	01-90		67	—	Congestive ♥ failure	1/05/89
L-8	662-L	03-90		84	—	Atherosclerotic ♥ disease	5/17/87

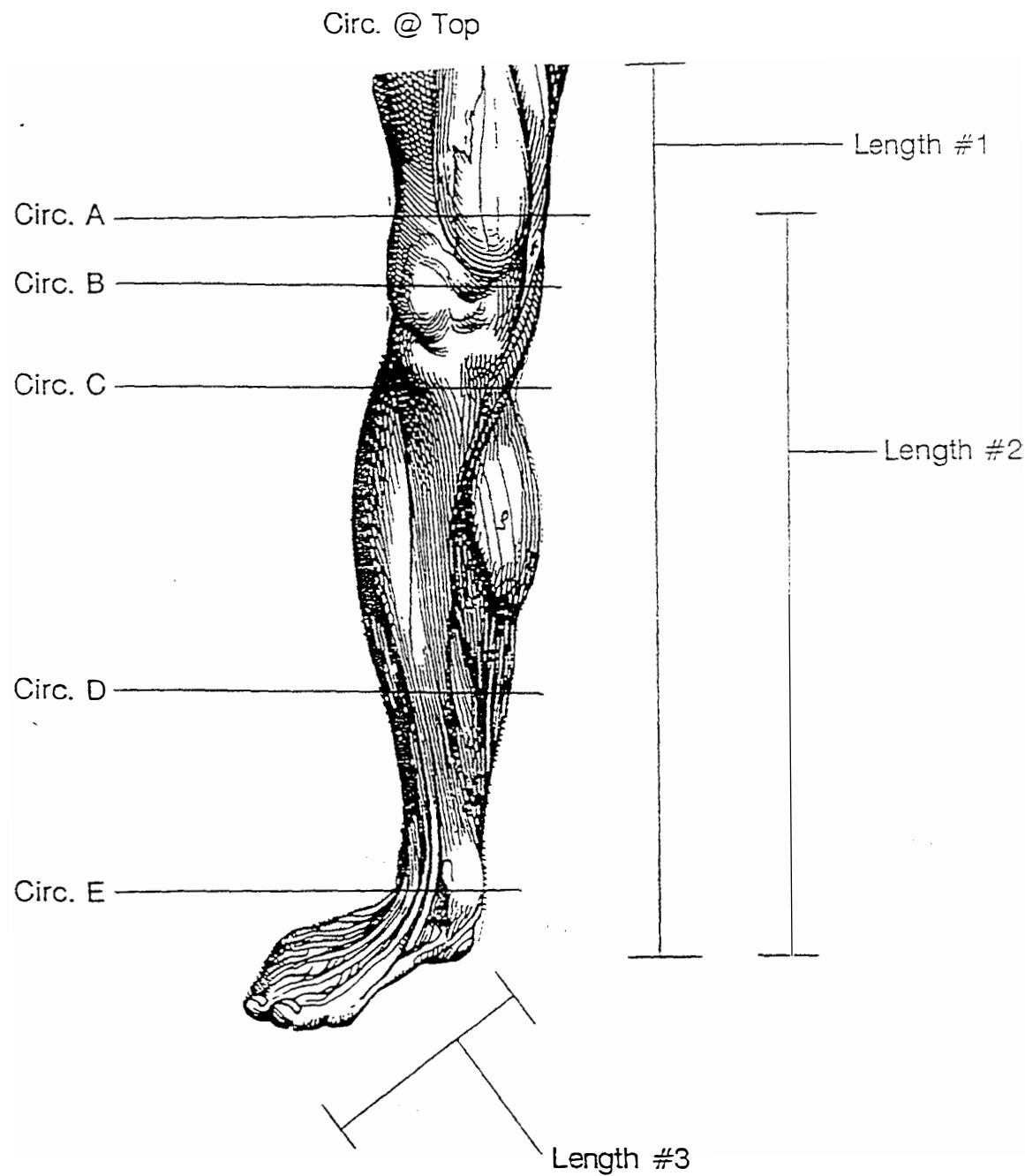
\* Cadaver Information not available for the given cadaver #.

## Measurements

<u>Test</u> <u># &amp; Vel.</u>	<u>Weight</u> <u>(kg.)</u>	<u>Lengths (")</u>			<u>Circumferences (")</u>					
		<u>#1</u>	<u>#2</u>	<u>#3</u>	<u>@ Top</u>	<u>A</u>	<u>B</u>	<u>C</u>	<u>D</u>	<u>E</u>
L-1, 20 mph	5	27½	19½	8½	16¾	11¼	11¼	10	8½	6½
L-2, 20	4	27½	20	9½	11¾	10	12½	10¾	8½	6¾
L-3, 16.4	5½	29	20½	10	14¾	11½	13	11¼	9½	7
L-4, 16.4	5	25	20	9	14½	14	14	12½	9	8
L-5, 13	6¾	31	22	10¼	13¾	12¾	14½	12	10¼	8
L-6, 13	4½	24¾	20½	8¾	12¾	12¾	12¼	11	9	7
L-7, 10	5¾	27¼	20½	9	14¼	11½	12¼	11½	9	6¾
L-8,	6¾	30	21	10¼	14¼	13	14½	12¼	9¾	8½

Lengths and Circumferences Noted on Diagram, Next Page.

Measurements Diagram



## **Appendix G**

### **Addendum to Biomechanical Effectiveness of a Safety Device: A Boat Motor Cage-type Propeller Guard**

## CONTENTS

ABSTRACT . . . . .	1
INTRODUCTION . . . . .	2
METHODOLOGY . . . . .	3
RESULTS . . . . .	6
DISCUSSION . . . . .	7
COMMENTARY . . . . .	8
APPENDIX A: Post-test Dissection and X-ray Data	
APPENDIX B: Dissection Measurements: Cortical Thicknesses and Weights	
APPENDIX C: Cadaver Information	



### **ABSTRACT**

This addendum discusses the results of the in-air tests that were mentioned in the second paragraph of the results section (page 9) of the main report.

The in-air results support the conjecture in the main report that the reason for lack of effect (vascular and neurological damage) was due to the altered condition of the soft tissue as a result of long-term storage and fixation.

Other commentary is intended to help clarify the meaning of the phrase, "loss of leg function," which is used throughout the main report. More detailed remarks with regard to injury are also included.

## INTRODUCTION

The principal reason for this addendum is to discuss the results of the in-air tests that were mentioned in the second paragraph of the results section (page 9) of the main report, Evaluation of a Boat Motor Cage-Type Propeller Guard as a Protection Device for the Human Leg (Tyler A. Kress, John N. Snider, et al., August 1991). Also, other pertinent commentary is included with the intention to further clarify or supplement the main report.

The expected vascular and neurological damage was not observed during post-test dissection of the legs from the tests discussed in the main report. It was noted that this lack of effect was due to the "leather-like" condition of the soft tissue as a result of long-term storage and fixation. The cadaver legs available for this study were all embalmed at various times ranging from about three to six years before testing with one exception (see asterick\* at bottom of this page); the tissue had changed to the point that soft tissue damage could only be inferred from the extent of bone damage. The two tests conducted in-air at the University of Tennessee laboratory used legs from the same population with similarly deteriorated states. The impact conditions for the two tests were known to produce extensive vascular and neurological damage to "fresher" legs. The intent of the in-air tests were to confirm the above conjecture that expected vascular and neurological damage should not have been observed during post-test dissection because of the deteriorated state of the legs.

\*Appendix C contains the cadaver information for each specimen. All cadavers were embalmed within a couple of days after death; note that tests discussed in the main report were conducted in December, 1990 and the two in-air tests were conducted in March, 1991 (test #L9) and March, 1992 (test #L10). So, specifically, the information with regard to embalment before testing is as follows: three legs - three years; two legs - four years; two legs - six years; two legs - eleven years; and one leg - one year.

## METHODOLOGY

A total of two embalmed human cadaver legs were used for the in-air comparison study. The legs were sectioned from the cadavers at mid-thigh region and were supported with a pin passing through the distal condyles of the femur. The lower leg was supported only by the inertial constraint of the foot. Pre-test photographs of the legs are shown in Appendix A of this addendum. **Table 1** presents the conditions for both tests.

For both tests conducted at the University of Tennessee laboratory, the following were the fixed conditions:

- 1) impactor: pipe,
- 2) object impacted: embalmed human cadaver legs similar to test population used in eight tests discussed in main report,
- 3) position of leg: vertical and in-air,
- 4) impact location: proximal one-third of tibia, and
- 5) impact direction: anterior-to-posterior.

**TABLE 1**  
**Test Conditions and Resultant Fractures**

TEST #	IMPACTOR	VELOCITY (MPH)	TRANSDUCER	FRACTURE DESCRIPTION
L9 <sup>1</sup>	PIPE	17.0	Yes	Comminution <sup>2</sup>
L10	PIPE	17.0	Yes	Comminution

<sup>1</sup>L9: Both of these tests, L9 and L10, were conducted in-air at the University of Tennessee laboratory.

<sup>2</sup>Comminution: Comminution fractures of the proximal tibia and fibula; for more detailed description of osteology see Appendix A.

The tests were videotaped and photographs were made of the legs after impact. Extensive dissection work was performed to evaluate the nature and extent of injury.

Each leg was characterized by utilizing the still photographs and by making various anthropometric measurements. Post-impact evaluation included dissection with particular attention directed toward bone fracture and fragmentation.

## RESULTS

The results for the two tests are summarized in **Table 1** (page 4) and more detailed results are presented in Appendices A and B.

The tibia and fibula fractures from the in-air tests were similar in severity to those from the water tests. As expected, there was no significant soft tissue damage observed during dissection of the in-air test legs.

Note that Appendix C outlines the cadaver information for the legs used in this study (with the inclusion of information for the in-air legs, L9 and L10). The average age at time of death for the two cadavers was approximately 70 years.

## DISCUSSION

The air-test results conclusively support the conjecture in the main report that the reason for lack of effect (vascular and neurological damage) was due to the altered condition of the soft tissue as a result of long-term storage and fixation.

Additional separate effects tests were conducted to provide further evidence that the embalming fluid (fixation) has an effect on the strength of soft tissue (specifically musculature structure). The modulus of elasticity was experimentally determined for both an embalmed muscle and a "fresh" muscle. The measured modulus of elasticity for the embalmed muscle was approximately ten times greater than the modulus of the "fresh" muscle. This provides additional support that the mechanical behavior of the soft tissue is dramatically altered via the fixation process. Specifically, the soft tissue becomes more stiff.

### COMMENTARY

The phrase, "loss of leg function," is used throughout the main report. The following remarks are intended to clarify the meaning of this phrase.

At impact velocities of 13.6 mph and above, the resultant leg injuries involved osteological damage that was so severe that loss of leg function would be expected. Loss of leg function means that the injured individual would experience permanent disabling damage to the leg (injury could be variable, ranging from a chronic limp to amputation).

The observed fractures have a high probability of resulting in a great many complications, some directly related to the fracture itself, and others attributable to subsequent effects. These effects (as discussed in Jeffrey Pike's book, Automotive Safety, published in 1990 by the Society of Automotive Engineers, Inc.) may include: infection; bone shortening; avascular necrosis; tears and lacerations to nearby vasculature (arteries, veins, and/or capillaries); injury to nerves and connective tissue and post-traumatic arthritis of joints; joint disruption; microembolism (also referred to as fat embolism); myositis and myositis ossificans; immobilization which could cause complications such as pressure sores and even pneumonia; compartment syndromes which can result in ischemia, hypoxia and anoxia which in turn can produce muscle necrosis and irreversible nerve damage.

Therefore, it should be apparent that the observed fractures are quite serious. There is a likelihood that the bone may not heal properly, or simply may not heal at all. Difficulty in



healing may even occur after surgical intervention. Also, these fractures can lead to a wide variety of soft tissue injuries, some of which are even fatal (e.g. fat embolism).

Resultant injuries (encompassed within the definition of loss of leg function) could be described using The Abbreviated Injury Scale (1990 Revision) published by the Association for the Advancement of Automotive Medicine. The severity of injuries could be coded as AIS 3 or AIS 4 indicating a level that is serious or severe (which includes amputation).

The Association for the Advancement of Automotive Medicine intend to publish an impairment scale later this year to be used in addition to The Abbreviated Injury Scale. The anticipated descriptive terms that will be used for the impairment scale are mobility, cognitive, cosmetic, sensory, sexual/reproductive, and pain. Direct or subsequent injuries related to the observed fractures from the six tests discussed in the main report would be expected to cause permanent mobility, cosmetic, sensory, and/or pain impairment. A microembolism that may result from these fractures could also cause permanent cognitive impairment and even death.

It may be of interest to discuss the relationship of injury to that of the geometry (or size) of the leading edge of the impactor (i.e. the edge of the cage vs. the edge of the strut, skeg or propeller). For simplicity, the cage impacting surface will be referred to as "blunt" and the strut, skeg and propeller edges as "fine." The blunt leading edge has a larger impacting surface area than the fine leading edge. Injuries produced from a fine leading edge are usually associated with more localized damage, however as speed increases to around 13 mph and above (such as

those of the six tests referred to in the main report) localized damage can be just as severe from a blunt impact and often worse (e.g., could be more difficult to surgically repair). In addition to causing severe localized damage, the blunt impactor can cause increased hip injury, flailing, and whole-body damage as opposed to the fine impactor.

Further discussion about injury mechanisms relevant to the impact conditions of the tests may be useful for comparison of expected real-life injuries resulting from collisions with outboard motors equipped and not equipped with a cage-type propeller guard. At speeds of about 13 mph and above it would be expected that both "impactors" (with and without cage-type guard) would cause damage so severe that loss of leg function would result which may require amputation (if traumatic amputation does not occur upon impact). Note, if traumatic amputation does not occur, then the motion of the two impacting objects (boat and human) will be in the direction of the boat's travel and initially will be at about the boat's velocity because of their relative masses. The inertial restraint imposed by the mass of the foot and the lower leg allows for a "wrapping" action of the leg around the impactor causing tremendous energy transfer to the rest of the body. Severe hip damage and other injuries should result from this dynamic action. It is expected that for impact conditions as in these tests, the caged motor would increase that "wrapping around" or grasping effect. So, in short, at speeds of about 13 mph and above, expected resultant real-life impact injuries from the caged guard impact are likely to lead to impairment equivalent to that of amputation to the leg; or, other serious whole-body injuries because the energy transfer from impact has to "go" somewhere. In other words, if the energy transfer is not completely transmitted locally as in amputation then it is sent elsewhere to do other damage probably

generating an increase in overall bodily injury of a more serious nature.

To put the results of these tests into perspective, the following example is offered. Consider a hypothetical case of impact onto the leg of a healthy young person at a velocity of about 13 mph or greater. The issue is whether or not a cage-type propeller guard is better or worse in this situation. According to the results in this study, one would expect more severe damage to both the hip joint and possibly to other areas of the leg with the cage present than without it. The injuries resulting from collisions with an outboard motor not equipped with a cage-type propeller guard have not been evaluated in this study, but it is believed that the resultant injuries would be of a different nature and less severe (i.e. local traumatic amputation is perhaps more likely with a strut or skeg which causes less hip damage and/or total bodily injury than the "gripping" action of the cage).

## **APPENDIX A**

### **Post-test and X-ray Dissection Data**

## Test L-9 Dissection Report

Cad # 59R (also listed as 57R), Impacted at the University of Tennessee Impacting Facility. Impacted in air with pipe, on anterior-posterior proximal one third of lower leg. Specimen had a metallic fixative plate on the tibia.

### Soft Tissue Damage

#### Anterior Leg:

**Muscles-** All muscles appeared to be intact except for tears in part of the tibialis anterior.

**Vasculature-** The anterior tibial artery and veins were intact as were the recurrent and muscular branches.

**Nerves-** The Common Fibular nerve and its Superficial and Deep branches were intact throughout the impact zone. Muscular and recurrent branches were also intact.

#### Posterior Leg:

**Muscles-** All muscles appeared to be intact.

**Vasculature-** Superficial vessels were unharmed. The Anterior & Posterior Tibial, and the Fibular arteries and veins were intact. Genicular and muscular branches seen were also intact.

**Nerves-** The Tibial nerve and its muscular branches were intact.

### Osteology

**Tibia:** Non-displaced comminuted fracture to the anterior proximal shaft of tibia.

**Fibula:** Non-displaced comminuted fracture at the level of the tibial fracture.

**Interosseous Membrane:** Appeared to be intact along the shafts of each bone.

**Impact Area:** The area of impact shows approximately 6 cm. of torn skin.

### SUMMARY:

- a) Approximate 6 cm. defect in the skin of anterior leg.
- b) No muscular damage to the musculature.
- c) No damage to the major neurovascular components.
- d) Non displaced comminuted fractures of the proximal Tibia and Fibula at the inferior border of the fixative plate.

### NEGATIVES:

30067-35,36, 56149-1 to 16

## Test Leg #9

Cadaver # 59-R (Incorrectly labelled 57-R in Photos).  
Impacted in air at the University of Tennessee.

L9-A) Pre-Test View of this leg at the Impact Lab.

L9-B) Actual Test of leg 59-R. Impacted at the proximal one third of the anterior lower leg without any restraint on the foot.

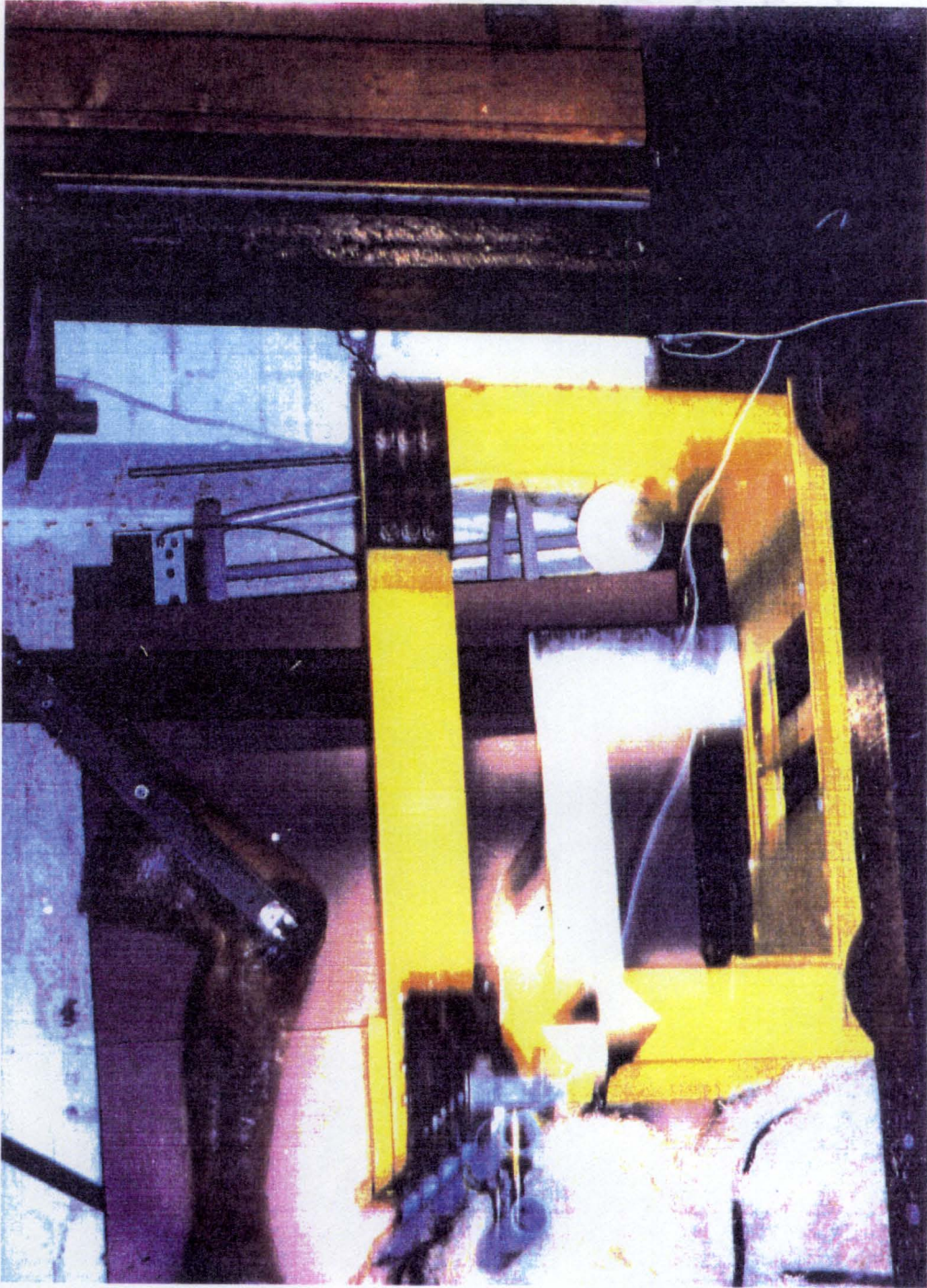
L9-C) Anterolateral View of the dissected leg. There is a tibial plate (**P**) just superior to the impact site. The Anterior tibial artery (**A**), as well as the Deep (**DN**) and Superficial (**SN**) branches of the common fibular nerve are intact throughout the impact zone. Fracturing of the Fibula (**F**) and the Tibia (**T**) is evident.

L9-D) Posterior View shows the Popliteal artery (**PA**) gives rise to the anterior tibial artery and posterior tibial artery (**PTA**) without interruption. The Fibular (**FA**) vessels are also intact. The tibial nerve (**TN**) has also escaped obvious injury.



L9-A





B-67



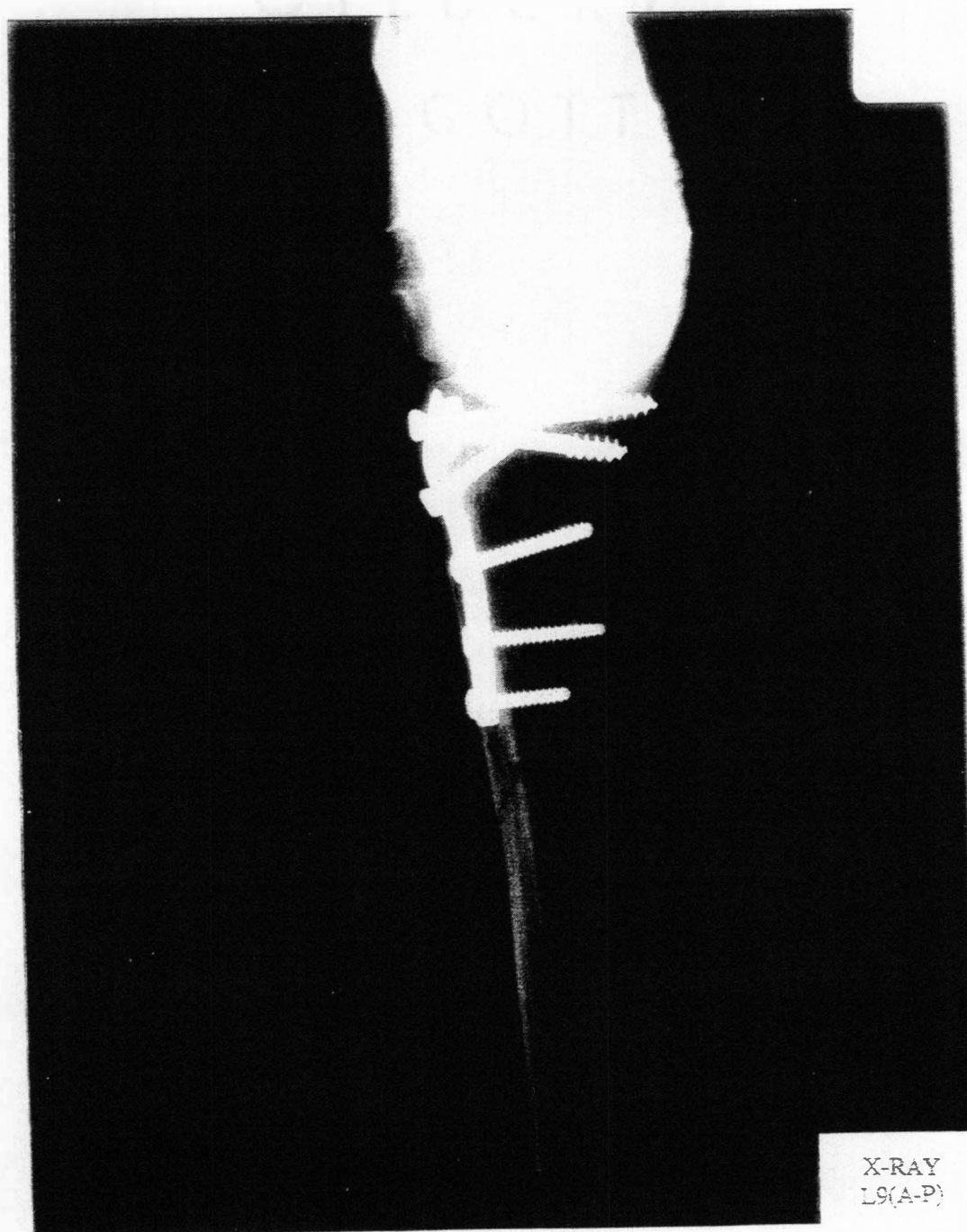


L9-C



Q-67





X-RAY  
L9(A-P)



X-RAY  
L9(L-M)

## Test L-10 Dissection Report

Cad # 582-R, Impacted at the University of Tennessee Impacting Facility.  
Impacted in air with pipe, on anterior-posterior, proximal one third of lower leg.

### Soft Tissue Damage

#### Anterior Leg:

**Muscles-** All muscles appeared to be intact except for longitudinal tears in the tibialis anterior.

**Vasculature-** The anterior tibial artery and veins were intact as were the recurrent and muscular branches.

**Nerves-** The Common Fibular nerve and its Superficial and Deep branches were intact throughout the impact zone. Muscular and recurrent branches seen were also intact.

#### Posterior Leg:

**Muscles-** All muscles appeared to be intact except the Flexor Digitorum Longus showed some longitudinal tears.

**Vasculature-** Superficial vessels were unharmed. The Anterior & Posterior Tibial, and the Fibular arteries and veins were intact through the impact zone. Genicular and muscular branches seen were also intact.

**Nerves-** The Tibial nerve and its muscular branches were intact.

### Osteology

**Tibia:** Non-displaced badly comminuted fracture to the proximal shaft of tibia.

**Fibula:** Non-displaced comminuted fracture at the level of the tibial fracture.

**Interosseous Membrane:** Appeared to be intact along the shafts of each bone.

**Impact Area:** There is a 10 cm. vertical laceration to the proximal anterior skin.

---

### SUMMARY:

- a) Approximate 10 cm. defect in the skin of anterior leg.
- b) Very little damage to the musculature.
- c) No damage to the major neurovascular components.
- d) Approximate 17 cm. of Non displaced comminuted fractures of the proximal Tibia and Fibula.

### NEGATIVES:

30502-2 to 11, 49075-4 to 6, 92625, 92644

# Test Leg #10

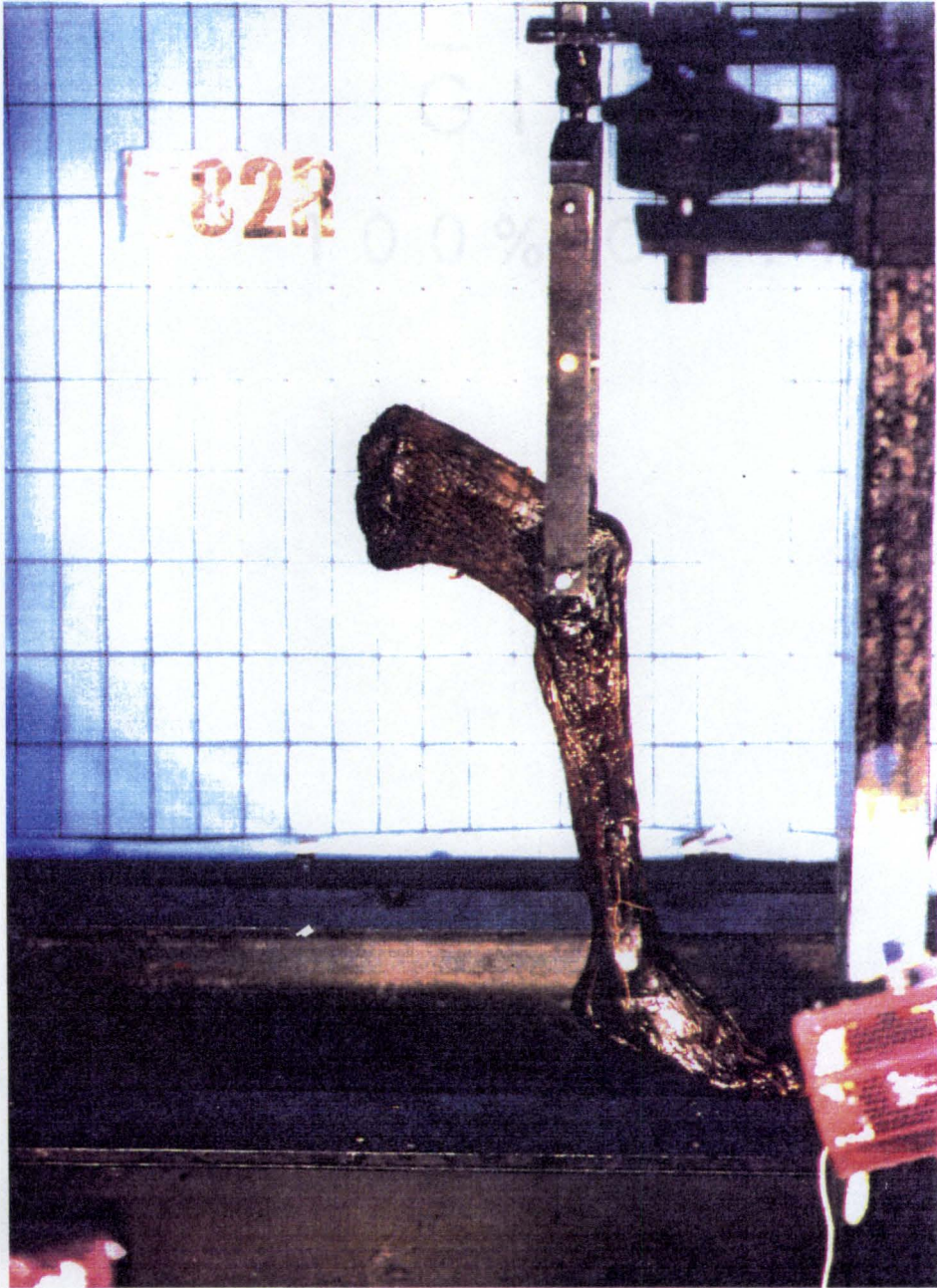
Cadaver #582-R.  
Impacted in air at the University of Tennessee.

L10-A) Pre-Test View of this leg at the Impact Lab.

L10-B) Actual Test of leg 582-R. Impacted at the proximal one third of the anterior lower leg without any restraint on the foot.

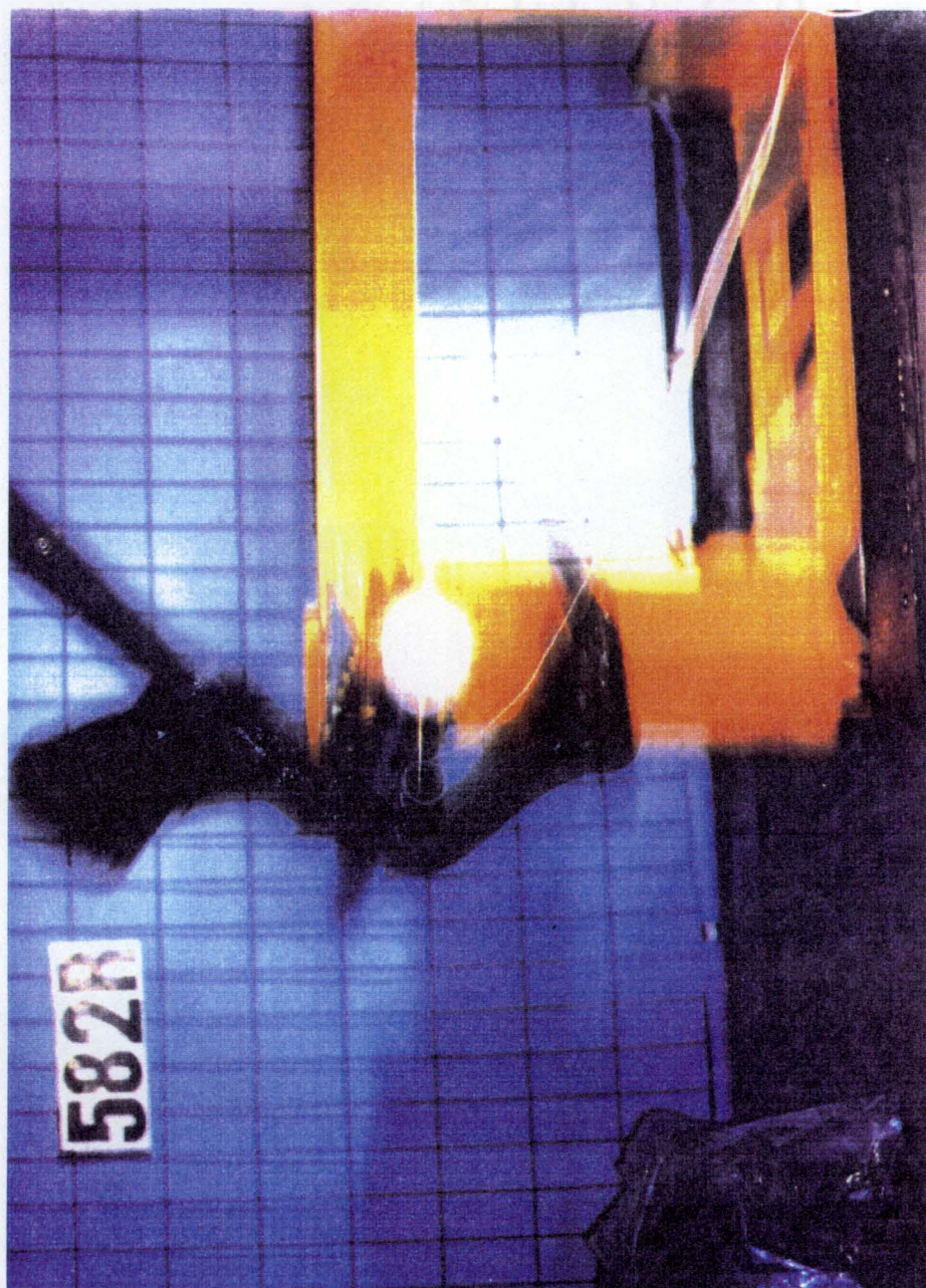
L10-C) Anterolateral View of the dissected leg. Badly comminuted fractures of the tibia (**T**) and fibula (**F**) are seen. However, the anterior tibial vessels (**ATA**) and the branches of the common fibular nerve (**FN**) are intact throughout the fracture zone.

L10-D) Posterior View shows the tibial nerve (**TN**), the posterior tibial vessels (**PTA**) and the common fibular nerve (**FN**) all escaped injury despite jagged bone fragments from the fibula (**F**) and tibia (**T**).



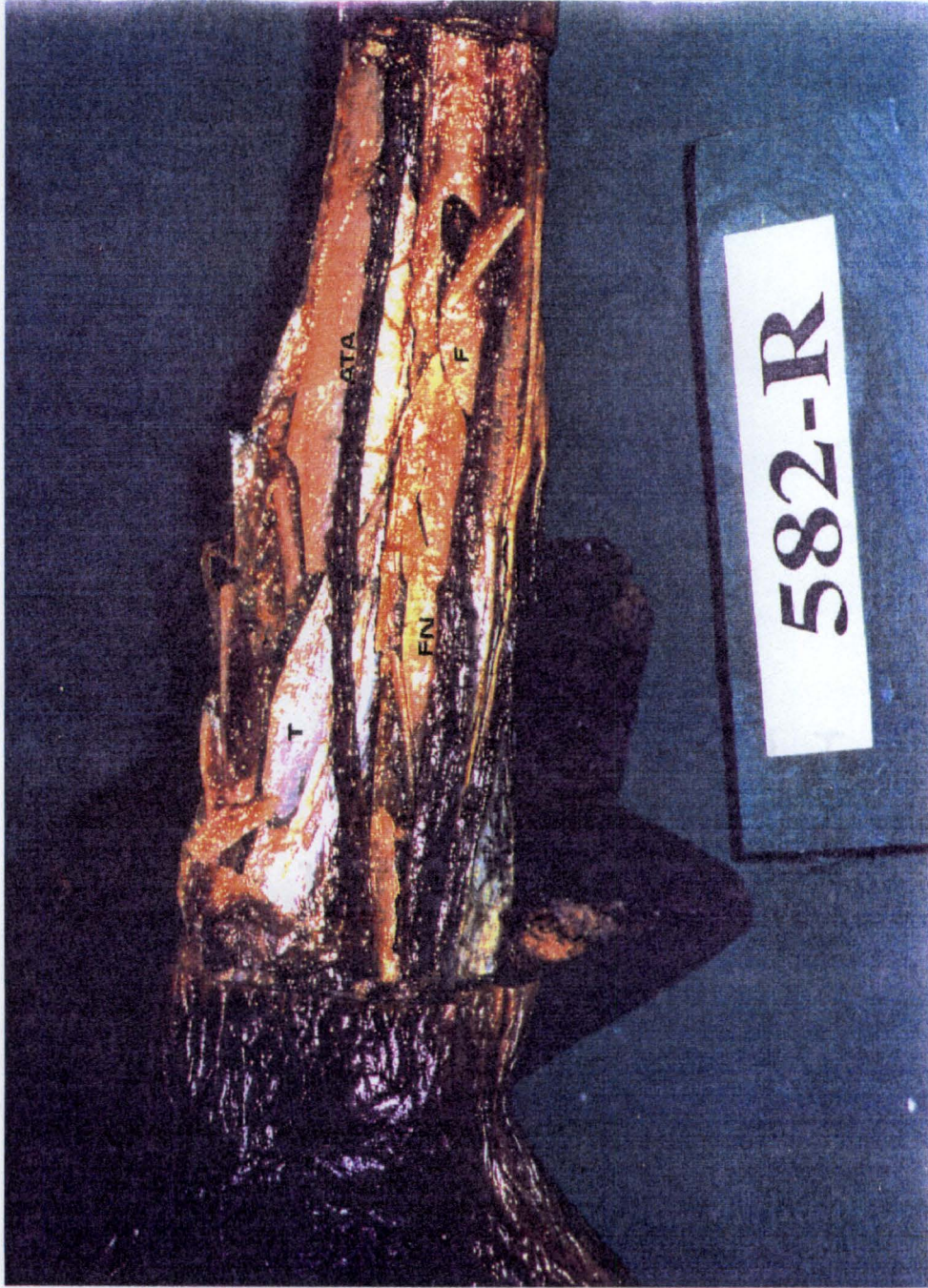
L10-A





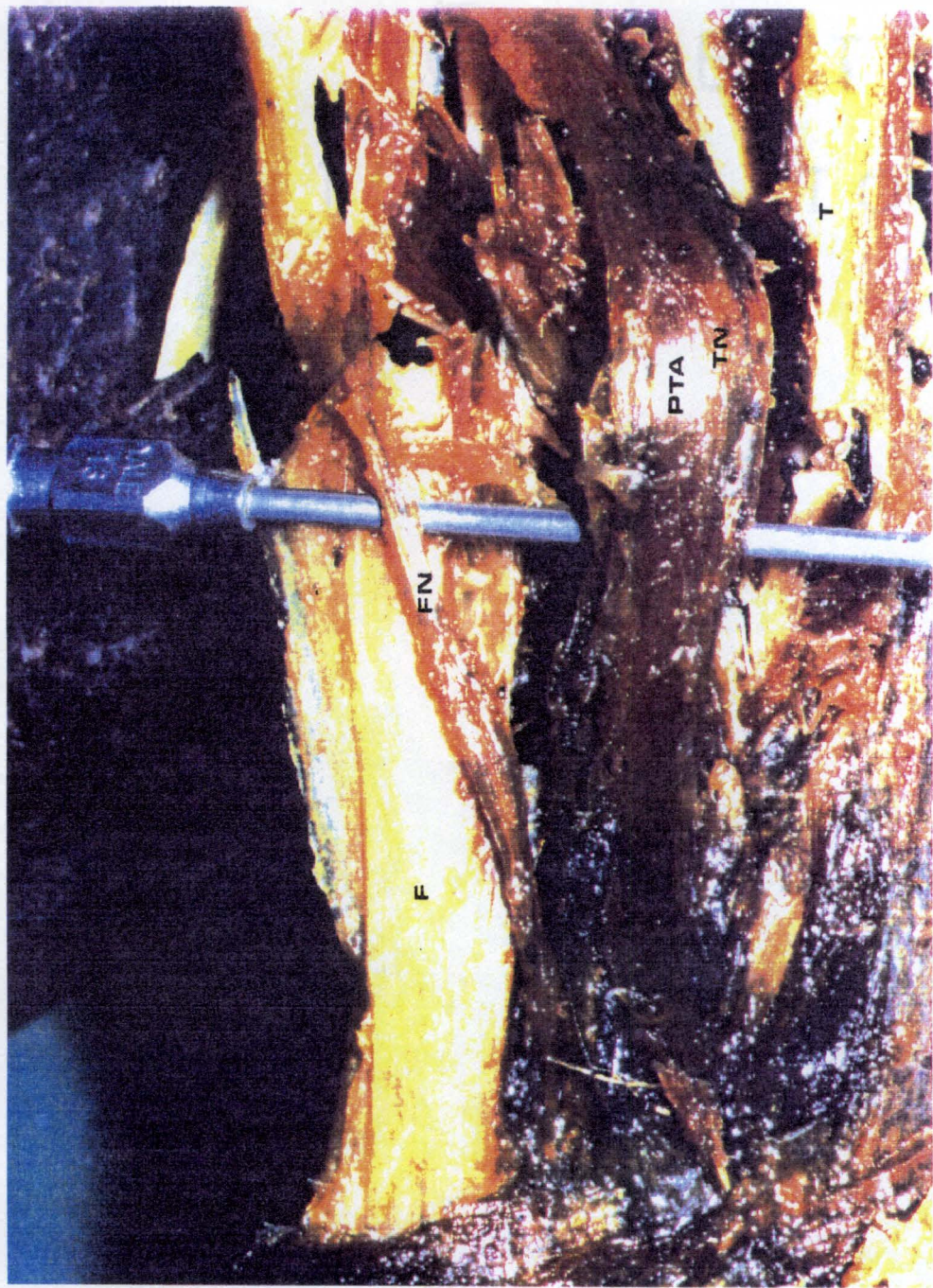
L10-B



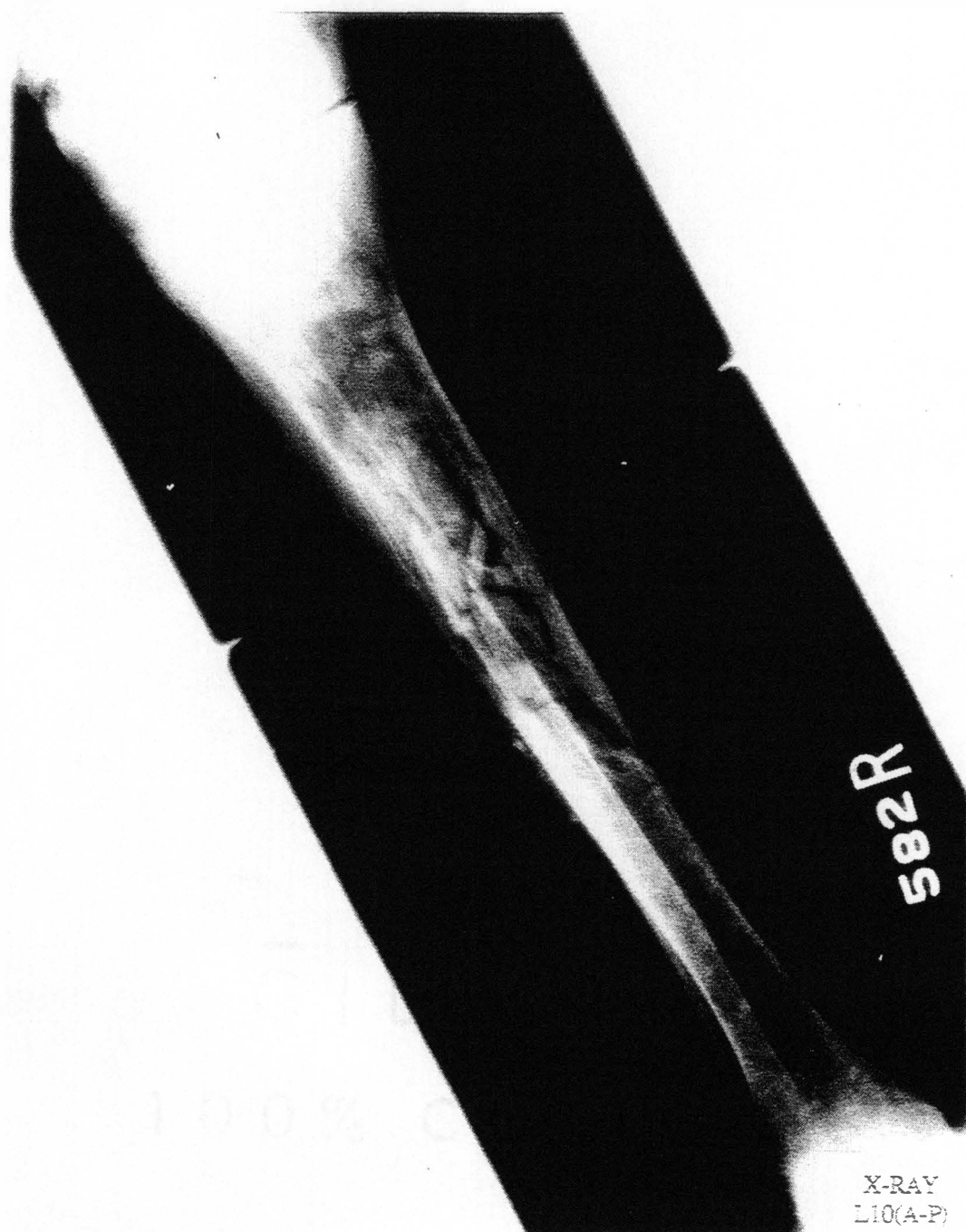


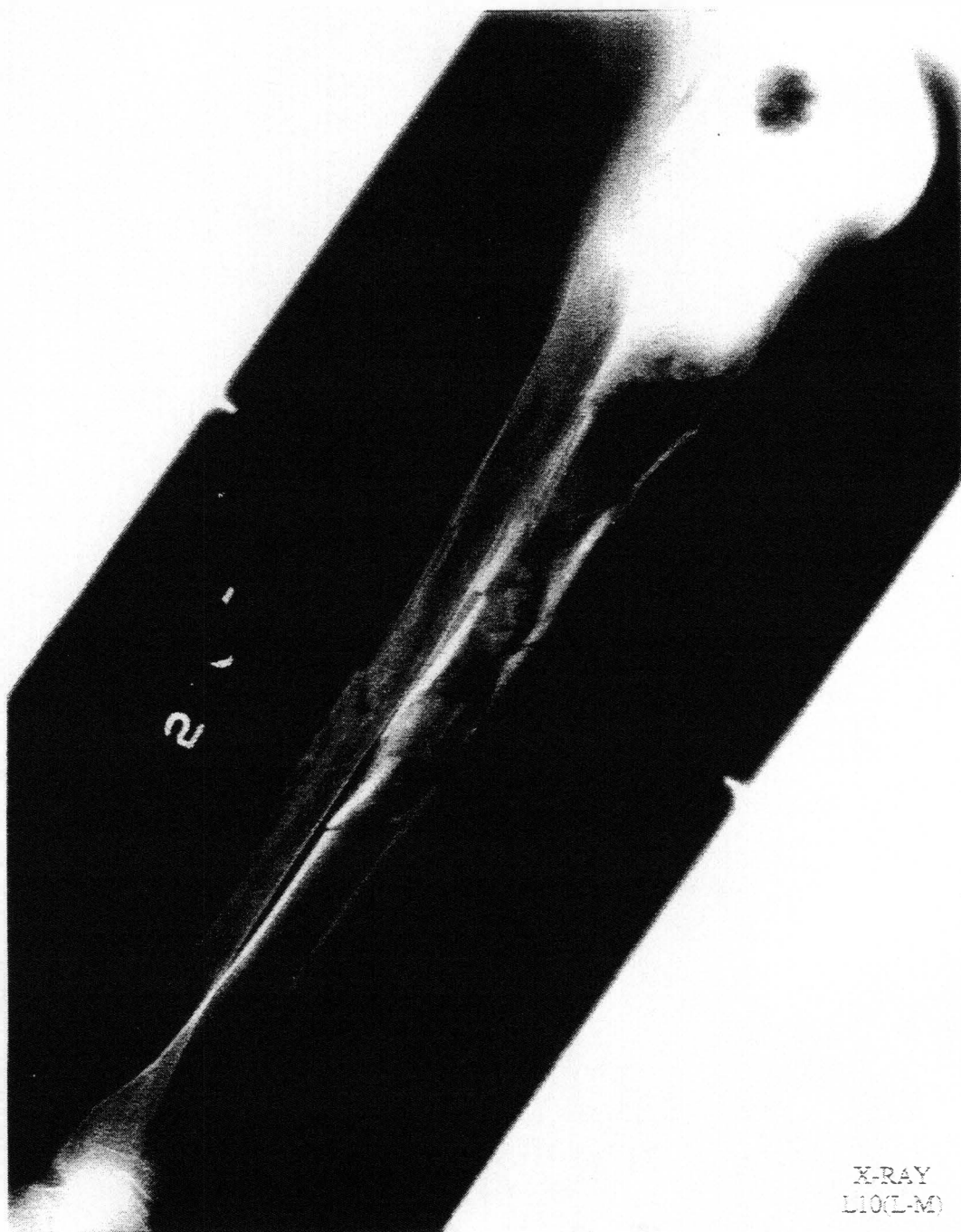
L10-C





L10-D





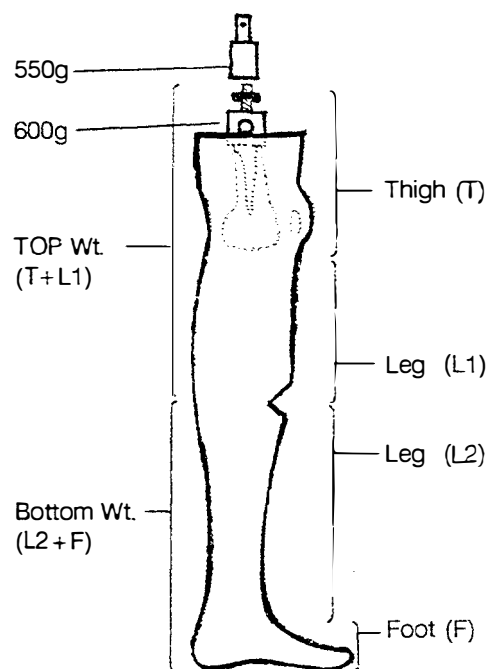
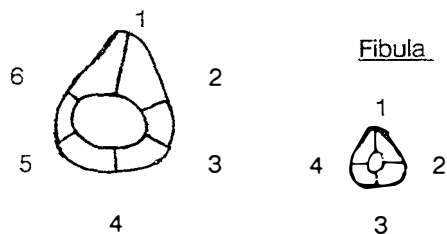
X-RAY  
L10(L-M)

## **APPENDIX B**

Dissection Measurements: Cortical Thicknesses and Weights

## Dissection Measurements

### Tibia Measuring Points



### CAD # 59-R, TEST L-9

#### CORTICAL THICKNESSES (cm.)

##### **Tibia:**

1) 0.839      3) 0.481      5) 0.477  
2) 0.305      4) 0.248      6) 0.305

##### **Fibula:**

1) 0.490      3) 0.346  
2) 0.368      4) 0.344

#### WEIGHTS (kg.)

Total = No weights taken since there was a metallic plate on the Tibia. Estimate weight to have been 5 Kg. In air testing so there was no artificial hip cemented into the femur.

### CAD # 582-R, TEST L-10

#### CORTICAL THICKNESSES (cm.)

##### **Tibia:**

1) 0.803      3) 0.423      5) 0.408  
2) 0.235      4) 0.402      6) 0.214

##### **Fibula:**

No measurements taken.

#### WEIGHTS (kg.)

Total = 6½ In air testing so there was no artificial hip cemented into the femur.

## APPENDIX C

### Cadaver Information



## Test Leg / Cadaver Information

<u>Test#</u>	<u>U of L #</u>	<u>Photo #</u>	<u>AGE</u>	<u>SEX</u>	<u>Cause of Death</u>	<u>Date of Death</u>
L-1	13-R	10-90	*	*	*	*
L-2	602-R	06-90	72	♂	Metastatic Cancer	9/17/86
L-3	629-L	05-90	68	♂	CA Prostate, ♥-resp arrest	12/31/86
L-4	646-R	04-90	72	♀	Pneumonia	3/11/87
L-5	662-R	05-90	84	♂	Atherosclerotic ♥ disease	5/17/87
L-6	436-L	08-90	76	♀	♥-respiratory arrest	9/04/84
L-7	762-R	01-90	67	♂	Congestive ♥ failure	1/05/89
L-8	662-L	03-90	84	♂	Atherosclerotic ♥ disease	5/17/87
L-9	59-R	09-90	66	♂	Stroke	6/01/79
L-10	582-R	07-90	73	♀	Emphysema	6/19/86

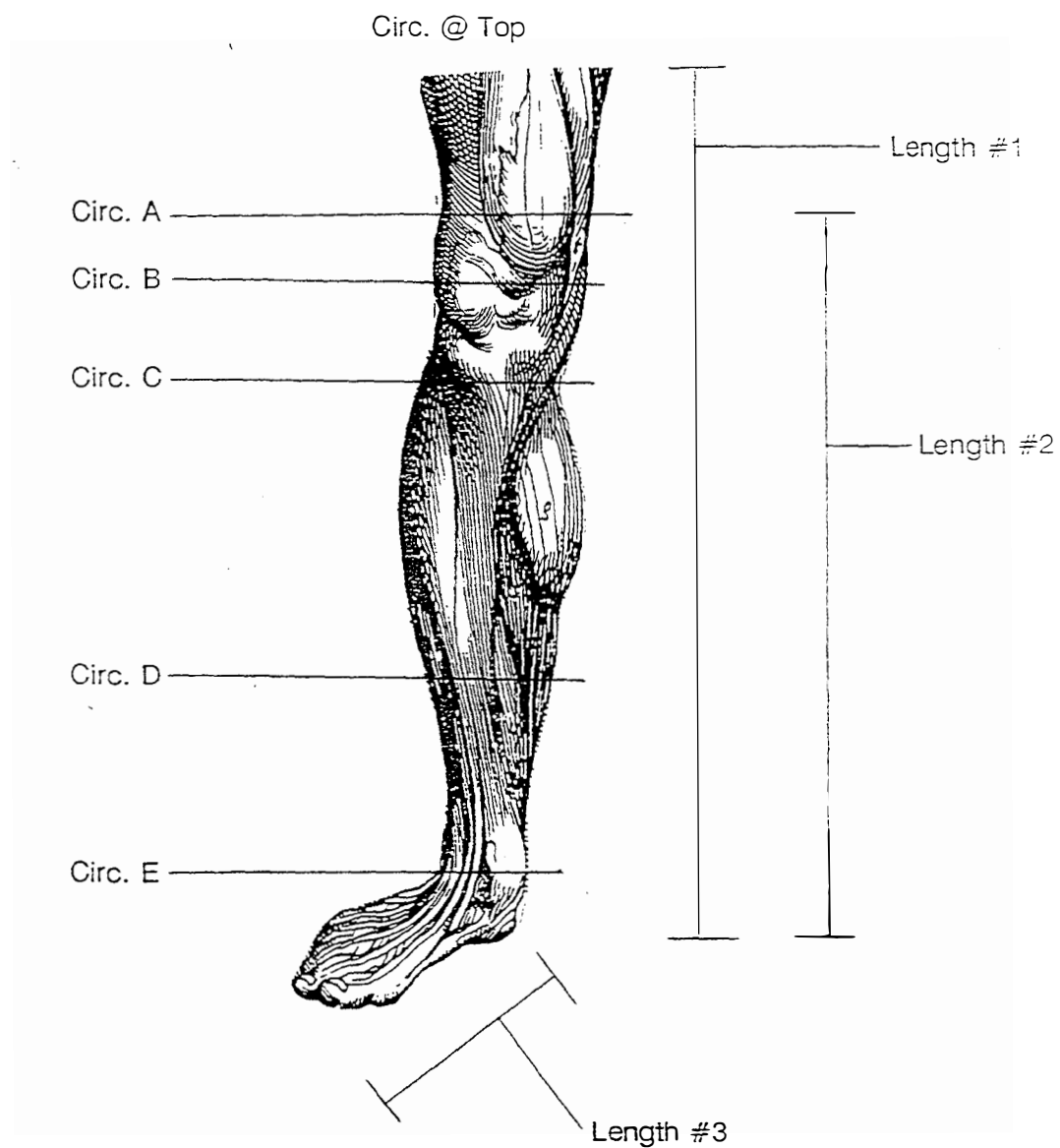
\* Cadaver Information not available for the given cadaver #.

## Measurements

<u>Test # &amp; Vel.</u>	<u>Weight (kg.)</u>	<u>Lengths (" )</u>			<u>Circumferences (" )</u>					
		<u>#1</u>	<u>#2</u>	<u>#3</u>	<u>@ Top</u>	<u>A</u>	<u>B</u>	<u>C</u>	<u>D</u>	<u>E</u>
L-1, 20 mph	5	27½	19½	8½	16¾	11¼	11¼	10	8½	6½
L-2, 20	4	27½	20	9½	11¼	10	12½	10¼	8½	6¼
L-3, 16.4	5½	29	20½	10	14¾	11½	13	11¼	9½	7
L-4, 16.4	5	25	20	9	14½	14	14	12½	9	8
L-5, 13	6¼	31	22	10¼	13¾	12¾	14½	12	10¼	8
L-6, 13	4½	24¾	20½	8¾	12¾	12¾	12¾	11	9	7
L-7, 10	5¾	27¾	20½	9	14¾	11½	12¾	11½	9	6¾
L-8, twice	6¼	30	21	10¼	14¾	13	14½	12¾	9¾	8½
L-9, in air	n/a	n/a				n/a		n/a		
L-10, in air	6¾	21¾	n/a	9	13	13	12½	10	n/a	6



## Measurements Diagram



**Appendix H**

**Causal Mechanisms of Air Bag Induced Eye  
Injuries from Actual Cases**

Case	Car	Person Injured				Collision Description*	Injury	Suggested Causal Mechanism
		Sex	Age	Ht	Wt			
		ys	cm	kg				
1	Ford Tempo 1985	M	25	189	86.2	front impact with concrete barrier, speed less than 96 km/hr	two tears of the left retina; minor abrasions of the left face, lower lip and chin;	-impact with deployed air bag
2	Ford Tempo 1985	M	32	177	72.6	front impact with earth embankment at 40 km/hr	left corneal abrasion	-impact with deployed air bag
3	Plymouth Gran Fury 1988	M	22	182	86.2	front impact with wooden pole at 40 km/hr	abrasions of right eyelid; abrasion of thumb	-impact with deployed air bag -deploying bag
4	Lincoln Continental 1989	F	60	170	70.3	vehicle rolled end over end several times, speed was 88 km/hr	left eye contusion; minor soreness	-impact with passenger air bag
5	Plymouth Sundance 1990	M	22	170	62.6	front end collision with rear of forward car, collision speed of 37 km/hr	laceration of the right retina; abrasions on right side of face; hematoma of forehead (loss of sight in right eye)	-impact with deployed air bag -contact with upper wheel
6	Ford Taurus GL Wagon 1990	F	54	165	55.3	front impact at 25 km/hr to rear of turning car wearing glasses	2 cm forehead laceration; lacerations at both eyebrows; hematoma of both upper and lower eyelids; abrasions of forehead, cheeks	-fractured eyeglass frames from impact with deployed air bag -impact with deployed air bag
7	Ford Mustang LX 1990	M	16	168	59	front impact with tree at 25.7 km/hr	detached left retina; hematoma of the left eye; abrasion from chin to left eye; superficial contusion to chest	-air bag module cover flap, the boy was extremely close to the wheel when it deployed -air bag deployment
8	Acura Legend 1991	F	50	154	58.5	right front impact with driver's car at 32 km/hr and seat in forward position non-tethered air bag	abrasion of left cornea with edema of the conjunctiva; left retinal hemorrhage; hemorrhage of the left eyelid; hyphema of the left eye	-impact with air bag
9	Geo Storm GSI 1991	M	25	183	79.8	right front impact at 96 km/hr with guardrail but did not come to stop, motion continued	bilateral commotio-retinae from compressed eye bilateral vitreous hemorrhage; contusions of forehead, eyelids; abrasions of forehead, eyelids	-impact with deploying and deployed air bag
10	Audi 100 1990	M	2	na	na	front impact with front of second car	thermal burns of the cheeks and both corneas (no long term visual impairments)	-unrestrained child was thrown onto the front driverside floor, air bag residue exhausted from vents onto child's face

Case	Car	Sex	Age	Ht	Wt	Collision Description	Injury	Suggested Causal Mechanism
11	Dodge Shadow 1990	F	36	160	49.9	fell asleep, resulting in front impact with utility pole impact speed was 26 km/hr <i>seat in forward position, non-tethered air bag</i>	contusions over both eyelids; abrasions under chin; abrasions and contusions of the anterior neck; contusions over both breasts; rupture of abdominal aorta; multiple bilateral rib fractures; ruptured spleen (Driver expired 3 hours later)	-Since asleep, it was assumed that at impact she was slumped over the wheel, and thus the deploying air bag did severe damage, as well as impact with the steering assembly. It was not determined which injuries were caused by which mechanism.
12	Plymouth Acclaim 1992	M	49	191	83.9	head-on collision with vel. changes of 62.6 km/hr and 56.3 km/hr for each car <i>wearing glasses</i>	contusion around left eye; multiple contusions and abrasions to upper extremities	-impact with deployed air bag and unbroken glasses
13	Mitsubishi 3000 GT 1992	F	58	168	61.3	frontal impact with tree yielding a velocity change of 16 km/hr	ecchymosis of left eyelids; contusions under right eye; bilateral corneal abrasions; bilateral conjunctiva hemorrhages; 10% hyphema in left eye; abrasions on left face, under chin (temporary loss of sight in left eye)	-Impact with deployed air bag
14	Acura Legend 1990	F	43	173	65.8	front impact at 19 km/hr to parked car <i>non-tethered bag</i>	hyphema of both eyes; dislocation of the temporo-mandibular joint; abrasions around both eyes left ear nerve damage; throat irritation	-impact with deployed air bag  -acoustic shock from air bag deployment -air bag exhaust
15	Lexus ES250 1990	M	40	179	77.1	front impact at 19.3 km/hr to a tree stump	tear + detachment of right retina; vitreous hemorrhage of right eye; abrasions of right face; (right eye sight now 20/400)	-impact with deploying bag
16	Mazda 929S 1992	M	60	177	72.6	front impact at 40 km/hr with median guardrail <i>non-tethered air bag</i>	minor concussion; scleral rupture of left eye 20%; laceration of the left iris; abrasion of left eye; partial left vitreous detachment; dilated left pupil; facial abrasions	-both the deploying motion of the air bag, and impact with deployed air bag
17	Chrysler Labaron 1989	F	39	168	64.4	Left front impact with oncoming second car, impact speeds of 84 and 74 km/hr <i>wearing glasses</i>	contusion on left eye; contusion on chin; contusion on nose; laceration of lip	-impact with air bag
18	Ford Taurus 1990	F	36	na	na	front impact with rear side of turning car, delta V=10 km/hr	thermal burns to the left eye, left face, neck, chest, left arm, and left hand (all were minor)	-fire from deploying air bag as the inflator burned two holes in the front of the bag

Case	Car	Sex	Age	Ht	Wt	Collision Description	Injury	Suggested Causal Mechanism
19	Acura Legend 1989	M	72	na	na	front impact at 40 km/hr with telephone pole <i>no seatbelt,</i> <i>wearing glasses</i>	left eye globe rupture  facial abrasions; left periorbital ecchymosis	-eyeglass frame via impact with deployed air bag -impact with deployed bag
20	Porsche Turbo 944 1987	M	35	173	83.9	48 km/hr impact with 12 cm steel grate protecting water pump off the road	laceration of the left eye; facial abrasions; abrasion to upper chest; (temporary loss of vision)	-impact with air bag
21	Acura Legend 1989	F	65	158	70.3	front side impact at 24km/hr with front of forward moving car at 72 km/hr	contusions around right eye; abrasion of right cornea; right vitreous humor detachment facial abrasions;	-impact and lateral slide against the deployed air bag
22	Ford LTD 1984	M	29	185	81.6	front impact at 83.6 km/hr with fence post	abrasion of left cornea; contusion on the lip; abrasion on the left cheek	-impact with deployed air bag
23	Dodge Daytona 1988	M	17	180	74.8	driver was hit from behind and then from the front <i>wearing glasses</i>	laceration of left eyelid; contusion of nose and left eye	-eyeglass frame via impact -impact with deployed air bag
24	Nissan Altima 1993	M	27	183	79	front impact with oncoming car at 35 km/hr <i>wearing contacts</i>	hyphema of left and right eye; corneal abrasion of left, right eye; laceration of left cheek; abrasion of left eyelid; contusion of left eyelid;	-impact with deployed air bag
25	Ford Crown Victoria 1991	F	60	175	90.7	front impact at 64.4 km/hr with earth embankment	vitreous hemorrhage of left eye abrasion of left cornea; laceration of left iris producing a hyphema of left eye; contusion of periorbital left eye; (lens was replaced due to traumatic cataract in left eye)	-impact with deployed air bag

## VITA

Tyler Kress, the youngest of three children of Tom and Dee Kress, was born in Oak Ridge, Tennessee, on May 15, 1964. His brother, Reid, was born in 1958 and his sister, Wendy, in 1961. Tyler graduated from Oak Ridge High School in 1982 and completed his Bachelor's degree in biomechanical engineering in 1986 at The University of Tennessee. He started working at The University and continued his education pursuing a Master's and a Ph.D. degree. His minors for his Bachelor's and Master's are mathematics and Engineering Management respectively. Upon acceptance of this dissertation, Tyler's Ph.D. will be completed and it will be a "dual degree" in that he has fulfilled the requirements of an Industrial Engineering Ph.D., yet his major concentrations are biomechanical engineering and human factors engineering (ergonomics). The degree will be a Ph.D. in "Engineering Science."

For the past ten years, Tyler has enjoyed a career in academics. He began teaching in 1986 and has essentially taught two classes per semester since 1989. Over 1000 junior- and senior-level and several master's students have taken a variety of courses from him - including courses in biomechanics, special topics in biomedical engineering and industrial engineering, human factors, work methods and measurement, engineering economy, quality control, operations research, computer programming, and others. He also spends a significant amount of time helping develop and promote The University of

Tennessee's Engineering Institute for Trauma and Injury Prevention and is currently the Manager of their impact biomechanics research.

On a more personal note, Tyler loves spending time with his family and friends, participates in a variety of different sports, and always enjoys a road trip or a good glass of red wine.